# NEXT TIER OFF-ROAD DIESEL TECHNOLOGY SELECTION, CALIBRATION, AND FINAL DEMONSTRATION

## OFF-ROAD LOW $NO_X$ DEMONSTRATION PROGRAM – STAGE 3

**ARB CONTRACT 20MSC005**

**FINAL REPORT**

**SwRI® Project Number 03.26778**

**Prepared for:**

**California Air Resources Board**

**Prepared by:**

**Christopher A. Sharp, Institute Engineer - Program Manager**

**Southwest Research Institute**
**6220 Culebra Road**
**San Antonio, TX 78238**

**April 28, 2024**

SwRI Benefiting government, industry and the public through innovative science and technology

# NEXT TIER OFF-ROAD DIESEL TECHNOLOGY SELECTION, CALIBRATION, AND FINAL DEMONSTRATION

## OFF-ROAD LOW $NO_X$ DEMONSTRATION PROGRAM – STAGE 3

**ARB CONTRACT 20MSC005**

**FINAL REPORT**

**SwRI® Project Number 03.26778**

**Prepared for:**

**California Air Resources Board**

**April 28, 2024**


**Prepared by:**

**Chris Sharp, Institute Engineer**
**Commercial Vehicle R&D Dept.**
**Powertrain Engineering Division**

**Approved by:**

**Charlie Roberts, Director**
**Commercial Vehicle R&D Dept**
**Powertrain Engineering Division**

**POWERTRAIN ENGINEERING DIVISION**



SwRI Benefiting government, industry and the public through innovative science and technology

## DISCLAIMER

The statements and conclusions in this Report are those of the contractor and not necessarily those of the California Air Resources Board. The mention of commercial products, their source, or their use in connection with material reported herein is not to be construed as actual or implied endorsement of such products.

## ACKNOWLEDGEMENTS

Southwest Research Institute (SwRI) would like to acknowledge the support and contributions of John Deere in the completion of this effort. John Deere provided engine hardware and engineering support as an in-kind contribution to this program, as well as providing access to source data for the development of a Low Load Application Cycle.

SwRI would also like to acknowledge the support and contributions of the Manufacturers of Emission Controls Association (MECA) and its member companies. MECA provided financial support for the program, and MECA member companies contributed a significant amount of hardware and engineering support in-kind. This support included both engine and aftertreatment technologies. Among the many supporting MECA member companies, SwRI would like to specifically acknowledge Jacobs Vehicle Systems who provided cylinder deactivation (CDA) technology for this program and Tula Technology who provided the use of their Diesel Dynamic Skip Fire (dDSF) algorithm.

In addition, SwRI would also like to acknowledge the contributions of the program Steering Committee, which was composed of various government and industry stakeholders, and which provided important input and feedback at various points in the program. In particular, SwRI would like to acknowledge the Truck and Engine Manufacturers Association (EMA) and the various off-road industry companies that provide both data and valuable feedback and guidance during the development of the Low Load Cycle.

This Report was submitted in fulfillment of CARB contract 20MSC005 titled “Next Tier Off-Road Diesel Aftertreatment Technology Fabrication and Optimization,” by Southwest Research Institute under the sponsorship of the California Air Resources Board. Technical efforts were completed as of November, 2023.

**TABLE OF CONTENTS**

ABSTRACT ..... 15
EXECUTIVE SUMMARY ..... 16
1.0 INTRODUCTION AND BACKROUND ..... 19
2.0 METHODS AND MATERIALS ..... 1
2.1 Test Engine ..... 1
2.2 Emission Test Cell ..... 4
2.3 Test Cycles, Test Procedures, and Preconditioning Procedures ..... 5
2.4 Low $NO_X$ Aftertreatment Hardware ..... 7
*2.4.1. Aftertreatment Team 1* ..... 8
*2.4.2. Aftertreatment Team 2* ..... 10
*2.4.3. Final Combined Team Aftertreatment Systems* ..... 13
*2.4.4. Aftertreatment e-Heater* ..... 16
*2.4.5. Aftertreatment Electrically Heated Mixer (EHM) Assembly* ..... 19
*2.4.6. Combined e-Heater and Heated Mixer* ..... 21
*2.4.7. Accounting for Heater Power Input* ..... 22
2.5 Low $NO_X$ Engine Hardware Options ..... 24
*2.5.1. EGR Cooler Bypass* ..... 24
*2.5.2. Cylinder Deactivation (CDA)* ..... 24
*2.5.3. Diesel Dynamic Skip Fire (dDSF™)* ..... 26
2.6 Low $NO_X$ Controls ..... 27
*2.6.1. Overall Strategy and Engine State Machine* ..... 28
*2.6.2. Aftertreatment Controller and DEF Dosing Controls for Conventional Architecture Systems* ..... 30
*2.6.4. Overall Aftertreatment System Control Strategy* ..... 35
2.7 Aging Methodology – Development Aging (Hydrothermal Only) ..... 36
2.8 Aging Methodology – DAAAC Aging (Hydrothermal and Chemical) ..... 37
3.0 RESULTS AND DISCUSSION ..... 44
3.1 Package 1 Testing and Previous Program Results ..... 44
*3.1.1. John Deere 6068 Baseline Tier 4 Final Emissions Results* ..... 44
*3.1.2. Package 1 Results* ..... 46
3.2 Impact of Crankcase Emissions and Closed Crankcase Ventilation (CCV) ..... 47
3.3 Package 2 Engine Calibrations ..... 50
3.4 Package 2 Results with Updated Engine Calibration ..... 52
3.6 Aftertreatment Heating – e-Heater and EHM Testing ..... 54
3.7 Combined Team Package 2 Results with Conventional Aftertreatment Architecture ..... 60

*3.7.1. Idle Emissions Testing*....62
3.8 Evaluation of Dual Dosing Dual SCR Architecture....63
3.9 Final Technology Comparison and Selection....71
3.10 Final Calibration and Zero-Hour Testing....73
3.11 8000-Hour Equivalent DAAAC Aging....78
3.12 Final 8000-Hour Demonstration Results....81
3.13 Impact of Infrequent Regeneration Adjustment Factor (IRAF)....108
*3.13.1. Team 2 Regeneration Results*....109
*3.13.2. Team 1 Regeneration Results*....113
3.13 Assessment of Idle Stop-Start Technology....117
3.14 Low Power Child Rating Tests....122
4.0 OFF-ROAD LOW LOAD CYCLE (LLC) DEVELOPMENT....140
4.1 Input Data Sets for LLC Development....141
4.2 Data Windowing....142
4.3 Identification of the Low Load Operating Region....144
4.4 k-Means Clustering Analysis to Identify Common Operating Modes....146
4.5 Idle Related Parameters....150
4.6 Selection of Profiles from each Cluster....153
4.6 Profile Testing....161
4.7 Candidate Cycle Assembly and Evaluation....163
4.8 Final Cycle Selection and Cleanup....170
5.0 SUMMARY AND CONCLUSIONS....171
5.1 Demonstration Results....171
5.2 Additional Discussion of Technology Considerations and Feasibility....174
6.0 REFERENCES....178
APPENDIX A - EMISSION DATA SUMMARIES FOR ALL TEST POINTS....179
APPENDIX B – Summary of Individual Test results for Low Load Cycle Cluster....188

## LIST OF FIGURES

**Figure** **Page**

Figure 1. Tailpipe BS$NO_X$ Emissions for Tier 5 Low $NO_X$ System Compared to Baseline Tier 4 Engine....16
Figure 2. Package 2 DEmonstration Aftertreatment System Architecture – Dual-Dosing, Dual SCR (MFC+zCSF+SCR)....17
Figure 3. $CO_2$ Emissions for Tier 5 Low $NO_X$ System Compared to Baseline Tier 4 Engine....17
Figure 4. $N_2O$ Emissions for Tier 5 Low $NO_X$ System Compared to Baseline Tier 4 Engine....18
Figure 5. PM Emissions for Tier 5 Low $NO_X$ System....18

Figure 6. Final Normalized Off-Road Low Load Cycle (LLC) ....19
Figure 7. Tier 4 john deere 6068 Engine....1
Figure 8. Baseline (Stock) Aftertreatment (Inlet Side) for 2018 Deere 6068 Engine ....3
Figure 9. Baseline (Stock) Aftertreatment System for Deere 6068 Engine – Outlet Side and dosing-mixing Pipe ....4
Figure 10. Normalized Off-Road Low Load Application Cycle (LLAC) ....6
Figure 11. Normalized Off-Road Low Load Cycle (LLC) ....6
Figure 12. Conventional Aftertreatment System Architecture – DOC+DPF+SCR (Package 1)...8
Figure 13. Team 1 Aftertreatment Primary Concept for Package 1 ....9
Figure 14. Team 1 Candidate Aftertreatment Package 2 Configuration....10
Figure 15. Team 2 aftertreatment Concept for Package 2....10
Figure 16. Team 2 Conventional Architecture Aftertreatment System ....11
Figure 17. Team 2 aftertreatment Concept for Package 2 with Dual SCR Dual Dosing Arrangement ....12
Figure 18. MFC and zCSF Installed at FRont of AT System Along with Upstream Heated Doser ....13
Figure 19. Schematic of Conventional Architecture Combined Aftertreatment System....14
Figure 20. Schematic of Dual SCR Dual Dosing Architecture Aftertreatment System ....14
Figure 21. Final Combined AT System with Dual Dosing Dual SCR architecture ....15
Figure 22. TRansfer Pipe from Engine for Dual Dosing Dual SCR Architecture Showing Heated Doser and Mixer Mounting ....16
Figure 23. 6.8kW e-Heater Assembly....17
Figure 24. Flanged e-Heater Assembly Ready for Installation ....17
Figure 25. Schematic of Conventional Architecture AT System with e-Heater Located After DPF ....18
Figure 26. e-Heater Assembly Installed in the Combined Conventional AT System Package (after DPF)....18
Figure 27. Heated Mixer Assembly (12-in Diameter) ....19
Figure 28. Heated Mixer Assembly Installed in the Low NOX Aftertreatment System in Place of the Inline Mixer ....20
Figure 29. Heated Mixer Assembly Installed with Insulation Wrap ....20
Figure 30. Combined e-Heater and EHM Assembly Installed in Series on TEam 2 Conventional System ....21
Figure 31. Examples of Heater Power Demand and Torque Correction During First 400 seconds of Cold NRTC....23
Figure 32. EGR Cooler bypass implementation ....24
Figure 33. Cylinder Deactivation System (Jacobs VEhicle Systems) ....26
Figure 34. Illustration of Dynamic Skip Fire (from Tula Presentation at 9th International Engine Congress, Baden-Baden, Germany)....27
Figure 35. High-Level Control Structure for Stage 3 Low $NO_X$ Demonstration....28
Figure 36. Low $NO_X$ Integration Controller Hardware Platform....28
Figure 37. Engine State M/C and Overall Strategy Control Diagrams....29

Figure 38. Example of Control Mode Switching during Cold-FTP .....30
Figure 39. Downstream SCR Dosing Controller Schematic .....31
Figure 40. Downstreatm SCR Controller Structure .....31
Figure 41. Example of Ammonia Storage Profiles during Hot-Start NRTC Cycle.....33
Figure 42. High-Level Schematic of Dual SCR Dual DEF Dosing Control Architecture.....34
Figure 43. Upstream (Lo-SCR/MFC) Dosing controller Schematic .....35
Figure 44. Upstream SCR Controller Structure.....35
Figure 45. SwRI ECTO-Lab$^{tm}$ Burner-Based Aging and Test Stand .....37
Figure 46. DAAAC Aging Cell with Deere 9.0L Aging Mule Engine and Final Low $NO_X$ Aftertreatment System .....42
Figure 47. DAAAC Engine Aging Stand Schematic .....42
Figure 48. Example Temperature Data for One DAAAC Aging Cycle .....43
Figure 49. Baseline Tier 4 Final Engine Tailpipe $NO_X$ Emissions for Base 187kw Engine Rating .....45
Figure 50. Baseline Tier 4 Final Engine $CO_2$ Emissions for BAse 187kw Engine Rating .....45
Figure 51. Baseline Tier 4 Final Engine $N_2O$ Emissions for BAse 187kw Engine Rating .....46
Figure 52. Compliance Margin Projections for Package 1 System at 8000-Hour FUL .....47
Figure 53. Impact of Crankcase Emissions of Deere 6068 Engine on Hot-Start NRTC Emissions .....48
Figure 54. crankcase Gas $NO_X$ Concentration as Compared to Engine-Out Level on NRTC ....49
Figure 55. Crankcase Gas Flow Rate as Compared to Engine Exhaust Flow on NRTC.....49
Figure 56. Crankcase Gas $NO_X$ Concentration as compared to Engine-Out Level on RMC .....50
Figure 57. Crankcase Gas Flow Rate as Compared to Engine Exhaust Flow on RMC .....50
Figure 58. $bsco_2$ emissions summary for baseline and Low $NO_X$ calibrations .....51
Figure 59. Margin Projections at 12,000 Hour FUL for Conventional Architecture with DSF...53
Figure 60. Margin Projections at 8,000 Hour FUL for Conventinal Architecture with DSF.....53
Figure 61. Engine-Out $NO_X$ in Early Cold-Start NRTC showing Heater Impact Before and After Calibration Adjustment .....54
Figure 62. Heater Power, System Temperatures, and Thermal Management Behavior for VArious Heater Configurations in Early Cold-Start NRTC .....56
Figure 63. DEF Dosing in Early Cold-Start NRTC for Various Heater Configurations .....57
Figure 64. Continuous Early Cold-Start NRTC Engine-Out and tailpipe NOX for Various Heater Configurations .....57
Figure 65. Early Cold-Start NRTC $NO_X$ Conversion for Various Heater Configurations.....58
Figure 66. Cumulative Early Cold-Start NRTC $NO_X$ and System Temperatures for Various Heater Configurations .....59
Figure 67. Extended Idle Test Results for Tier 5 Demonstration Engine with Combined Team Conventional Aftertreatment and Development Aged Parts .....63
Figure 68. Ammonia Storage Versus Temperature for System Catalysts.....64
Figure 69. Feed-Forward ANR Targets for Upstream and Downstream Dosers Versus Temperature.....65
Figure 70. Updated Dosing Calibration During Early Cold-STart NRTC.....66

Figure 71. Impact of Updated Doser Strategy on Early Cold-Start NRTC $NO_X$ Conversion over MFC ....66
Figure 72. Margin Projections for MFC-Enabled Configuration at 12,000 hour FUL Without DSF ....68
Figure 73. Behavior of Exotherm Across MFC and zCSF with Late Post Injection from Engine at Various Inlet Temperatures ....70
Figure 74. Final Tier 5 Demonstration Aftertreatment Schematic ....73
Figure 75. Filter Differential Pressure over Repeat Hot NRTC cycles....74
Figure 76. Hot-Start NRTC $NO_X$ Emissions Before and After passive Soot Oxidation CAlibration change ....75
Figure 77. 0-Hour $NO_X$ Emissions for Final Tier 5 Demonstration Package With and Without DSF, CCV....76
Figure 78. 0-Hour $CO_2$ Emissions for Final Tier 5 Demonstration Package With and Without DSF, CCV....76
Figure 79. 0-Hour $N_2O$ Emissions for Final Tier 5 Demonstration Package With and Without DSF, CCV....77
Figure 80. Aftertreatment System Temperatures during DAAAC Aging Cycle for Tier 5 Demonstration Aging....78
Figure 81. $NO_X$ Emissions over DAAAC Aging Cycle Early in Aging ....79
Figure 82. Accumulation of Sulfur Exposure Mass During 800-hour DAAAC Aging Run....80
Figure 83. MFC Outlet Ammonia on the LLAC – 8000-hr Initial Calibration Versus 0-hr without DSF....81
Figure 84. Tailpipe $N_2O$ Emissions on the LLAC - 8000-hr Initial Calibration Versus 0-hr without DSF....82
Figure 85. Tailpipe $NO_X$ Emissions on the LLAC - 8000-hr Initial Calibration Versus 0-hr without DSF....82
Figure 86. Changes to MFC Ammonia Storage Targets from 0-Hour Calibration to 8000-Hour Calibration ....83
Figure 87. Ammonia Storage Targets and Actual Values – Before and After 8000-Hr Calibration Change....84
Figure 88. Hot-Start NRTC DEF Dosing Before and After 8000-Hr Calibration change....85
Figure 89. Tailpipe $N_2O$ Emissions on the LLAC - 8000-hr Final Versus Initial Calibration without DSF....86
Figure 90. Tailpipe $NO_X$ Emissions Without DSF – 8000-Hr Versus 0-Hr, CCV ....86
Figure 91. Tailpipe $CO_2$ Emissions Without DSF Compared to Tier 4 Final Baseline – 8000-Hr Versus 0-Hr, CCV....87
Figure 92. Tailpipe $N_2O$ Emissions Without DSF Compared to Tier 4 Final Baseline – 8000-Hr Versus 0-Hr, CCV....87
Figure 93. Tailpipe PM Emissions Without DSF – 8000-Hr Versus 0-Hr, CCV ....88
Figure 94. Continuous Cold-Start NRTC $NO_X$ Data – 8000-Hr Versus 0-Hr without DSF, CCV ....90

Figure 95. Continuous Hot-Start NRTC $NO_X$ Data – 8000-Hr Versus 0-Hr without DSF, CCV ....91
Figure 96. Continuous LLAC $NO_X$ Data – 8000-Hr Versus 0-Hr without DSF, CCV....92
Figure 97. Continuous LLC $NO_X$ Data at the 8000-Hr Point without DSF, CCV....92
Figure 98. Continuous RMC $NO_X$ Data – 8000-Hr Versus 0-Hr without DSF, CCV ....93
Figure 99. Continuous RMC Tailpipe $N_2O$ Data – 8000-Hr Versus 0-Hr without DSF, CCV ...94
Figure 100. Tailpipe $NO_X$ Emissions With DSF – 8000-Hr Versus 0-Hr, CCV ....95
Figure 101. Tailpipe $CO_2$ Emissions With DSF – 8000-Hr Versus 0-Hr, CCV ....95
Figure 102. Tailpipe $N_2O$ Emissions With DSF – 8000-Hr Versus 0-Hr, CCV....96
Figure 103. Continuous Cold-Start NRTC $NO_X$ Data – 8000-Hr Versus 0-Hr with DSF, CCV.97
Figure 104. MFC Ammonia Storage for Cold-START NRTC with DSF at 8000-hr and 0-hr Test Points....97
Figure 105. Continuous Hot-Start NRTC $NO_X$ Data – 8000-Hr Versus 0-Hr with DSF, CCV ..98
Figure 106. Hot-Start NRTC SCR Catalyst TEmperatures – 8000-hr versus 0-hr with DSF....98
Figure 107. Continuous LLAC $NO_X$ Data – 8000-Hr Versus 0-Hr with DSF, CCV....99
Figure 108. NOX Conversion across MFC on LLAC – 8000-Hr versus 0-hr with DSF....99
Figure 109. Continuous LLC $NO_X$ Data – 8000-Hr with DSF, CCV ....100
Figure 110. Continuous LLC Temperature and Thermal Management Data – 8000-Hr with DSF, CCV ....100
Figure 111. Continuous RMC $NO_X$ Data – 8000-Hr Versus 0-Hr with DSF, CCV ....101
Figure 112. Continuous Cold-Start NRTC Data – DSF versus noDSF at 8000 Hours FUL....102
Figure 113. Continuous Hot-Start NRTC Data – DSF versus noDSF at 8000 Hours FUL....103
Figure 114. Continuous LLAC Data – DSF versus noDSF at 8000 Hours FUL ....105
Figure 115. Continuous LLC Data – DSF versus noDSF at 8000 Hours FUL....106
Figure 116. Continuous RMC Data – DSF versus noDSF at 8000 Hours FUL....107
Figure 117. Team 2 $NO_X$ Conversion under DPF Regeneration Conditions at 22.5K $Hr^{-1}$ space velocity....110
Figure 118. Team 2 $NO_X$ Conversion under DPF Regeneration Conditions at 40k $HR^{-1}$ space velocity....111
Figure 119. IRAF Calculations for Team 2 System on NRTC Cycle at 570°C Target Temperature....111
Figure 120. IRAF Calculations for Team 2 System on NRTC Cycle at 585°C target temperature ....112
Figure 121. IRAF Calculations for Team 2 System on RMC Cycle ....112
Figure 122. IRAF Calculations for Team 2 System on LLAC Cycle....113
Figure 123. Team 1 $NO_X$ Conversion under DPF Regeneration Conditions at 22.5K $Hr^{-1}$ space velocity....114
Figure 124. Team 1 $NO_X$ Conversion under DPF Regeneration Conditions at 40k $HR^{-1}$ space velocity....114
Figure 125. IRAF Calculations for Team 1 System on NRTC Cycle at 570°C Target Temperature....115

Figure 126. IRAF Calculations for Team 1 System on RMC Cycle at 570°C Target Temperature .....115
Figure 127. IRAF Calculations for Team 1 System on LLAC Cycle at 570°C Target Temperature.....116
Figure 128. IRAF Calculations for Team 1 System on LLC Cycle at 570°C Target Temperature .....116
Figure 129. Idle Stop-Start Test Cycle – Concatenated from Low Load Clusters 11 and 3.....117
Figure 130. LLAC Cycles on MFC-Enalbed System – With and Without Stop-Start Compared to DSF .....119
Figure 131. Cluster 113 Idle Cycles on MFC-Enalbed System – With and Without Stop-Start Compared to DSF .....120
Figure 132. Cluster 113 Evalution with Longer extended Idle modes (40-min and 25-min) ....122
Figure 133. Range of available Child Ratings for the John Deere 6068 Demonstration Engine family .....123
Figure 134. Low power Child Rating versus Base Rating – Hot-Start NRTC SCR Catalyst Temperaures .....124
Figure 135. MFC Storage Calibration Adjustments from Base (187kw) Rating to Child (126kw) Rating .....124
Figure 136. Child vs Base Rating – Cold NRTC Behavior without DSF at 8000-hr Test Point127
Figure 137. Child vs Base Rating – Cold NRTC $NO_X$ Conversion and Cumulative $NO_X$ without DSF at 8000-hr Test Point.....128
Figure 138. Child vs Base Rating – Hot NRTC Behavior without DSF at 8000-hr Test Point.129
Figure 139. Child vs Base Rating – Hot NRTC $NO_X$ Conversion and Cumulative $NO_X$ without DSF at 8000-hr Test Point.....130
Figure 140. Child vs Base Rating – LLAC Behavior without DSF at 8000-hr Test Point.....131
Figure 141. Child vs Base Rating – LLAC $NO_X$ Conversion, $N_2O$, and Cumulative $NO_X$ without DSF at 8000-hr Test Point .....132
Figure 142. Child vs Base Rating – LLC Behavior without DSF at 8000-hr Test Point.....133
Figure 143. Child vs Base Rating – LLC $NO_X$ Conversion, $N_2O$, and Cumulative $NO_X$ without DSF at 8000-hr Test Point.....134
Figure 144. Child vs Base Rating – LLAC Behavior with DSF at 8000-hr Test Point.....135
Figure 145. Child vs Base Rating – LLAC $NO_X$ Conversion, $N_2O$, and Cumulative $NO_X$ withDSF at 8000-hr Test Point.....136
Figure 146. Child vs Base Rating – LLC Behavior with DSF at 8000-hr Test Point.....137
Figure 147. Child vs Base Rating – LLC $NO_X$ Conversion, $N_2O$, and Cumulative $NO_X$ without DSF at 8000-hr Test Point.....138
Figure 148. Application breakdown in the LLC Development Input Data Set.....142
Figure 149. Histogram of Engine Power Levels in the LLC Development Input Data Set.....142
Figure 150. Example of 5-Microtrip Analysis on a Machine Data Segment .....143
Figure 151. Distribution of Window Loads using Load at Current Speed Metric .....145
Figure 152. Distribution of Window Loads Using Percent of Maximum Engine Power Metric .....146

Figure 153. Example of Clustering Output with Two Parameters and Two Clusters .....147
Figure 154. population of clusters versus Number of Clusters for the Low Load Data Set .....149
Figure 155. Variance Versus Number of Clusters for Low Load Data Set k-Means Analysis..149
Figure 156. Cumulative EDF of Idle Duration for Various Minimum Idle Durations.....151
Figure 157. Cumulative EDF for Idle Load at Various Minimum Idle Durations .....152
Figure 158. Example of Six Selected Profiles for Cluster 11.....154
Figure 159. Example of Six Selected Profiles for Cluster 6.....154
Figure 160. Distribution application type for Cluster 11 by Engine Population and NUmber of Windows.....155
Figure 161. Normalized Profiles for each Cluster .....158
Figure 162. Normalized Speed-Torque Scatterplots of Selected Profiles from each Cluster ....159
Figure 163. Machines Represented by the Selected Profiles for each Cluster .....160
Figure 164. Example of Profile Testing for Cluster 6 Profile on John Deere 6068 Tier 4 Final Engine .....162
Figure 165. LLC Beta Candidate Cycle 14 .....165
Figure 166. LLC BeTa Candidate Cycle 15 .....166
Figure 167. LLC Beta Candidate Cycle 16 .....167
Figure 168. Example of Low Load Cycle Testing on Candidate 14 with Baseline Tier 4 Final Engine .....168
Figure 169. Example of Low Load Cycle Testing on Candidate 14 with Teir 5 Low $NO_X$ Demonsration Engine using Development Aged Parts.....169
Figure 170. Final Off-road Low Load Cycle (LLC).....170
Figure 171. Summary of Tailpipe $BSNO_X$ for Low $NO_X$ Demonstration Compared to Baseline – With and Without DSF.....171
Figure 172. Tailpipe NOX Compliance Values for Tier 5 Low $NO_X$ Demonstration Engine ..172
Figure 173. Summary of Tailpipe $BSCO_2$ for Low $NO_X$ Packages Compared to Baseline.....173
Figure 174. Summary of Tailpipe $BSN_2O$ for Low $NO_X$ Packages Compared to Baseline .....173
Figure 175. Tailpipe $NO_X$ Emissions for Base and child Ratings – 8000-Hr Data With and Without DSF.....174

## LIST OF TABLES

**Table** **Page**

Table 1. John Deere 6068 Engine Parameters.....2
Table 2. Cycle Average Power for Compliance Cycles.....7
Table 3: Team 1 Candidate Aftertreatment System Catalyst Specifications .....9
Table 4. Catalyst Specifications for Team 2 Conventional Architecture System .....11
Table 5. Team 2 Catalyst Specifications for Dual-SCR Dual Dosing Architecture System.....13
Table 6. Combined System Catalyst Specifications for Single Def Doser System.....14
Table 7. Combined System Catalyst Specifications for Dual DEF Doser System.....15
Table 8. Initial Set of Potential DAAAC Non-Regeneration Aging Modes .....39

Table 9. Final Set of DAAAC Non-Regeneration AGing Modes ....39
Table 10. Regeneration Intervals and Weight Factors by Test Cycle....40
Table 11. Final DAAAC Aging Cycle for OffRoad Low NOx Demonstration....40
Table 12. Final Package 1 Test Results with Development Aged Parts ....46
Table 13. Package 2 Results with Team 2 Conventional Architecture and Updated Calibration with DSF and Development Aged Parts ....52
Table 14. Heater COnfiguration Impact on Cold-Start NRTC BS$NO_X$ ....60
Table 15. Best Heater Enabled Results (EH or EHM ~ 6.5kw Capacity) with DSF, CCV ....60
Table 16. Package 2 Results with Combined Team Conventional Archtecture on Development Aged Parts with Updated Calibration and DSF, CCV ....61
Table 17. Package 2 Results with Combined Team Conventional Architecture on Development Aged Parts with Updated CAlibration and no DSF, CCV ....61
Table 18. Extended Idle Test Results....62
Table 19. Cold-Start NRTC Emissions for Various Test Configurations with Development Aged Parts, CCV....67
Table 20. Tailpipe Emissions with MFC and DSF on All Cycles with Development Aged Parts, CCV ....67
Table 21. Tailpipe Emissions with MFC on All Cycles Without DSF with Development Aged Parts, CCV....68
Table 22. Comparison of Tier 5 Demonstration Technology Options and Recommendations ...72
Table 23. Improvement in $CO_2$ Emissions Compared to Tier 4 Baseline Engine for 0-Hour Tier 5 Demonstration Engine....77
Table 24. Selected Oil Properties for 15W40 Oil Used during DAAAC Aging....80
Table 25. Initial Test Results Without DSF for 8000-Hr Aged Parts with 0-Hour Calibration, CCV ....81
Table 26. $CO_2$ Emission Results at FUL Without DSF Compared to BAseline Tier 4 Engine...88
Table 27. $CO_2$ Emission Results at FUL With DSF Compared to BAseline Tier 4 Engine ....96
Table 28. Final Infrequent Regeneration UAFs for Tier 5 Demonstration Engine ....116
Table 29. LLAC Evaluation Results with Stop-Start....118
Table 30. Cluster 113 Idle Cycle Evaluation Results with Stop-Start on MFC-Enabled AT System ....121
Table 31. Cluster 113 Idle Cycle Evaluation Results with Stop-Start on conventional AT System ....121
Table 32. Tailpipe Emissions for Low Power Child Rating with Development Aged parts – Without DSF, CCV....125
Table 33. Tailpipe Emissions for Low Power Child Rating with 8000-Hr DAAAC-Aged Parts – Without DSF, CCV....125
Table 34. Tailpipe Emissions for Low Power Child Rating with 8000-Hr DAAAC-Aged Parts – With DSF, CCV....126
Table 35. Clustering Parameters....147
Table 36. Centroid Values and Populations for the 12 Clusters....150

Table 37. Selected Quantiles of Idle Load for the 30-Second minimum Idle Duration Data Set .....153
Table 38. Application and Engine Information for selected Profile from each Cluster .....157

## LIST OF ACRONYMS

| | |
|---|---|
| 3B-MAW | 3-Bin Moving Average Window |
| AMT | Automated Manual Transmission |
| ANR | Ammonia to $NO_X$ Ratio |
| ASC | Ammonia Slip Catalyst |
| AT | Aftertreatment |
| BMEP | Brake Mean Effective Pressure |
| BSFC | Brake Specific Fuel Consumption |
| CAN | Controller Area Network |
| CARB | California Air Resources Board |
| CDA | Cylinder Deactivation |
| CE-CERT | Bourns College of Engineering, Center for Environmental Research & Technology |
| $CH_4$ | Methane |
| CITT | Curb Idle Transmission Torque |
| CNG | Compressed Natural Gas |
| CO | Carbon Monoxide |
| $CO_2$ | Carbon Dioxide |
| COV | Coefficient of Variation |
| CSF | Catalyzed Soot Filter |
| CWF | Carbon Weight Fraction |
| DAAAC | Diesel Aftertreatment Accelerated Aging Cycles |
| DEF | Diesel Exhaust Fluid (32% urea by weight) |
| dDSF | Diesel Dynamic Skip Fire |
| dsSCR | Downstream SCR |
| $deSO_X$ | Desulfation |
| DOC | Diesel Oxidation Catalyst |
| DPF | Diesel Particulate Filter |
| ECM | Electronic Control Module |
| ECTO-Lab | Exhaust Composition Transient Operation Burner System (SwRI) |
| EGR | Exhaust Gas Recirculation |
| EO | Engine Out |
| EOL | End of Useful Life |
| EU | European Union |
| FTP | U.S. Heavy Duty Transient Federal Test Procedure |
| FUL | Full Useful Life |
| GHG | Greenhouse Gas |
| HDIUT | Heavy Duty In-Use Testing |
| HW | Hardware |
| IMAP | Intake Manifold Absolute Pressure |
| IMT | Intake Manifold Temperature |
| LLC | Low Load Cycle |
| LLAC | Low Load Application Cycle |
| LO-SCR | Light Off SCR Catalyst |
| LTT | Long term trim |
| MAB2 | MicroAutoBox II |
| MAW | Moving Average Window |

| | |
|---|---|
| MB | Mini-burner |
| MECA | Manufacturers of Emission Controls Association |
| MFC | Multi-Function Catalyst (LO-SCR) |
| MT | Manual Transmission |
| MY | Model Year |
| $N_2O$ | Nitrous Oxide |
| $NH_3$ | Ammonia |
| NIST | National Institute of Standards and Technology |
| $NO_X$ | Oxides of Nitrogen |
| NRTC | Nonroad Transient Cycle |
| NTE | Not-to-Exceed |
| NVH | Noise, Vibration, and Harshness |
| OBD | Onboard Diagnostics |
| PAG | Program Advisory Group |
| PGM | Platinum Group Metals |
| PM | Particulate Matter |
| PNA | Passive $NO_X$ Adsorber |
| RMC | Ramped Modal Cycle |
| RMC-C1 | Ramped Modal Cycle C-1 8-Mode for Variable Speed Nonroad Engines |
| RMC-SET | Ramped Modal Cycle Supplemental Emission Test |
| RMS | Root Mean Square |
| SCR | Selective Catalytic Reduction (ammonia-based) |
| SCRF | SCR on Filter (SCR coated on DPF) |
| SwRI | Southwest Research Institute |
| SPN | CAN Suspect Parameter Number |
| THC | Total Hydrocarbons |
| TM | Thermal Management |
| TP | Tailpipe |
| UAF | Upward Adjustment Factor (for Infrequent Regeneration) |
| VGT | Variable Geometry Turbine |
| zCSF | Zone-coated Catalyzed Soot Filter |

## ABSTRACT

This program was the culmination of a continuing effort aimed at demonstration of the capability of certain diesel emission control technologies to reach Low $NO_X$ levels on an offroad diesel engine. This program used incremental improvements and technology additions that were available within the time and budget available without resorting to the further tools afforded by fundamental redesign of the block, heads and rotating assembly. The program objective was to demonstrate the feasibility of technologies to reach tailpipe $NO_X$ emission reductions of up to 90% from the current Tier 4 standards, and PM emission reductions of at least 75% from the current Tier 4 standards. Two different systems were developed to meet these targets, the first of which was intended to meet the target $NO_X$ and PM levels with no impact on GHG emissions. The second system was intended to meet the target $NO_X$ and PM levels while also demonstrating a 5% to 8.5% improvement in $CO_2$ emissions. This report is focused primarily on the development and performance of the second system, which was designated as Package 2. The demonstration was targeted primarily at offroad engines rated between 56kw and 560kw. The offroad Low $NO_X$ demonstration reported here builds on previous extensive efforts to demonstrate Low $NO_X$ technologies for on-highway engines [1][2][3][4][5][6], as well as previous offroad test programs for CARB [7][8] that were intended to lay the groundwork for the current effort. The focus of this final effort was on a final robust performance demonstration of an optimized system configuration and durability out to a full-useful life (FUL) of 8,000 hours. The final emission control systems developed and evaluated in this program demonstrated levels 25% to 50% below the target emission levels at end of life (EOL) with technologies generally suitable for implementation in production, allowing for a reasonable potential compliance margin. In addition to these efforts, a Low Load Cycle (LLC) representative of off-road engine operation was developed using field data provided by CARB and other stakeholders, and the performance of the emission control system mentioned above over this cycle was also demonstrated.

## EXECUTIVE SUMMARY

Despite decades of progress in cleaning the air in California, challenges remain. The California Air Resources Board (CARB) has stated that meeting federally mandated ozone limits in the National Ambient Air Quality Standard (NAAQS) will require significant reductions in ozone forming oxides of nitrogen ($NO_X$) emissions across a wide range of applications. $NO_X$ emissions contribute heavily to ambient fine particulate matter pollution as well. Offroad diesel engines remain one of the most significant contributors to the overall $NO_X$ inventory, and CARB has indicated that further reductions from current standards are necessary to achieve air quality goals.

Previously, CARB has initiated a series of programs at SwRI to demonstrate the technical feasibility of reaching Low $NO_X$ levels up to 90% below the current standards for on-highway engines.[1][2][3][4][5][6] The goal of this program was to leverage that previous research and extend the Low $NO_X$ technology demonstration to the offroad market. The program goal for Low $NO_X$ was to demonstrate a level below 0.040 g/kw-hr over the current regulatory test cycles, with low load and in-use emissions as low as feasible. In addition, the program would also demonstrate PM levels below 0.005 g/kw-hr, 75% below the current Tier 4 standard. At the same time, the target was also to have the system demonstrate reductions in $CO_2$ on the order to 5 to 8.6% (equivalent to Phase 1 on-highway GHG reductions) compared to the Tier 4 baseline engine. The program's intent was to reach these targets with technologies that are feasible for production in the off-road market by the 2029.

Figure 1 shows a summary of the tailpipe $NO_X$ emission levels demonstrated in this program. It should be noted that these levels were demonstrated with aftertreatment hardware that was Diesel Accelerated Aftertreatment Aging Cycle (DAAAC)-aged to full useful life (FUL) on the primary engine rating of 187kw. The DAAAC aging methodology is an accelerated aging protocol that considers both thermal and chemical aging mechanisms, and it has been adopted by EPA as an accepted approach for demonstration the durability of emission controls systems for compliance testing, as well as by CARB on the On-Highway Low $NO_X$ Omnibus rule.

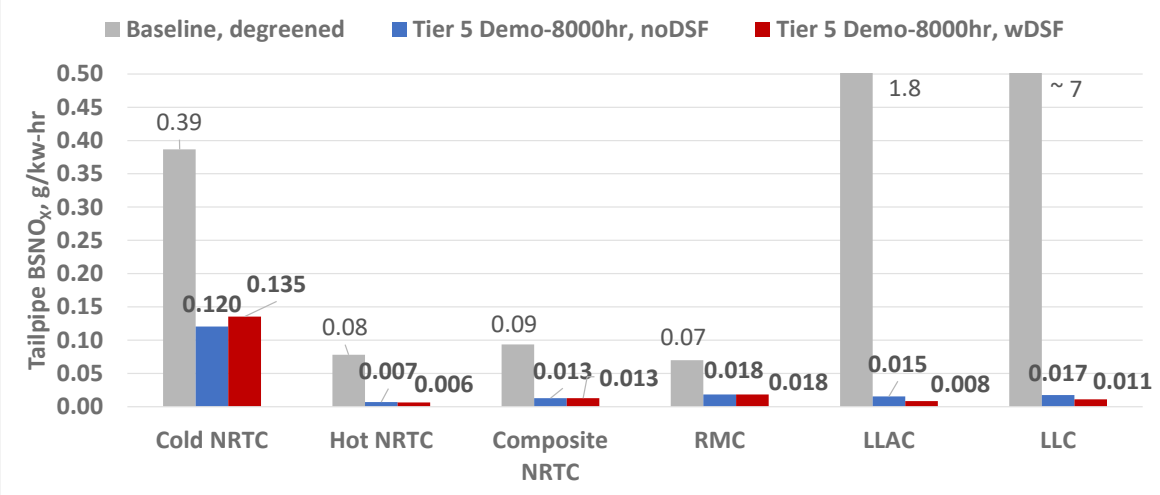



**FIGURE 1. TAILPIPE $BSNO_X$ EMISSIONS FOR TIER 5 LOW $NO_X$ SYSTEM COMPARED TO BASELINE TIER 4 ENGINE**

As can be seen in the figure above, tailpipe emissions were reduced by 90% compared to the Tier 4 engine on the Nonroad Transient Cycle (NRTC), by 75% on the high load RMC cycle, and by over 99% under the light load conditions of the Low Load Application Cycle (LLAC) that are below the loads of the current certification cycles.

The final demonstration aftertreatment system is depicted below in Figure 2, which was a dual-SCR dual dosing architecture. The upstream SCR system was a multi-function catalyst (MFC) which comprised both SCR and oxidation capability in-situ on the catalyst surface. The use of both the MFC and a zone-coated catalyzed soot filter (zCSF) allowed for the use of a dual SCR architecture without a substantial change in package size, which was important for nonroad application. The final demonstration architecture incorporates closed crankcase ventilation (CCV), which is already in use on some on-highway engines.

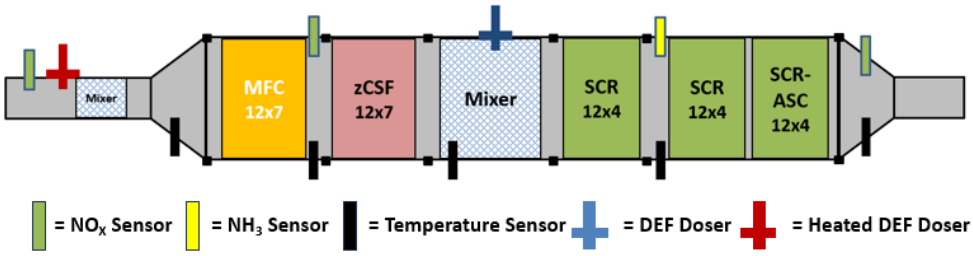



**FIGURE 2. PACKAGE 2 DEMONSTRATION AFTERTREATMENT SYSTEM ARCHITECTURE – DUAL-DOSING, DUAL SCR (MFC+ZCSF+SCR)**

Figure 3 gives a summary of $CO_2$ emissions for the Low $NO_X$ systems as compared to the Tier 4 baseline engine. The baseline levels are shown in g/kw-hr and the data labels for the two final test configurations (with and without DSF) show the percent reduction on $CO_2$ from the baseline. The Tier 5 Low $NO_X$ demonstration engine was able to reach the target range of 5% to 8.6% reduction from the Baseline engine on the NRTC, both with and without DSF, while achieving the $NO_X$ levels shown in Figure 1. Without DSF, these reductions were smaller on the RMC and low load cycles. The use of DSF resulted in an additional 1% $CO_2$ reduction on the NRTC and RMC, but it also resulted in a 6% reduction on the LLAC and a 10% reduction on the LLC.

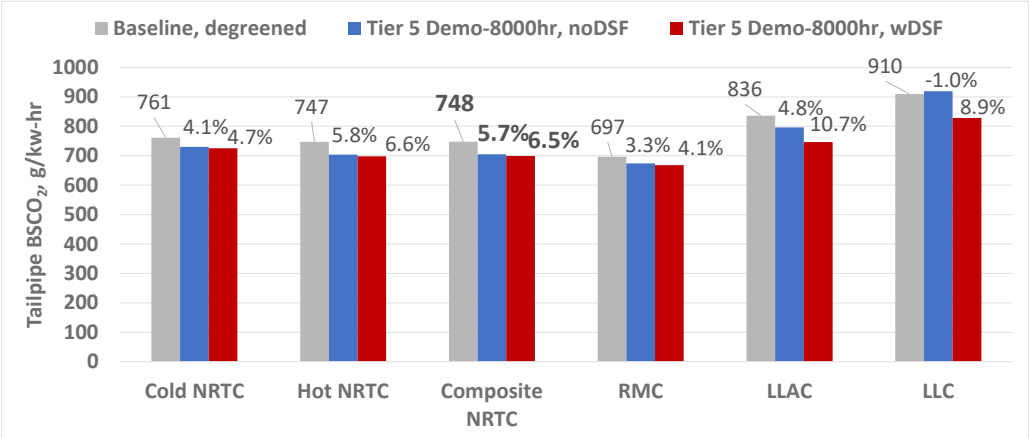



**FIGURE 3. $CO_2$ EMISSIONS FOR TIER 5 LOW $NO_X$ SYSTEM COMPARED TO BASELINE TIER 4 ENGINE**

A summary of $N_2O$ emissions for the Low $NO_X$ systems as compared to the Tier 4 baseline engine is given in Figure 4. The Tier 5 demonstration system, both with and without DSF, had $N_2O$ levels below those of the Tier 4 baseline engine on the NRTC. $N_2O$ levels on other cycles were generally at or below the levels observed on the baseline engine, and in all cases were well below the proposed Tier 5 $N_2O$ capping standard of 0.15 g/kw-hr.

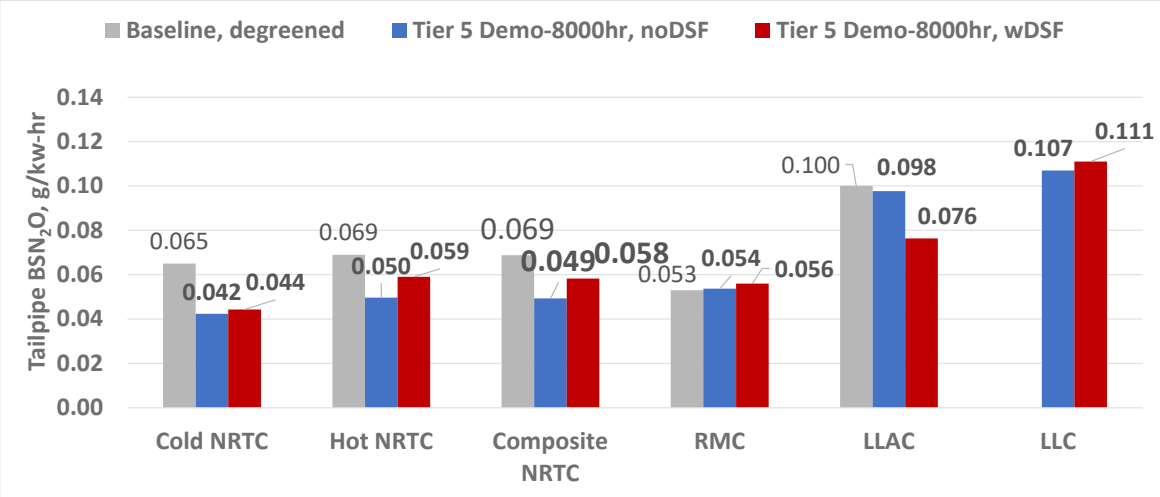



**FIGURE 4. $N_2O$ EMISSIONS FOR TIER 5 LOW $NO_X$ SYSTEM COMPARED TO BASELINE TIER 4 ENGINE**

Figure 5 shows a summary of FUL tailpipe PM emissions both with and without DSF. PM emissions were on average an order of magnitude below the proposed 0.005 g/kw-hr. It should be noted that individual test results were observed as high as 0.001 g/kw-hr, but this is still well below the 0.005 g/kw-hr level.

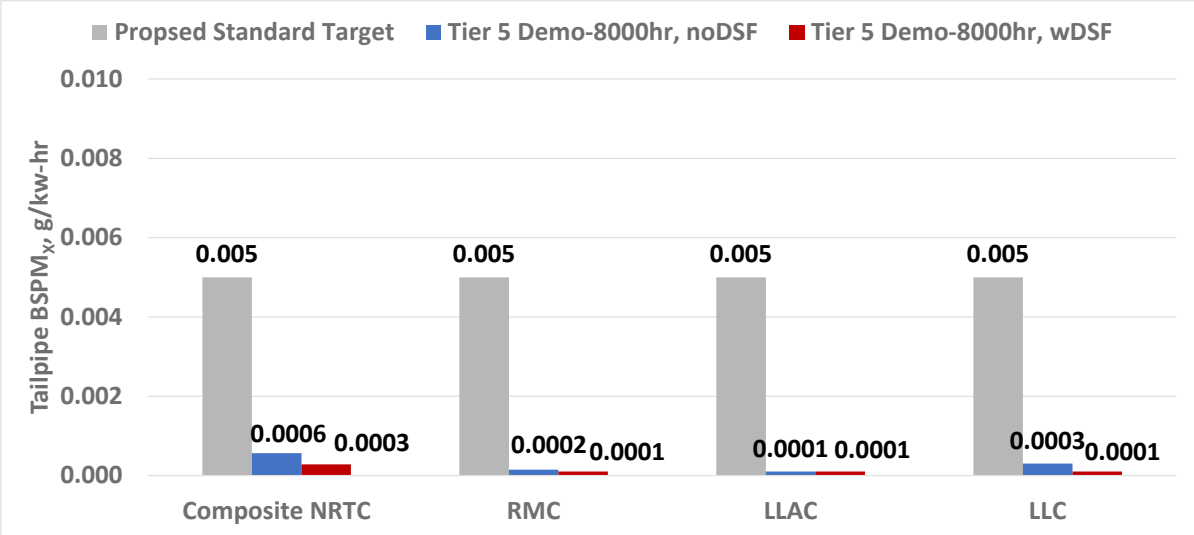



**FIGURE 5. PM EMISSIONS FOR TIER 5 LOW $NO_X$ SYSTEM**

A key part of this program was the development of a new offroad Low Load Cycle (LLC). This cycle was developed based on field data recorded on 240 different engines from a wide variety of off-road and nonroad mobile machine applications, with data contributions from both CARB funded CE-CERT studies and industry engine and equipment manufacturers. These data sets were

used to identify low load operating regions that could be sampled for examples of low load operation (generally below 27% load or power). Common operating modes in this low load region were identified using a k-means clustering process, and representative operating profiles from those modes were randomly sampled and screened to be the building blocks of the final cycle. A total of 16 different candidate cycles were evaluated before the final cycle was determined. The final normalized Offroad LLC is depicted in Figure 6.

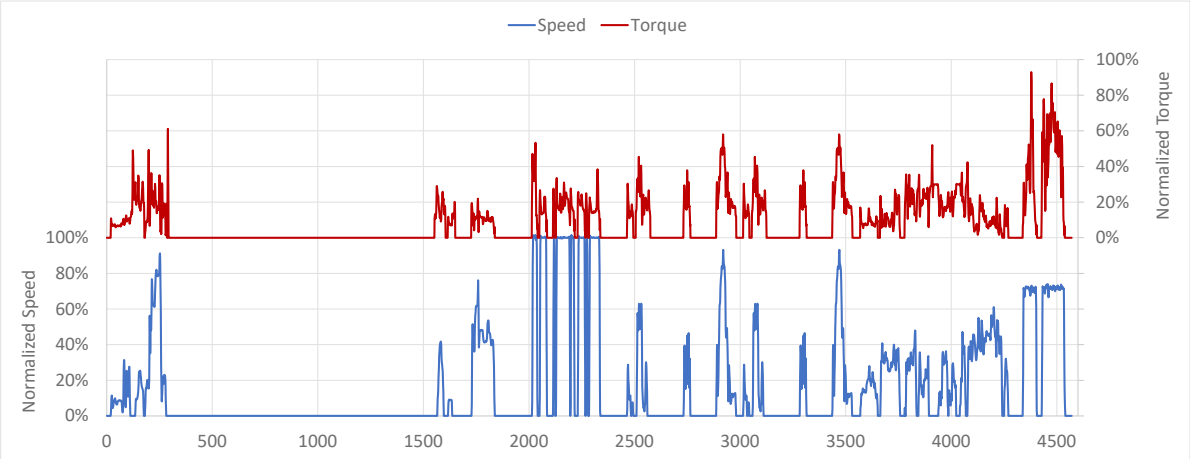



**FIGURE 6. FINAL NORMALIZED OFF-ROAD LOW LOAD CYCLE (LLC)**

## 1.0 INTRODUCTION AND BACKROUND

This report details the results of SwRI's continuing efforts to demonstrate low oxides of nitrogen ($NO_X$) emission control technologies for off-road diesel engines on behalf of the California Air Resources Board (CARB) since 2018. In particular, this report supplements those previously documented efforts. The effort detailed herein comprises what is generally referred to as Stage 3 of the Offroad Low $NO_X$ Demonstration Program and was conducted under CARB Contract 20MSC005. This Stage 3 program builds on previous efforts conducted under the Stage 1 offroad program (CARB Agreement No. 18RD006)[7] and the Stage 2 offroad program (CARB Contract 19RD025)[8].

This program also leveraged experience and understanding that were gained during previous technology demonstration efforts conducted in support of the development of the CARB on-highway Low $NO_X$ Omnibus rule, which was approved for adoption by the Board in August 2020. It is understood that the efforts documented in this report will be used to support the development of a 5$^{th}$ tier of off-road diesel engine standards in California. The proposed elements of the Tier 5 regulation were most recently released during a two-day workshop on October 30-31, 2023[9].

The target for this program was to demonstrate emission technologies which would be scalable for offroad diesel engine having rated power between 56 kW and 560 achieve tailpipe $NO_X$ emission levels 90% below the current Tier 4 standards, and PM emission levels 75% below the current Tier 4 standards. This would translate to a tailpipe $NO_X$ target of 0.040 g/kw-hr and a tailpipe PM target of 0.005 g/kw-hr. At the same time, for at least one technology package, a parallel target was set to achieve a $CO_2$ reduction of between 5% and 8.6% from the Tier 4 baseline engine. These targets needed to be demonstrated at the end of the regulatory full useful life (FUL) for offroad engines, which is currently set at 8,000 hours of operation for Tier 4 engines with rated power above 37kw. Under the originally contracted scope of 20MSC005, the demonstration also

included an extended life demonstration target of 12,000 hours. However, CARB later determined that an increased hourly period for useful life was not warranted for off-road diesel engines, and elected to remove the 12,000 hour target to focus instead on a more robust demonstration at 8,000 hours, including testing both with and without dynamic skip fire (DSF) and the examination of the system on a low power child rating.

The program focused on offroad certification duty cycles, which for the target engine are the Nonroad Transient Cycle (NRTC) and the 8-Mode C1 Ramped Modal Cycle (RMC) for variable speed engines. In addition, the low load operating space was initially covered through the use of the offroad Low Load Application Cycle (LLAC) that was developed in the previous program under contract 18RD006. The LLAC did not have a specific emission target, but instead the intent was to reach as low a tailpipe $NO_X$ level as feasible while at least maintaining $CO_2$ emissions.

It should be noted that the PM targets for the program were met in a relatively straightforward fashion through the incorporation of the latest generation DPF technology that is already in production for both offroad and on-highway engines. Therefore, the majority of the program effort was expended on examining $NO_X$ control options and balancing those options with the desire to not increase $CO_2$ emissions. However, maintaining reasonable engine-out soot levels and good passive regeneration capability over most of the operating cycles were still important priorities for the program. The final engine calibration that was used for the demonstration testing was specifically designed to balance engine-out $NO_X$ and engine out PM emissions, such that good passive soot oxidation performance was maintained over most cycles, and to insure that soot oxidation and loading were balance over the NRTC cycle as well as higher loaded duty cycles.

With the addition of scope under this contract 20MSC005, the original program targets from the Stage 2 program were split into two emission control "packages" as follows:

- Package 1, designated as the "Low Cost" package, would be targeted to demonstrate the original program goals of meeting tailpipe emission targets of 0.040 g/kw-hr $NO_X$ and 0.005 g/kw-hr PM, while targeting $CO_2$ levels that did not exceed the baseline Tier 4 engine.

- Package 2, designated as the "Low GHG" package, would be targeted to demonstrate tailpipe emission targets of 0.040 g/kw-hr $NO_X$ and 0.005 g/kw-hr PM, while at the same time targeting a reduction in $CO_2$ of 5% to 8.6% from the baseline Tier 4 engine.

The initial evaluation of technology options and the demonstration of the Package 1 system were generally the focus of the Stage 2 program, and these results have been previously reported in the Stage 2 Final Report for CARB Contract 19RD025 [9]. The Stage 3 program was primarily focused on the final development and technology selections for the Package 2 system, demonstrating both $NO_X$ and $CO_2$ reductions. That demonstration included representative FUL aging of the final aftertreatment system using the Diesel Aftertreatment Accelerated Aging Cycle (DAAAC) methodology, and final demonstration testing using those DAAAC-aged parts. In addition, there was a portion of scope under the Stage 3 effort to examine the potential for idle

stop-start technology for $NO_X$ and $CO_2$ emission reduction, which will also be discussed in this report.

The Stage 3 program contract was later amended as 20MSC005-1, expanding the scope to include the development of an offroad Low Load Cycle (LLC), working in partnership with CARB staff. The newly developed LLC was also added to the demonstration targets for the program, with the intent being to demonstrate the lowest feasible tailpipe $NO_X$ levels at FUL, while at least maintaining $CO_2$ emissions. The development of the LLC will be described within this report.

# 2.0 METHODS AND MATERIALS

## 2.1 Test Engine

The test engine for this program was a 2019 MY John Deere 6068 diesel engine which met Tier 4 final emissions standards. The engine installed in the transient emission test cell at SwRI is shown in Figure 7. The engine selected for this program was calibrated at a nominal 187 kw maximum power rating at 2200 rpm. It was supplied to the program by Deere, along with the stock aftertreatment (AT) system. Both the engine and the AT system had previously been de-greened as part of the prior baseline work under contract 18RD006. The engine was later reinstalled for Low $NO_X$ development and demonstration efforts under contract 19RD025. A summary of some basic engine parameters for this test engine is given in Table 1 below.



**FIGURE 7. TIER 4 JOHN DEERE 6068 ENGINE**

**TABLE 1. JOHN DEERE 6068 ENGINE PARAMETERS**

| Parameter | Value |
|---|---|
| **Configuration** | Inline 6 cylinder |
| **Bore x Stroke** | 106 x 127 mm |
| **Displacement** | 6.8 L |
| **Compression Ratio** | 16.7 : 1 |
| **Rated Power** | 187 kW (251 hp) |
| **Rated Speed** | 2200 rpm |
| **Peak Torque** | 1026 Nm |
| **Peak Torque Speed** | 1600 rpm |
| **Test Fuel** | 2-D Cert. Diesel |

Later in the program, an additional lower power "child" rating of the engine was also used. A child rating is a lower torque curve calibration on the same hardware within an engine family. Child ratings are of interest here because they share the same absolute thermal mass and heat loss characteristics of the common hardware, but the lower power rating can result in less fuel supplied enthalpy through the system. For this engine, that lower power rating operated on the same engine and aftertreatment hardware had a rated power of 126 kw and a peak torque of 780 Nm.

The engine was an inline 6-cylinder diesel engine that was turbocharged and intercooled, with a dual stage series turbocharger arrangement featuring a variable geometry turbine (VGT) as the high pressure turbocharger. The engine utilized cooled exhaust gas recirculation (EGR) as a primary means of engine-out $NO_X$ control. The engine also featured an intake throttle to help regulate engine air flow and drive EGR under some engine conditions. The fuel injection system was capable of supporting multiple pilot and post injection events and was capable of both near and far post injections. For the stock engine, diesel particulate filter (DPF) regeneration was generally performed using post-injection, rather than in-exhaust injection.

Deere also supplied a significant amount of hardware and engineering support for this program, including calibration access to the engine electronic control module (ECM) using proprietary engineering tools. Deere also supplied a cylinder head machined and prepared to allow the measurement of cylinder pressure in all 6 cylinders. Significant additional electronic and engineering support for controls development was also provided by Deere, as detailed later in the section covering Controls.

The stock Deere AT system was a conventional DOC+DPF+SCR architecture, with the canning arrangement being two can "switchback" style assembly. The DOC and DPF are in the first can followed by a dosing and mixing tube, and finally a second can, containing the SCR catalysts. The stock AT system is shown in Figure 8 and Figure 9, depicted from the inlet and outlet sides, respectively. The outlet view also shows the transfer pipe from the engine, which was sized to match a representative (but somewhat long) machine installation and verified to be within the temperature drop specifications given by Deere. The system used a Bosch Denoxtronic 2.2

Diesel Exhaust Fluid (DEF) injection system, which utilized an engine-water cooled injection nozzle. An ammonia slip catalyst was coated on the rear of the SCR catalyst.



**FIGURE 8. BASELINE (STOCK) AFTERTREATMENT (INLET SIDE) FOR 2018 DEERE 6068 ENGINE**



**FIGURE 9. BASELINE (STOCK) AFTERTREATMENT SYSTEM FOR DEERE 6068 ENGINE – OUTLET SIDE AND DOSING-MIXING PIPE**

## 2.2 Emission Test Cell

This program was performed by the Powertrain Division at SwRI in the primary emissions laboratory in Building 87, with the engine installed in Transient Emission Cell 19. This test cell was a transient capable test cell meeting the requirements of 40 CFR Part 1065 and 40 CFR Part 1039 for emission certification testing on offroad engines. It features a full-flow constant volume sampling dilution tunnel and incorporates both Raw and Dilute emission measurements.

Primary tailpipe emission measurements were performed via Dilute Continuous sampling using the constant volume sampling dilution tunnel. A Horiba MEXA 7200D dilute emission bench was used for measurements of THC, $CH_4$, NMHC, CO, $CO_2$, and $NO_X$. Tailpipe particulate matter (PM) measurements were made via SwRI's proprietary secondary dilution system. In addition to the Dilute measurements, an FTIR was also used in the Raw exhaust at the tailpipe to monitor NO, $NO_2$, $NH_3$, $N_2O$, and $SO_2$, as well as $CO_2$ and other gases for quality assurance purposes. The FTIR was attached to a manifold that allowed measurements at multiple points along the AT system to aid in AT development and calibration, as well as to understand various aspects of AT behavior.

Engine-out emissions were also monitored using Raw measurement techniques. A Horiba MEXA 7100DEGR raw emission bench was used for engine-out measurements of THC, CO, $CO_2$, $NO_X$, NO, and $O_2$, as well as intake manifold $CO_2$ measurement to allow for independent calculation of the EGR rate. Raw exhaust flow measurement was performed via intake air flow measurement using a laminar flow element (LFE) and the chemical balance calculations in 40 CFR

Part 1065.650 and 1065.655. During initial baseline tests, engine-out PM was also measured via a Sierra BG3 partial flow dilution system. The partial flow dilution system was used only to establish baseline engine-out PM rates, and again later to verify engine-out PM rates on the Low $NO_X$ engine during development.

To support combustion and hardware development, an SwRI proprietary high-speed data acquisition system was used to monitor cylinder pressure and fuel injector current on all 6 cylinders. This system was also used to monitor valve proximity sensors to verify CDA actuation when that technology was being examined. This was crucial for the development and monitoring of systems such as cylinder deactivation, as well as for monitoring combustion stability and performance during calibration development. This system was also used to monitor the timing and triggering of the CDA valve actuators during the initial implementation and development stages for that system.

Most of the additional sensors and actuators used for the program were Controller Area Network (CAN)-based, and multiple CAN buses were monitored and recording along with the test cell data. In addition, proprietary control channels were monitored via both ASAP3 for the engine, and CAN for the SwRI integration controller systems. This allowed all data to be recorded and synched onto the SwRI test cell host computer for later ease of use and analysis.

All testing, emission calculations, and test cell quality assurance procedures were conducted in accordance with procedures given on 40 CFR Part 1065, Part 86, and Part 1039. It should also be noted that, in general, SwRI worked to keep carbon balance for Dilute and Raw emission measurements within the recommended 2% level, although this was not always maintained on some of the tests using some of the prototype Low $NO_X$ AT systems. Even when maintained within the recommended 2% range, this still allowed for variation over time and among systems. In order to enable meaningful comparison of $CO_2$ emission results over the long performance periods and multiple systems of this program, tailpipe $CO_2$ emission results were corrected to place them on the same carbon balance basis as the baseline emission results. The approach to this is detailed later under the Results section of the report.

It was observed under this program that the day-to-day variability for the various test cycles, as characterized by the standard deviation of the brake-specific results was in the range of ±2 mg/kw-hr for the NRTC and RMC cycles, ±3 mg/kw-hr for the LLAC, and ±5 mg/kw-hr for the LLC.

## 2.3 Test Cycles, Test Procedures, and Preconditioning Procedures

The targets for this program were demonstrated over the relevant off-road regulatory cycles, including the NRTC, RMC-C1, and the Low Load Application Cycle (LLAC) that was developed during the previous Stage 1 effort under CARB Contract 18RD006. In addition, an off-road Low Load Cycle (LLC) was developed as part of this program, as described later. The LLC was not initially available prior to the start of this effort, and the cycle only became available in its final form in time for the 8000-hour testing.

The NRTC and RMC-C1 cycles are well documented in 40 CFR Part 1039 and are currently used for certification of Tier 4 engines. The LLAC cycle, on the other hand, was developed specifically to represent lower load operations, as described above. The LLAC is depicted in Figure 10 below. A comparison of the average power of all of these cycles, in comparison to each other and the OH cycles is given in Table 2.

When the final off-road LLC became available, it was added to the test sequence. The normalized off-road LLC is shown in Figure 11. More details on this cycle and its development are given in Section 4 of this report. To maintain a consistent preconditioning, the following sequence was run for each LLC cycle. In the event that the LLC was run before the LLAC, it replaced the LLAC in the sequence given above. If the LLC was run at a different point in the sequence, or if there was a need to repeat a cycle, the following sequence was used. It should be noted that this sequence was used for the LLAC in the event of a repeat (except replacing the LLC with LLAC in the third step).

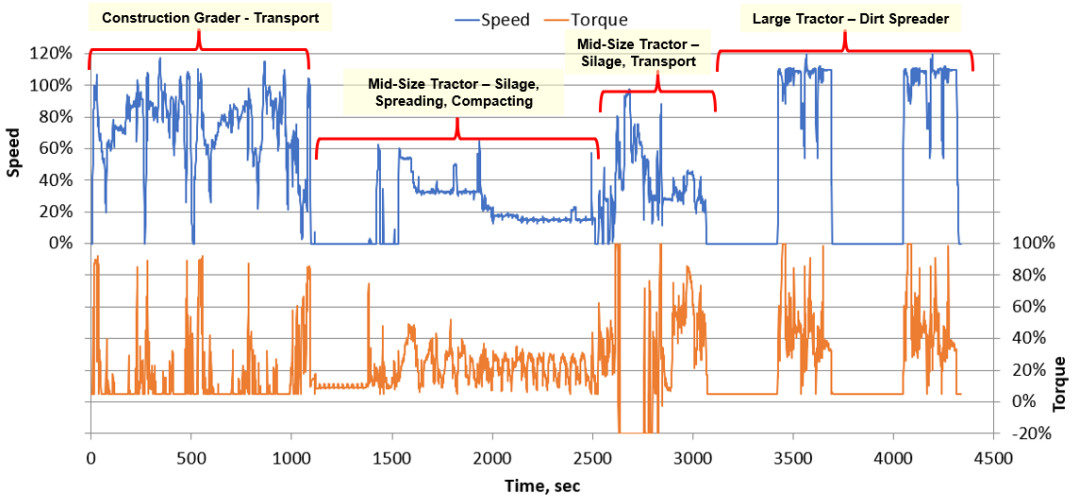



**FIGURE 10. NORMALIZED OFF-ROAD LOW LOAD APPLICATION CYCLE (LLAC)**

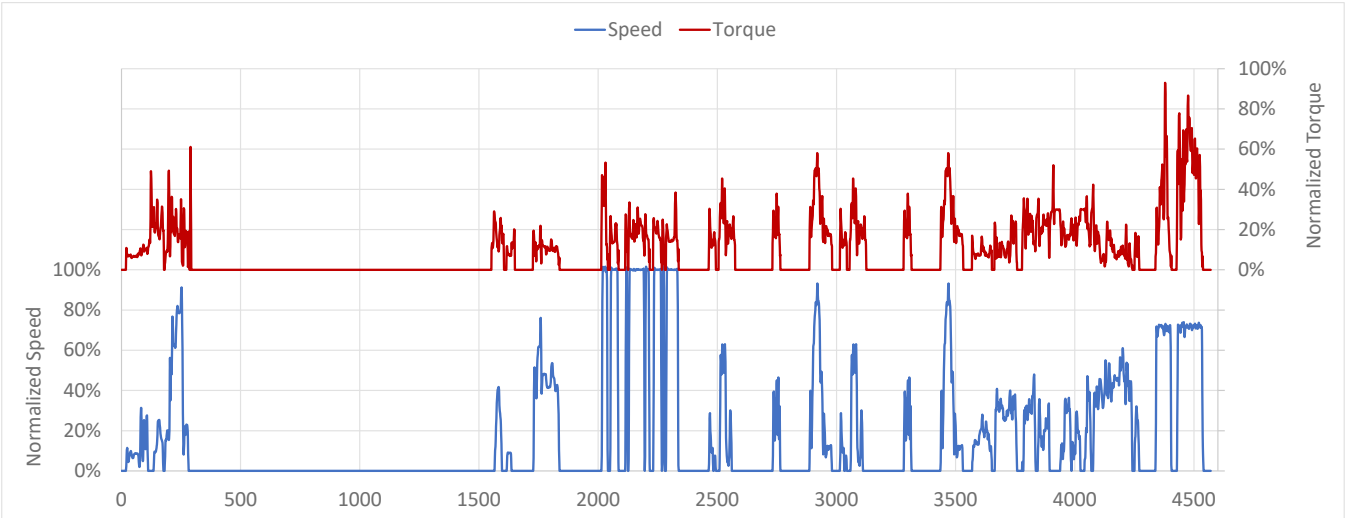



**FIGURE 11. NORMALIZED OFF-ROAD LOW LOAD CYCLE (LLC)**

**TABLE 2. CYCLE AVERAGE POWER FOR COMPLIANCE CYCLES**

| Operation | On-Highway | | Off-road | |
|---|---|---|---|---|
| | Cycle | %Max Power | Cycle | %Max Power |
| Transient | FTP | 22 % | NRTC | 37 % |
| Steady-State | RMC-SET | 48 % | RMC C1 | 55 % |
| Low Load | LLC | 6 – 7 % | LLAC | 15 % |
| | | | LLC | 10% |

All testing and preconditioning was conducted in accordance with the procedures given in 40 CFR Part 1039 and 40 CFR Part 1065.

Preconditioning for the NRTC cycle involved two NRTC transient hot-start tests, with a 20-minute soak between the two tests, as outlined in 40 CFR Part 1065. The engine was then placed in overnight cold-soak. Operations prior to the preconditioning NRTC tests were not specified, but if a DPF regeneration was needed it was run prior to the start of the preconditioning NRTCs. It was found that operations prior to the preconditioning NRTCs did not have any impact on the result of the NRTC tests. The emission control system was designed and tuned to reach emissions stability with the NRTC duty cycle after two NRTC preconditioning tests.

Preconditioning for the RMC-C1 was conducted as outlined in 40 CFR Part 1065, wherein an RMC-C1 cycle is run immediately prior to the start of the RMC test for record. The preconditioning and test cycles were run head-to-tail, with no dwell between the end of the preconditioning cycle and the start of the test for record.

Preconditioning for either the LLC or the LLAC involves running at least one hot-start NRTC transient cycle. If the test sequence is run as described above, the final NRTC hot-start test of the NRTC test sequence serves as preconditioning for the LLC or LLAC, such that no additional engine operation is needed, and the LLC or LLAC can be run following a 20-minute soak. However, in the event the sequence was interrupted, two preconditioning hot-start NRTC transient cycles would be run, followed by a 20-minute engine-off soak and then the LLAC test itself as noted earlier.

## 2.4 Low $NO_X$ Aftertreatment Hardware

Advanced AT hardware for this program was supplied in kind by members of the Manufacturers of Emission Controls Association (MECA). The MECA suppliers for this program were organized into two supplier teams, each consisting of a catalyst company, substrate supplier and canning company. Each team was supplied a set of data from SwRI to aid in system design and simulation. These data sets were taken from SwRI engine calibration efforts and projections of expected performance from technologies like CDA. The supplier teams used this data to

develop two sets of AT technology offerings, each with several optional elements. This approach provided SwRI with a wide variety of technology to choose from in developing a final AT system approach to reach the $NO_X$ and $CO_2$ goals of the program. It was understood that these systems were developed with the intention of reaching a at least 8,000 hour FUL, but with the potential to reach an extended 12,000 hour FUL.

Initial simulations from the previous program effort under 18RD006 indicated that it might be feasible to reach program targets, at least for Package 1, using a more conventional AT system architecture, as depicted in Figure 12. Later modeling work from the suppliers indicate similar results, and therefore Package 1 system designs reflected this. On the other hand, depending on the final engine-out $NO_X$ level for Package 2 chosen in trying to reach the GHG targets, Package 2 might require a more complicated architecture. Therefore, an option to use LO-SCR technology and dual DEF dosing was also procured. In addition, several hardware options were also procured for the systems, including heated dosing, electric heaters (e-heater), and an electrically heated mixer.

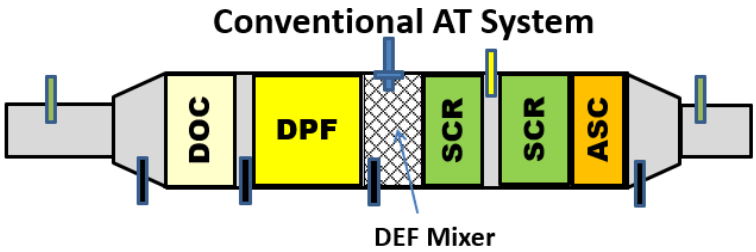



**FIGURE 12. CONVENTIONAL AFTERTREATMENT SYSTEM ARCHITECTURE – DOC+DPF+SCR (PACKAGE 1)**

Individual aftertreatment system options are described in more detail in the report sections below.

### *2.4.1. Aftertreatment Team 1*

Aftertreatment Team 1 supplied a system primarily designed for Package 1 usage, although it could be utilized for Package 2 with the optional added volume if sufficient performance and durability reserve is observed. The Team 1 system was a conventional architecture having a DOC+DPF+SCR arrangement. The system was designed as a single inline module featuring a "compact mixer" design and a production style side-inlet cone. The base system design, originally intended for 8000-hour useful life had two 12x4 inch SCR bricks, the second of which had 2 inches of ASC coating on the back. This system is depicted below in Figure 13.

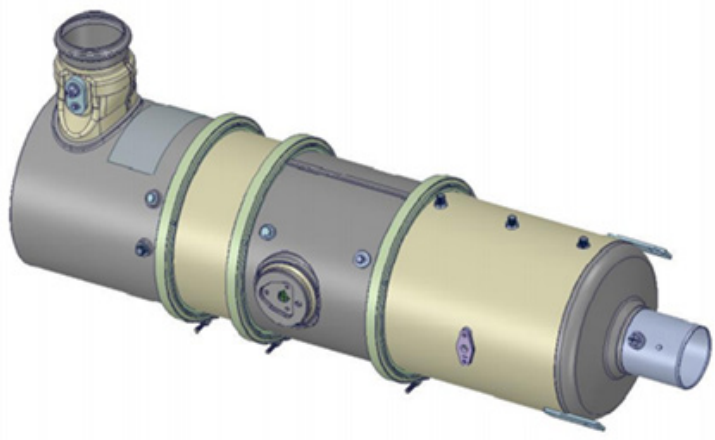


**FIGURE 13. TEAM 1 AFTERTREATMENT PRIMARY CONCEPT FOR PACKAGE 1**

More detail about the catalysts is given below in Table 3. The system was also designed to allow the installation of a third 12x4 SCR brick to insure sufficient durability reserve for 12000 hours of aging. This same arrangement could also be potentially used as a Package 2 candidate, although that is not the original intent. The actual system is shown in Figure 14 in the Package 2 arrangement with the additional 4-in SCR brick installed. Some testing was actually done for Package 2 in the smaller configuration without that extra brick installed in the front, as discussed later under the Results section.

**TABLE 3: TEAM 1 CANDIDATE AFTERTREATMENT SYSTEM CATALYST SPECIFICATIONS**

| Component | D x L, in | CPSI/Wall, mm | Volume |
|---|---|---|---|
| DOC | 12x4 | 400/4 | 7.4 L |
| DPF | 12x4.7 | 300/7 | 8.7 L |
| *SCR*[1] | *12x4* | *600/4.5* | *7.5 L* |
| SCR | 12x4 | 600/4.5 | 7.5 L |
| SCR-ASC | 12x4 | 600/4.5 | 7.5 L |
| [1] If necessary for 12k hours or Package 2 | | | |

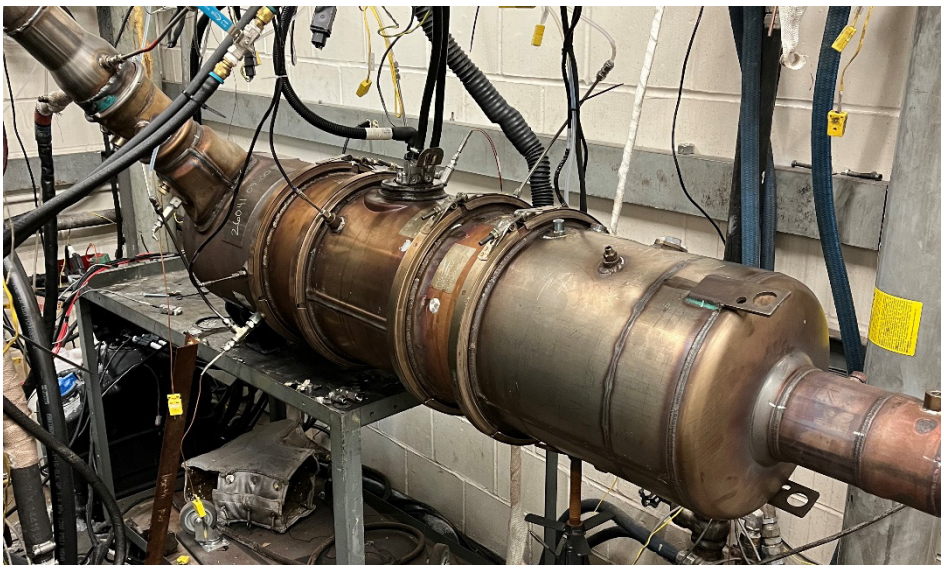


**FIGURE 14. TEAM 1 CANDIDATE AFTERTREATMENT PACKAGE 2 CONFIGURATION**

The system was designed to mount a conventional Bosch Denoxtronic 2.2 DEF injector with a 6-hole configuration.

### *2.4.2. Aftertreatment Team 2*

AT Team 2 also designed their system around a single inline module approach. Team 2 also provided two different options for the portion of the catalysts system before the post-DPF DEF injector. The first option was designed for use on Package 1, and potentially Package 2 if performance was sufficient. This system is depicted below in Figure 15, shown with the third 12x4 brick installed upstream of the other two SCR bricks for the Package 2 configuration. Catalyst details are given in Table 4 for this system, and the system is shown installed in the test cell in Figure 16.

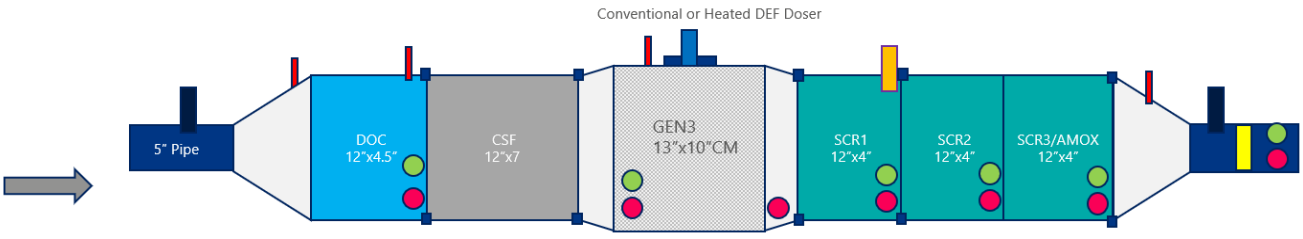



**FIGURE 15. TEAM 2 AFTERTREATMENT CONCEPT FOR PACKAGE 2**



**FIGURE 16. TEAM 2 CONVENTIONAL ARCHITECTURE AFTERTREATMENT SYSTEM**

**TABLE 4. CATALYST SPECIFICATIONS FOR TEAM 2 CONVENTIONAL ARCHITECTURE SYSTEM**

| Component | D x L, in | CPSI/Wall, mm | Volume |
|---|---|---|---|
| DOC | 12x4.5 | 400/4 | 8.3 L |
| DPF | 12x7 | 300/7 | 13 L |
| *SCR*[1] | *12x4* | *600/4.5* | *7.5 L* |
| SCR | 12x4 | 600/4.5 | 7.5 L |
| SCR-ASC | 12x4 | 600/4.5 | 7.5 L |
| [1] If necessary for 12k hours or Package 2 | | | |

Team 2 also supplied a second option for the Package 2 system which included a light-off SCR (LO-SCR) catalyst option. This second architecture was a dual dosing, dual SCR approach, and it is shown schematically in Figure 17. However, due to the significant packaging challenges associated with many machines in the off-road market, it was desirable to take an approach that would minimize the impact of the addition of LO-SCR to the overall package size. Therefore, a technology approach was selected which would allow the use of a LO-SCR in a package profile that was similar to the conventional system, minimizing the additional space claim challenge. In addition, it was also not desirable in this case to have to package in exhaust hydrocarbon (HC) injection downstream of the LO-SCR, as was the case in the Stage 3 on-highway demonstration. Therefore, it was important that the LO-SCR should be compatible with the use of post-injected

HC from the engine to enable exotherms for DPF regeneration to enable this simplification of the aftertreatment system package and its installation constraints.

The technology approach that enabled this was the use of a Multi-Function Catalyst (MFC) in combination with a zone-coated Catalyzed Soot Filer (zCSF). The MFC is a specialized type of LO-SCR that includes oxidation capacity coated in-situ alongside the Cu-zeolite SCR. This oxidation capacity serves to protect the SCR catalyst from exposure to hydrocarbons. In addition, the oxidation capacity gives the MFC the capability to generate an exotherm, though it is not as effective as a DOC for this function. Nevertheless, the MFC can generate exotherms effectively at temperatures above 300°C. It should be noted that the presence of this in-situ oxidation does compromise the $NO_X$ reduction performance of the MFC somewhat in comparison to a typical zeolite SCR catalyst, especially at higher temperatures. However, the LO-SCR function is primarily needed at lower temperatures anyway, and at higher temperatures the strategy is to allow $NO_X$ through the MFC to reach the downstream filter and enable passive soot oxidation. As a result, the MFC is a good fit for this application. It should be noted that the MFC also included a layer of ammonia slip catalysts (ASC) on the back 2 inches of the MFC brick.

Because the MFC has limited HC oxidation capacity at lower temperatures compared to a DOC, it was paired with a zCSF. The front 2 inches of the zCSF are coated with a higher precious metal loading, similar to what would normally be used on a DOC, while the rest of the zCSF has a much lower precious metal loading (more like a conventional coated DPF). The DOC coating layer allowed the zCSF to help to handle the generation of exotherms for filter regeneration at the low exhaust temperatures, in the range of 250°C to 300°C. The use of the combination of the MFC and the zCSF meant that the LO-SCR option would replace the DOC and DPF assembly of the conventional system, with the MFC package being only 3 inches longer. Thus, the LO-SCR option can still fit in the same package envelope as a conventional system. It is still necessary to package an upstream doser and in-pipe mixer, but this is much easier than finding a remove for a full size aftertreatment can and additional mixer assembly.

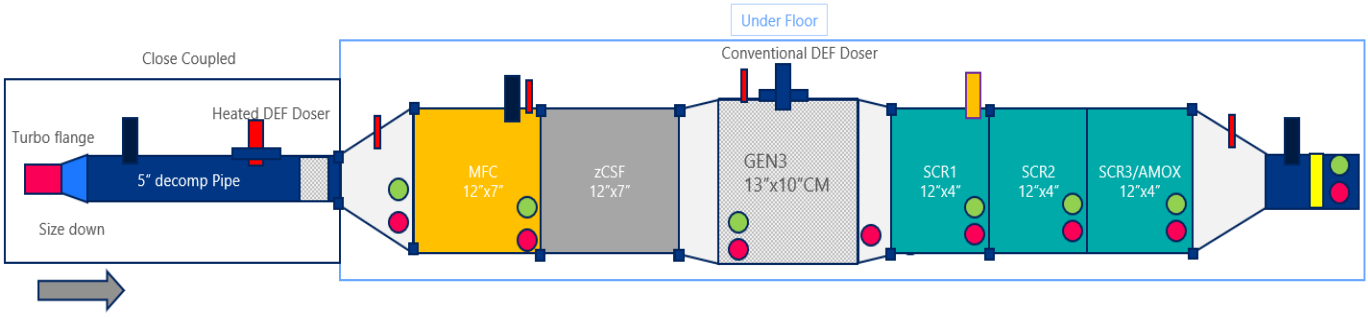



**FIGURE 17. TEAM 2 AFTERTREATMENT CONCEPT FOR PACKAGE 2 WITH DUAL SCR DUAL DOSING ARRANGEMENT**

Catalyst details for this system are given in Table 5, and the system is shown installed in the test cell in Figure 18. In this installation the upstream doser is in the form of a heated doser, but an un-heated doser could also be used at this position.

**TABLE 5. TEAM 2 CATALYST SPECIFICATIONS FOR DUAL-SCR DUAL DOSING ARCHITECTURE SYSTEM**

| Component | D x L, in | CPSI/Wall, mm | Volume | Notes |
|---|---|---|---|---|
| MFC (LO-SCR) | 12x7 | 400/4 | 13 L | 2-in ASC layer at back |
| Zone-coated CSF | 12x7 | 300/7 ACT | 13 L | 2-in DOC layer at front |
| *SCR*[1] | *12x4* | *600/4.5* | *7.5 L* | *Cu-Zeolite* |
| SCR | 12x4 | 600/4.5 | 7.5 L | Cu-Zeolite |
| SCR-ASC | 12x4 | 600/4.5 | 7.5 L | Cu-Ze, 2-ASC layer at back |
| [1] If necessary for 12k hours or Package 2 | | | | |

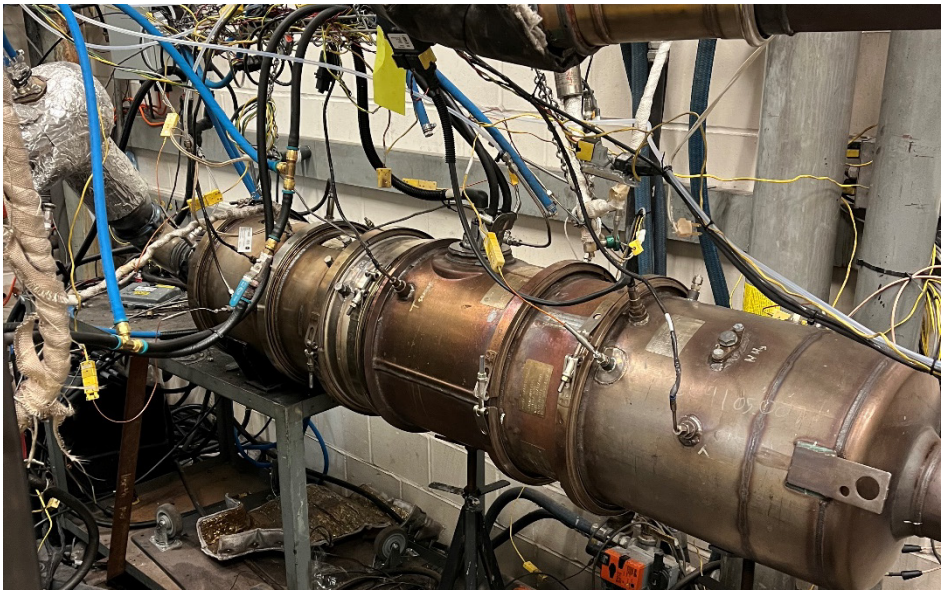


**FIGURE 18. MFC AND ZCSF INSTALLED AT FRONT OF AT SYSTEM ALONG WITH UPSTREAM HEATED DOSER**

### *2.4.3. Final Combined Team Aftertreatment Systems*

Testing of the two sets of aftertreatment hardware from the two different teams was described in the previous Stage 2 program report [9]. Following the completion of those efforts, it was determined that the most optimal aftertreatment package would be one that combined some of the characteristics of both systems. This optimal arrangement was important to maximize the performance of the system given the increased $NO_X$ reduction demand for Package 2. As a result,

a combined system was assembled, and this system would form the basis for all the subsequent evaluations. This combined package is depicted schematically in Figure 19, and catalyst details for this system are given in Table 6.

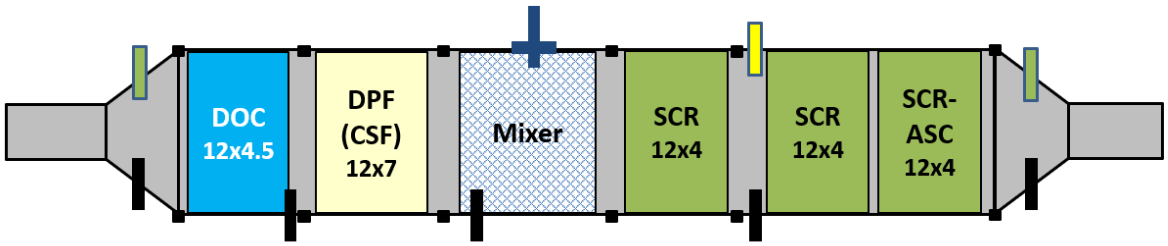



**FIGURE 19. SCHEMATIC OF CONVENTIONAL ARCHITECTURE COMBINED AFTERTREATMENT SYSTEM**

**TABLE 6. COMBINED SYSTEM CATALYST SPECIFICATIONS FOR SINGLE DEF DOSER SYSTEM**

| Component | D x L, in | CPSI/Wall, mm | Volume | Supplier Team | Notes |
|---|---|---|---|---|---|
| DOC | 12x4.5 | 400/4 | 8.3 L | 2 | |
| DPF | 12x7 | 300/7 ACT | 13 L | 2 | |
| SCR[1] | *12x4* | *600/4.5* | *7.5 L* | *1* | *Cu-Zeolite* |
| SCR | 12x4 | 600/4.5 | 7.5 L | 1 | Cu-Zeolite |
| SCR-ASC | 12x4 | 600/4.5 | 7.5 L | 1 | Cu-Ze, 2-ASC layer at |
| [1] This brick was omitted for testing of a reduced package size where | | | | | |

A second combined team system was also assembled for use when the LO-SCR option was utilized. This system combined the downstream SCR catalysts of Team 1 with the MFC+zCSF elements of the Team 2 LO-SCR option system. This combined system is depicted below in Figure 20, and catalyst details for this system are given in Table 7. This system is shown installed in the test cell in Figure 21. Figure 22 shows the mounting of the heated doser and plenum mixer assembly in the transfer tube from the engine, which was kept at the same total length as was used for the conventional architecture systems previously.

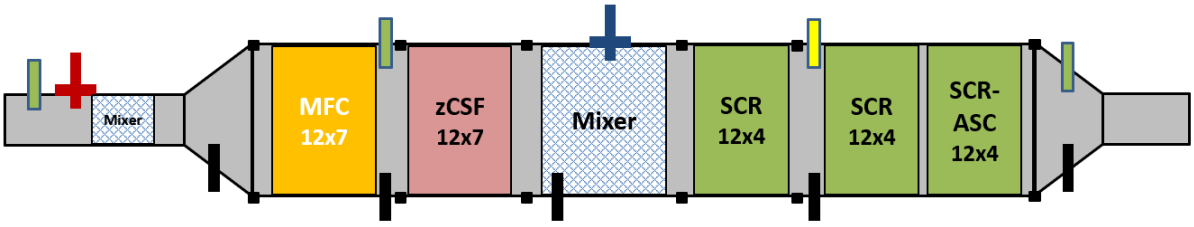



**FIGURE 20. SCHEMATIC OF DUAL SCR DUAL DOSING ARCHITECTURE AFTERTREATMENT SYSTEM**

**TABLE 7. COMBINED SYSTEM CATALYST SPECIFICATIONS FOR DUAL DEF DOSER SYSTEM**

| Component | D x L, in | CPSI/Wall, mm | Volume | Supplier Team | Notes |
|---|---|---|---|---|---|
| MFC (LO-SCR) | 12x7 | 400/4 | 13 L | 2 | 2-in ASC layer at back |
| Zone-coated CSF | 12x7 | 300/7 ACT | 13 L | 2 | 2-in DOC layer at front |
| SCR[1] | *12x4* | *600/4.5* | *7.5 L* | *1* | *Cu-Zeolite* |
| SCR | 12x4 | 600/4.5 | 7.5 L | 1 | Cu-Zeolite |
| SCR-ASC | 12x4 | 600/4.5 | 7.5 L | 1 | Cu-Ze, 2-ASC layer at |
| [1] This brick was omitted for testing of a reduced package size where noted. | | | | | |

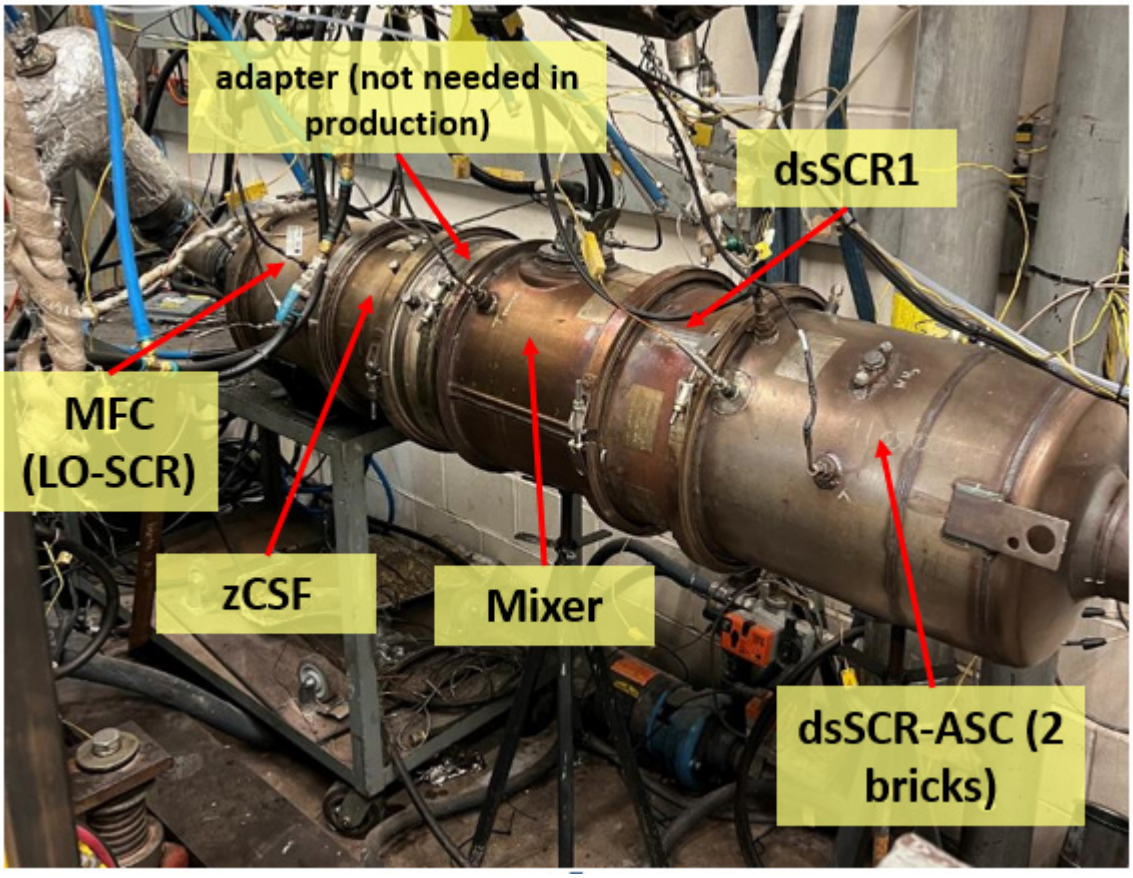



**FIGURE 21. FINAL COMBINED AT SYSTEM WITH DUAL DOSING DUAL SCR ARCHITECTURE**



**FIGURE 22. TRANSFER PIPE FROM ENGINE FOR DUAL DOSING DUAL SCR ARCHITECTURE SHOWING HEATED DOSER AND MIXER MOUNTING**

### *2.4.4. Aftertreatment e-Heater*

As an option to augment the performance of the AT systems for Package 2, an electric heater (or e-Heater) assembly was provided by one of the MECA suppliers. This compact heater assembly that was designed to provide 6.8kw of heat at 48 volts. It was optimally designed for a 48V electrical system but could also be used at a lower power level in a 24V system. However, from an electrical standpoint, it was felt that more than 2.5kw of power was not likely to be practical in a 24V system, due to the need to handle high current levels in excess of 100A. This is a level beyond what many current off-road machines are currently prepared for and would require a significant and costly electrical system upgrade. Therefore, at higher power levels it was felt that a 48V electrical system could be necessary to power an e-Heater.

The e-Heater is shown in Figure 23 as it came from the supplier, and features are very compact design that could be readily incorporated into a production AT system with relatively little impact on the overall package size. For the modular installation that was needed in this

demonstration, however, additional flanges had to be added to allow installation of the heater. Figure 24 shows the e-Heater assembly after the flanges were added.



**FIGURE 23. 6.8KW E-HEATER ASSEMBLY**

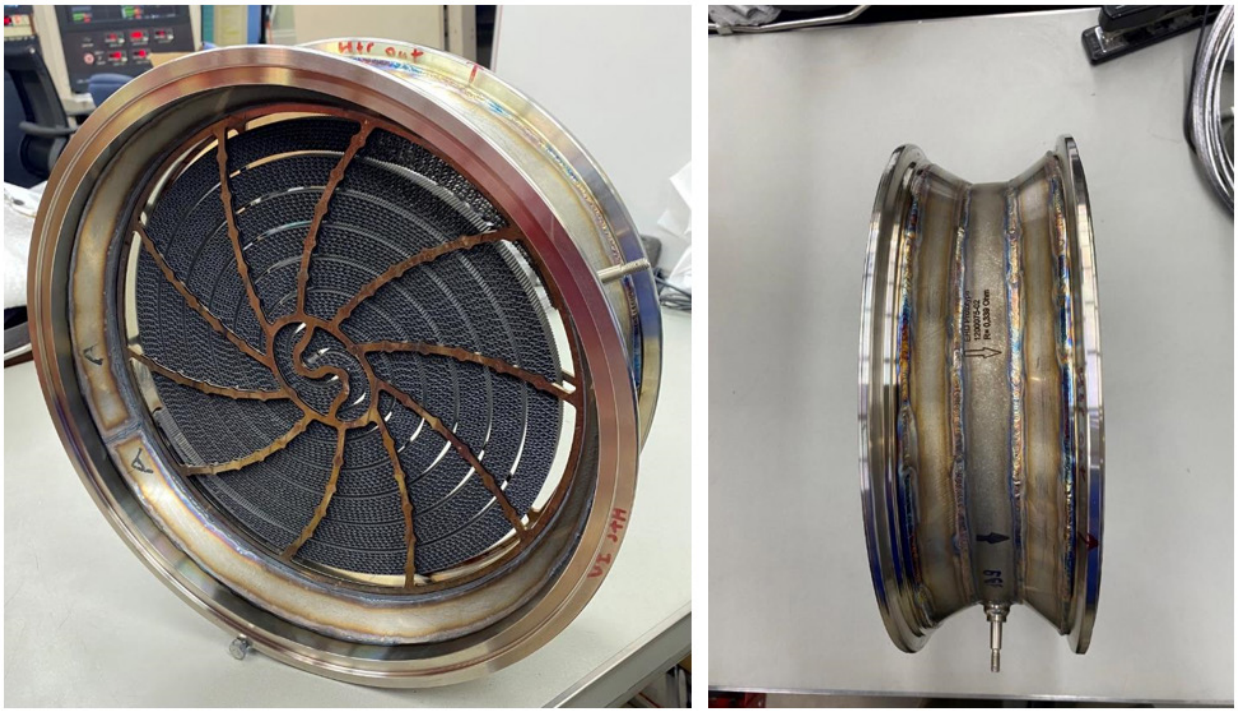


**FIGURE 24. FLANGED E-HEATER ASSEMBLY READY FOR INSTALLATION**

The e-Heater assembly was initially installed in a location downstream of the DPF in the Conventional architecture AT system, just upstream of the DEF mixer. This would allow the heater to also warm the mixer allowing for earlier injection of DEF during cold-start warm-up. A schematic of the system with the e-Heater installed in shown below in Figure 25. It was also

considered to install the e-Heater before the DOC in the system, to also allow the use of the heater to enable DPF regeneration under lower temperature conditions and perhaps allow the earlier use of post-injection upstream of the DOC for warm-up. However, those concepts were not pursued following the initial test results with the system shown in Figure 25. The actual e-Heater installation in the system is shown in Figure 26. Note that an additional flange adapter was needed in the modular development system that would not have been required in the final assembly.

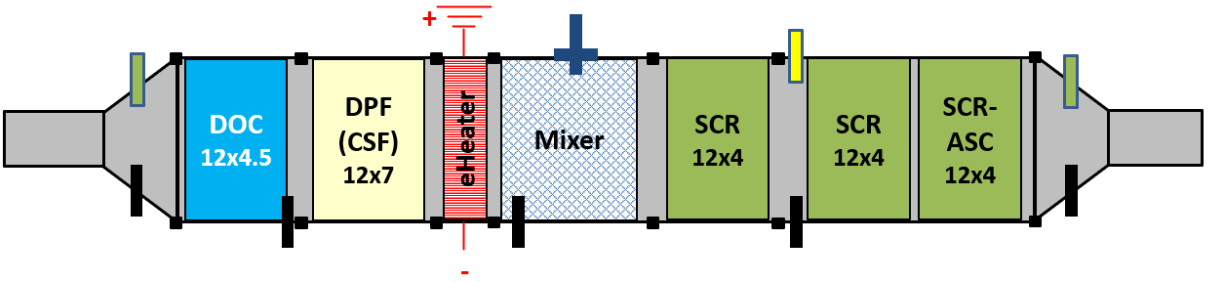



**FIGURE 25. SCHEMATIC OF CONVENTIONAL ARCHITECTURE AT SYSTEM WITH E-HEATER LOCATED AFTER DPF**

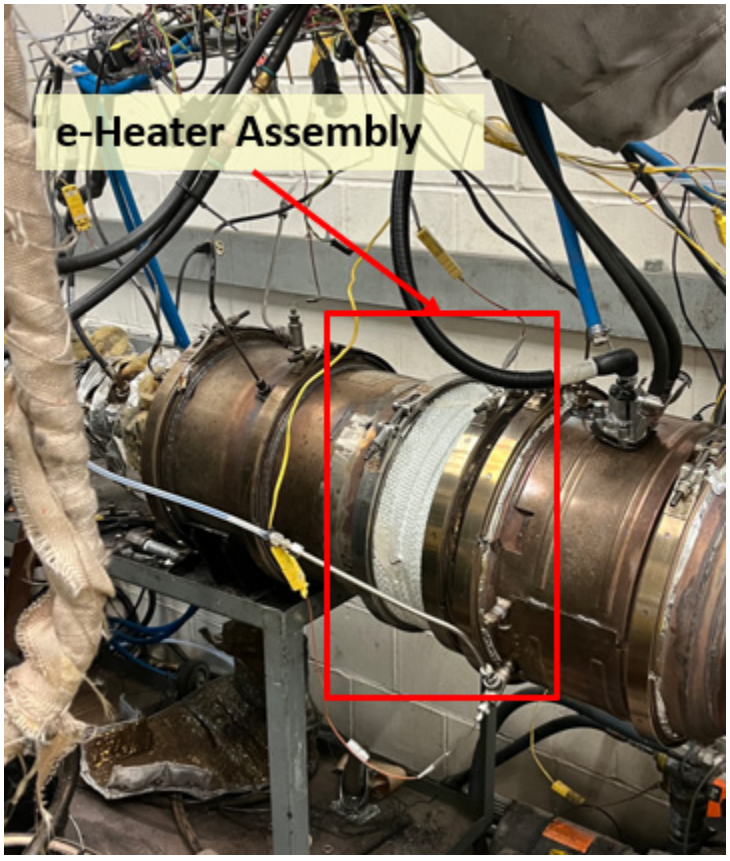



**FIGURE 26. E-HEATER ASSEMBLY INSTALLED IN THE COMBINED CONVENTIONAL AT SYSTEM PACKAGE (AFTER DPF)**

To power the e-Heater, a pair of 5kW variable voltage power supplies were used which had a maximum voltage capability of 60V. For this experiment, the heater power was controlled by adjusting the power supply voltage, which was accomplished via an analog output channel from the aftertreatment control system. It should be noted that in production it would be expected that a power electronics unit would likely be used at a fixed system voltage, and the power would be varied using pulse width modulation.

The heater control strategy for the e-Heater was run from the aftertreatment control system on the dSPACE MAB2 platform. This control strategy was designed to target a particular temperature at the DPF outlet, as measured by the DPF-out temperature sensor. Heater power was controlled via a PID loop, but with a maximum power limit that could be calibrated as part of the strategy. Heater safety features for low flow rates were also incorporated in the strategy.

### *2.4.5. Aftertreatment Electrically Heated Mixer (EHM) Assembly*

A second electrical heat based approach was provided by Emissol in the form of an electrically heated mixer (EHM) assembly. This unit was designed to replace the existing mixer in the system, and in this case, electrical energy was applied directly to the mixer itself. This was done both for bulk exhaust gas heating, and to allow for DEF dosing at temperatures below 180°C without the risk of deposit formation. The heated mixer assembly also incorporated an additional supplement heater strictly for bulk gas heating. The EHM assembly is shown in Figure 27. The EHM was flanged and prepared for installation into the Team 2 aftertreatment system, therefore it was necessary to adapt to the 13-in flange size of that unit. Figure 28 shows the EHM mounted in the aftertreatment system replacing the Team 2 compact mixer. Figure 29 shows a closer shot of the EHM assembly and electrical connections, as well as the insulation wrap that was used on the assembly because it did not come with production insulation like the other mixers.



**FIGURE 27. HEATED MIXER ASSEMBLY (12-IN DIAMETER)**

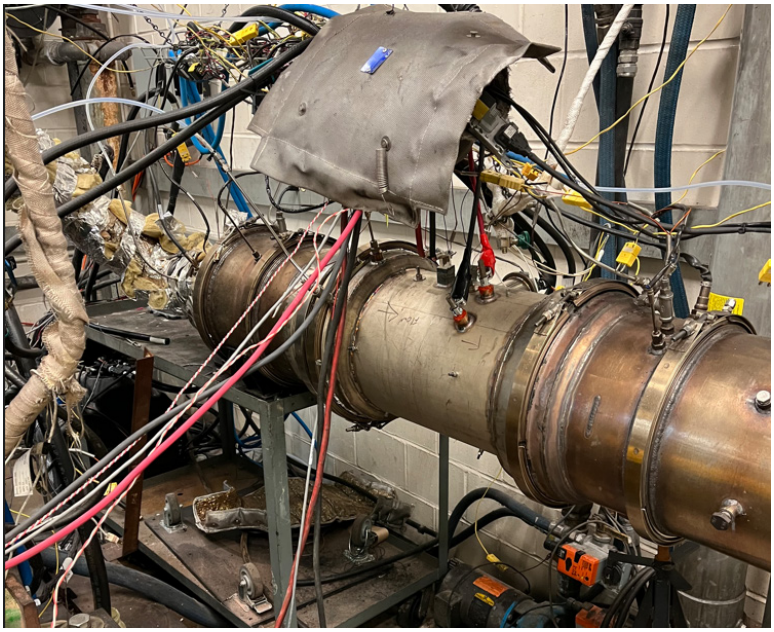


**FIGURE 28. HEATED MIXER ASSEMBLY INSTALLED IN THE LOW NOX AFTERTREATMENT SYSTEM IN PLACE OF THE INLINE MIXER**



**FIGURE 29. HEATED MIXER ASSEMBLY INSTALLED WITH INSULATION WRAP**

The EHM incorporates two different heater elements. The first is designed to enable low temperature dosing operation and assist in evaporation of DEF. The DEF doser is mounted so that the spray is targeted directly at the heated mixer element. The second heater element is

downstream of the first and is designed to supplement the bulk gas exhaust heater. The combined capacity of the two elements is 6.3kw at 48 volts.

The actual heater control for the EHM was accomplished via a separate controller that was supplied by Emissol. The first element was generally controlled in heated dosing mode, wherein the heater current was controlled by an internal model in the EHM control unit to enable successful evaporation and mixing at any inlet temperature. That first element could also be set to a heating mode to assist in bulk gas heating, regardless of DEF flow rate. The second element was only controlled in a heating mode to assist in bulk gas heating to reach a target exhaust gas temperature. Details of the EHM control strategy are proprietary in nature and thus not discussed in this report.

### *2.4.6. Combined e-Heater and Heated Mixer*

After initial testing of both heater options, it became apparent that more heat input was needed for the Package 2 system to reach its targets with sufficient margin for aging. To evaluate this, a combined package was assembled wherein both the e-Heater and the EHM were installed in series. This allowed for greater heat input into the exhaust. The heat input potential of the combined system was still limited by the power supply configuration that could be readily controlled in this case, but the system was still capable of 10kw of heating power at 48V. This was sufficient to evaluate the impact of additional heater power. In addition, 10kw was considered to be the practical limit of what might be feasible on a machine with an engine the size of the John Deere 6068, even at 48V. It should be noted that on a hybrid machine with more voltage available, higher power might be practical, but evaluating that potential does not fall with the scope of this program.

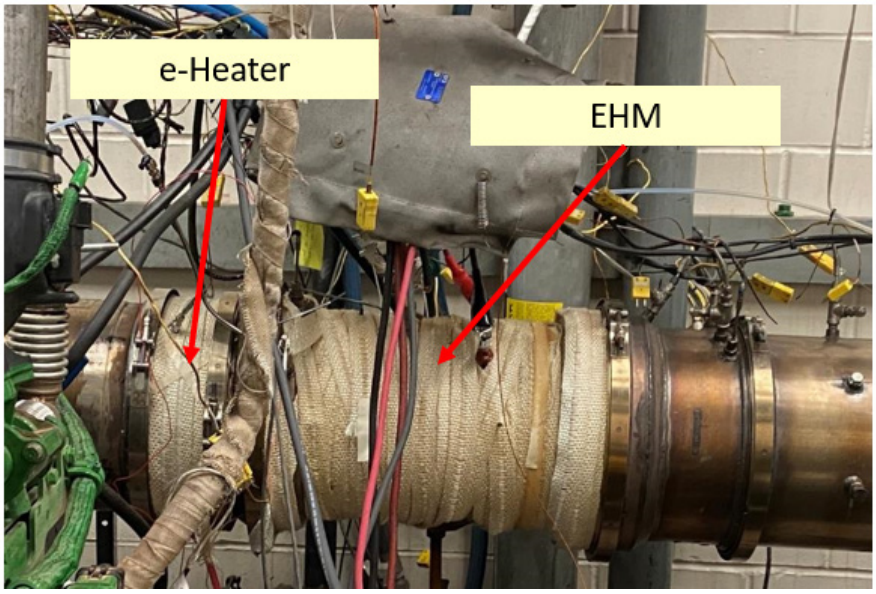



**FIGURE 30. COMBINED E-HEATER AND EHM ASSEMBLY INSTALLED IN SERIES ON TEAM 2 CONVENTIONAL SYSTEM**

In this case the controls of the two systems were essentially linked to provide the maximum potential heat output.

### *2.4.7. Accounting for Heater Power Input*

In the case of all of the previously described heater systems, a significant amount of power is being supplied to these systems. For lab operation, these systems were all powered by a bank external variable voltage power supplies that could supply up to 48V, with each power supply being capable of up to 4.8kw. To make sure that the results are representative and accurate, it is necessary to account for this power flow into the system so that the impact of these systems in temperature and fuel consumption is likewise representative of real machine operation.

The methodology used to account for the heater power in this program was originally developed for the on-highway Low $NO_X$ demonstration programs, and is a very representative approach to this problem. The methodology is applied in several steps, ultimately leading to representative loading of the engine in real-time to account for the heater power draw. The key steps of the methodology are as follows:

- The voltage and current for each device are measured in real-time at the device connections in the aftertreatment system, using a voltage meter and a current shunt.
- System power draw for each device is calculated from the measured voltage and current.
- The power draw from all devices is summed to provide a total power draw.
- The power draw is corrected for an assumed generator efficiency. In the case of the work under this program, a fixed 80% efficiency was used, but a variable speed curve could also be applied. For example, if 1kw was measured, then the load to the engine was calculated at 1.2kw.
- The corrected power drawn from the previous step is used along with engine speed to calculate an equivalent engine torque. This calculation is done at 10hz.
- The derived engine torque demand is subtracted from the shaft measured torque in the test cell. The corrected torque is then used by the test cell for both torque feedback and work calculation (thus accounting for the inflow of power).

At the end of this process, a negative torque offset is being applied in real-time to the measured torque. As a result, when driving a test cycle, the test cell controls will increase the operator demand (e.g. more pedal command) to reach the cycle torque targets. This results in increased fuel flow to meet a given cycle torque target at the output shaft, which is an accurate simulation of what would happen if an that load were being generated by a crankshaft driven alternator or generator. However, because the fuel is actually being burned to generate the added load, the resulting exhaust temperature behavior from that fuel burn is also accurately accounted for. For instance, a 5 kw electrical heater load demand might actually result in a net exhaust heat input of 8kw due to exhaust heat from the engine, although that heat is coming from the turbine outlet through the system, rather than being applied where the heater is. Examples of this methodology

in action are shown in Figure 31 for early cold-start NRTC tests at various power levels. As can be seen, the method is flexible enough to provide an accurate real-time accounting of power from even complex heater controls strategies. As seen in the bottom graph of this figure, the resulting engine torque traces are all comparable and following the cycle targets, regardless of the different strategies and power levels. Note that at some high heater demands, the engine may be expending enough fuel to offset as much as 140Nm of electrical demand just to maintain a zero torque target.

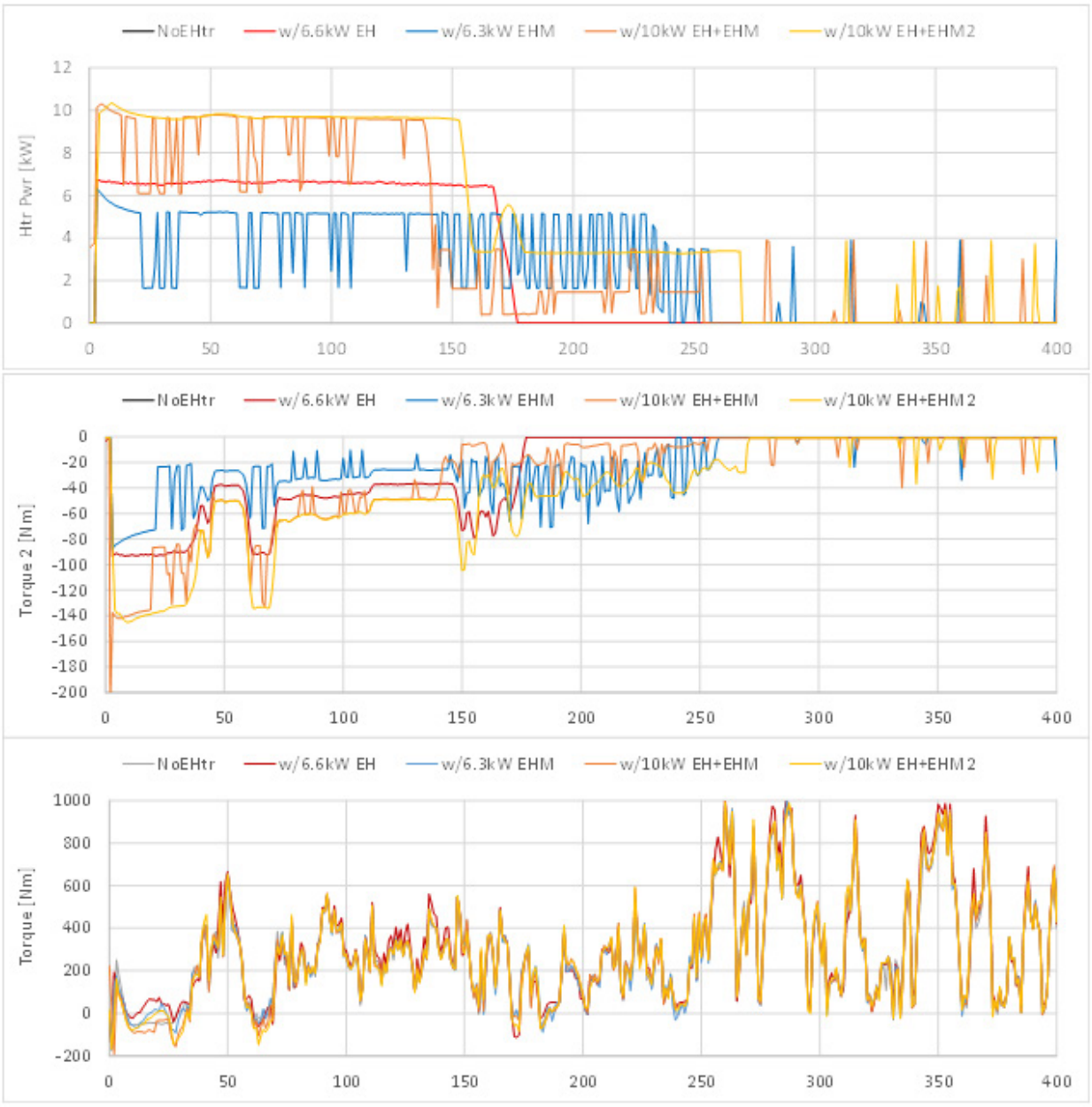



**FIGURE 31. EXAMPLES OF HEATER POWER DEMAND AND TORQUE CORRECTION DURING FIRST 400 SECONDS OF COLD NRTC**

In this manner then, the $CO_2$ impact of these electrical power draws is seen in the emissions data in a representative fashion because the extra fuel to power the devices is actually being burned during the test. All results shown for any tests using an e-Heater or any other significant power draw use this methodology.

## 2.5 Low $NO_X$ Engine Hardware Options

### *2.5.1. EGR Cooler Bypass*

To alleviate concerns of HC condensation within the EGR cooler, which can lead to fouling, the base engine calibration does not use EGR below 1200 RPM engine speed. However, no EGR operation increases engine-out $NO_X$ and exhaust flow rate which can accelerate aftertreatment cooling. To address these issues, an EGR cooler bypass was implemented on the test engine. The stock EGR transfer elbow located before the high-pressure turbine was modified to provide hot exhaust gas, which was controlled with an electronically-controlled wastegate, before being introduced downstream of the stock EGR valve. Photos of the EGR cooler bypass implementation are shown in Figure 32. Test results obtained with the EGR cooler bypass will be discussed in the results section.

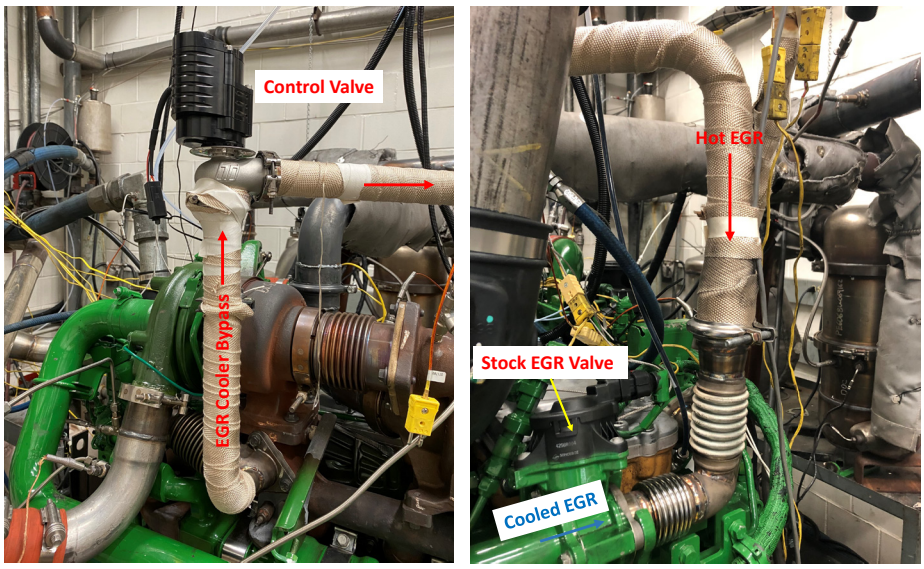



**FIGURE 32. EGR COOLER BYPASS IMPLEMENTATION**

### *2.5.2. Cylinder Deactivation (CDA)*

Another major hardware lever evaluated for inclusion in Package 2 was cylinder deactivation (CDA). This was a primary technology leveraged in the on-highway Low $NO_X$ effort and was also evaluated here for application to the offroad market. It should be noted that due to the significant differences between on-highway and offroad, it was necessary to re-evaluate

whether CDA would continue to provide enough value to justify the cost and effort to deploy the technology.

CDA is a viable technology lever for the off-road market, and the systems developed for the on-highway application can be applied to off-road engines. CDA technology options have been developed for all of the valvetrain architectures commonly seen in off-road engines. CDA is likely to be primarily applicable to engines 56kw and above, where the combination of low $NO_X$ standards and required $CO_2$ reductions could potentially create enough value to justify the engineering effort and cost, especially considering the wide range of engine power ratings often observed in off-road engine families. However, it should be noted that while viable, the application of CDA to off-road engine families is made more challenging by the wide array of machine applications seen in the off-road market. This application variety will require more engineering effort to account for the individual vibration and mounting characteristics of each application.

The CDA system hardware used in this program was supplied by Jacobs Vehicle Systems (JVS). The system is shown below in Figure 33, installed on the Deere 6068 engine. As can be seen in the figure, there is an individual control solenoid for each cylinder, allowing independent deactivation of any or all cylinders. This allowed maximum flexibility for any CDA strategy, as well as enabling the use of Dynamic Skip Fire, as discussed below. The system was controlled via the dSPACE MAB2 integration controller that was deployed by SwRI, using software that was developed working with JVS for control, and a solenoid driver system developed by SwRI for this application.

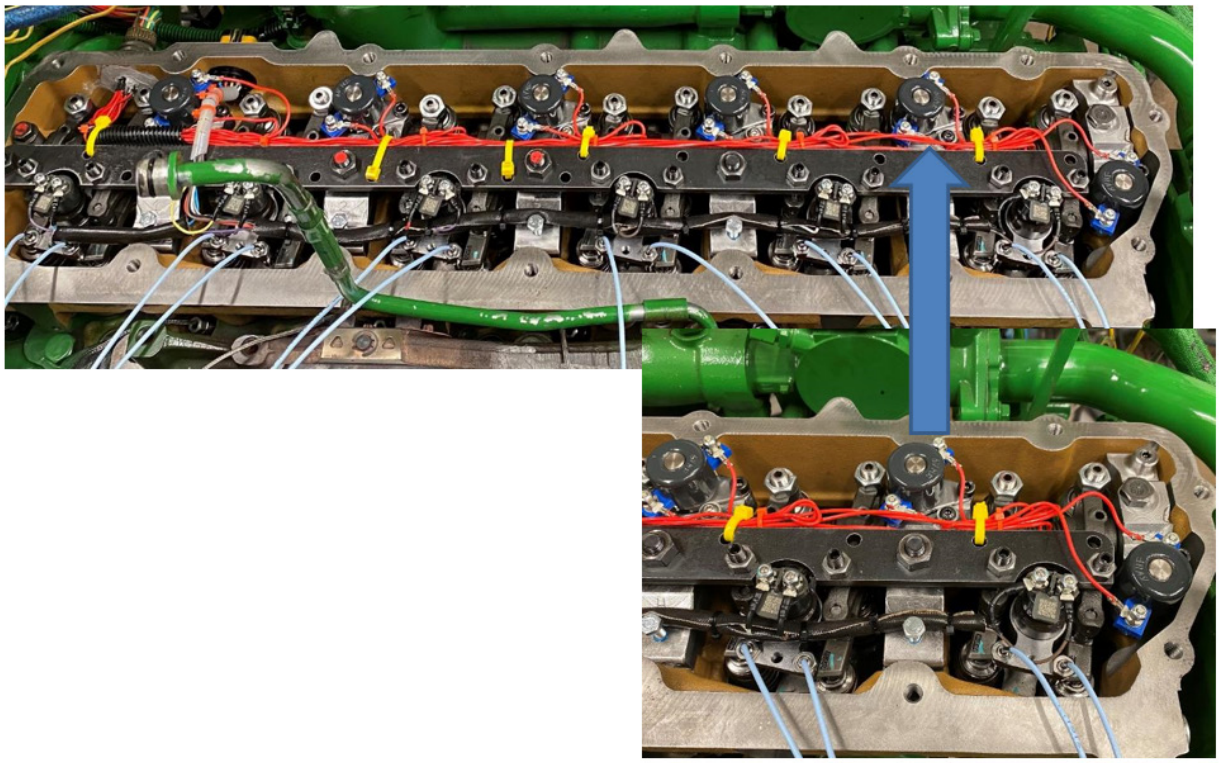


**FIGURE 33. CYLINDER DEACTIVATION SYSTEM (JACOBS VEHICLE SYSTEMS)**

### *2.5.3. Diesel Dynamic Skip Fire (dDSF™)*

A further innovation in the control of CDA hardware technology is the use of a more flexible control architecture developed by Tula Technology which is known as Diesel Dynamic Skip Fire (dDSF). Rather than utilizing a strategy which moves between fixed modes of CDA operation, dDSF uses a more sophisticated algorithm to continuously vary the number of cylinders being operated at lighter load. An illustration of how this concept works is given below in Figure 34. The use of dDSF can enable a wider range of more frequent cylinder deactivation under transient cycles, thus enabling a larger benefit than map-based CDA. In addition, dDSF can be used to avoid NVH resonances in more dynamic fashion, thus enabling CDA to be used more readily in areas that might otherwise be limited in flexibility due to vibration limits. When DSF is referred to in this report it is referring to the combined use of CDA with the dDSF control algorithm.

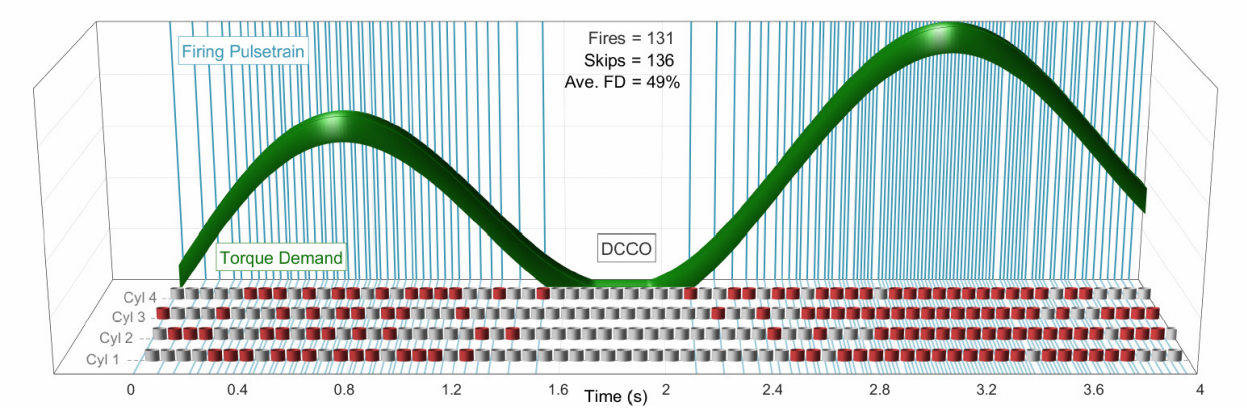



**FIGURE 34. ILLUSTRATION OF DYNAMIC SKIP FIRE (FROM TULA PRESENTATION AT 9TH INTERNATIONAL ENGINE CONGRESS, BADEN-BADEN, GERMANY)**

## 2.6 Low $NO_X$ Controls

A significant portion of the effort in the Low $NO_X$ demonstration program involved the development of the hardware and software controls needed to make the combined engine-AT system function, and to provide the flexibility needed to minimize tailpipe $NO_X$ and maximize engine efficiency. Although the controls were implemented in an open development platform, the controls used on the offroad Low $NO_X$ engine were designed using a production-oriented approach based on SwRI's experience working with production engine controls. As with a production controller, a single unified strategy and calibration were developed that could run on any duty cycle without cycle specific tuning. The single calibration architecture was developed to balance the needs of all the various duty cycle requirements, as would be done in a normal production environment. It should be noted that this generalized control architecture is designed to deal not only with laboratory certification cycles, but also with field cycles wherein prior knowledge of the duty cycle is not available.

The basic control architecture for the Stage 3 demonstration is shown in Figure 35. The core strategy and much of the custom controls were operating from the SwRI Controller, which resided in a dSPACE MicroAutoBox II (MAB2) platform. The controller hardware itself is shown in Figure 36. The SwRI Controller had overall supervisory control of the system, and several key controls were located there. These included the Engine State Machine, the main CDA controller, and the AT Controller.

The SwRI Controller was linked to the engine via a proprietary link allowing the SwRI controller to override various engine functions and operating modes as needed to implement the Low $NO_X$ strategy. John Deere also provided proprietary tools to enable ECM calibration access, as well as provided calibration engineering support to the program for areas that would have been too complicated for SwRI to adjust directly.

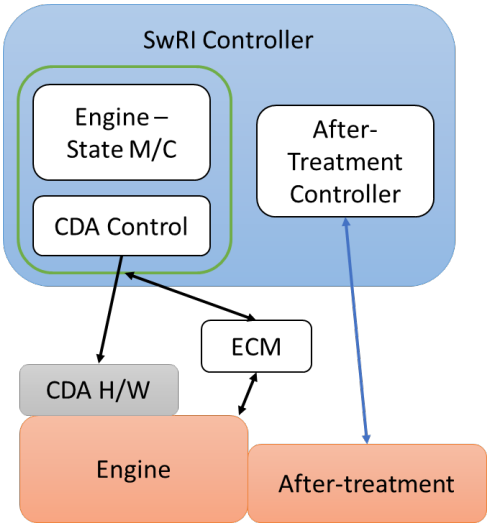
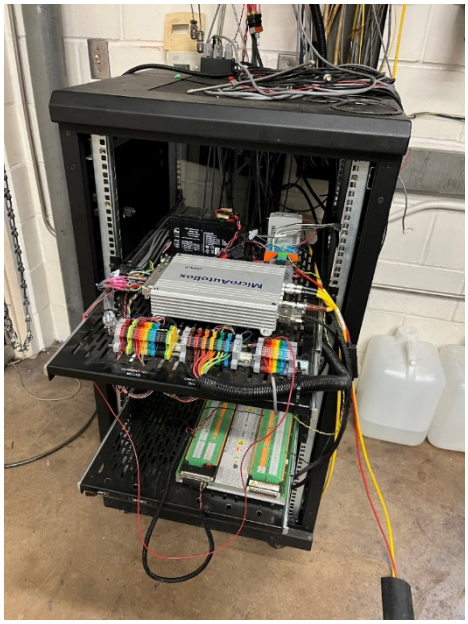



**FIGURE 35. HIGH-LEVEL CONTROL STRUCTURE FOR STAGE 3 LOW $NO_X$ DEMONSTRATION**

**FIGURE 36. LOW $NO_X$ INTEGRATION CONTROLLER HARDWARE PLATFORM**



*2.6.1. Overall Strategy and Engine State Machine*

The Engine State Machine contained the primary Strategy controls for the engine-AT system. The Strategy control was implemented a series of Engine Modes that allowed the implementation of different calibration targets, depending on the state of the system. This strategy was driven by a combination of Engine Coolant Temperature (ECT) and AT system temperatures. In particular, the LO-SCR temperature and the temperature of the first brick of the downstream SCR system (SCR1 in the diagrams) were used to drive state switching. The Strategy is shown in Figure 37 and involved three primary Engine States that were defined as follows:

- **Fuel Economy (FE)** – this mode was the desired endpoint of the strategy and can be considered the "Default" operating mode when the engine and AT system are at optimal temperatures for maximum $NO_X$ efficiency. It has the highest engine-out $NO_X$ emissions and the lowest $CO_2$ emissions. In some cases, this mode actually was calibrated to higher engine-out $NO_X$ levels than the baseline engine.
- **Aggressive Thermal Management (TM-1)** – this mode was used when both catalyst beds were below optimal temperature, and represents the most aggressive thermal management mode used outside of cold-start. TM-1 had the lowest engine-out $NO_X$ level and the highest $CO_2$ emissions. Features of this mode included higher EGR rates, significant use of multiple injections, combustion phasing, intake throttling, and modifications to the CDA mode table that prioritized system temperature at certain speeds. Due to the impact on $CO_2$ this mode was used only to the degree necessary.
- **Low Thermal Management (TM-2)** – this mode was a transitional mode that was added to provide an intermediate point between FE and TM-1. This was used in cases where the AT system temperatures were at temperatures slightly below optimal, but still able to reach high conversion on at least one of the catalyst beds. TM-2 provided a less drastic mode of intervention allowing moderate thermal management and some $NO_X$ reduction, but with significantly less $CO_2$ penalty than the TM-1 mode. The flexibility added by TM-2 was essential for optimizing $CO_2$ emissions in part load duty cycles.

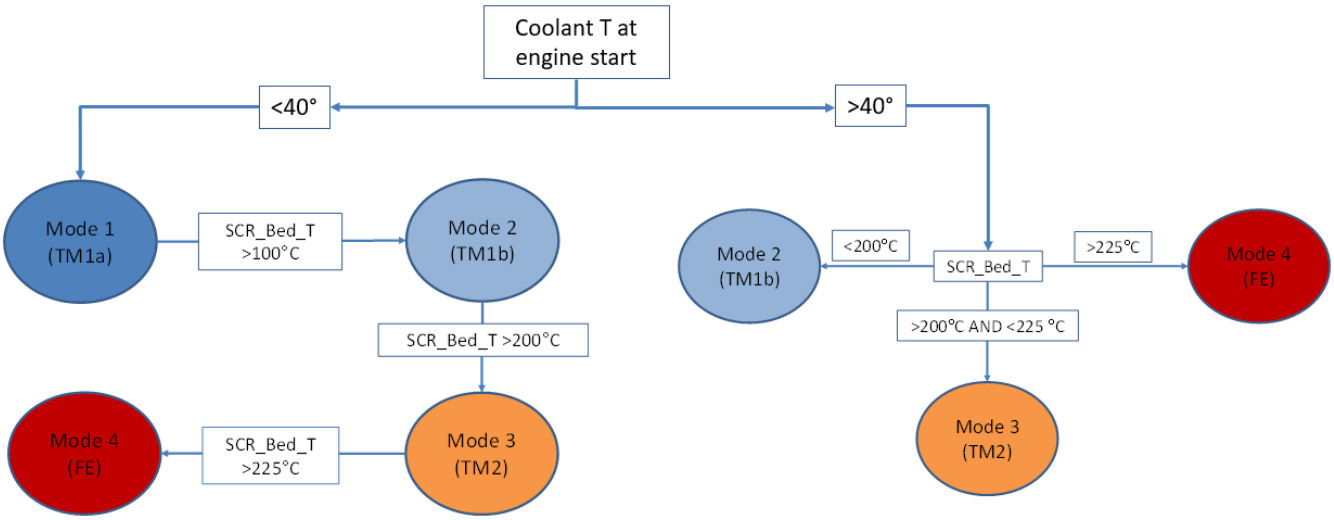



**FIGURE 37. ENGINE STATE M/C AND OVERALL STRATEGY CONTROL DIAGRAMS**

Under normal operations after engine-start and when ECT was above 40°C, these three modes were the only active modes, and the strategy work cycle between these modes as dictated by the AT system temperatures. Each of these modes was tied to a set of maps in the engine ECM

for various systems, leveraging the existing controls within the engine ECM as much as possible. SwRI then recalibrated these maps to implement the desired strategy.

If at engine start the ECT was below 40°C, additional sub-modes (Engine Modes TM1a in Figure 37) was enabled under the TM-1 mode to implement early stages of the cold-start warmup strategy. Transition out of these modes was based on ECT and the SCR temperature, given that the primary purpose of these modes was to warm up the SCR as rapidly as possible. An example of the control switching over a cold-start NRTC is shown in Figure 38 below. A different duty cycle during cold-start would likely result in a different progression through these modes, as would different ambient conditions, and an example of this behavior over a different cold-start duty cycle with a much longer initial idle is shown later in the Results section.

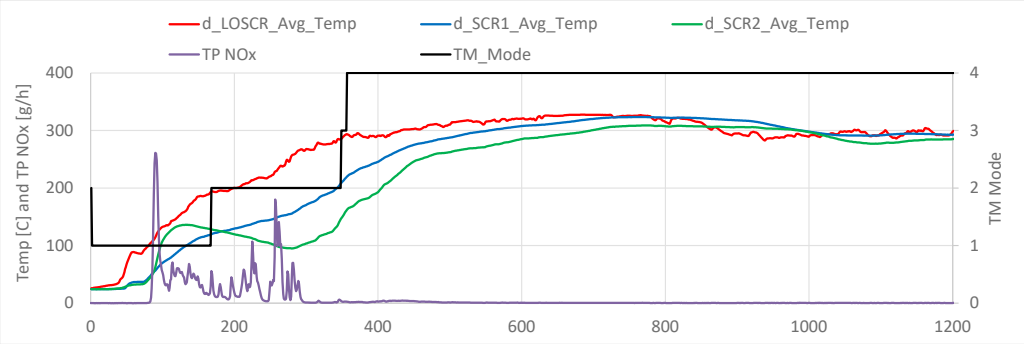



**FIGURE 38. EXAMPLE OF CONTROL MODE SWITCHING DURING COLD-NRTC**

Additional specialized controls modes were also implemented for specific functions, such as DPF Regeneration or SCR de$SO_X$. DPF regeneration also involved control of post injection via the Deere ECM. More discussion on the strategy associated with these modes is given under the AT Controls section. Due to scope limitations, these specialized modes were not fully calibrated for transient cycle implementation as part of this demonstration program.

### *2.6.2. Aftertreatment Controller and DEF Dosing Controls for Conventional Architecture Systems*

The downstream SCR sub-controller is depicted in Figure 39, and the basic control structure is shown in Figure 40. This system was patterned from the controller used for the downstream SCR system under the on-highway Low $NO_X$ program.

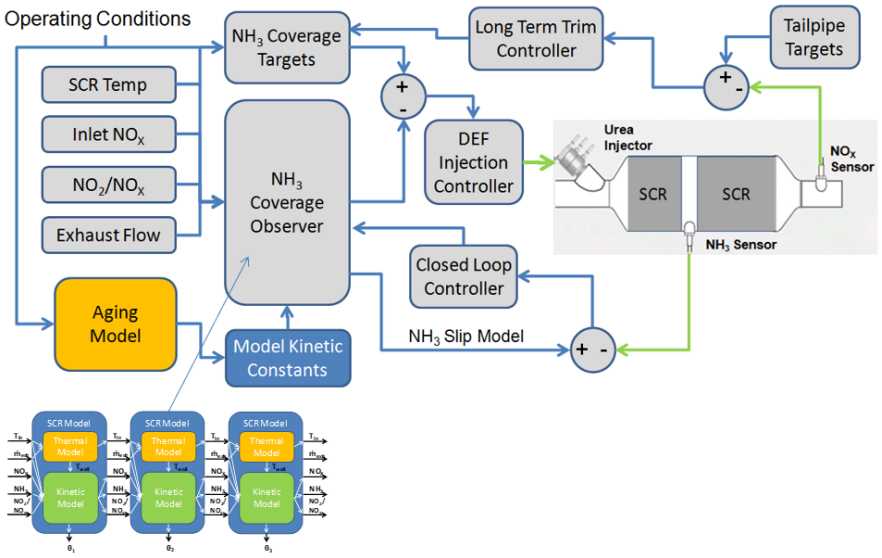



**FIGURE 39. DOWNSTREAM SCR DOSING CONTROLLER SCHEMATIC**

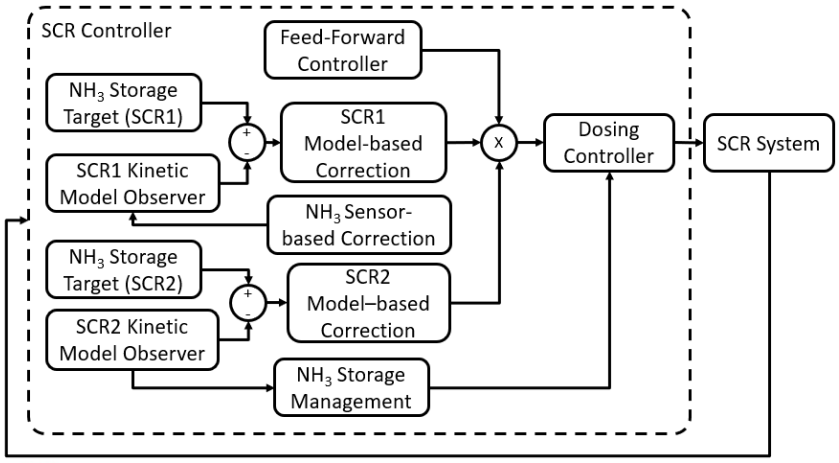



**FIGURE 40. DOWNSTREATM SCR CONTROLLER STRUCTURE**

As shown in Figure 40, the downstream command is the sum of corrections for both the first downstream SCR bed (SCR1) which is before the $NH_3$ sensor, and the second downstream SCR bed (SCR2) after the $NH_3$ sensor, with each bed having both an average storage correction, and a profile-based correction. However, the two beds target a different desired profile, given that the first bed must provide ammonia to the second bed, while the second bed profile is targeted to avoid tailpipe $NH_3$ slip. A further bias function is used to help drive coverage to desired levels by allowing the first bed to exceed its targets in cases where the second bed is too far below targets. The downstream catalyst controller also contains the same deposit avoidance limiting of maximum dosing and accelerated dosing features as the upstream controller.

The primary added feature was the high-speed feedback element, driven by the mid-bed $NH_3$ sensor. To meet tailpipe $NO_X$ targets and in-use requirements, the warmed up AT system

must be able to maintain $NO_X$ conversion in excess of 99.5%. Given even a small margin for degradation of 0.25%, this translates to a control demand to be above 99.75% conversion consistently before any degradation. From a control standpoint, maintaining such a high performance level consistently requires a high amount of precision, and it is very difficult to maintain that kind of precision on any system without some form of real-time feedback. Slower long-term trim adjustments, while also important for long-term precision, are not enough by themselves. For the model-based DEF controls, the key parameter modeled is ammonia storage, and therefore some real-time feedback element is needed that can provide information about how accurate the storage model actually is. Either $NO_X$ or $NH_3$ could be used for this purpose. However, the tailpipe $NO_X$ sensor cannot be used for this function because the downstream SCR catalyst itself is such a large filter that any tailpipe sensor signal, whether $NO_X$ or $NH_3$, is simply too slow to be of use. A tailpipe $NH_3$ sensor would have a similar attenuation problem, in addition to the fact that tailpipe $NH_3$ levels are generally low, and the presence of the ASC would eliminate most of the remaining signal.

For this reason, the downstream catalyst was split into two regions with a mid-bed sensor to provide feedback. At this location a mixture of both high $NO_X$ and high $NH_3$ is expected, therefore a $NO_X$ sensor would not be useful due to the cross-sensitivity of currently available sensors. Therefore, a mid-bed $NH_3$ sensors was the only viable option for real-time feedback. However, the currently available production $NH_3$ sensor is known to have issues with accuracy at lower $NH_3$ levels (below 30ppm) and is also subject to significant drift over time. It was necessary to use the $NH_3$ sensor in a manner that was not sensitive to these issues. As shown in Figure 39 above, the mid-bed $NH_3$ sensor was used for model state correction based on comparison to the model predicted value at the mid-bed location. Because the $NH_3$ sensor is used as a state sensor, rather than in a traditional feedback loop, the absolute accuracy of the $NH_3$ sensor is not as important, and the sensor functions primarily to detect the presence of an unexpected ammonia wave, or the absence of a predicted ammonia "wave." The detection of the rapid concentration rise of this "wave" does not shift a practical amount in time regardless of the accuracy of the NH3 sensor gain. On the timescale of the concentration rise, detecting at 10% or at 50% of rise both yield a practical and useful signal for shimming the dosing schedule. This allows the feedback algorithm to correct storage over a timescale of seconds to minutes, and the more accurate storage prediction allows the controller to correct catalyst behavior better.

Figure 41 shows an example of how the ammonia storage profiles look during a typical hot-start FTP cycle. Storage is tracked in the model as the variable "theta," which is a fractional ratio of ammonia storage compared to the maximum capacity of the system at a reference condition of 200°C. As temperature increases, this coverage ratio (theta) can be seen to drop exponentially. For each catalyst both the actual (black) and target (red) average storage values are shown, along with the actual coverage values for each of the seven model cells on a given bed. As can be seen in the figures, the individual cell coverage values can be very dynamic, and they illustrate how

storage evolves though a given catalyst bed over time. This profile information can be very useful for high efficiency SCR control, as it can be used to spot a wave of ammonia moving through the catalyst, allowing controls to react to that profile to prevent ammonia slip before it occurs, while also maximizing coverage and preparing the next wave of ammonia. In this way, the controls can be thought of as arranging a succession of waves of ammonia to pass through the catalysts as the temperature cycles.

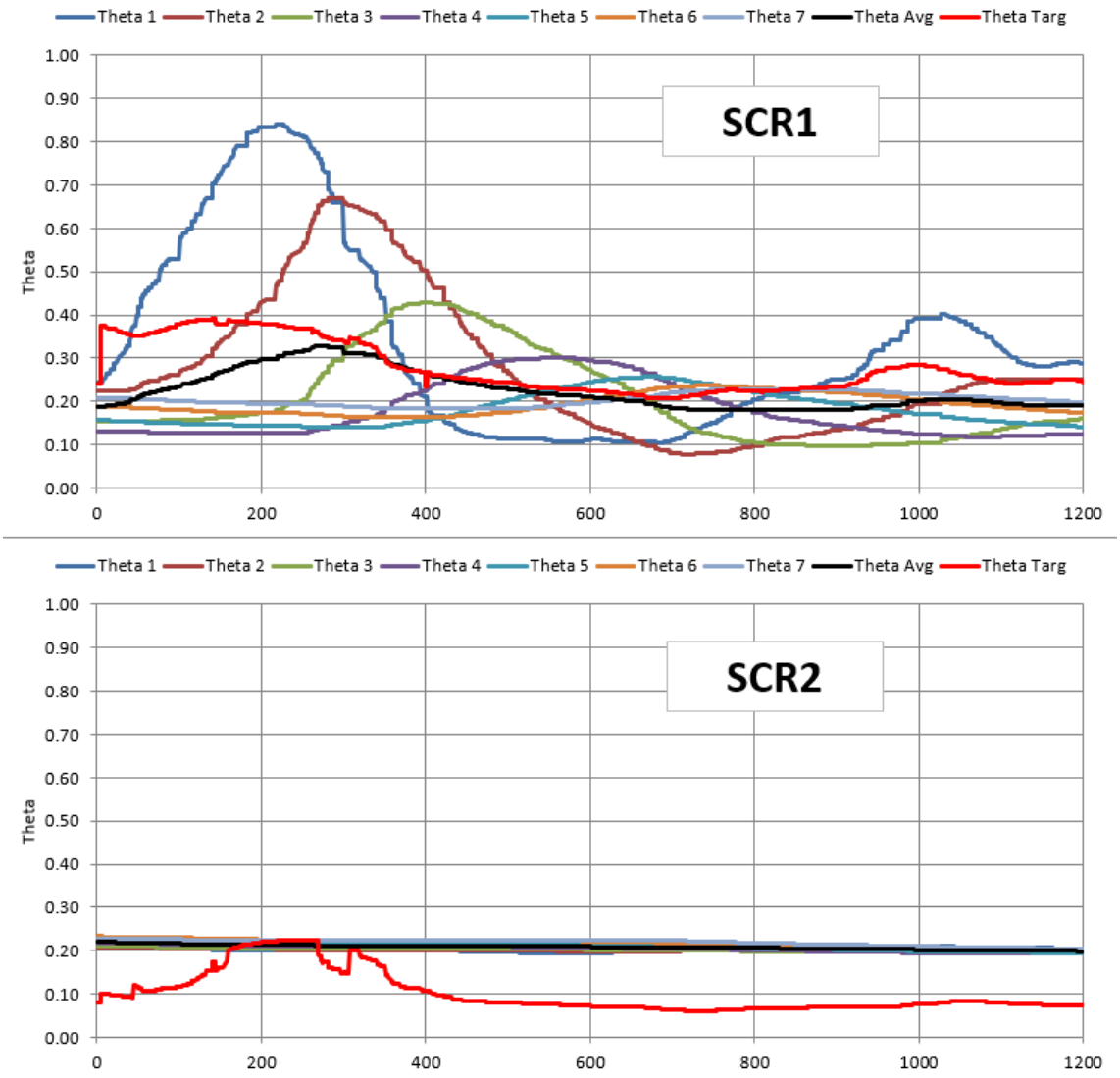



**FIGURE 41. EXAMPLE OF AMMONIA STORAGE PROFILES DURING HOT-START NRTC CYCLE**

*2.6.3. Aftertreatment Controller and DEF Dosing Controls Dual DEF Dosing Architecture Systems*

For systems with the MFC and a dual DEF dosing architecture, a more complex control strategy is required. A third model-based coverage observer of controller is added to the controller, and more sophisticated algorithms are utilized to manage the combined system. A high level representation of this approach is given below in Figure 42.

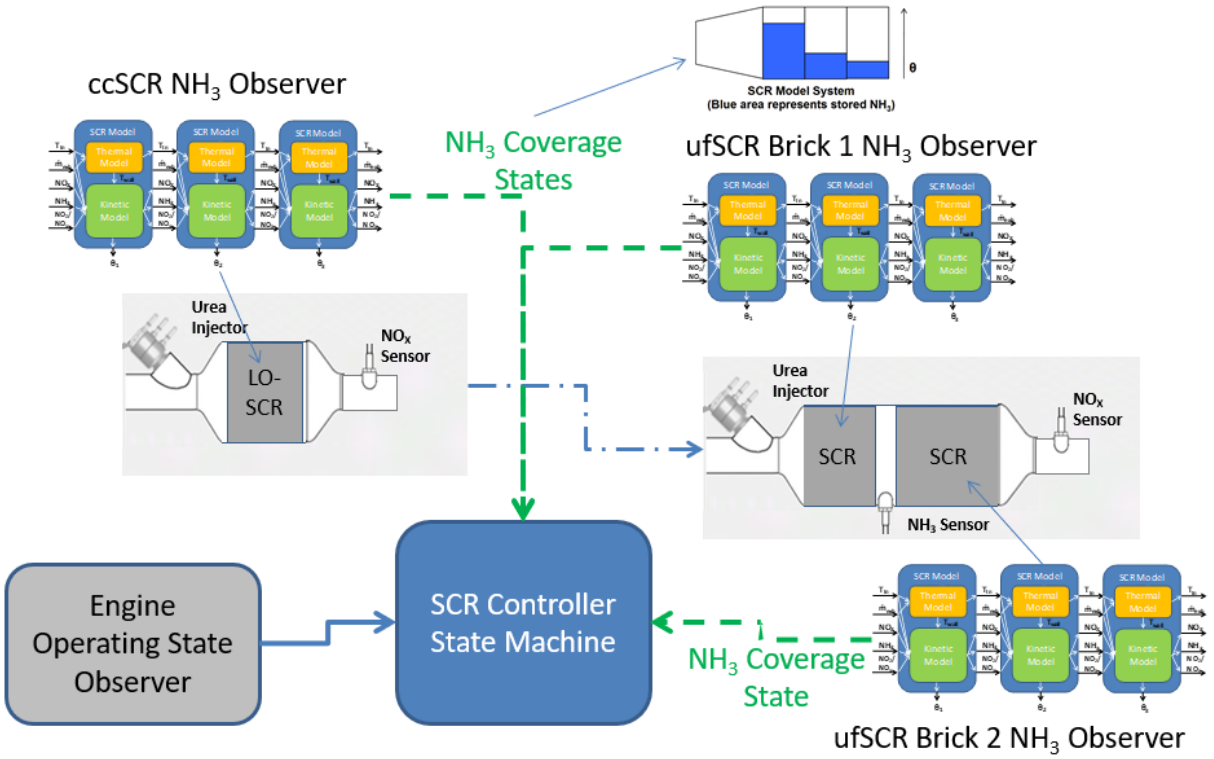



**FIGURE 42. HIGH-LEVEL SCHEMATIC OF DUAL SCR DUAL DEF DOSING CONTROL ARCHITECTURE**

The upstream SCR sub-controller is depicted in Figure 43, and the basic control structure is shown in Figure 44. This system was patterned from the controller used for the LO-SCR system under the on-highway Low $NO_X$ program. As with the downstream system controller, the key calibration parameters are the coverage targets, the feed forward ammonia-to-$NO_X$ ratio, and various system gains and thresholds.

It should be noted that the overall strategy for systems with a LO-SCR (MFC) is to target coverage at low temperatures for maximum conversion, and then to back off on dosing at higher temperatures, allowing the upstream SCR to empty of ammonia and thus permit most of the engine-out $NO_X$ to reach the filter to facilitate passive soot oxidation. At these higher temperatures, the larger downstream SCR takes on the majority of the effort of $NO_X$ reduction, and the MFC is only used to target a relatively modest 20-30% $NO_X$ conversion.

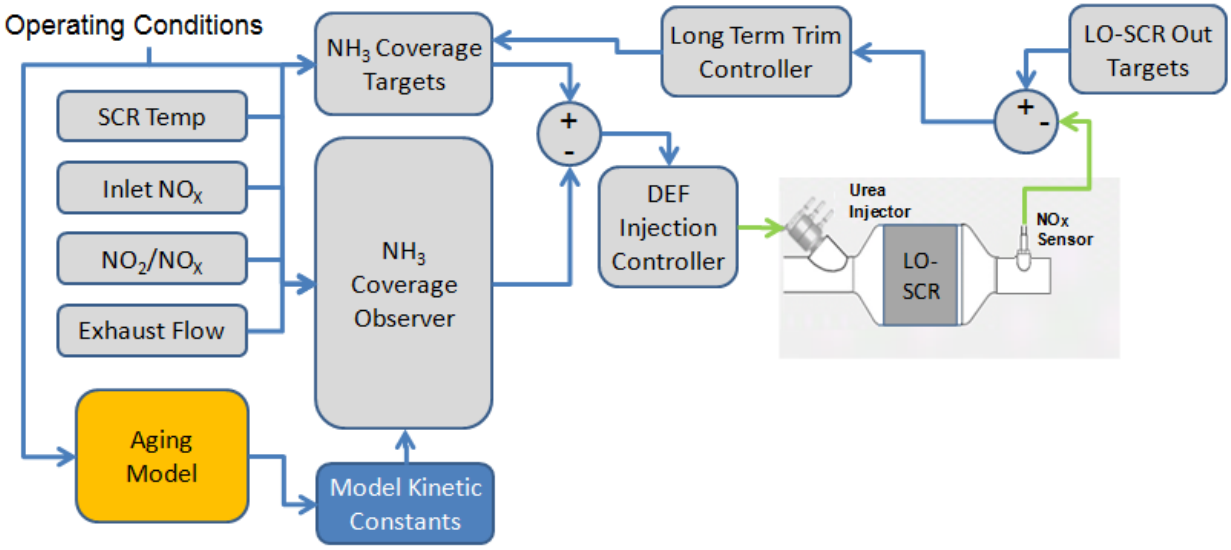



**FIGURE 43. UPSTREAM (LO-SCR/MFC) DOSING CONTROLLER SCHEMATIC**

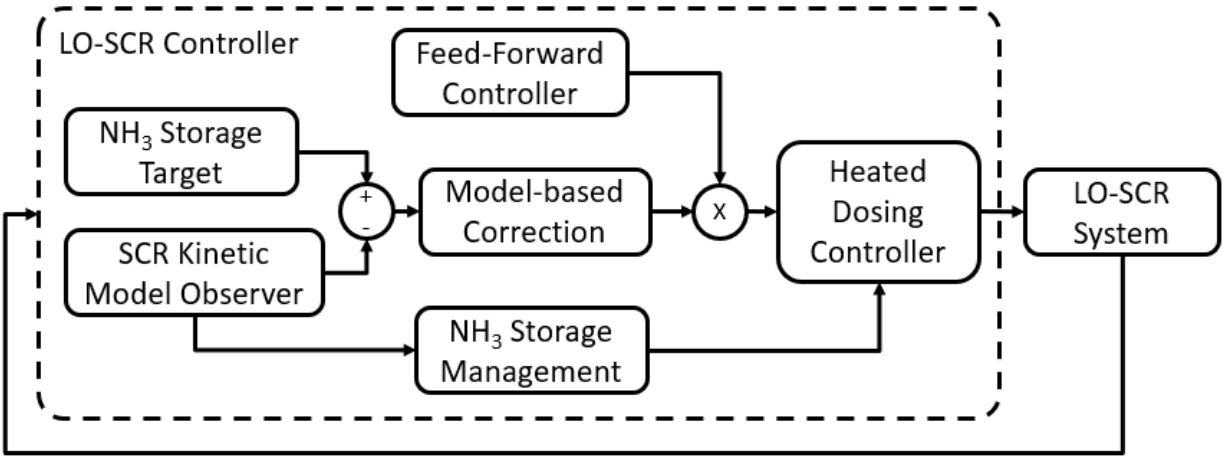



**FIGURE 44. UPSTREAM SCR CONTROLLER STRUCTURE**

*2.6.4. Overall Aftertreatment System Control Strategy*

The DEF dosing controls described above allow for a great degree of flexibility in designing a strategy to manage the usage of the two (or three) SCR catalysts systems to try to reach the program targets for $NO_X$ and $CO_2$ in a robust manner. At the same time, other system priorities, such as removal of soot from the DPF, must also be considered. The planned strategy was considered at the time of the AT hardware design, and implemented in the calibration of the DEF dosing controls and the Engine State Machine thermal states.

Under cold-start warm-up conditions, stored ammonia on the surface of the catalysts is crucial to maximizing performance during catalyst light-off. Although the lower temperature capability of the heated dosing is helpful in this case, the high storage capacity of the zeolite SCR

catalysts at low temperatures makes it difficult to push enough ammonia through the catalysts to achieve coverage. Therefore, previously stored ammonia is useful for reaching Low $NO_X$ levels during cold-start which creates a design aim to continuously maintain target coverage prior to each (time-unknown) engine shutdown. A significant amount of the strategy is designed to enable rapid recovery of SCR storage that will be needed for the next start event. Although this is useful under many field situations, for the off-road duty cycles, the NRTC poses a particular challenge in that it operates at temperatures that do not readily allow for recovery of ammonia storage before engine shut down. This poses a challenge different from the on-highway cycles, which will be discussed later under the Results section of the report. The accelerated dosing modes of the controller and the low deposit risk, high DEF dosing rate capabilities of the heated dosing system are both important features for this to work on an optimal fashion over a wide variety of duty cycles and entry conditions. With regard to the heated dosing system, it should be noted that there are several heat-enabled options for low temperature dosing, including dosing onto a small heater or heated mixer, in addition to the option chosen for this program, which involved direct heating of the DEF fluid under pressure.

## 2.7 Aging Methodology – Development Aging (Hydrothermal Only)

The Development Aging process was designed to simulate FUL of hydrothermal aging only. This process by its design did vary slightly from one set of hardware to the other, given that there were some characteristic chemical/physical differences in key parameters like those that led to different Active Regeneration target temperatures used by the respective AT systems. The basic approach to Development Aging was to again leverage the exponential relationship of temperature and thermal deactivation, but without the extra time for the chemical poisoning elements of the full DAAAC aging protocol In effect, all of the high temperature exposure events were collected together, with little or no time in between. Because the final systems were not yet developed, conservative choices were made regarding regeneration durations and frequencies.

Development Aging was conducted on the ECTO-Lab burner system, illustrated in Figure 45. This system allows the simulation of exhaust conditions of many different engines and can be used for aging and evaluation of full-size engine AT systems for engines ranging from 3-15L in displacement.

For the conventional DOC+DPF+SCR architectures, the estimated regeneration frequency used to scale aging was 45 minutes every 80 hours, which is equivalent to the baseline engine regeneration frequency. This worked out to 113 hours of total regeneration over the course of 12,000 hours of operation. A conservative target temperature of 600°C at the DPF was chosen for the development aging. This temperature is higher than the 565 to 575°C temperature typically seen for offroad DPF regenerations but was selected primarily due to experience on the on-highway Low $NO_X$ program. This was due to the earlier success in that program controlling long-term sulfur poisoning at these temperatures. It is possible that a lower temperature would be

successful for deSO$_X$, but for Development aging early in the program, the conservative higher temperature was used to avoid under-prediction of aging for the purposes of comparing technologies to each other. A DOC inlet temperature of 350°C was used, and then the target temperature was reached using HC injection over the DOC, as would be the case in the real application.

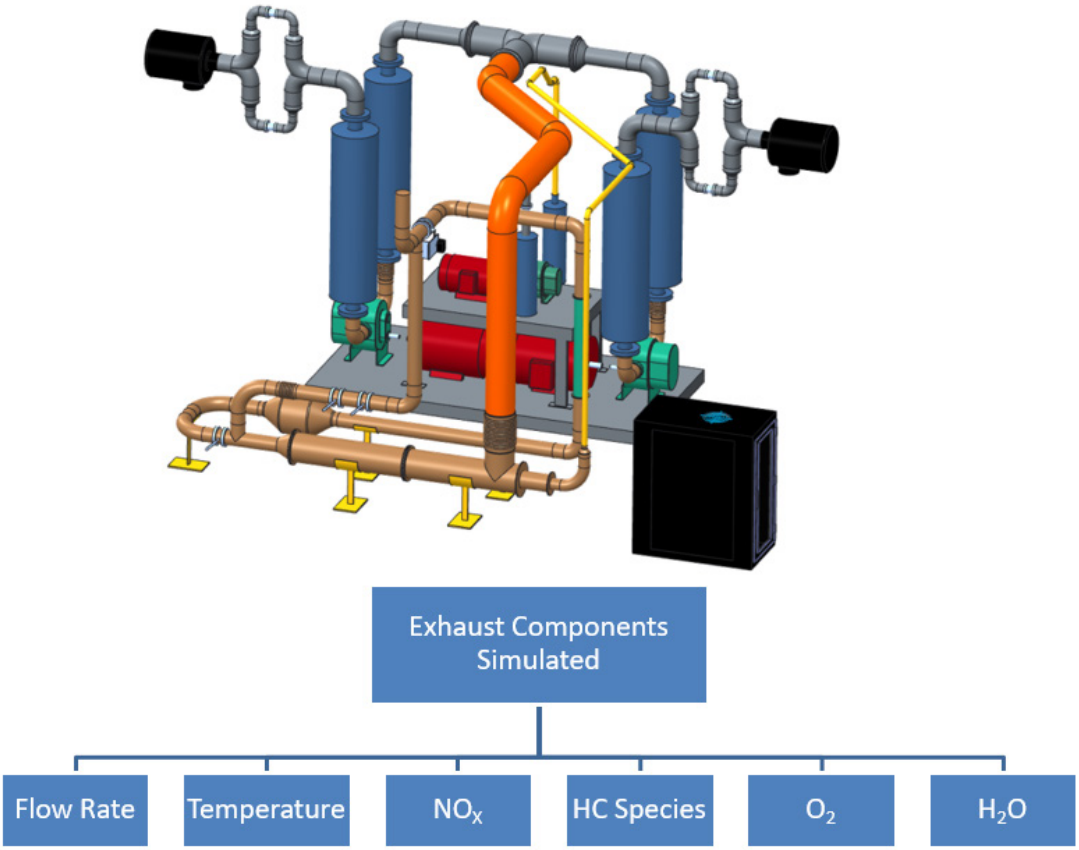



**FIGURE 45. SWRI ECTO-LAB™ BURNER-BASED AGING AND TEST STAND**

This approach was used for all systems except the Team 2 LO-SCR (MFC) option. In this case, a lower target temperature of 575°C was used for two-thirds of the time as a result of the different configuration, but temperature of 600°C was used one-third of the time to represent an end of regeneration kick of temperature that would be used to remove any residual sulfur still stored on the downstream SCR.

## 2.8 Aging Methodology – DAAAC Aging (Hydrothermal and Chemical)

For the final demonstration effort, a more representative form of aging was essential to provide for a robust demonstration of the final selected emission control system. Consistent with methods used during previous Low NO$_X$ demonstration programs, SwRI utilized the DAAAC methodology (Diesel Aftertreatment Accelerating Aging Cycle) to perform FUL useful life aging

on the final demonstration aftertreatment system. The DAAAC methodology has been described in detail in previous publications [10][11][12], and is an accelerated bench aging methodology for demonstration of aftertreatment system durability. The DAAAC methodology generally applies a 10X acceleration on aftertreatment system aging (e.g. 1000 aging hours in 100 hours of time), and it does so in a manner that produces results representative of un-accelerating aging on engine. The DAAAC protocol is a method of generating application specific aging cycles and executing those cycles to age parts in an accelerated fashion. The DAAAC protocol considers both thermal and chemical aging, and it has been adopted into 40 CFR Part 1065 Subpart L as the official bench aging methodology for diesel aftertreatment used for durability demonstration for compliance and certification purposes.

For this program, the aging cycle was generated using DAAAC Method 2, which is intended for use when field temperature and flow data are not available for the application. This method was chosen because there is no available field exhaust temperature and flow data available, given the developmental nature of this demonstration program. Under Method 2, activity data recorded in the field is used, via a k-means clustering analysis, to produce weighting factors for the appropriate lab certification cycles for the given application. In this case, those cycles were the NRTC, the RMC 8-mode, and the LLAC. Data recorded from those test cycles is then used to provide the temperature and exhaust flow setpoints required for aging. The application of these methods to the Deere 6.8L engine and Low $NO_X$ emission control system is described below.

The activity data analysis and k-means clustering were for DAAAC Method 2 was performed by John Deere, who leveraged recorded data sets from several different machine applications. The source data sets were all proprietary in nature, and therefore the analysis was performed directly by Deere using the methods described in 40 CFR § 1065.1139(b)(2). The final weight factors determined for the 6068 engine were 46% for the NRTC, 22% for the RMC, and 32% for the LLAC. Data was then extracted from those test cycles run in the lab with the final aftertreatment system installed, in accordance with the methods described in the CFR section noted above. The resulting set of 9 potential aging modes for non-regeneration operation is shown in Table 8. Modes with very similar conditions were then consolidated to a smaller set, again in accordance with the DAAAC procedures in Part 1065. The modes that were consolidated together are indicated in Table 8 by matching colors, for example the modes in the 3 rows shaded in green were consolidated into a single mode.

**TABLE 8. INITIAL SET OF POTENTIAL DAAAC NON-REGENERATION AGING MODES**

| Cycle WF | Percentile WF (1065) | Cycle | Percentile | AT Inlet degC | DPF Out degC | Exh Flow kg/hr | Fuel Flow kg/hr | NOX g/hr | Overal Weighting |
|---|---|---|---|---|---|---|---|---|---|
| 46% | 0.25 | **NRTC** | **25th** | **274** | **247** | **328** | **8.6** | **168** | 0.115 |
| 46% | 0.65 | **NRTC** | **50th** | **299** | **284** | **422** | **14.7** | **240** | 0.299 |
| 46% | 0.1 | NRTC | 90th | 335 | 320 | 674 | 27.6 | 479 | 0.046 |
| | | | | | | | | | |
| 22% | 0.25 | RMC | 25th | 304 | 289 | 430 | 12.3 | 254 | 0.055 |
| 22% | 0.65 | **RMC** | **50th** | **347** | **332** | **555** | **22.1** | **403** | 0.143 |
| ***22%*** | ***0.1*** | ***RMC*** | ***90th*** | ***379*** | ***364*** | ***880*** | ***38.2*** | ***694*** | *0.022* |
| | | | | | | | | | |
| 32% | 0.25 | LLAC | 25th | 191 | 176 | 186 | 2.0 | 65 | 0.08 |
| 32% | 0.65 | **LLAC** | **50th** | **208** | **193** | **253** | **4.7** | **126** | 0.208 |
| 32% | 0.1 | LLAC | 90th | 284 | 269 | 464 | 16.6 | 255 | 0.032 |

The final consolidated set of 5 non-regeneration aging modes is given in Table 9. It should be noted that aging Mode 5 would have a duration shorter than the 15 minute minimum mode length specific in 1065. Therefore, that mode is only run on alternating cycle repeats at 15 minute duration.

**TABLE 9. FINAL SET OF DAAAC NON-REGENERATION AGING MODES**

| Mode | Mode Reference | | AT Inlet degC | DPF Out degC | Exh Flow kg/hr | Fuel Flow kg/hr | NOX g/hr | WF | Duration mins |
|---|---|---|---|---|---|---|---|---|---|
| 1 | NRTC | 50th | 299 | 284 | 422 | 14.7 | 240 | 0.386 | 119 |
| 2 | NRTC | 25th | 274 | 247 | 328 | 8.6 | 168 | 0.115 | 35 |
| 3 | RMC | 50th | 347 | 332 | 555 | 22.1 | 403 | 0.189 | 58 |
| 4 | LLAC | 50th | 208 | 193 | 253 | 4.7 | 126 | 0.288 | 89 |
| 5 | RMC | 90th | 379 | 364 | 880 | 38.2 | 694 | 0.022 | 7 |

In addition to these non-regeneration modes, the regeneration mode must be considered. The expected regeneration frequency and interval between regenerations was already known as a result of experiments and projections used to adjust emission for infrequent regeneration, as will be discussed later under the Results section in detail. Those intervals are summarized below in Table 10. Combining these results in a final weighted average DAAAC aging interval of 58 hours. The regeneration duration was 40 minutes, with a target temperature at the DPF outlet of 570°C. Therefore, during DAAAC aging, regeneration was conducted every 5.8 hours at the specified temperature. This meant that over the course of 800 DAAAC aging hours (8000 field equivalent hours), 138 regenerations were conducted.

**TABLE 10. REGENERATION INTERVALS AND WEIGHT FACTORS BY TEST CYCLE**

| Cycle | Regeneration Interval hours | Weight Factor |
|---|---|---|
| NRTC | 69 | 46% |
| RMC | 80 | 22% |
| LLAC | 28 | 32% |
| **Weighted Composite** | **58** | **n/a** |

Combining both regeneration and non-regeneration modes, the final DAAAC aging cycle is shown in Table 11. Note that Mode 5 is only run every other set of mode repeats. Also, the two regenerations in each cycle happen at two different system inlet temperatures, to make sure the location of the HC exotherm moves around over the course of aging. This temperature choices are discussed later in the Results section when examining the regeneration performance of the MFC. This cycle was repeated 69 times to reach 800 DAAAC-hours and 8000 field hours.

**TABLE 11. FINAL DAAAC AGING CYCLE FOR OFFROAD LOW NOX DEMONSTRATION**

| Mode | Mode Reference | | **AT Inlet T** **degC** | DPF Outlet T degC | **Exhaust Flow** **kg/hr** | *Fuel Flow Ref* *kg/hr* | *NOX Mass* *g/hr* | Duration min | **NOX Concentration** **ppm** |
|---|---|---|---|---|---|---|---|---|---|
| 1 | NRTC | 50th | **299** | 284 | **422** | *14.7* | *240* | 119 | **357** |
| 2 | LLAC | 50th | **208** | 193 | **253** | *4.7* | *126* | 89 | **313** |
| 3 | RMC | 50th | **347** | 332 | **555** | *22.1* | *403* | 58 | **457** |
| 4 | NRTC | 25th | **274** | 247 | **328** | *8.6* | *168* | 35 | **322** |
| | Regen | | **300** | 570 | **400** | | *350* | 40 | **551** |
| 1 | NRTC | 50th | **299** | 284 | **422** | *14.7* | *240* | 119 | **357** |
| 2 | LLAC | 50th | **208** | 193 | **253** | *4.7* | *126* | 89 | **313** |
| 3 | RMC | 50th | **347** | 332 | **555** | *22.1* | *403* | 58 | **457** |
| 4 | NRTC | 25th | **274** | 247 | **328** | *8.6* | *168* | 35 | **322** |
| 5 | RMC | 90th | **379** | 364 | **880** | *38.2* | *694* | 15 | **497** |
| | Regen | | **350** | 570 | **400** | | *350* | 40 | **551** |

For the chemical aging due to oil exposure, the base engine oil consumption was 5.5 g/hr on a duty cycle average basis. Therefore, considering the 10X exposure the DAAAC exposure target was 55 g/hr. Similarly based on a fuel sulfur level of 10ppm (as specified of 40 CFR §1065.1139(i)) and considering the 13 kg/hr average field fuel consumption, the total sulfur exposure target was 1039 grams of sulfur over 8000 hours.

The aging was run on a John Deere 6090HFC09 aging mule engine, which is a 9L 6-cylinder diesel engine with a rated power of 242kw. The engine was modified according to DAAAC protocol procedures to increase oil consumption via changes to the piston rings. This

involved flipping the second compression rings (oil scraper ring), as well as modifications to the oil control rings to reduce the spring tension on the ring expander. This engine was installed in a DAAAC aging cell, along with an exhaust heat exchanger and bypass assembly, and a constant oil sump volume system for extended aging operation. The DAAAC engine installation is shown in Figure 46. A schematic of the DAAAC aging cell components is shown in Figure 47.

A sample of exhaust temperature data from one repeat of the cycle shown in Table 11 is shown in Figure 48, showing aftertreatment system temperatures at various locations through the system. The two regeneration events can clearly be seen in the middle of the cycle and towards the end. In addition, the different evolution of the regeneration exotherm across the MFC and the zCSF can be seen between the first regeneration event that occurs with a system inlet of 350°C and the second regeneration event that occurs with a system inlet of 300°C. In the first event, the exotherm is nearly completed within the first two inches of the MFC, while in the second (lower inlet temperature event), a significant portion of the exotherm does not happen until the high PGM region of the zCSF downstream. This was expected based on previous data.

It should be noted that although LO-SCR technology in the form of the MFC was used, a separate LO-SCR de$SO_X$ event was not deemed necessary. This is because the periodic exotherm across the MFC during regeneration was expected to be sufficient for de$SO_X$ of the MFC itself. However, this was not known for certain until a significant portion of the aging was completed, and the $NO_X$ performance could be assessed via the system $NO_X$ sensors. In the end, excessive deterioration of the MFC $NO_X$ conversion was not observed due to sulfation, indicating that this strategy was successful, and the exotherm across the MFC during DPF regeneration was sufficient for MFC de$SO_X$ as well.

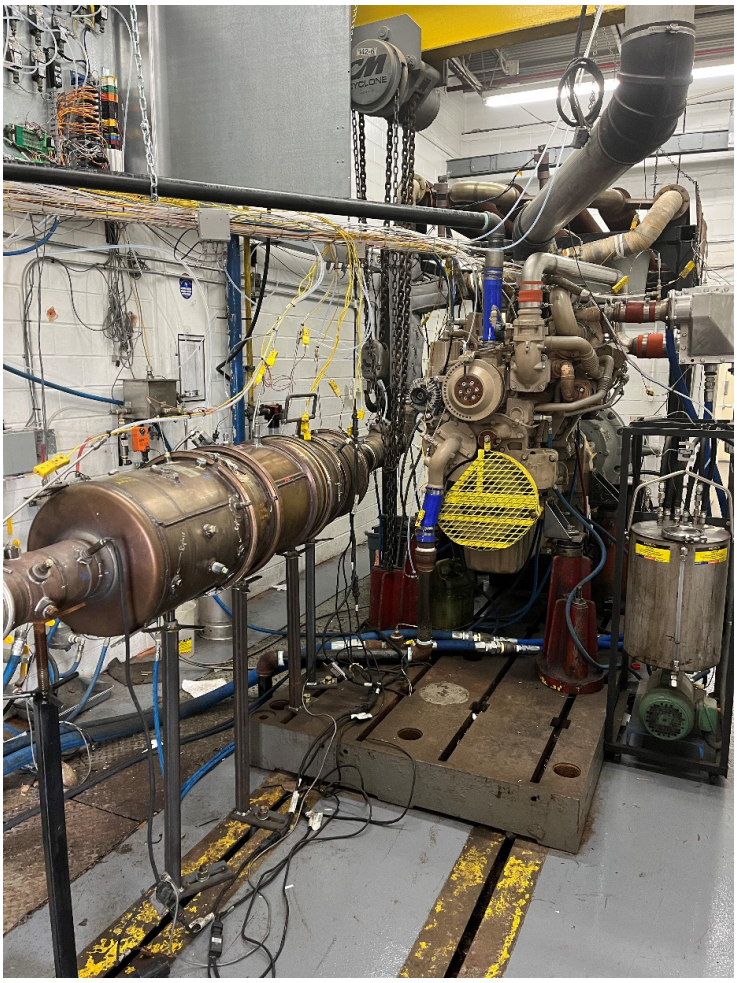


**FIGURE 46. DAAAC AGING CELL WITH DEERE 9.0L AGING MULE ENGINE AND FINAL LOW $NO_X$ AFTERTREATMENT SYSTEM**

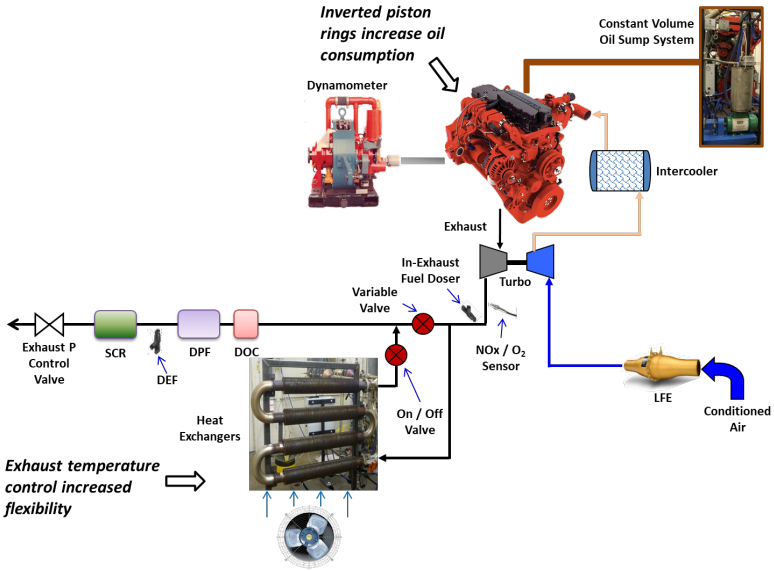



**FIGURE 47. DAAAC ENGINE AGING STAND SCHEMATIC**

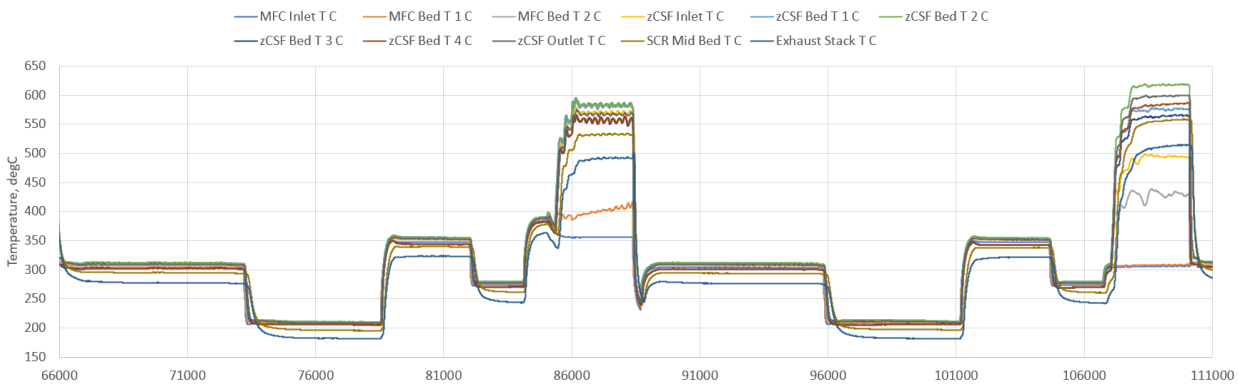



**FIGURE 48. EXAMPLE TEMPERATURE DATA FOR ONE DAAAC AGING CYCLE**

# 3.0 RESULTS AND DISCUSSION

This section of the report provides detail on the results of the program and the development process for reaching the final test configuration and associated emission performance levels. In this section program results are often referred to as being for either Development Aged or DAAAC-Aged aftertreatment parts. In the case of Development Aged parts, these were hydrothermally aged according to the procured outlined in Section 2.7, and these were used only for initially hardware development and screening prior to the down-select of the final configuration. The DAAAC-aged parts were more rigorously aged to account for both thermal and chemical aging in accordance with the procedures described in Section 2.8.

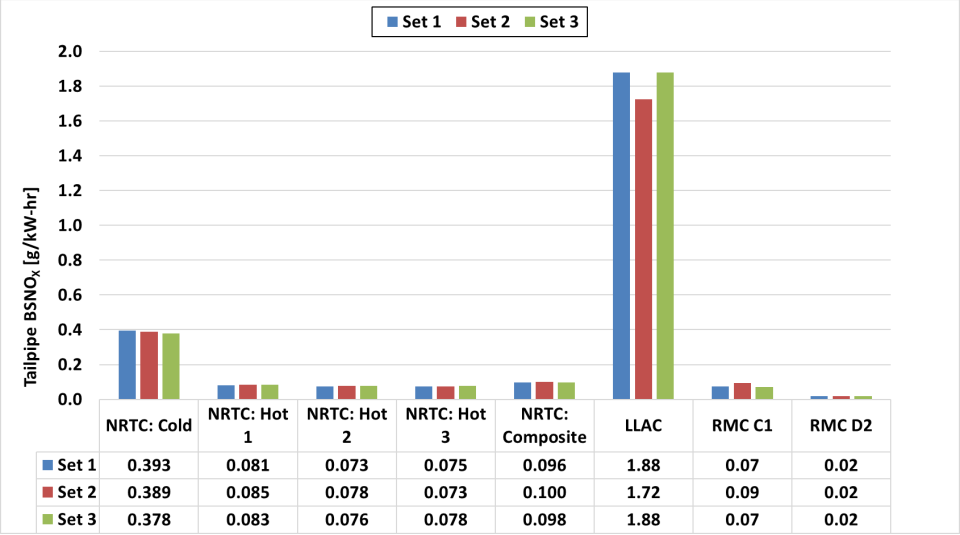
## 3.1 Package 1 Testing and Previous Program Results

As mentioned earlier, this program discussed in this report is a continuation of work that was started under earlier CARB programs. The Stage 1 program conducted under CARB Contract 18RD006 produced the baseline test results used for the rest of the program comparison. In the Stage 2 program under CARB Contract 19RD025, Low $NO_X$ hardware options were screened and Package 1 results were generated looking at $NO_X$ reduction to reach Tier 5 program targets without impacting GHG emissions. Some efforts under the Stage 2 program were also conducted looking at Package 2. Some of the aftertreatment and hardware options were also examined using in-kind services and supplemental funding that were provided by the Manufacturers of Emission Controls Association (MECA).

The previous results were already covered in detail in the Stage 2 program final report [9], and in general those results will not be repeated here. However, certain results will be included in this report section for ease of comparison, to prevent readers from having to refer back to those other documents for comparisons.

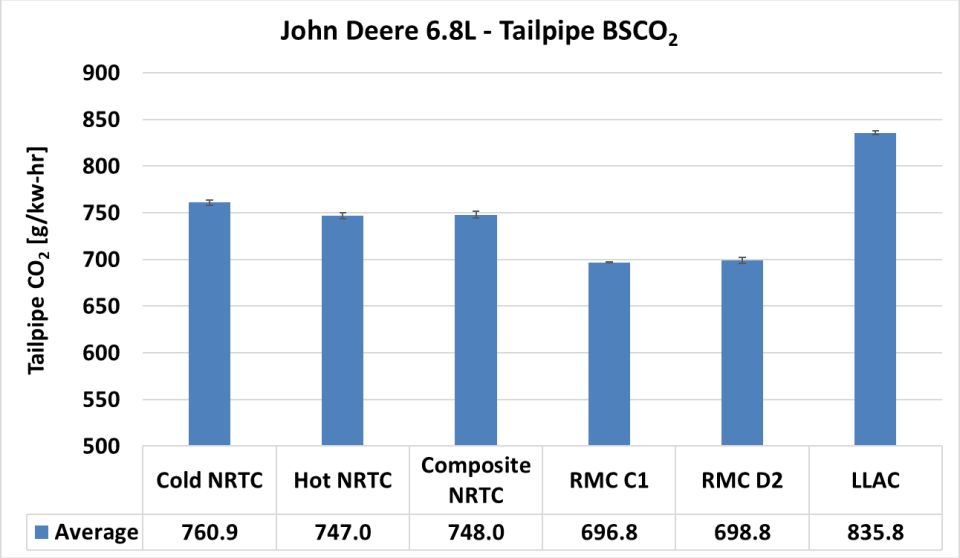
### *3.1.1. John Deere 6068 Baseline Tier 4 Final Emissions Results*

A brief summary of relevant emission results for comparison to the results of this demonstration program is given below. Tailpipe $NO_X$ emission levels are summarized on Figure 49, while $CO_2$ emissions are given in Figure 50, and $N_2O$ emissions are summarized in Figure 51.




| | NRTC: Cold | NRTC: Hot 1 | NRTC: Hot 2 | NRTC: Hot 3 | NRTC: Composite | LLAC | RMC C1 | RMC D2 |
|---|---|---|---|---|---|---|---|---|
| Set 1 | 0.393 | 0.081 | 0.073 | 0.075 | 0.096 | 1.88 | 0.07 | 0.02 |
| Set 2 | 0.389 | 0.085 | 0.078 | 0.073 | 0.100 | 1.72 | 0.09 | 0.02 |
| Set 3 | 0.378 | 0.083 | 0.076 | 0.078 | 0.098 | 1.88 | 0.07 | 0.02 |

**FIGURE 49. BASELINE TIER 4 FINAL ENGINE TAILPIPE $NO_X$ EMISSIONS FOR BASE 187KW ENGINE RATING**




| | Cold NRTC | Hot NRTC | Composite NRTC | RMC C1 | RMC D2 | LLAC |
|---|---|---|---|---|---|---|
| Average | 760.9 | 747.0 | 748.0 | 696.8 | 698.8 | 835.8 |

**FIGURE 50. BASELINE TIER 4 FINAL ENGINE $CO_2$ EMISSIONS FOR BASE 187KW ENGINE RATING**

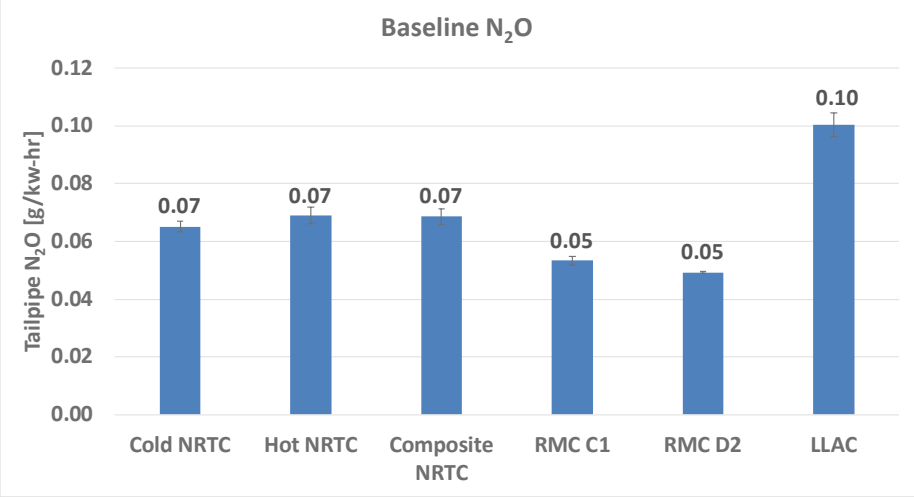



**FIGURE 51. BASELINE TIER 4 FINAL ENGINE $N_2O$ EMISSIONS FOR BASE 187KW ENGINE RATING**

Later in the program, a second set of baseline emission levels were generated for the Low Power Child engine rating at 126kw. These will be summarized in the result section dealing with testing of the Low Power Child Rating.

### *3.1.2. Package 1 Results*

Package 1 test results were discussed in detail for a variety of configurations and development steps in the Stage 2 final report. For purposes of comparison, a summary a Package 1 results for $NO_X$, $CO_2$, and $N_2O$ is given in Table 12. The results shown are for a closed crankcase ventilation system (CCV). Based on these results, projected margins were calculated for an 8000-hour FUL DAAAC aged scenario based on deterioration rates observed during the on-highway program (as the Package 1 system would not be DAAAC aged in the scope of this program). The projections are shown in Figure 52.

**TABLE 12. FINAL PACKAGE 1 TEST RESULTS WITH DEVELOPMENT AGED PARTS**

| Cycle | EO $NO_X$, g/kw-hr | TP $NO_X$, g/kw-hr | $NO_X$ Efficiency, % | $CO_2$, g/kw-hr | Baseline $CO_2$, g/kw-hr | TP N2O, g/kw-hr |
|---|---|---|---|---|---|---|
| Cold NRTC | 2.3 | 0.138 | 93.9 | 763 | 761 | 0.06 |
| Hot NRTC | 2.4 | 0.004 | 99.8 | 741 | 747 | 0.07 |
| **Composite NRTC** | **2.4** | **0.011** | **99.5** | **745** | **748** | **0.07** |
| **RMC C1** | **2.6** | **0.006** | **99.7** | **690** | **697** | **0.05** |
| **LLAC** | **4.1** | **0.011** | **99.7** | **832** | **836** | **0.11** |

| | | NRTC | | | |
|---|---|---|---|---|---|
| | | 5% | 95% | | |
| | | Cold | Hot | RMC | LLC |
| | | g/kw-hr | g/kw-hr | g/kw-hr | g/kw-hr |
| Standard | | 0.04 | | 0.04 | 0.10 |
| Certification Targets | Engine-Out | 2.3 | 2.4 | 2.6 | 4.1 |
| | Conversion | 94.0% | 99.8% | 99.8% | 99.7% |
| | Tailpipe | 0.138 | 0.004 | 0.006 | 0.011 |
| | TP Composite | | 0.011 | | |
| | EO Composite | | 2.4 | | |
| | Composite Conversion | | 99.6% | | |
| FUL Compliance | FUL Durability Loss Margin | 0.4% | 0.3% | 0.3% | 0.7% |
| | FUL Conversion | 93.6% | 99.5% | 99.5% | 99.0% |
| | FUL Tailpipe | 0.148 | 0.011 | 0.014 | 0.040 |
| | FUL Composite Conversion | | 99.2% | | |
| | IRAF | | 0.004 | 0.004 | 0.007 |
| | Final TP Composite | | 0.022 | 0.018 | 0.047 |
| | Margin to Standard | | 45% | 56% | 53% |
| | | | 0.018 | 0.022 | 0.053 |

**FIGURE 52. COMPLIANCE MARGIN PROJECTIONS FOR PACKAGE 1 SYSTEM AT 8000-HOUR FUL**

The margin projections indicated that for the 8000-hour FUL DAAAC-aged system using a CCV configuration, the expected emission levels generally provided margins on the order of 50%, or roughly 20 mg/kw-hr, to a NRTC/RMC standard of 0.040 g/kw-hr. As a reminder, the Package 1 system was a conventional DOC+DPF+SCR system with no additional hardware and featuring a modified engine calibration that maintained engine-out $NO_X$ and $CO_2$ levels at levels similar to those of the Baseline engine.

## 3.2 Impact of Crankcase Emissions and Closed Crankcase Ventilation (CCV)

In working to further reduce tailpipe emissions on the hot NRTC cycle, it was observed the aftertreatment temperatures were essentially satisfactory over the entire cycle, and that further adjustments to dosing strategy did not result in further changes in tailpipe emission behavior. At this point SwRI conducted several additional investigations into both the system and the measurements. One of these included disconnecting the crankcase vent line from the tailpipe to see of this affected the measurement significantly. However, this last change resulted in a substantial drop in measured $NO_X$ levels observed by the CVS instrumentation indicating that the previously connected/collected crankcase ventilation gas was a significant source of $NO_x$. A comparison continuous tailpipe $NO_X$ behavior of the system with and without the crankcase line hooked up to the tailpipe is shown below in Figure 53. As can be seen, following the very early tailpipe spike, there is a continuous but low level of $NO_X$ accumulation occurring with the crankcase line plumbed to the tailpipe, and that is essentially gone after about 300 seconds into the cycle with the line disconnected. The difference between these two cycles was on the order of 0.01 g/kw-hr, which represents a dominating two-thirds of the total tailpipe $NO_X$ shown in Figure 53**Error! Reference source not found.** for the OCV configuration and a clear target for further $NO_x$ reduction actions.

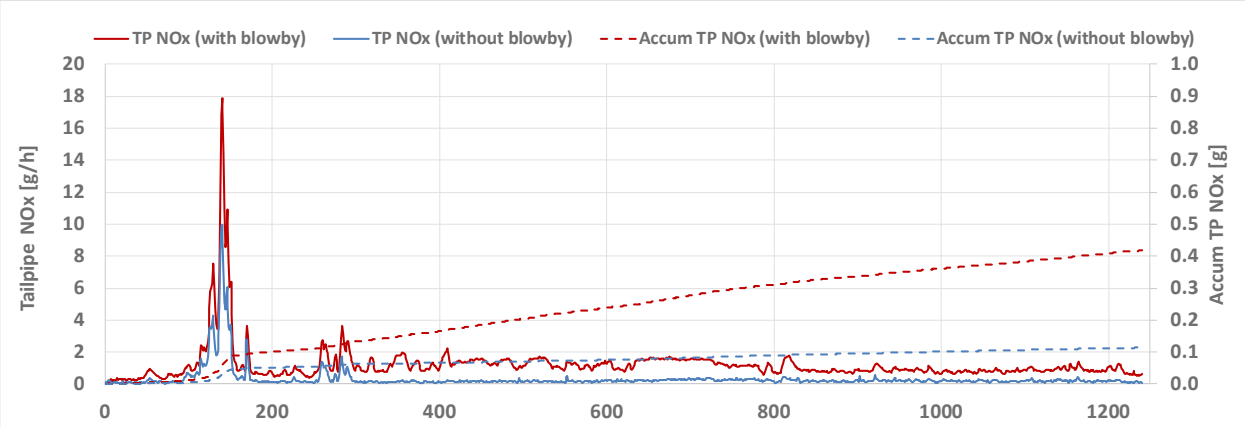



**FIGURE 53. IMPACT OF CRANKCASE EMISSIONS OF DEERE 6068 ENGINE ON HOT-START NRTC EMISSIONS**

To facilitate a better understanding of the crankcase emissions, additional measurement instrumentation was installed to directly monitor the crankcase gas flow rate and $NO_X$ concentration. The results for direct crankcase gas measurements on the NRTC are shown below in Figure 54 for $NO_X$ concentration, and Figure 55 for flow rate, respectively. The $NO_X$ concentration in the blowby gases is generally between about 70ppm and 120ppm, and it can be seen to vary somewhat weakly with in-cylinder (engine-out) $NO_X$ levels. Overall, the crankcase $NO_X$ concentration appears to be roughly 20-35% of the in-cylinder level. It should be noted that this damped response makes sense given that the crankcase itself will serve as something of a mixing and dilution chamber for the gases that escape the combustion chamber past the piston rings. The crankcase gas flow rate, shown in Figure 55**Error! Reference source not found.**, demonstrates a very strong correlation to the exhaust flow rate, with the crankcase flow rate generally seen at about 1 percent of exhaust flow. This is a blowby flowrate level that is consistent with other engines, though on the higher end of the typical range. The data from shown in these figures was used to determine a $BSNO_X$ rate from direct crankcase measurement, and that values was 0.011 g/kw-hr, consistent with the 0.01 g/kw-hr level predicted by the difference between the measured dilute levels with and without the crankcase line connected to the tailpipe providing two independent measurement methods that both showed the importance of this NOx emission physical pathway.

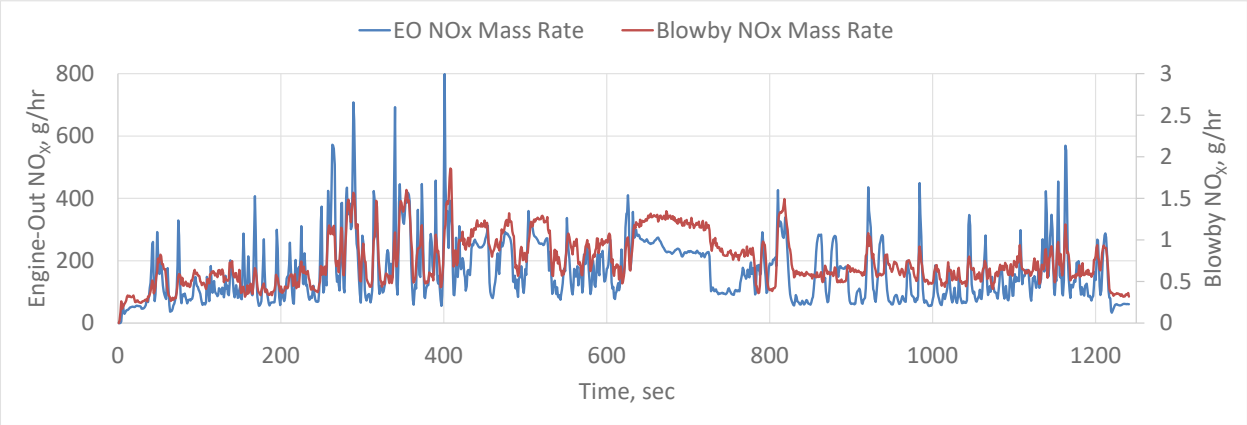



**FIGURE 54. CRANKCASE GAS $NO_X$ CONCENTRATION AS COMPARED TO ENGINE-OUT LEVEL ON NRTC**

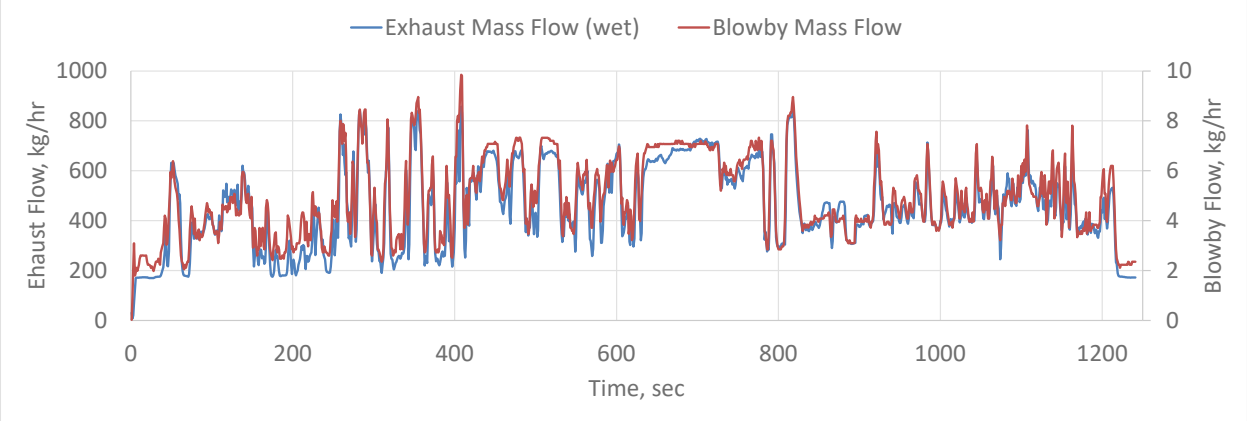



**FIGURE 55. CRANKCASE GAS FLOW RATE AS COMPARED TO ENGINE EXHAUST FLOW ON NRTC**

Similar results are shown for the RMC in Figure 56 for $NO_X$ concentration and Figure 57 for crankcase flow rate, respectively. Here the measured tailpipe $NO_X$ impact of the crankcase gases is 0.013 g/kw-hr, slightly higher given the higher load cycle. Given the steady-state nature of this cycle from an engine standpoint, the relationship between engine out $NO_X$ and crankcase $NO_X$ concentration is more apparent, but still somewhat damped. Blowby flow rate remains highly correlated to exhaust flow rate, with the blowby flow rate generally at about 1% of the exhaust flow.

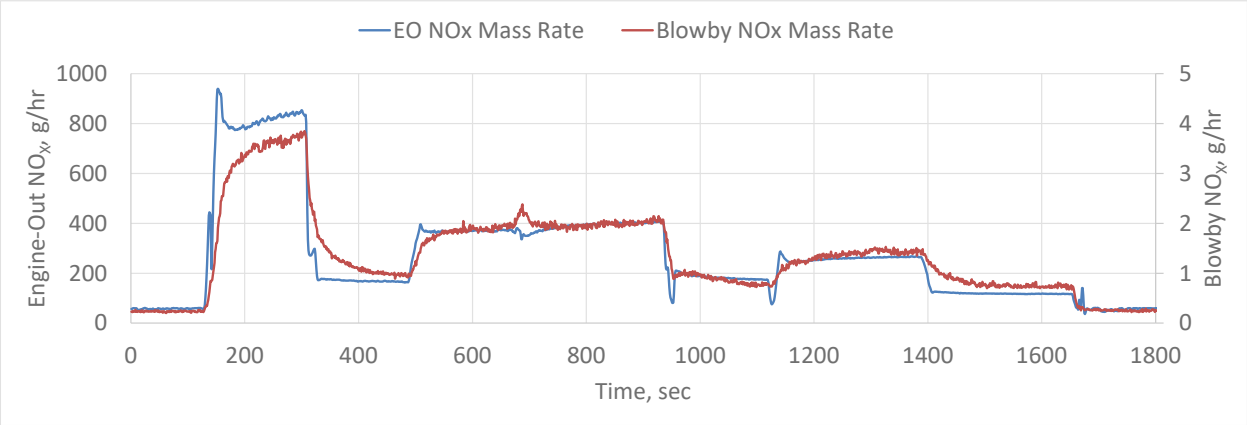



**FIGURE 56. CRANKCASE GAS $NO_X$ CONCENTRATION AS COMPARED TO ENGINE-OUT LEVEL ON RMC**

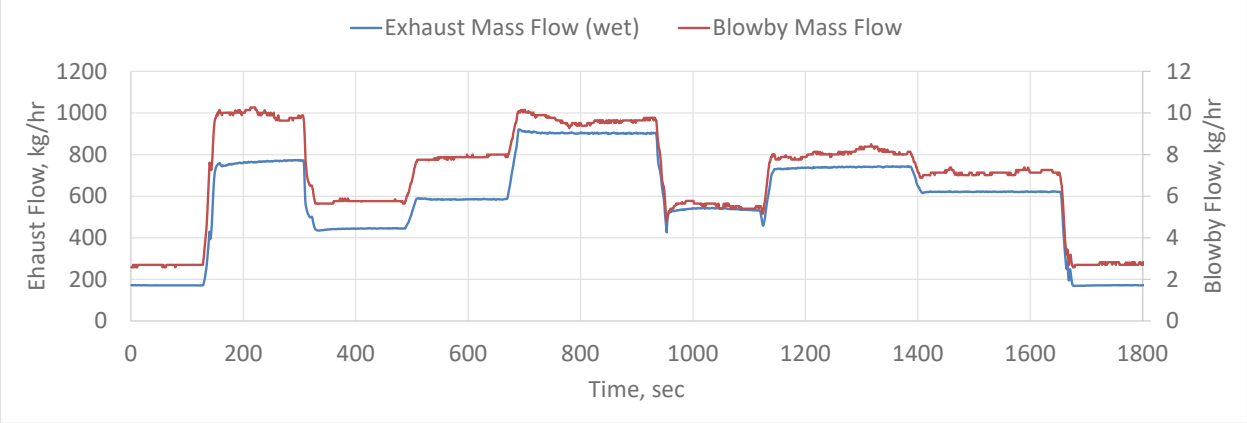



**FIGURE 57. CRANKCASE GAS FLOW RATE AS COMPARED TO ENGINE EXHAUST FLOW ON RMC**

Additional testing in the Stage 2 program indicated that crankcase emission levels remained consistent test-to-test and day-to-day. As a result of these experiments, it was decided that the remainder of the demonstration effort would be carried out using a CCV configuration. This is consistent with existing regulatory requirements that primarily require CCV when doing emissions testing, with OCV as an option under certain conditions. The impact of moving to OCV can be readily estimated by adding a factor of 0.01 g/kw-hr to the tailpipe emission levels observed for any Package 2 system to the levels showing for CCV.

## 3.3 Package 2 Engine Calibrations

Significant detail was given in the Stage 2 final report regarding the development of the modified engine calibrations, and those details will not be repeated in this report. Because this report is focused primarily on Package 2 results targeting both tailpipe $NO_X$ and $CO_2$ reductions, only the Package 2 calibration and further modifications and optimization will be discussed in this report.

The Package 2 calibration differs from Package 1 primarily by modifications made to reduce $CO_2$ emissions, while at the same time maintaining the thermal management modes necessary to assist in achieving Low $NO_X$ levels. This included a more fuel efficient "normal" operating mode calibration with advanced injection timing and higher engine-out $NO_X$. It was expected that the advanced aftertreatment systems would have the capability to handle the higher engine-out $NO_X$ levels and still achieve the program tailpipe $NO_X$ targets.

The base aftertreatment system and Deere's proprietary ECU access software were used for developing the Package 2 calibrations. The control software for the CDA hardware was implemented in a supervisory controller with fast communication access with the engine ECU and special provisions to allow individual cylinder fuel control on a cycle-by-cycle basis. In addition, combustion quality was monitored with cylinder pressure measurement in each cylinder.

At the end of the initial development effort in the Stage 2 program, the modified calibrations had achieved $CO_2$ reductions noted in Figure 58, and these had been achieved through a combination of engine calibration, thermal management modes, and the application of DSF. These levels did not reach the program target levels of a 5% to 8.6% reduction in $CO_2$, especially on the NRTC cycle. Therefore, more work was needed to further refine the Package 2 calibration, both with and without DSF. It should be noted that the Package 2 calibrations that generated these $NO_X$ levels had an engine-out $NO_X$ level on the NRTC of 2.8 g/kw-hr, and 3.7 g/kw-hr on the RMC.

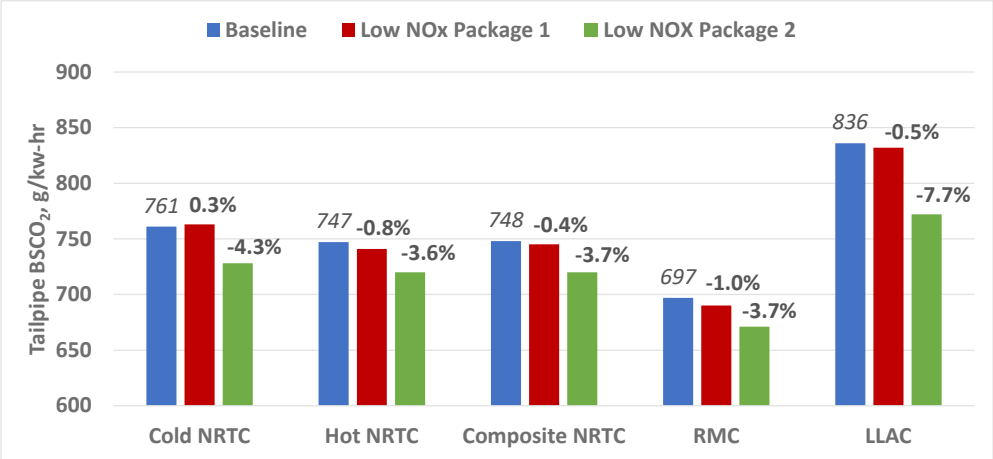



**FIGURE 58. $BSCO_2$ EMISSIONS SUMMARY FOR BASELINE AND LOW $NO_X$ CALIBRATIONS**

To reach the desired $CO_2$ reduction targets, further changes were made to both the modified "normal" mode calibration, and to the thermal management strategy triggers, leveraging the capability of the advanced aftertreatment systems. The final Package 2 calibration had an engine-out level of nominally 4.1 g/kw-hr on both the NRTC and the RMC. This final calibration proved capable of reaching the desired $CO_2$ levels, but the elevated engine-out $NO_X$ levels put more pressure on the aftertreatment system, resulting in the need for more technology.

## 3.4 Package 2 Results with Updated Engine Calibration

Initial experiments on Package 2 focused on whether sufficient $NO_X$ margins could be achieved using a conventional DOC+DPF+SCR aftertreatment architecture. Evaluations were run with both Team 1 and Team 2 conventional aftertreatment packages. These were combined with the modified Package 2 calibration which was able to meet $CO_2$ reduction targets for the program.

Table 13 shows the results for the Team 2 conventional AT package (DOC+DPF+SCR) with the updated Package 2 calibration using DSF with a CCV system. Figure 59 shows margin projection at 12,000-hour FUL for this system even though the decision had been made to retain 8,000-hour useful life periods under Tier 5. While the $CO_2$ emissions are reaching targets, tailpipe $NO_X$ levels are higher, and do not appear to be sufficient to achieve the desired margins at FUL. In addition, given the known impact of DSF of about 1% $CO_2$ improvement on the NRTC and RMC, the modified engine calibration appeared capable of reaching the $CO_2$ reduction targets even without the use of DSF. However, this would place even more pressure on the tailpipe $NO_X$ levels. These results indicated that more technology was needed on the AT system to achieve both $NO_X$ and $CO_2$ targets for Package 2, even with the use of DSF.

**TABLE 13. PACKAGE 2 RESULTS WITH TEAM 2 CONVENTIONAL ARCHITECTURE AND UPDATED CALIBRATION WITH DSF AND DEVELOPMENT AGED PARTS**

| Cycle | EO $NO_X$, g/kw-hr | TP $NO_X$, g/kw-hr | $NO_X$ Efficiency, % | $CO_2$, g/kw-hr | Baseline $CO_2$, g/kw-hr | $CO_2$ Reduction, % | $N_2O$, g/kw-hr |
|---|---|---|---|---|---|---|---|
| Cold NRTC (DSF) | 3.7 | 0.128 | 96.6 | 720 | 761 | 5.4% | 0.049 |
| Hot NRTC (DSF) | 4.3 | 0.006 | 99.9 | 690 | 747 | 7.6% | 0.077 |
| **Composite NRTC (DSF)** | **4.2** | **0.012** | **99.7** | **692** | **748** | **7.5%** | **0.076** |
| **RMC C1 (DSF)** | **4.1** | **0.014** | **99.7** | **660** | **699** | **5.6%** | **0.062** |
| **LLAC (DSF)** | **5.9** | **0.012** | **99.8** | **738** | **836** | **11.7%** | **0.10** |

Figure 60 shows a margin projection at an 8000-hour FUL point for this same system. As noted earlier this projection was based on system durability experience over similar periods from the on-highway system. In this case, projected $NO_X$ margins on the NRTC and RMC are better, though still not ideal. It is for this reason that additional technology beyond simply a conventional DOC+DPF+SCR system was needed for the final system configuration.

| | | NRTC | | | |
|---|---|---|---|---|---|
| | | 5% | 95% | | |
| | | Cold | Hot | RMC | LLC |
| | | g/kw-hr | g/kw-hr | g/kw-hr | g/kw-hr |
| Standard | | 0.04 | | 0.04 | 0.10 |
| Certification Targets | Engine-Out | 3.7 | 4.3 | 4.1 | 5.9 |
| | Conversion | 96.6% | 99.9% | 99.7% | 99.8% |
| | Tailpipe | 0.128 | 0.006 | 0.014 | 0.012 |
| | TP Composite | | 0.013 | | |
| | EO Composite | | 4.3 | | |
| | Composite Conversion | | 99.7% | | |
| FUL Compliance | FUL Durability Loss Margin | 0.7% | 0.5% | 0.5% | 1.0% |
| | FUL Conversion | 95.8% | 99.4% | 99.2% | 98.8% |
| | FUL Tailpipe | 0.155 | 0.028 | 0.035 | 0.071 |
| | FUL Composite Conversion | | 99.2% | | |
| | IRAF | | 0.002 | 0.002 | 0.004 |
| | Final TP Composite | | 0.036 | 0.037 | 0.075 |
| | Margin to Standard | % std | 9% | 8% | 25% |
| | | g/kw-hr | 0.004 | 0.003 | 0.025 |
| Urea Consumption Relative to Fuel | | | | | 3.5% |

**FIGURE 59. MARGIN PROJECTIONS AT 12,000 HOUR FUL FOR CONVENTIONAL ARCHITECTURE WITH DSF**

| | | NRTC | | | |
|---|---|---|---|---|---|
| | | 5% | 95% | | |
| | | Cold | Hot | RMC | LLC |
| | | g/kw-hr | g/kw-hr | g/kw-hr | g/kw-hr |
| Standard | | 0.04 | | 0.04 | 0.10 |
| Certification Targets | Engine-Out | 3.7 | 4.3 | 4.1 | 5.9 |
| | Conversion | 96.6% | 99.9% | 99.7% | 99.8% |
| | Tailpipe | 0.128 | 0.006 | 0.014 | 0.012 |
| | TP Composite | | 0.013 | | |
| | EO Composite | | 4.3 | | |
| | Composite Conversion | | 99.7% | | |
| FUL Compliance | FUL Durability Loss Margin | 0.4% | 0.3% | 0.3% | 0.7% |
| | FUL Conversion | 96.1% | 99.6% | 99.4% | 99.1% |
| | FUL Tailpipe | 0.144 | 0.019 | 0.026 | 0.053 |
| | FUL Composite Conversion | | 99.4% | | |
| | IRAF | | 0.002 | 0.002 | 0.004 |
| | Final TP Composite | | 0.028 | 0.028 | 0.057 |
| | Margin to Standard | % std | 31% | 30% | 43% |
| | | g/kw-hr | 0.012 | 0.012 | 0.043 |
| Urea Consumption Relative to Fuel | | | | | 3.5% |

**FIGURE 60. MARGIN PROJECTIONS AT 8,000 HOUR FUL FOR CONVENTINAL ARCHITECTURE WITH DSF**

## 3.6 Aftertreatment Heating – e-Heater and EHM Testing

Given the previous results, it was clear that more aftertreatment technology was needed to reach Package 2 targets, even with the use of DSF. The various aftertreatment heating options were fabricated to be mounted on the Team 2 conventional system to examine the potential for exhaust heating in enabling the systems to reach targets. Given that hot-start NRTC values were already at 0.006 g/kw-hr, there was not much additional room to gain there. As a result, the initial focus was on improved cold-start performance. All of the initial heater evaluations were conducted using the DSF-enabled calibration, because that was the one which was closest to demonstrating the desired $CO_2$ reductions. However, it should be noted that DSF was not active during the early cold-start, therefore this would not affect the cold-start comparisons on early warm up.

While the EHM enabled low temperature dosing, the primary limiting factor on early cold-start conversion was the initial warmup. Therefore, the EHM and e-Heater systems generated similar results, and the primary driver of changes in this configuration was the heat capacity of the system. The EHM had a combined capacity of 6.3 kw, while the e-Heater had a capacity of 6.8kw. A later test configuration to add even more heat was also testing using a combination of both of these systems in series, with combined total heat capacity of 10kw. As noted earlier, for all of these tests the heater power was applied as an offset to measured torque in real-time, accounting for the input heater power in a representative fashion.

It should be noted that this additional load actually impacted the engine calibration causing an unexpected early increase in the engine-out $NO_X$. This issue was resolved with a relatively minor change to the cold-start thermal mode calibration, but it does serve to illustrate the complexity of these system interactions. This behavior is illustrated in Figure 61, both before and after the calibration adjustment, as compared to the systems without an aftertreatment heating. It should be noted that without the realistic application of heater power to load in real-time, this real issue would not have been observed in the lab testing. This highlights the importance of proper application of heater power to the engine for a representative result.

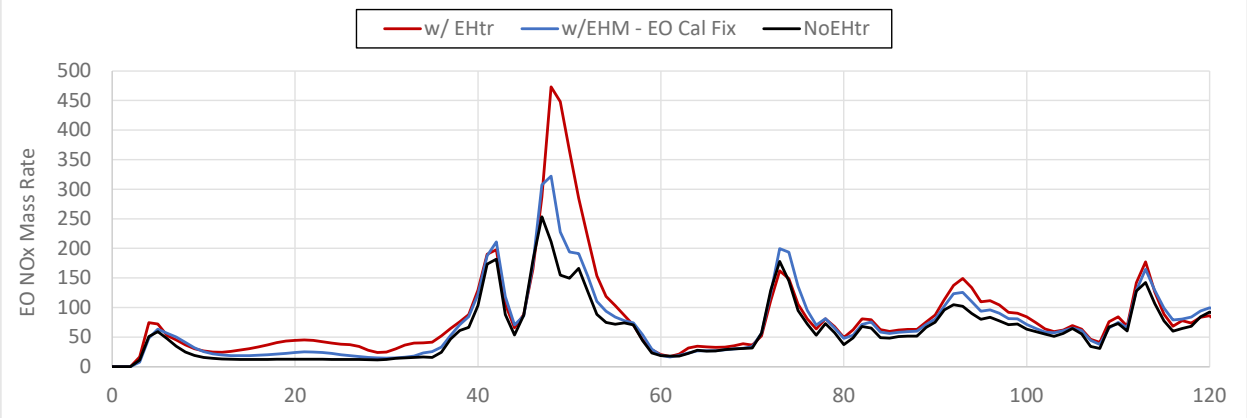
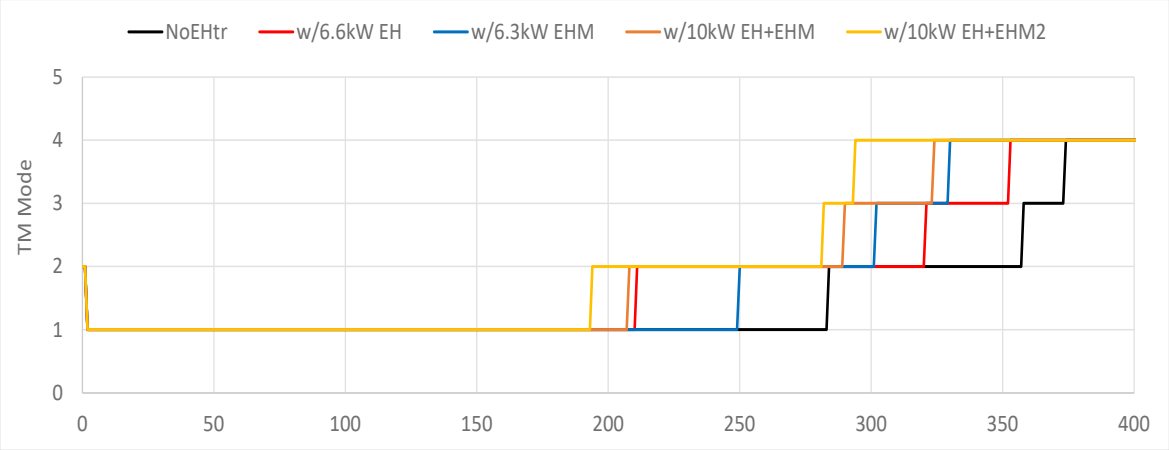



**FIGURE 61. ENGINE-OUT $NO_X$ IN EARLY COLD-START NRTC SHOWING HEATER IMPACT BEFORE AND AFTER CALIBRATION ADJUSTMENT**

Each of the heaters was initially tested separately and different strategies were implemented and tried for each. The heaters and strategy were generally compared using the cold-start NRTC first, because this was one of the cycles where the heater was needed the most. The RMC cycle needed no additional temperature, and it was generally found that a relatively small amount of heater power was sufficient to address the LLAC with DSF. On that cycle, all the heaters performed equally well at all maximum power levels, because the amount of heat needed for the LLAC was small. For the hot NRTC cycle, which was already at 6 mg/kw-hr, there was not much more room for improvement, although some heat could gain an additional 2-3 mg/kw-hr. To reach a reasonable margin, especially at a 12,000-hour durability target, it would be necessary to improve cold-start efficiency to 98% or better, reach a tailpipe level of less than 0.08 g/kw-hr. For 8000-hr durability an improvement to 97% would be sufficient at 0.11 g/kw-hr.

Rather than look at each heater result separately, the results for all the primary heater configurations tested are compared in Figure 62 which shows the early portions of the cold-start NRTC in terms of power consumption, key system temperatures, and the behavior of the engine-based thermal management in response to the input of additional heat to the system. Figure 63 shows the impact of the heaters on DEF dosing, and in particular shows the ability to start DEF dosing earlier with the additional system heat. Figure 64, shows the impact of the heater configurations on both engine-out $NO_X$ and tailpipe $NO_X$ on a continuous basis over the first 200 seconds of the cycle. Note that engine-out $NO_X$ impacts are due primarily to increased fueling in the early cycle as a result of the need to power the heater, as well as change in thermal management behavior. Figure 65 shows $NO_X$ conversion during the early cold-start, showing the onset and ramp up of SCR activity in the system. Finally, Figure 66 shows a comparison of cumulative tailpipe $NO_X$ and system temperatures, to help evaluate the final impact of the heater input on tailpipe emissions.

Figure 62 shows the Mixer Inlet temperature downstream of the heater, and also the mid-bed SCR system temperature at the outlet of the first SCR brick (which is the temperature that governs the thermal management choices in the conventional architecture aftertreatment system). Note that the EHM will not cause an increase in mixer inlet temperature because it is downstream



of this measurement, but the same increase is seen later at the outlet of the heater and is comparable to the heat increase of the e-Heater. However, the EHM still allows a significantly earlier start to DEF dosing due to the impact of the heated DEF mixer surface. As seen in Figure 63, the system with no heater does not reach sufficient temperature to allow DEF dosing until 365 second into the cycle. The higher system temperatures near the mixer allowed all of the heated-enabled systems to begin DEF dosing before 150 seconds into the cycle. However, due to the cold SCR temperatures this did not result in any $NO_X$ conversion behavior until later, although it did help build storage somewhat faster so that conversion was better once temperatures were high enough. Therefore, the primary limiting factor in the early cycle for $NO_X$ conversion is temperature, rather than DEF availability. Figure 62 also shows the earlier changes in thermal management, with the higher modes representing less thermal management, as the system warms up more quickly. However, these changes in thermal management don't begin to show until about 200 seconds into the cycle.

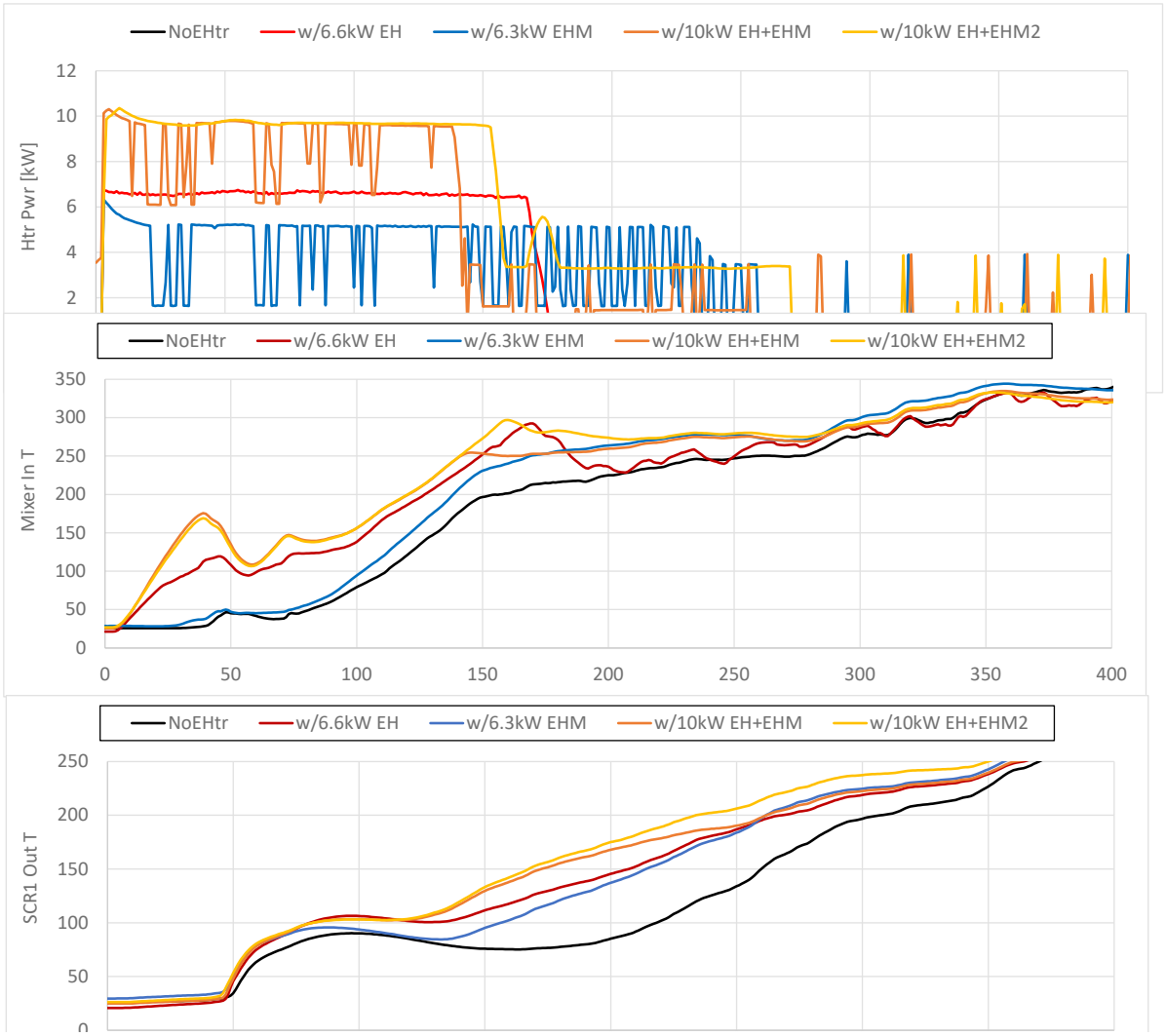



**FIGURE 62. HEATER POWER, SYSTEM TEMPERATURES, AND THERMAL MANAGEMENT BEHAVIOR FOR VARIOUS HEATER CONFIGURATIONS IN EARLY COLD-START NRTC**

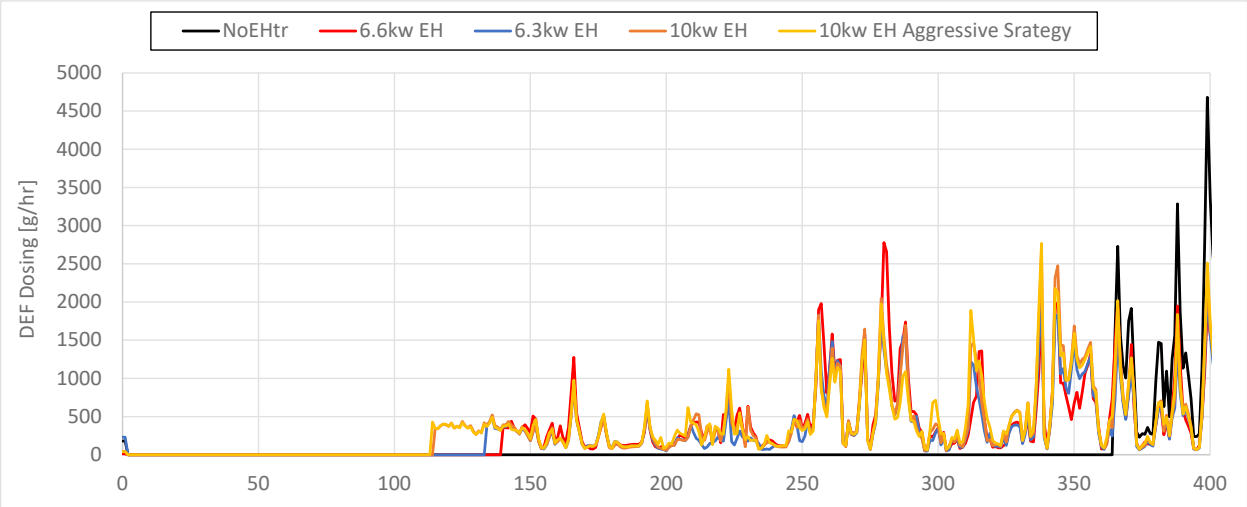



**FIGURE 63. DEF DOSING IN EARLY COLD-START NRTC FOR VARIOUS HEATER CONFIGURATIONS**

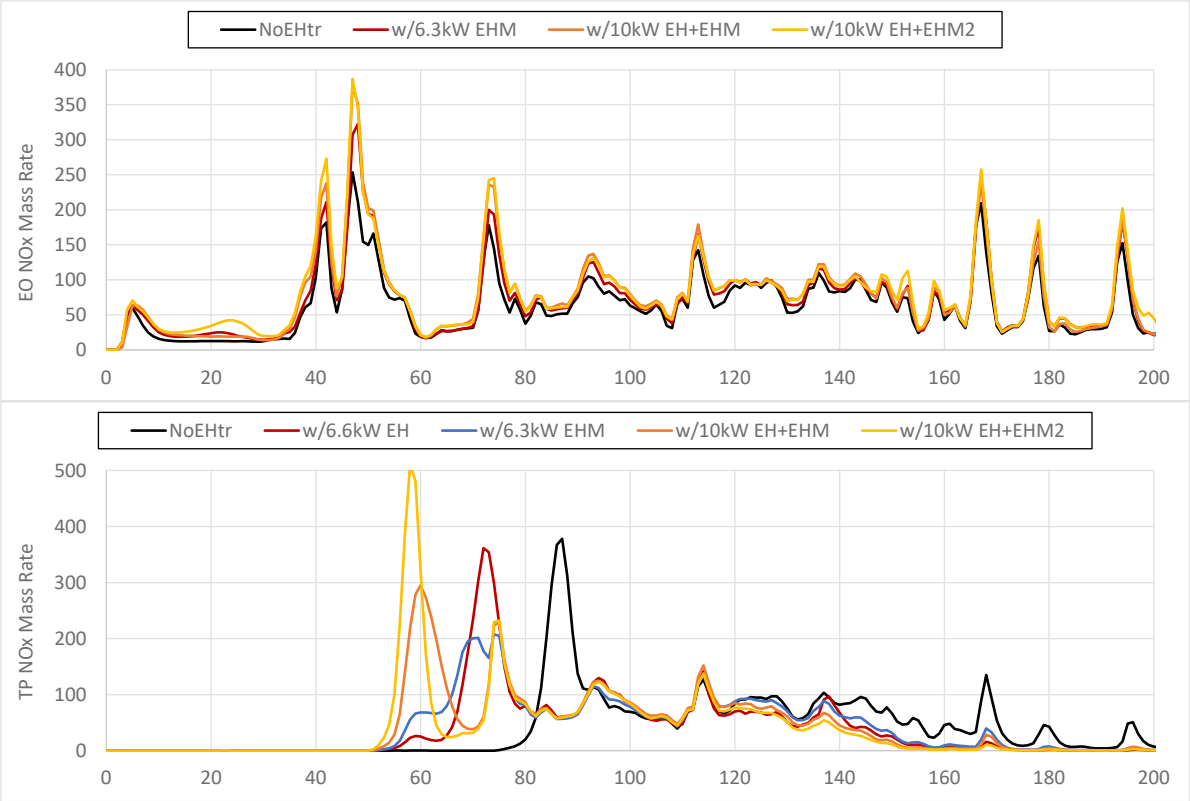



**FIGURE 64. CONTINUOUS EARLY COLD-START NRTC ENGINE-OUT AND TAILPIPE NOX FOR VARIOUS HEATER CONFIGURATIONS**

Looking at the data in Figure 64, it can be seen that the onset of improvement in tailpipe $NO_X$ behavior compared to the unheated case begins around 120 to 140 seconds into the cycle. The $NO_X$ conversion chart in Figure 65 gives a clear indication of the heater impact on SCR activity. All of the heaters resulted in an improvement of at least 40 seconds in the onset of SCR

light-off (the point at which the system first reaches 50% conversion). Furthermore, the SCR conversion reach in excess of 95% by 200 seconds, about 100 seconds earlier than without the heaters. However, the increase in heat from 6 kw to 10kw resulted in little further improvement, perhaps only 10 more seconds of improvement in light-off for an 80% increase in heat input. This indicates that further improvement would have required substantially more heat, and as noted earlier it was felt that heater capacity beyond 10kw was considered impractical for this size engine.

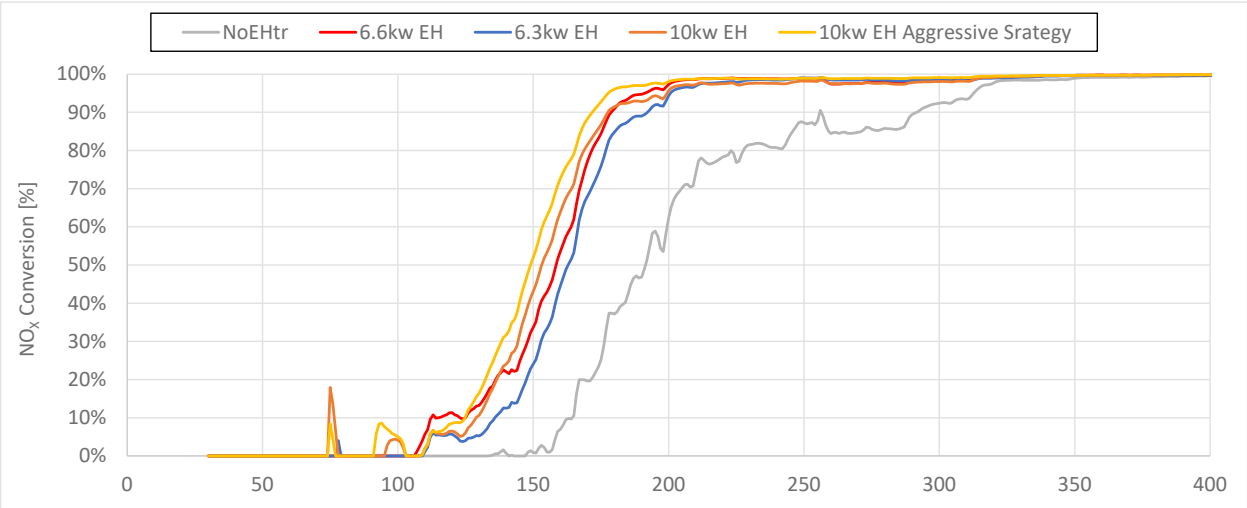



**FIGURE 65. EARLY COLD-START NRTC $NO_X$ CONVERSION FOR VARIOUS HEATER CONFIGURATIONS**

The impact of these changes on tailpipe $NO_X$ is illustrated in Figure 66, along with system temperatures again for reference. The key point in these cumulative graphs that indicates SCR function is the point where the accumulation of $NO_X$ has substantially ended, indicated that the "cold-start peak" is now over. For the baseline conventional system without a heater, this point does not occur until 250 seconds into the cycle, with another secondary bump in $NO_X$ until the 300-second mark. For all of the heater configurations, this point occurs around the 150-second point, fully 100 seconds sooner. However, the initial rate of $NO_X$ accumulation is somewhat faster, and that rate increases with increased heater power. This is because in the earlier cycle, engine-out $NO_X$ rates are higher due to the extra power required to drive the heater at high input. This causes an increase in $NO_X$ that occurs well before SCR light-off, and it serves to offset some of the improvements in the pace of SCR light-off. This is part of the reason why increased heater power did not actually result in much tailpipe $NO_X$ improvement.

Table 14 shows cold-start NRTC cycle $NO_X$ levels for the various heater configurations. Both the 6.6kw e-Heater and the 6.3 kw EHM assembly were able to reach cold-start NRTC levels of 0.10 g/kw-hr or a $NO_X$ conversion of 97.4%. This was considered sufficient to enable desired margins at 8,000 hours of aging, but not at 12,000 hours of aging, as noted earlier. However, the application of more heater power did not further improve tailpipe $BSNO_X$ levels, but it did result

in increased $CO_2$ levels by about 1.5%. Use of electrical heating does not necessarily incur a fuel consumption penalty: for the lower power heater configurations, Cold-start $CO_2$ levels were unchanged, with the heater power cost being offset by fuel savings due to earlier switching out of aggressive engine thermal management, as shown in Figure 62 earlier.

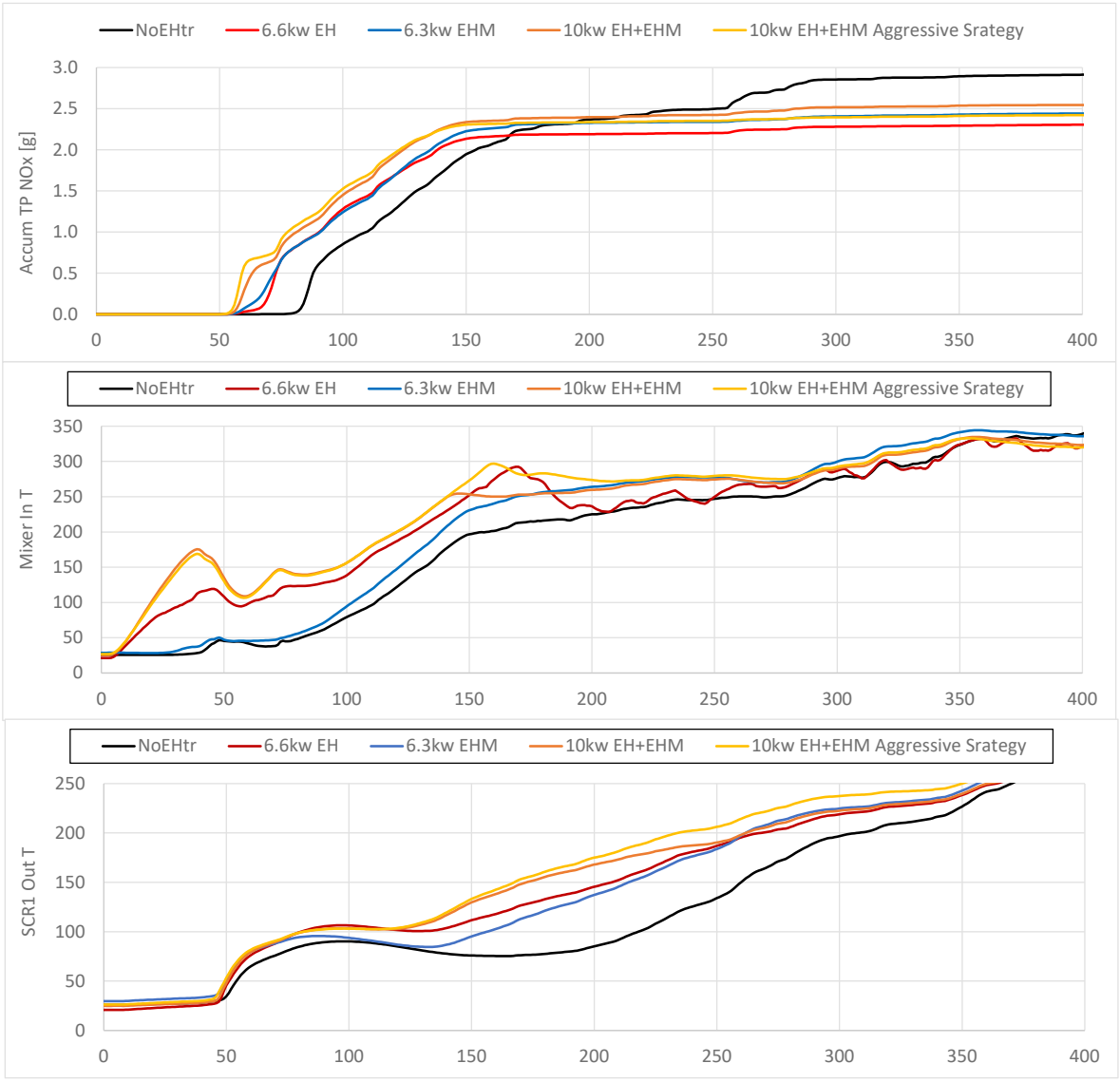



**FIGURE 66. CUMULATIVE EARLY COLD-START NRTC $NO_X$ AND SYSTEM TEMPERATURES FOR VARIOUS HEATER CONFIGURATIONS**

**TABLE 14. HEATER CONFIGURATION IMPACT ON COLD-START NRTC BSNO$_X$**

| Configuration | Cold-Start NRTC Tailpipe Emissions, g/kw-hr | |
|---|---|---|
| | $NO_X$ | $CO_2$ |
| No Heater | 0.13 | 715 |
| 6.6kw EH | 0.10 | 716 |
| 6.3kw EHM | 0.10 | 720 |
| 10kw EH+EHM | 0.11 | 728 |
| 10kw EH+EHM Aggressive Strategy | 0.10 | 726 |

Table 15 shows the best cycle results obtained with either the 6.6kw e-Heater or the 6.3kw EHM assembly. It should be noted that the heaters were barely active during the hot-start NRTC, though it was also noted that the $N_2O$ emissions were higher than expected during these cycles, likely indicating a need to re-optimize the dosing targets. Similarly, the heaters were on during the LLAC but it was clear that to see further $NO_X$ reduction a larger heater power would be needed. However, it was noted that the engine was able to stay in fuel economy mode over the entire LLAC, therefore some room was available. The additional available heat capacity would also likely be useful in low ambient temperature situations. These strategies would be optimized further, along with a re-tuning of storage targets, if the heater technology was selected for the final Package 2 configuration.

**TABLE 15. BEST HEATER ENABLED RESULTS (EH OR EHM ~ 6.5KW CAPACITY) WITH DSF, CCV**

| Cycle | EO $NO_X$, g/kw-hr | TP $NO_X$, g/kw-hr | $NO_X$ Efficiency, % | $CO_2$, g/kw-hr | Baseline $CO_2$, g/kw-hr | $CO_2$ % Change | TP $N_2O$, g/kw-hr |
|---|---|---|---|---|---|---|---|
| Cold NRTC | 3.8 | 0.104 | 97.3 | 723 | 761 | 5.0% | 0.088 |
| Hot NRTC | 4.2 | 0.003 | 99.9 | 691 | 747 | 7.4% | 0.115 |
| **Composite NRTC** | **4.3** | **0.007** | **99.8** | **693** | **748** | **7.3%** | **0.114** |
| **RMC C1** | **4.0** | **0.010** | **99.7** | **668** | **699** | **4.4%** | **0.060** |
| **LLAC** | **6.0** | **0.012** | **99.8** | **746** | **836** | **10.8%** | **0.111** |

Ultimately, it was determined that the combination of an aftertreatment heater located after the DPF, in combination with some of the other package catalyst updates discussed below, would be sufficient for a system to demonstrate acceptable margins with 8000-hour aged catalysts. However, it was likely that further optimization would be needed for 12,000 hours of aging that would be 50% beyond current CARB staff assessments of in-use usage data.

### 3.7 Combined Team Package 2 Results with Conventional Aftertreatment Architecture

The system was to combine the best elements of the AT systems between Team 1 and Team 2. The Team 1 SCR catalysts seemed to produce lower $N_2O$ levels, and it was already also

known that they had better high temperature performance under regeneration conditions, leading to lower UAF adjustments for infrequent regeneration. On the other hand, The Team 2 DOC+DPF components appeared to perform better and also appeared to generate better $NO_2$ levels in the SCR feedgas. Therefore a combination of these elements could make for a superior final system. Table 16 shows the results with the modified calibration for the combined conventional AT system with DSF. This combined package produced better $NO_X$ results than the results for Team 1 and Team 2 and had lower $N_2O$ emissions as well. These levels appear to be sufficient to provide the desired margin at 12,000 hour FUL, though LLAC emission levels appeared to have room for improvement compared to other configurations. Based on the previous heater testing results, it was evident that the addition of an aftertreatment heater to this combined system could address the LLAC emissions with only a small amount of heater power input, and there was plenty of room to still maintain substantial $CO_2$ reductions while paying the relatively small fuel cost of a low power heater input.

**TABLE 16. PACKAGE 2 RESULTS WITH COMBINED TEAM CONVENTIONAL ARCHTECTURE ON DEVELOPMENT AGED PARTS WITH UPDATED CALIBRATION AND DSF, CCV**

| Cycle | EO $NO_X$, g/kw-hr | TP $NO_X$, g/kw-hr | $NO_X$ Efficiency, % | $CO_2$, g/kw-hr | Baseline $CO_2$, g/kw-hr | $CO_2$ % Change | TP $N_2O$, g/kw-hr |
|---|---|---|---|---|---|---|---|
| Cold NRTC | 3.7 | 0.116 | 96.9 | 724 | 761 | 4.9% | 0.049 |
| Hot NRTC | 4.3 | 0.004 | 99.9 | 698 | 747 | 6.5% | 0.071 |
| **Composite NRTC** | **4.3** | **0.007** | **99.8** | **701** | **748** | **6.3%** | **0.070** |
| **RMC C1** | **4.0** | **0.007** | **99.8** | **667** | **699** | **4.6%** | **0.033** |
| **LLAC** | **5.9** | **0.019** | **99.7** | **741** | **836** | **11.4%** | **0.111** |

Performance for the combined system was also briefly examined without DSF, but only over the NRTC. The results are shown in Table 17. As expected, for the conventional architecture without DSF, significantly more thermal management was needed without DSF and the $CO_2$ targets could not be met. Based on these results, it was apparent that a conventional DOC+DPF+SCR architecture could not meet the Package 2 targets without the additional engine technology lever of DSF (or something equivalent).

**TABLE 17. PACKAGE 2 RESULTS WITH COMBINED TEAM CONVENTIONAL ARCHITECTURE ON DEVELOPMENT AGED PARTS WITH UPDATED CALIBRATION AND NO DSF, CCV**

| Cycle | EO $NO_X$, g/kw-hr | TP $NO_X$, g/kw-hr | $NO_X$ Efficiency, % | $CO_2$, g/kw-hr | Baseline $CO_2$, g/kw-hr | $CO_2$ Reduction, % | $N_2O$, g/kw-hr |
|---|---|---|---|---|---|---|---|
| Cold NRTC (noDSF) | 3.4 | 0.117 | 96.5 | 734 | 761 | 3.5% | 0.048 |
| Hot NRTC (noDSF) | 3.6 | 0.007 | 99.8 | 720 | 747 | 3.6% | 0.062 |
| **Composite NRTC (noDSF)** | **3.6** | **0.012** | **99.7** | **721** | **748** | **3.6%** | **0.060** |

Ultimately the combined package proved to have a combination of slightly better tailpipe $NO_X$ emissions and significantly lower $N_2O$ emissions. The combined system would also benefit from the lower impact of regeneration emissions with the Team 1 SCR catalysts. Therefore, the Team 1 SCR catalysts would be used moving forward in whichever architecture was finally selected, regardless of the technologies chosen before the mixer.

### *3.7.1. Idle Emissions Testing*

An additional assessment was carried out at this point in the program to examine idle emissions in the context of a potential clean idle standard for off-road engines. This testing was run on the combined conventional aftertreatment system using the Package 2 configuration. Methodology had not yet been defined for this testing, therefore, SwRI ran the engine over a test protocol similar to what is used for extended clean idle testing for on-highway engines. The test sequence used was as follows:

- A preconditioning of one hot-start NRTC cycle.
- Transition immediately to Mode 1 consisting of 30 minutes of low idle with a representative load (52 Nm was used in this case).
- Transition immediately to Mode 2 consisting of 30 minutes of operation at 1100rpm with a representative load (88 Nm was used in this case).

The test loads were decided based on consultation with Deere. In discussions regarding the idle loads chosen for the LLAC, Deere indicated that a load of 10% (measured as a percentage of available torque at that speed) was more broadly applicable to their applications than the original 5% used for the LLAC. Therefore, SwRI used this guidance of 10% of torque available at speed to set the loads for both Modes of the extended idle test. It should be noted that the resulting load for Mode 1 (low idle) was very close to the final idle load later determined for the LLC at 2.5% of maximum power. Therefore, it is felt that this scaling was appropriate for both speeds. The calibration used for this cycle was unmodified from the calibration used to generate the results in Table 17. It should be noted that this calibration does not include the use of EGR during idle operations, because an EGR cooler bypass was not selected for the engine configuration and there were concerns about the risks of condensation in the EGR cooler during extended idle.

The result for this test is illustrated in Figure 67. The top graph shows the speed and torque for the test, while the middle graph illustrates system temperatures and the behavior of the thermal management over the test. The bottom graph shows engine out and tailpipe $NO_X$ emissions. The final results for the test are given in Table 18, showing the average of the last 20-minutes of each test mode. In the case of Mode 1, the SCR catalyst stabilized in thermal management at 185°C, with the mixer upstream at the dosing temperature having a 190°C inlet temperature. In the case of Mode 2, the engine cycles through thermal management modes in a stable pattern at this condition, varying between all three modes as AT temperature varied, with an average temperature of 215°C.

**TABLE 18. EXTENDED IDLE TEST RESULTS**

| Test Mode | $NO_X$ Mass Rate, g/hr | | Stable SCR Temperature |
|---|---|---|---|
| | Engine-Out | Tailpipe | degC |
| Mode 1 | 41 | 2.9 | 185 |
| Mode 2 | 68 | 0.3 | 180-250 oscillating |

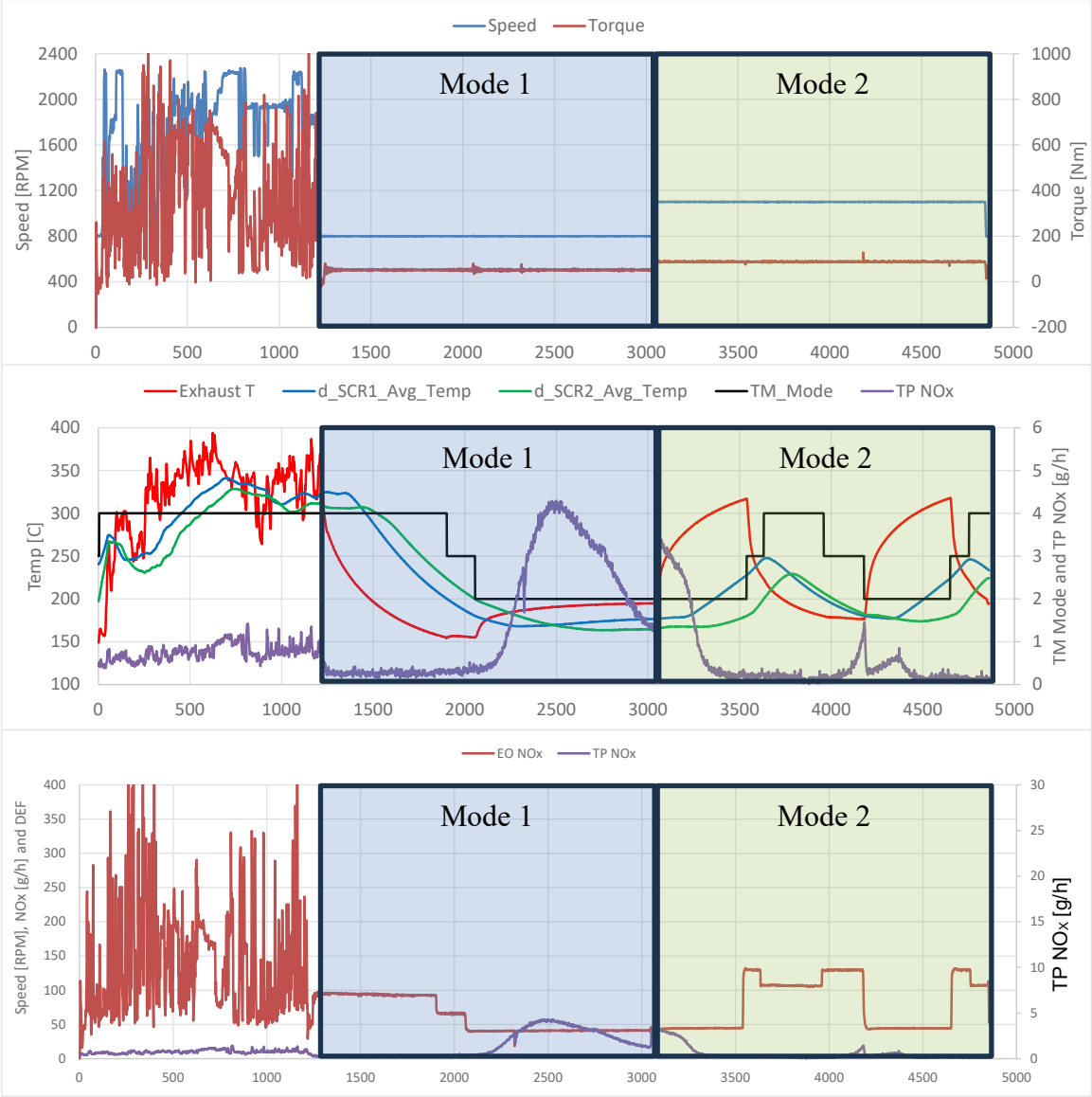



**FIGURE 67. EXTENDED IDLE TEST RESULTS FOR TIER 5 DEMONSTRATION ENGINE WITH COMBINED TEAM CONVENTIONAL AFTERTREATMENT AND DEVELOPMENT AGED PARTS**

## 3.8 Evaluation of Dual Dosing Dual SCR Architecture

It was apparent from the previous testing that with conventional DOC+DPF+SCR architecture Package 2 targets could only be met using DSF, possibly in conjunction with some form of aftertreatment heater after the DPF to ensure robust capability and margin on all cycles with a 12,000-hour durability requirement.

The alternate approach was to move to a dual-dosing dual SCR architecture, reminiscent of the on-highway Low $NO_X$ approach. This would involve adding a LO-SCR option upstream of the DPF. However, as mentioned earlier a different technology was selected for off-road, primarily due to packaging constraints, in the form of the multi-function catalyst (MFC). The

MFC was paired with a zone-coated catalyzed soot filter (zCSF), and this assembly replaced the DOC+DPF from the previous architecture. As noted earlier, these components came from Team 2, but they were paired with the Team 1 downstream SCR catalysts. The MFC technology was also paired with a heated doser to allow maximum leveraging of upstream SCR at low temperatures. It was hoped that this improved AT system capability would enable the engine to meet Package 2 targets without having to rely solely on DSF.

Following preliminary tests with the MFC+zCSF and the heated doser, it became clear that the added capability would allow additional flexibility with the engine calibration. It was also possible to relax some of the thermal management targets, allowing for better $CO_2$ emissions on the NRTC cycle. This resulted in higher engine-out $NO_X$ for tests without DSF than previously observed, but the improved $NO_X$ reduction capability of the aftertreatment system was able to handle that change.

The strategy for the dual SCR architecture is more complicated because there are now two dosing locations and an additional catalyst bed to track with the model-based controller. This was described earlier. The overall strategy must also consider the need to allow sufficient $NO_X$ to reach the filter at higher temperatures to enable passive soot oxidation to continue to function effectively. This means the dosing on the MFC must back off substantially at higher temperatures. An example of this is shown in Figure 68, which shows ammonia storage and temperature over a cold-start NRTC cycle. Ammonia storage is tracked as a dimensionless ratio of maximum capacity, and targets are shown with dashed lines while actual storage is shown in solid lines. It can be seen that as the temperature rises, the storage level on the MFC drops rapidly above 250°C to a near zero level above 300°C. At the same time the downstream SCR catalysts maintain a certain storage target level at those same temperatures.

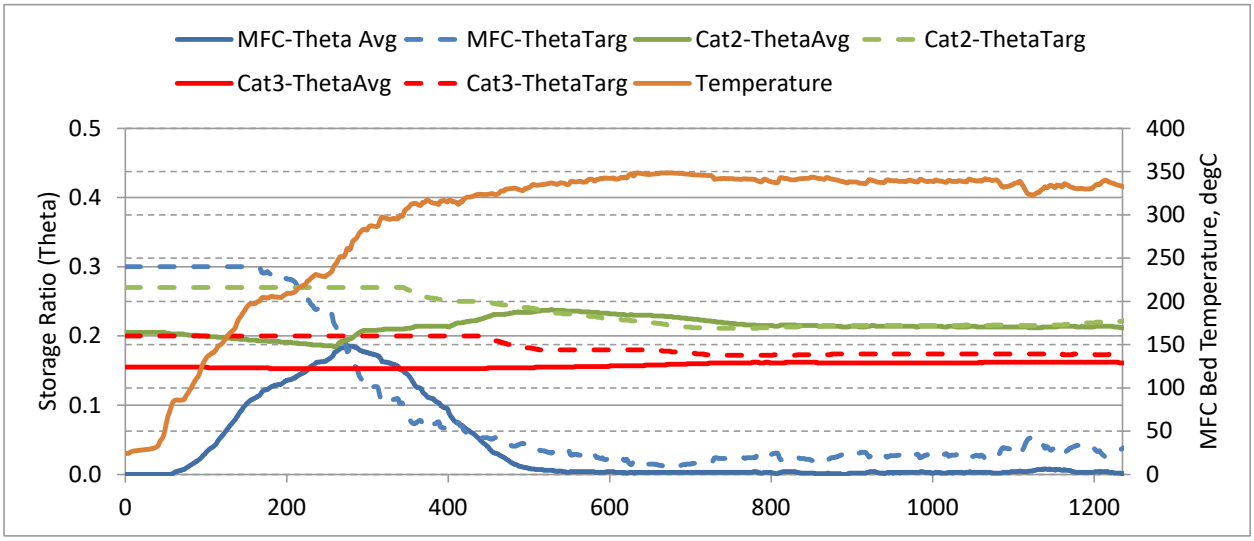



**FIGURE 68. AMMONIA STORAGE VERSUS TEMPERATURE FOR SYSTEM CATALYSTS**

The strategy is further illustrated by looking at the feed-forward ammonia-to-$NO_X$ molar ratio (ANR), which shows the target dosing when the system has reached equilibrium with its storage targets (which generally only occurs during relatively steady operations). An example of these targets over a cold-start NRTC is given in Figure 69. Note that the MFC targets (Doser 1) vary over a wide range from a number greater than 1 at low temperatures, to significantly

underdosing at only 0.3 at temperatures over 325°C. On the other hand, the downstream targets (Doser 2) stay at or above ANR = 1 over the whole temperature range.

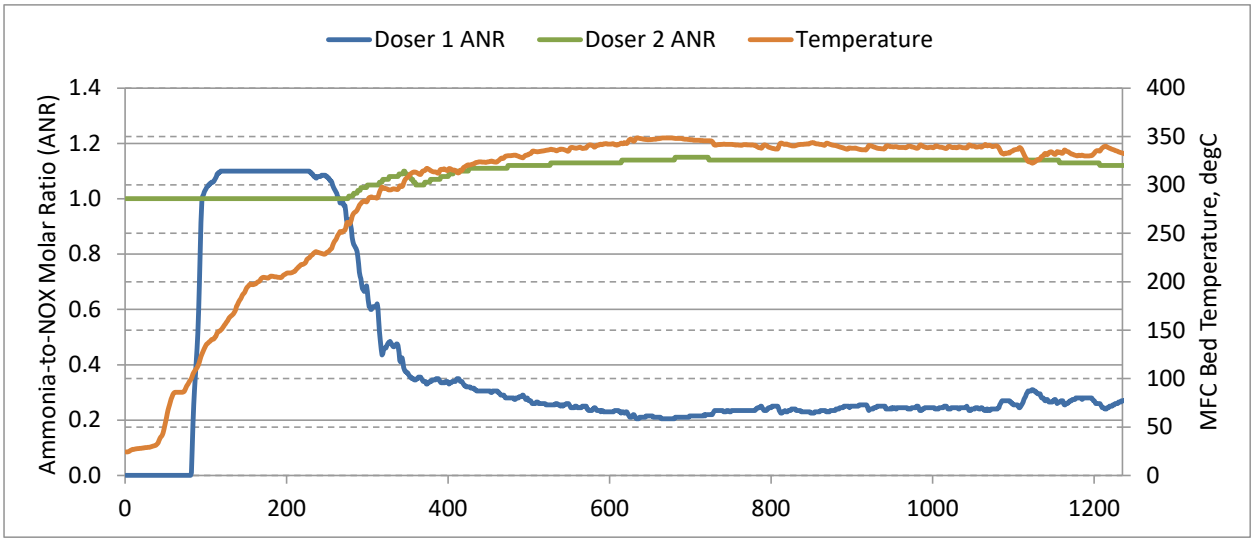



**FIGURE 69. FEED-FORWARD ANR TARGETS FOR UPSTREAM AND DOWNSTREAM DOSERS VERSUS TEMPERATURE**

This illustration also serves to bring up a particular challenge related to the use of LO-SCR (or any SCR) over the NRTC. Note from the temperature trace of the NRTC in Figure 69 that the MFC never falls below 325°C for most of the later part of the cycle. This means that the upstream doser is always in an underdosing mode at this part, as part of the strategy to enable passive soot oxidation. Unfortunately, this also means that there is no opportunity to build any ammonia coverage on the MFC before the engine is shut down. This is quite different from the on-highway FTP cycle, where temperatures are generally cooling down before shutdown, allowing for coverage to be established on the LO-SCR before the engine is turned off. This coverage is important to maximizing the effectiveness of the LO-SCR, but there is no way to leverage that in the NRTC, presenting a unique challenge for cold-start on the off-road duty cycle.

This challenge was apparent in the early tests with the MFC, and it was necessary to change the cold-start dosing strategy to respond to this issue. Because of the lack of initial ammonia coverage on the MFC at the beginning of the cold-start it was necessary to dose aggressively early to get as much ammonia on the catalyst at possible. However, if the strategy was too aggressive at low temperatures there was a risk of deposit formation over repeated cold-starts, and with the mixer being upstream of the aftertreatment it would be very difficult to generate sufficient temperature to remove them. The heated doser proved useful at this point because it allowed a more aggressive strategy with injection starting at 130°C and going to higher early dosing rates than un-heated dosing would allow. The impact of these changes on upstream dosing can be seen in Figure 70 which shows upstream DEF dosing before and after the updates. The start of dosing is moved up in the revised calibration to 53 seconds from 85 seconds, and early dosing rates are increased by 50 percent or more. Accelerated dosing modes where dosing is based on the ability to dose safely without deposit issues at a given temperature and exhaust flow, rather than being tied to engine-out $NO_X$, are calibrated more aggressively. At times the ANR approached 10 or more. This is necessary to force ammonia through the empty catalyst at low temperatures to get as much coverage as possible.

The impact of this change on $NO_X$ behavior can be seen in Figure 71, which shows system temperatures and $NO_X$ emission mass rates in the early cold-start NRTC both before and after the dosing calibration change. The advent of significant $NO_X$ conversion over the MFC is advanced by 35 seconds, and more conversion is achieved earlier. It should be noted that this is only the case because even the outlet MFC has already reached temperatures above 150°C within 90 seconds of cold-start. For the conventional architecture, temperature had been the limited factor for cold-start. With MFC as a LO-SCR, the initial limiting factor was now ammonia availability, and the revised calibration addressed that.

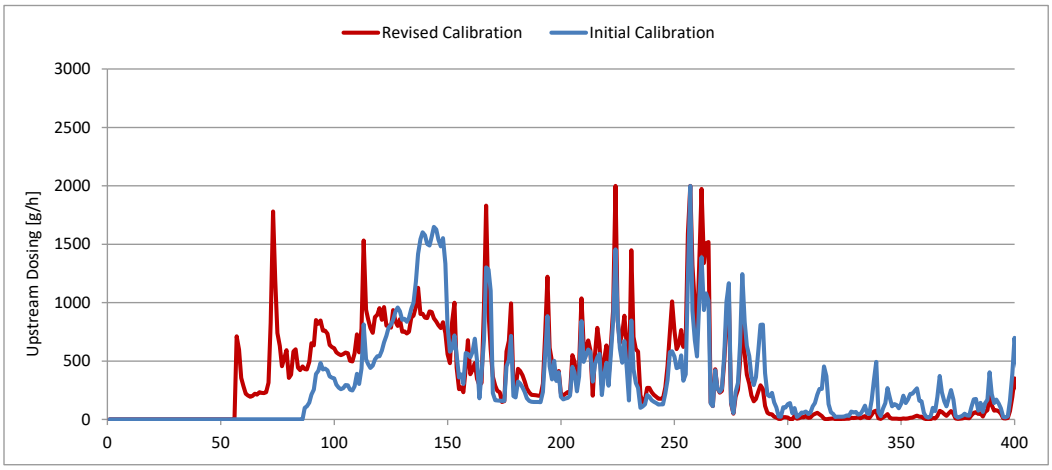



**FIGURE 70. UPDATED DOSING CALIBRATION DURING EARLY COLD-START NRTC**

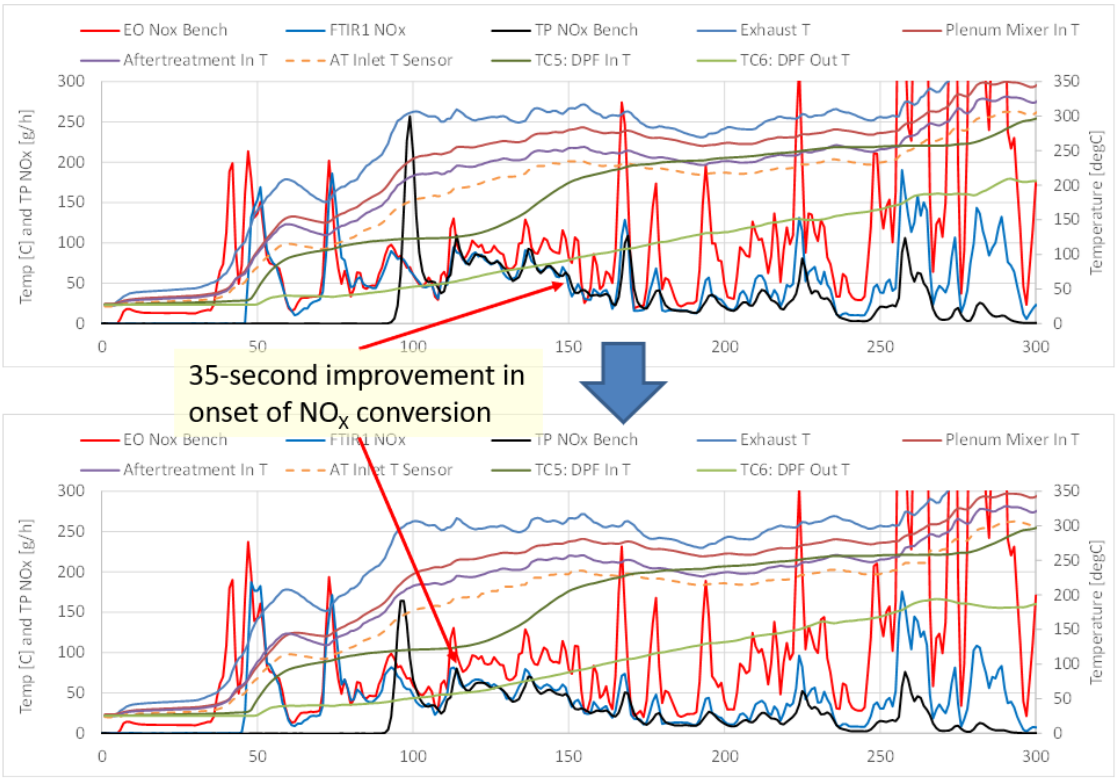



**FIGURE 71. IMPACT OF UPDATED DOSER STRATEGY ON EARLY COLD-START NRTC $NO_X$ CONVERSION OVER MFC**

This configuration was also tried without DSF but still using a revised Package 2 calibration to reach $CO_2$ targets. It turned out that even without DSF, leveraging the MFC and a revised thermal management calibration, along with a few small engine adjustments that did slightly increase engine-out $NO_X$, Package 2 targets could still be reached without DSF with the MFC, which was not the case with the conventional architecture system. A summary of cold-start NRTC emissions in various test configurations is given below in Table 19. With DSF the MFC-enabled configuration was able to reach similar table emission levels as the e-Heater enabled conventional system. However, as noted above, with the MFC it was also possible to reach Package 2 targets without DSF, although the $CO_2$ reduction is somewhat smaller. In addition, with the MFC-enabled configuration, $N_2O$ emissions were well below the Tier 4 baseline engine.

**TABLE 19. COLD-START NRTC EMISSIONS FOR VARIOUS TEST CONFIGURATIONS WITH DEVELOPMENT AGED PARTS, CCV**

| Configuration | Cold-Start NRTC Tailpipe Emissions, g/kw-hr | | |
|---|---|---|---|
| | $NO_X$ | $N_2O$ | $CO_2$ |
| Tier 4 Baseline | 0.387 | 0.065 | 761 |
| **Conventional DOC+DPF+dos+T2SCR with e-Heat, DSF** | **0.104** | **0.088** | **716** |
| Conventional DOC+DOF+dos+T1SCR, DSF | 0.117 | 0.044 | 724 |
| ***Conventional DOC+DOF+dos+T1SCR, no DSF*** | ***0.116*** | ***0.048*** | ***734*** |
| dos+MFC+zCSF+dos+T1SCR, DSF | 0.102 | 0.056 | 719 |
| **dos+MFC+zCSF+dos+T1SCR Revised, DSF** | **0.073** | **0.040** | **721** |
| ***dos+MFC+zCSF+dos+T1SCR Revised, no DSF*** | ***0.080*** | ***0.036*** | ***722*** |

A summary of tailpipe emissions with the MFC-enabled configuration is given in Table 20 for testing with DSF, and for Table 21 without DSF. Both sets of testing were able to meet the Package 2 targets, and with more margin on $NO_X$ than was observed for the conventional system with DSF and e-heater. $N_2O$ emissions were generally lower with the MFC as well, which makes sense considering that with the MFC most of the low temperature $NO_X$ reduction will be based on the standard (NO only) reaction, which does not generate significant $N_2O$. DSF does provide better $CO_2$ reductions generally on the order of 1 to 1.5% on the NRTC and RMC, and 3.5% on the LLAC.

**TABLE 20. TAILPIPE EMISSIONS WITH MFC AND DSF ON ALL CYCLES WITH DEVELOPMENT AGED PARTS, CCV**

| Cycle | EO $NO_X$, g/kw-hr | TP $NO_X$, g/kw-hr | $NO_X$ Efficiency, % | $CO_2$, g/kw-hr | Baseline $CO_2$, g/kw-hr | $CO_2$ Reduction, % | $N_2O$, g/kw-hr |
|---|---|---|---|---|---|---|---|
| Cold NRTC (DSF) | 3.7 | 0.073 | 98.0 | 722 | 761 | 5.1% | 0.040 |
| Hot NRTC (DSF) | 4.3 | 0.003 | 99.9 | 697 | 747 | 6.7% | 0.049 |
| **Composite NRTC (DSF)** | **4.1** | **0.007** | **99.8** | **698** | **748** | **6.6%** | **0.049** |
| **RMC C1 (DSF)** | **4.0** | **0.003** | **99.9** | **662** | **699** | **5.3%** | **0.040** |
| **LLAC (DSF)** | **5.6** | **0.006** | **99.9** | **738** | **836** | **11.1%** | **0.11** |

**TABLE 21. TAILPIPE EMISSIONS WITH MFC ON ALL CYCLES WITHOUT DSF WITH DEVELOPMENT AGED PARTS, CCV**

| Cycle | EO $NO_X$, g/kw-hr | TP $NO_X$, g/kw-hr | $NO_X$ Efficiency, % | $CO_2$, g/kw-hr | Baseline $CO_2$, g/kw-hr | $CO_2$ Reduction, % | $N_2O$, g/kw-hr |
|---|---|---|---|---|---|---|---|
| Cold NRTC (noDSF) | 3.5 | 0.080 | 97.7 | 723 | 761 | 5.0% | 0.036 |
| Hot NRTC (noDSF) | 3.9 | 0.003 | 99.9 | 702 | 747 | 6.0% | 0.049 |
| **Composite NRTC (noDSF)** | **3.9** | **0.007** | **99.8** | **703** | **748** | **6.0%** | **0.049** |
| **RMC C1 (noDSF)** | **4.0** | **0.005** | **99.9** | **672** | **699** | **3.9%** | **0.030** |
| **LLAC (noDSF)** | **5.2** | **0.008** | **99.9** | **773** | **836** | **7.5%** | **0.123** |

Figure 72 shows projected margins for the MFC-enabled system using the Development Aged part results without DSF as the zero-hour values, again assuming degradation rates similar to the on-highway program observations. These show a reasonable margin of 11-13 mg/kw-hr for the NRTC and RMC, and a 36 mg/kw-hr margin to an assumed 0.10 standard for the LLAC (as the placeholder for LLC at this point in the program). This is better than what could be achieved by the e-heater enabled conventional architecture. The 8000-hour projections for the same system (not shown here) actually showed very good margins on the order of 20 mg/kw-hr for the NRTC and RMC.

| | | NRTC | | | |
|---|---|---|---|---|---|
| | | 5% Cold | 95% Hot | RMC | LLC |
| | | g/kw-hr | g/kw-hr | g/kw-hr | g/kw-hr |
| | Standard | **0.04** | | **0.04** | **0.10** |
| Certification Targets | Engine-Out | 3.5 | 3.9 | 4.0 | 5.2 |
| | Conversion | **97.7%** | **99.9%** | **99.9%** | **99.8%** |
| | Tailpipe | **0.080** | **0.003** | **0.005** | **0.008** |
| | TP Composite | | **0.007** | | |
| | EO Composite | | **3.9** | | |
| | Composite Conversion | | **99.8%** | | |
| FUL Compliance | FUL Durability Loss Margin | **0.7%** | **0.5%** | **0.5%** | **1.0%** |
| | FUL Conversion | **97.0%** | **99.4%** | **99.4%** | **98.8%** |
| | FUL Tailpipe | 0.106 | 0.023 | 0.025 | 0.060 |
| | FUL Composite Conversion | | **99.3%** | | |
| | IRAF | | 0.002 | 0.002 | 0.004 |
| | Final TP Composite | | **0.029** | **0.027** | **0.064** |
| | Margin to Standard (% std) | | **28%** | **33%** | **36%** |
| | Margin to Standard (g/kw-hr) | | **0.011** | **0.013** | **0.036** |

**FIGURE 72. MARGIN PROJECTIONS FOR MFC-ENABLED CONFIGURATION AT 12,000 HOUR FUL WITHOUT DSF**

An important factor in assessing the MFC-enabled system was to understand the behavior of the system under regeneration conditions. This is because the MFC was at least partially responsible for generating the exotherm required for filter regeneration. In addition, it was anticipated that this exotherm might also facilitate $deSO_X$ on the MFC, removing the need for a separate LO-SCR $deSO_X$ event, as was needed in the on-highway program which could be a reduction in controls complexity and potentially fuel consumption related to desulfation. Recall

that in this system for the Tier 5 demonstration, HC injection for filter regeneration is provided via late post-injection from the engine.

It was understood that the MFC would not be as effective as a DOC in generating an exotherm, especially at lower temperatures. Figure 73 shows examples of the exotherm of the MFC and zCSF at various MFC inlet temperatures at exhaust flow rates in the range of 500-600 kg/hr. The target temperature for the exotherm in all cases with a DPF (zCSF) outlet temperature of 570°C. The DPF (zCSF) inlet temperature is also shown, which indicates the exotherm across the MFC. At 325°C inlet, it can be seen that the entire exotherm occurs on the MFC, with a slight loss of temperature across the zCSF. This indicates that all the HC was consumed on the MFC. This is also the case at inlet temperatures above 325°C. At 300°C, the exotherm is still mostly across the MFC, but it takes more time to ramp, and some exotherm does occur across the zCSF, indicating that not all HC was consumed on the MFC. At 275°C inlet temperature, nearly half the exotherm occurs on the zCSF, indicating that the MFC is not as effective in generating temperature form post injection at these temperatures. Temperatures below 275°C were not investigated as it was felt that at inlet temperatures below this, near post injection would likely to be used to raise the inlet temperature to near that level before trying to initiate regeneration.

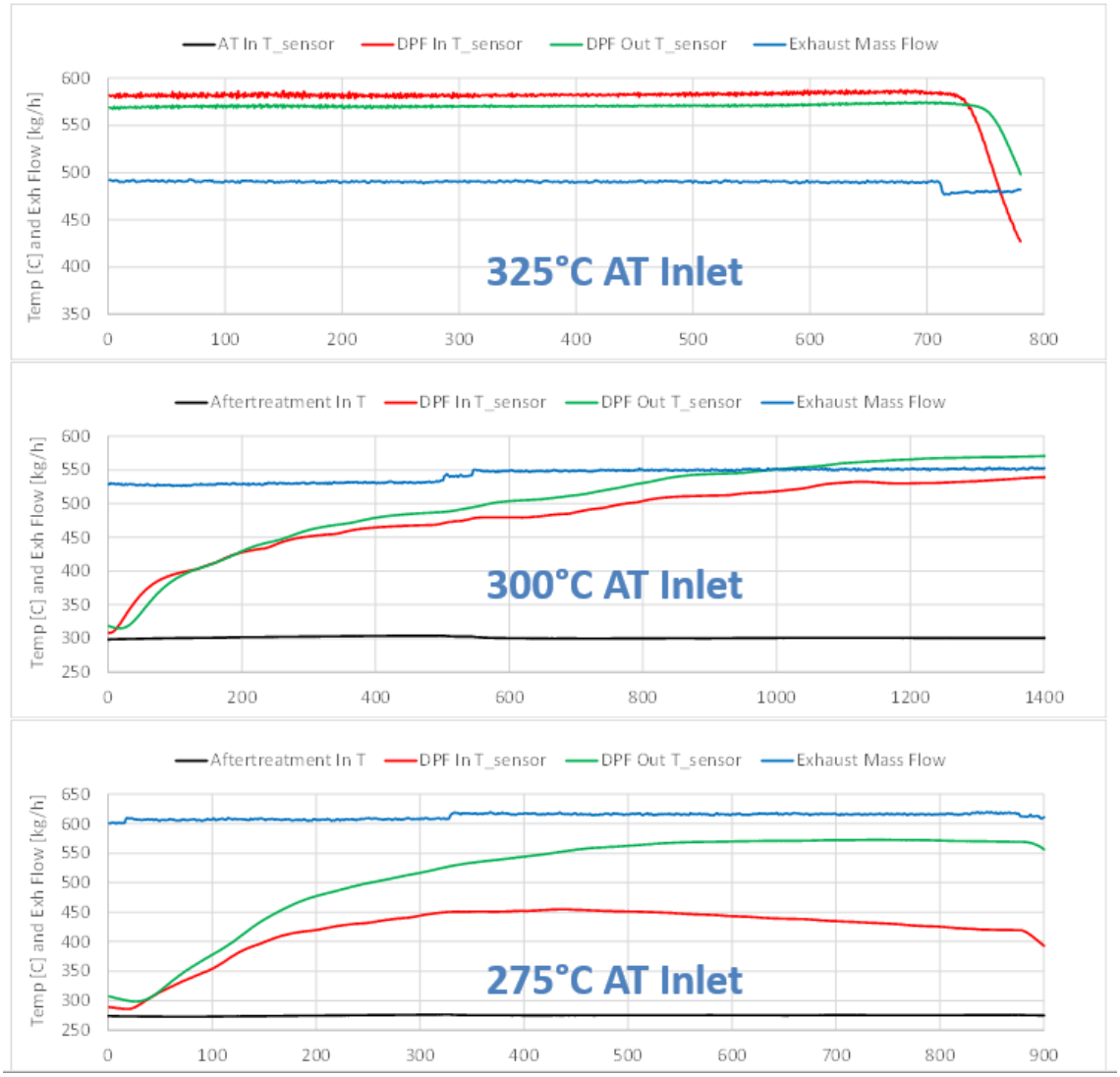



**FIGURE 73. BEHAVIOR OF EXOTHERM ACROSS MFC AND ZCSF WITH LATE POST INJECTION FROM ENGINE AT VARIOUS INLET TEMPERATURES**

Measurements taken later during aging indicate that the majority of the exotherm above 325°C inlet took place in the first two inches of the MFC, indicating that most of the MFC was at temperatures near 580°C. This means that during regeneration the majority of the MFC was above temperatures required for de$SO_X$, and some of the remaining front 2 inches would likely exceed 550°C via conduction by the end of the regeneration. At or below 300°C inlet, it is likely that the MFC would only reach 525°C and the front part would be lower, which might not facilitate fully effective de$SO_X$. Regeneration frequency is expected to be on the order of every 60 to 80 hours, while it is expected that de$SO_X$ would likely be needed only every 150 hours or more (depending on temperature history). As long as roughly one in every two to three regenerations occurs at an inlet temperature of 325°C or higher for at least part of its duration, this would likely be sufficient for MFC de$SO_X$. This would be validated during the DAAAC aging run, and this information was used to set the DAAAC aging cycle conditions that would be used.

There was evidence that little $NO_X$ conversion was accomplished across the MFC during regeneration exotherms. However, the downstream system had already shown capability for $NO_X$ reduction at 570°C filter outlet temperature using the Team 1 SCR catalysts. As a result, it was assumed that the MFC-enabled system would perform similarly to the conventional system in terms of $NO_X$ reduction during regeneration. As a result, the same upwards adjustment factor (UAF) for infrequent regeneration was used for the MFC-enabled system as for the Team 1 conventional system.

## 3.9 Final Technology Comparison and Selection

Following the completion of the various technology evaluations with Development Aged parts, it was necessary to go through a selection process to decide which final architecture would be used for the fully DAAAC-aged demonstration. To facilitate this selection, SwRI prepared a comparison of the technology options, including both performance data, margin projections, and relative assessments of other factors such as complexity and durability. A summary of this comparison in given in Table 22, showing the characteristics of the various options. All projected margins assumed degradation rates similar to those from the on-highway Low $NO_X$ program, and the "certification" data for those projections actually came from the Development Aged results (making the margin projections somewhat conservative). This information as well as the detailed performance data was shared with CARB staff and the stakeholders of the Program Advisory Group at the 5th PAG meeting. Feedback was solicited and compiled from stakeholders, along with the recommendations from SwRI.

For the various non-performance factors, such as complexity and durability, the symbols were meant to provide a relative assessment. A "0" would indicate where a characteristic was considered equivalent to the baseline engine. A "-" would indicate where a characteristic was worse, with the number of marking indicated increasing levels of concern. On the other hand, a "+"indicated areas of higher confidence and better performance than the baseline engine. For durability the "+" and "_" marking were indicators of more or less confidence in the system durability. For instance, while reduced size SCR configurations were evaluated, there was concern that they would not have sufficient durability for an 8,000-hr or especially 12,000-hour demonstration, and thus these were given "-" scores for that. Cost is not explicitly stated as a factor, but it was assumed the increasing complexity in any category would mean increasing costs as well.

## TABLE 22. COMPARISON OF TIER 5 DEMONSTRATION TECHNOLOGY OPTIONS AND RECOMMENDATIONS

| | | | Package 2 | | | | | | | |
|---|---|---|---|---|---|---|---|---|---|---|
| | | | 1 | 2 | 3 | 4 | 5 | 6 | 7 | 8 |
| CDA | | | **n/a** | **DSF** | **DSF** | **DSF** | **DSF** | **DSF** | **n/a** | **n/a** |
| eHeater | | | **n/a** | **n/a** | **n/a** | **6.6kw @ 48V** | **n/a** | **n/a** | **n/a** | **n/a** |
| AT Archictecture | | | DOC+DPF+SCR+ASC | DOC+DPF+SCR+ASC | DOC+DPF+SCR+ASC | DOC+DPF+SCR+ASC | **MFC+zCSF+SCR+ASC** | **MFC+zCSF+SCR+ASC** | **MFC+zCSF+SCR+ASC** | **MFC+zCSF+SCR+ASC** |
| Upstream Doser | | | n/a | n/a | n/a | n/a | **Heated DEF** | **Heated DEF** | **Heated DEF** | **Heated DEF** |
| Downstream Doser | | | Conventional DEF | Conventional DEF | Conventional DEF | Conventional DEF | Conventional DEF | Conventional DEF | Conventional DEF | Conventional DEF |
| DOC | | | 12X4 | 12X4 | 12X4 | 12X4 | n/a | n/a | n/a | n/a |
| DPF | | | 12X7 CSF | 12X7 CSF | 12X7 CSF | 12X7 CSF | **12X7 zone-coated CSF** | **12X7 zone-coated CSF** | **12X7 zone-coated CSF** | **12X7 zone-coated CSF** |
| Upstream SCR | | | n/a | n/a | n/a | n/a | 12 X 7 MFC | 12 X 7 MFC | 12 X 7 MFC | 12 X 7 MFC |
| Downstream SCR | | | 2 x 12X4 SCR | 2 x 12X4 SCR | **1 x 12X4 SCR** | 2 x 12X4 SCR | 2 x 12X4 SCR | **1 x 12X4 SCR** | 2 x 12X4 SCR | **1 x 12X4 SCR** |
| | | | 1 x 12X4 SCR-ASC | 1 x 12X4 SCR-ASC | 1 x 12X4 SCR-ASC | 1 x 12X4 SCR-ASC | 1 x 12X4 SCR-ASC | 1 x 12X4 SCR-ASC | 1 x 12X4 SCR-ASC | 1 x 12X4 SCR-ASC |
| CCV | | | Yes | Yes | Yes | Yes | Yes | Yes | Yes | Yes |
| NRTC | g/kw-hr | 0.04 | 0.015 | 0.012 | 0.007 | 0.007 | 0.007 | 0.007 | 0.007 | 0.008 |
| RMC | g/kw-hr | 0.04 | 0.020 | 0.014 | 0.004 | 0.008 | 0.003 | 0.005 | 0.005 | 0.006 |
| LLAC | g/kw-hr | 0.1 | *0.078* | 0.012 | 0.003 | 0.011 | 0.006 | 0.003 | 0.008 | *0.031* |
| NRTC Margin - 12k/8k | mg/kw-hr | 40 | -2 / 8 | 4 / 12 | 7 / 15 | 8 / **17** | 10 / 19 | *11 / 15* | 11 / **19** | *10 / 14* |
| RMC Margin - 12k/8k | mg/kw-hr | 40 | -2 / 6 | 3 / 12 | 11 / 19 | 10 / **18** | 15 / 23 | *13 / 17* | 13 / **21** | *12 / 20* |
| LLAC Margin - 12k/8k | mg/kw-hr | 100 | -31 / -16 | 25 / 43 | 35 / 50 | 26 / **44** | 34 / 51 | *37 / 46* | 36 / **51** | *<15 / 23* |
| NRTC CO2 Delta | % reduction | | 4.8% | 7.5% | 3.6% | **6.6%** | 6.6% | 6.0% | **6.0%** | **6.3%** |
| RMC CO2 Delta | % reduction | | 3.6% | 5.6% | 4.1% | 4.6% | 5.3% | 4.8% | 3.9% | 3.1% |
| LLAC CO2 Delta | % reduction | | *8.1%* | 11.7% | 7.5% | 10.8% | 11.1% | 11.1% | 7.5% | 7.1% |
| NRTC N2O | g/kw-hr | | 0.080 | 0.076 | 0.076 | **0.078** | 0.049 | 0.083 | **0.049** | 0.089 |
| | | | | | | | | | | |
| Durability Confidence | | | +++ | ++ | + | ++ | + | - | + | - |
| Engine Complexity | | | 0 | -- | -- | -- | -- | -- | 0 | 0 |
| Electrical Complexity | | | 0 | 0 | 0 | - | 0 | 0 | 0 | 0 |
| AT Complexity | | | 0 | 0 | 0 | - | -- | -- | -- | -- |
| AT Packaging | | | - | - | 0 | - | -- | 0 | -- | 0 |

Performance data highlighted in red indicates areas where program targets were not likely to be met.
Performance data highlighted in yellow indicates areas where program targets were marginal and might be improved with further effort.
Performance data highlighted in green indicates areas where program targets were met.

The two configurations shaded at the top in gray represent the two candidate configurations recommended by SwRI. SwRI ultimately recommended the use of Configuration 7 involving the MFC-enabled system with dual dosing.

Ultimately, it was up to CARB staff to assess the feedback and recommendations, with assistance and input from SwRI. CARB staff chose to select Configuration 7, with input from the regulated industry, which was the dual-dosing, dual-SCR system with the MFC and the full size downstream SCR catalysts. Although shown earlier, the final configuration is illustrated the schematic below in Figure 74 for ease of reference.

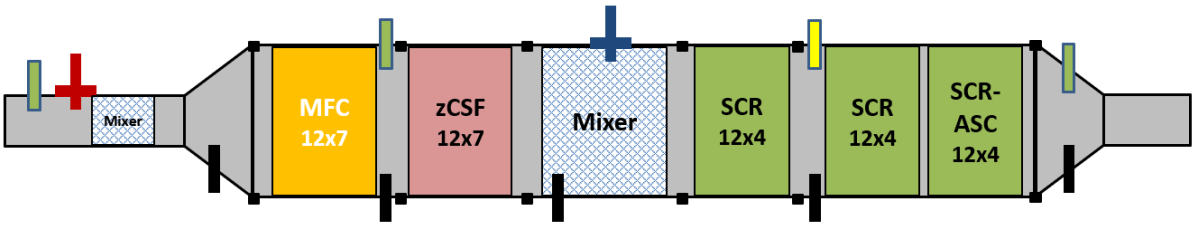



**FIGURE 74. FINAL TIER 5 DEMONSTRATION AFTERTREATMENT SCHEMATIC**

Given the information in the program about margins, and also considering other market information, CARB ultimately elected to stay with an 8000-hour FUL, and therefore the demonstration would be limited to 8000-hours of equivalent aging This decision freed some of the original program scope, which was redirected in two ways. First the system performance would be characterized both with and without the use of DSF, to examine the full capability of that technology. In addition, system performance would be assessed both for the primary engine rating of 187kw, which most of the program was conducted on, and a lower power child rating of 126kw with a lower torque curve using the same engine and AT hardware.

## 3.10 Final Calibration and Zero-Hour Testing

With the final configuration selected, a reserve set of parts matching the final aftertreatment configuration was assembled. The final demonstration system was slightly shorter in length because some of the adapters that were used to permit modularity in the development system were no longer needed. In addition, insulation equivalent to production thickness was added the MFC assembly because it did not initially include any insulation when canned.

That final demonstration system was de-greened on the ECTO-Lab burner system. The de-green protocol was a cycle consisting of the following steps:

- 24 hours of 450°C system inlet temperature
- Reduce inlet temperature to 350°C and introduce HC injection upstream of the system to generate and exotherm to reach a zCSF outlet temperature of 570°C. Note that HC injection is ramped over the course of 5 minutes to reach this temperature.
- 40 minutes at 350°C system inlet temperature and 570°C filter outlet temperature.

The de-green cycle was repeated twice for a total of 50 hours of de-greening operation including two regeneration events. This is consistent with previous experiments, and industry practice observed across multiple manufacturers. The de-greened system was then installed on the demonstration engine for performance checks.

Following initial system performance checks, a final optimization and calibration effort was carried out. This was done to reach the maximum practical performance of the system, while also ensuring that it would be robust over FUL aging and operation.

The final optimized calibration without DSF did result in somewhat higher engine-out $NO_X$ levels, and a small improvement in $CO_2$ emissions. The dosing calibration was also adjusted to maximize conversion while trying to balance $N_2O$ emissions to some extent. In addition to these changes, a final evaluation of passive soot oxidation was carried out over the NRTC. Although earlier checks had been done on the partial systems, it was important to ensure good passive soot oxidation with the presence of the MFC. There was some concern that the MFC dosing calibration used for the Development Aged system might have potentially compromised passive soot oxidation by targeting a little too much conversion over the MFC, thus limited the amount of $NO_X$ reaching the zCSF to promote passive soot oxidation over the smaller high PGM zone of the zCSF (as compared to a full DOC).

These passive soot oxidation experiments came in the form of repeat hot-start NRTC cycles (with soaks in between). The rate of increase in filter differential pressure was observed over these tests. The result of this experiment is given below in Figure 75. The initial cycles do show a gradual rise in differential pressure on the order of 0.05 kpa per cycle but slowing as more soot loaded on the filter to about 0.025kpa per cycle after the first 8 cycles.

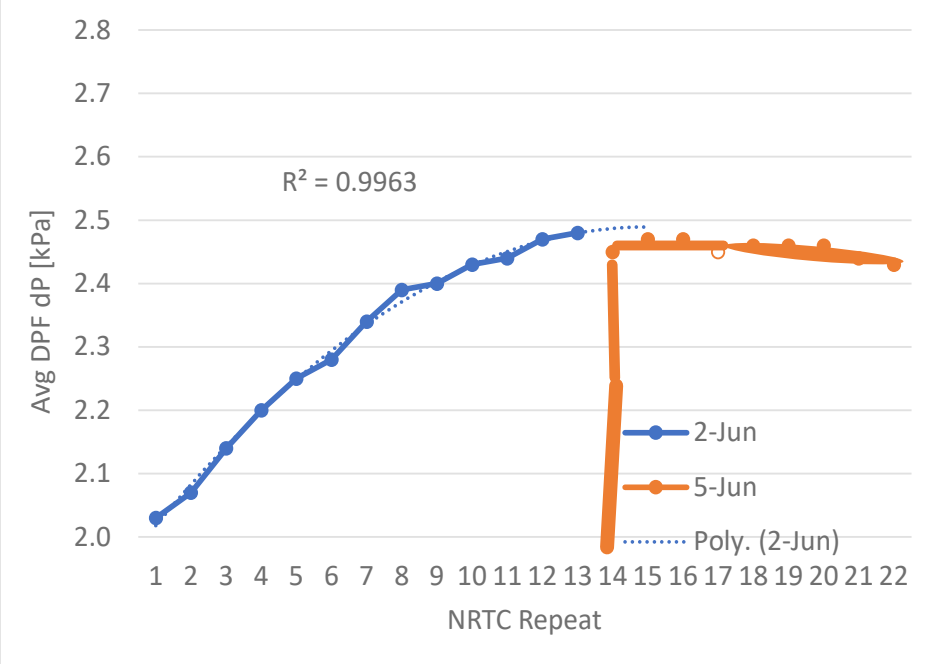



**FIGURE 75. FILTER DIFFERENTIAL PRESSURE OVER REPEAT HOT NRTC CYCLES**

However, to ensure a calibration that would be robust under more real-world conditions, and after consultation with Deere for feedback, it was decided to adjust the calibration to ensure that no differential pressure rise was seen on the system. The balance of conversion between the MFC and the downstream system was adjusted to allow more $NO_X$ to reach the filter and enable improved passive soot oxidation. Following that adjustment, the subsequent cycles indicate no further increase, and in fact showed a very modest decreasing trend. This indicates that the system

was at the balance point between soot loading and soot oxidation over the NRTC. This was considered satisfactory.

The impact of this change on hot-start NRTC $NO_X$ performance can be seen in Figure 76. The change is visible in the higher levels of MFC-outlet $NO_X$ observed in the highlighted region between 400 and 900 seconds in the cycle. Note that tailpipe emissions in green are unaffected by this change, indicating that the downstream system is capable of absorbing this increased $NO_X$ input. However, this doubled the cumulative mass of $NO_X$ reaching the zCSF in this region of the cycle, facilitating passive soot oxidation and helping eliminate the cycle-to-cycle increase in differential pressure across the filter.

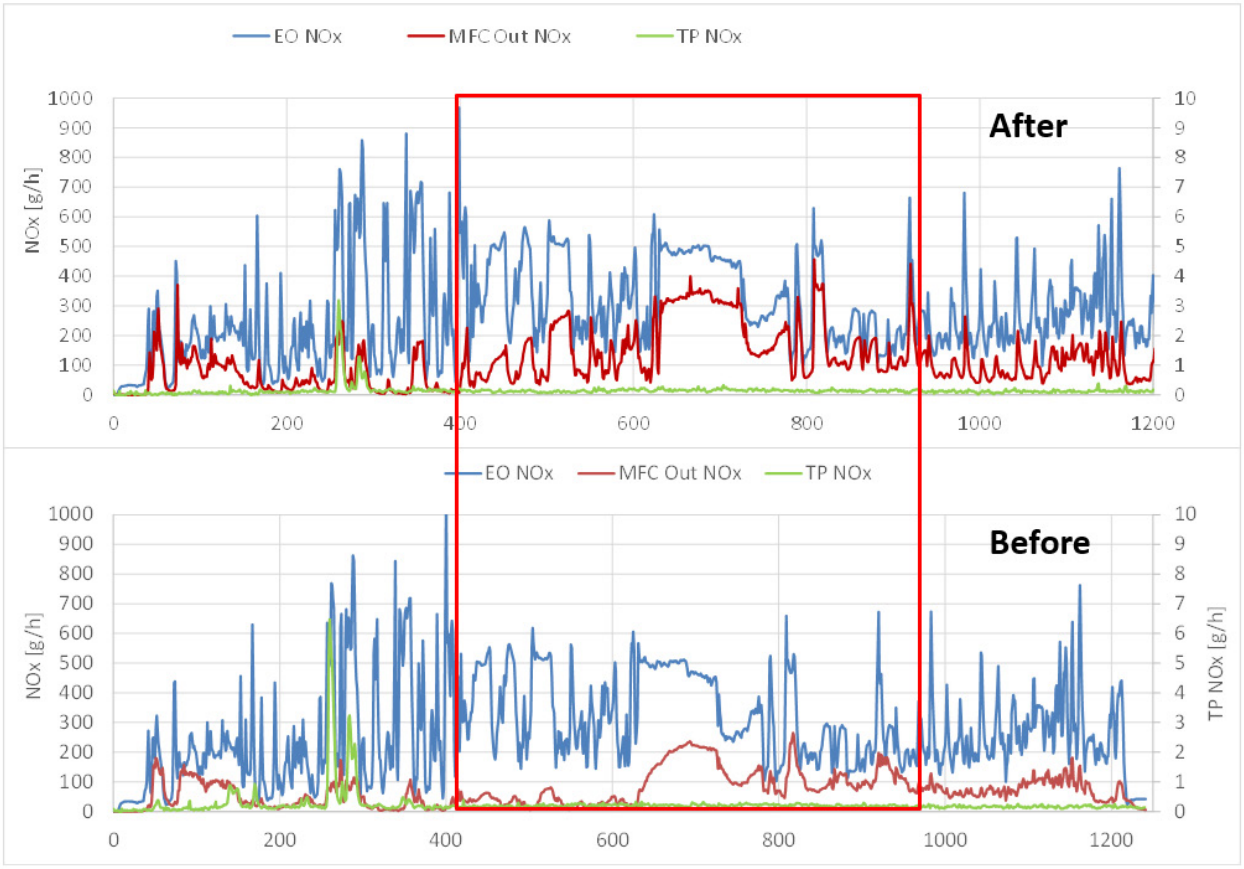



**FIGURE 76. HOT-START NRTC $NO_X$ EMISSIONS BEFORE AND AFTER PASSIVE SOOT OXIDATION CALIBRATION CHANGE**

With the final calibration optimization completed, 0-hour results were generated both with and without DSF active. A summary of the tailpipe $NO_X$ emission results for the 0-hour hour test point is given in Figure 77. The results shown are the average of triplicate test sequences, with the error bars showing one standard deviation. All of these results were for a closed crankcase ventilation (CCV) configuration. As noted earlier, open crankcase ventilation results would have been 0.01 g/kw-hr higher for all cycles. Results were similar with and without DSF for the NRTC and the RMC, but for the LLAC the $NO_X$ level with DSF was half that of the level observed without DSF.

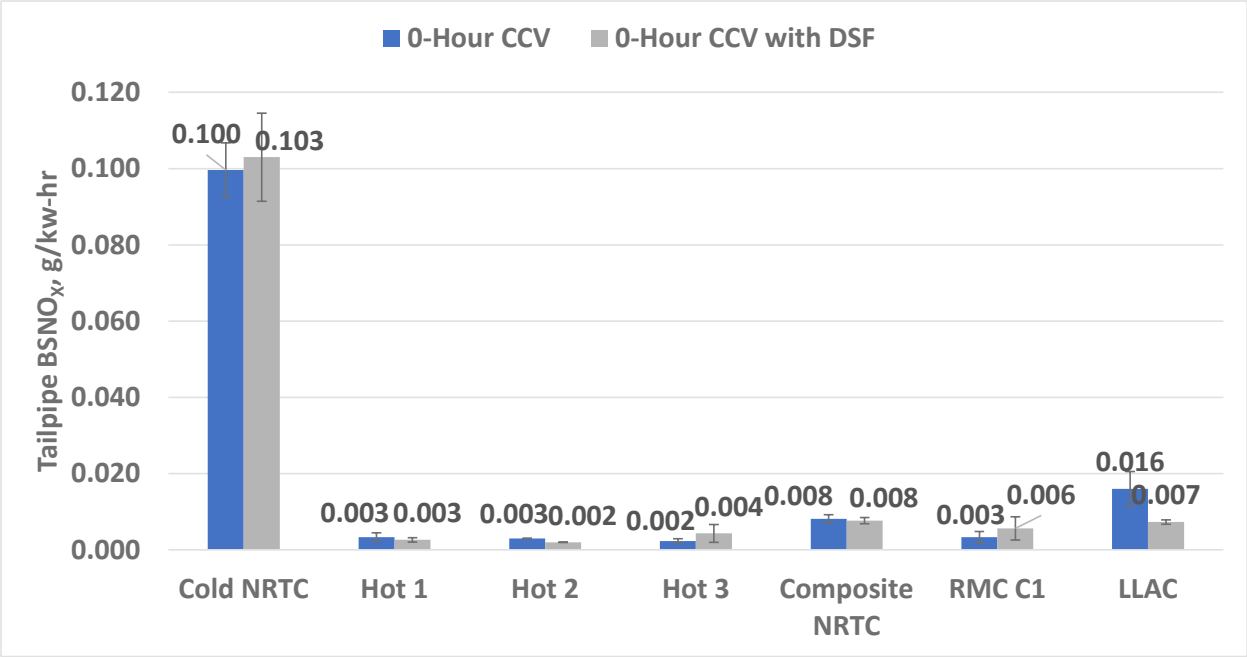



**FIGURE 77. 0-HOUR $NO_X$ EMISSIONS FOR FINAL TIER 5 DEMONSTRATION PACKAGE WITH AND WITHOUT DSF, CCV**

Figure 78 shows $CO_2$ emissions for the 0-hour test point in comparison to the results for the Baseline Tier 4 engine, while Table 23 shows the $CO_2$ improvement in percent change both with and without DSF from the Tier 4 baseline. The Tier 5 demonstration engine met the initial Package 2 target of achieving a reduction of 5% to 8.6% reduction in $CO_2$ from the baseline engine both with and without DSF on both the NRTC and the LLAC, while the RMC improvement was somewhat less at 3.5 to 4.5 %. Results with DSF showed roughly a 1% greater reduction in $CO_2$ compared to results without DSF for the NRTC and RMC, and a 5% greater reduction on the LLAC.

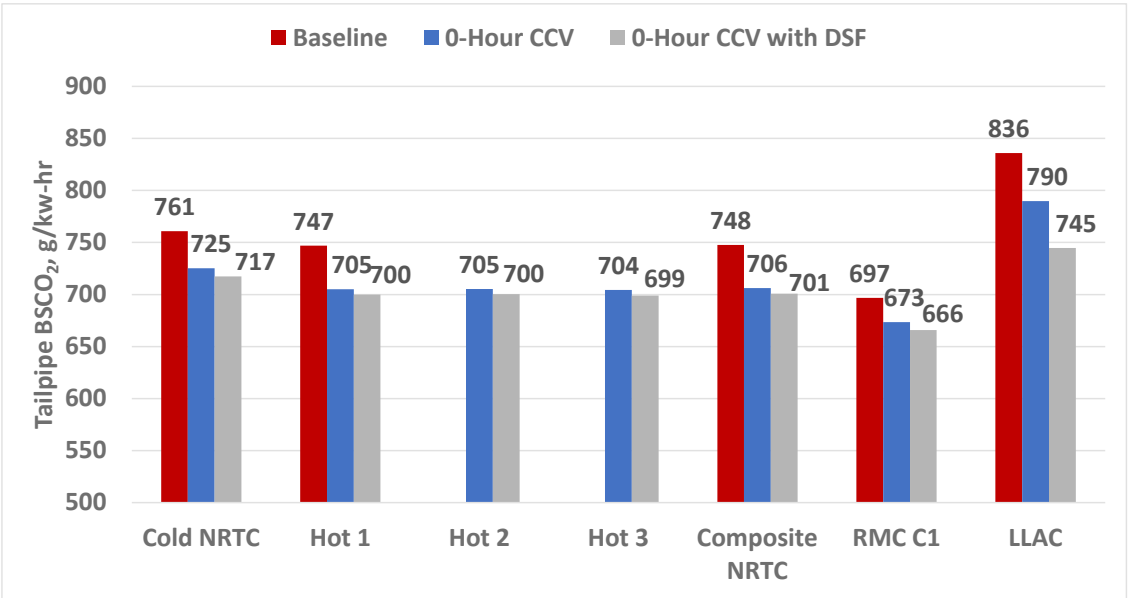



**FIGURE 78. 0-HOUR $CO_2$ EMISSIONS FOR FINAL TIER 5 DEMONSTRATION PACKAGE WITH AND WITHOUT DSF, CCV**

**TABLE 23. IMPROVEMENT IN $CO_2$ EMISSIONS COMPARED TO TIER 4 BASELINE ENGINE FOR 0-HOUR TIER 5 DEMONSTRATION ENGINE**

| Cycle | Improvement in CO2, % | |
|---|---|---|
| | Pkg 2 without DSF | Pkg 2 with DSF |
| Cold NRTC | 4.7% | 5.7% |
| Hot NRTC | 5.6% | 6.3% |
| **Composite NRTC** | **5.6%** | **6.3%** |
| RMC C1 | 3.3% | 4.4% |
| LLAC | 5.5% | 10.9% |

Figure 79 shows a summary of $N_2O$ emissions at the 0-hour test point, again compared to $N_2O$ emissions from the Tier 4 baseline engine. For the NRTC and RMC cycles, $N_2O$ emissions from the Tier 5 demonstration engine were below the baseline engine both with and without DSF. For the LLAC, $N_2O$ emissions were significantly higher without DSF than the baseline, while they were significantly lower with DSF. This difference was due primarily to the higher temperatures on the LLAC with DSF. While $N_2O$ levels without DSF could likely have been reduced via calibration, at this point in the program it was not clear how much margin was available to do so while maintaining sufficient $NO_X$ reduction after FUL aging, therefore the data were taken as shown. In addition, it was not yet clear from CARB what the final targets were, and whether $N_2O$ would be regulated on low load cycles or not.

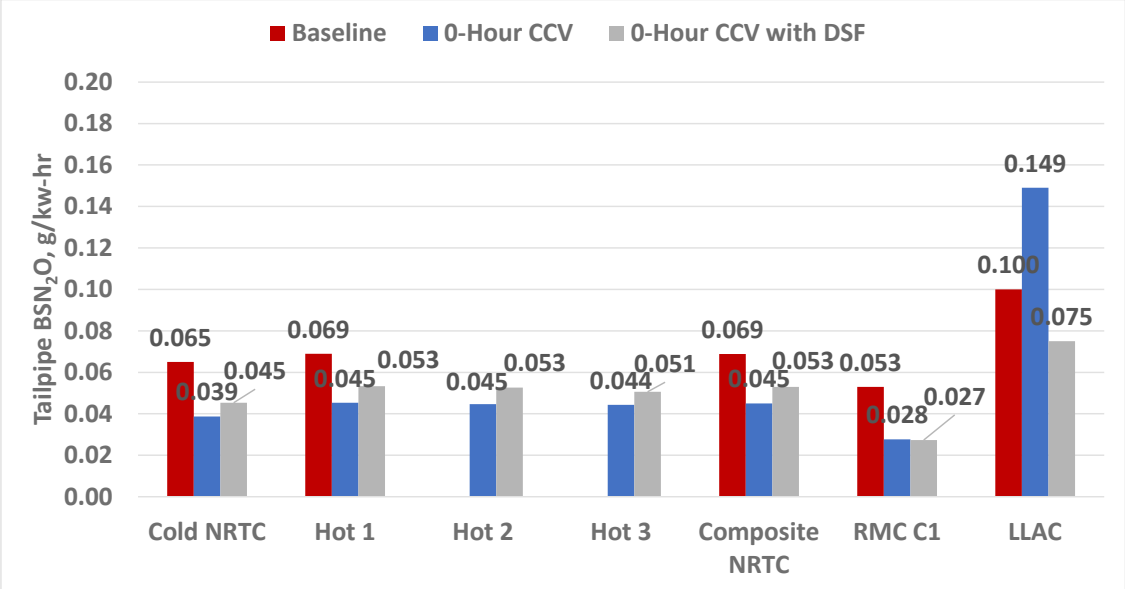



**FIGURE 79. 0-HOUR $N_2O$ EMISSIONS FOR FINAL TIER 5 DEMONSTRATION PACKAGE WITH AND WITHOUT DSF, CCV**

Following 0-hour testing, the aftertreatment system was removed from the Tier 5 demonstration engine and relocated to the DAAAC mule engine for the 8000-hour equivalent aging.

## 3.11 8000-Hour Equivalent DAAAC Aging

As noted in Section 2 of this report, the 8000-hour equivalent aging was conducted on a John Deere 6090HFC09 9 liter mule engine and aging stand that was modified and set up to meet the requirements of the DAAAC protocol, as given in 40 CFR 1065.1141. Initially, the Development Aged parts were used to set up the test stand, as well as for the tuning of the final DAAA cycle to meet the cycle targets for both regeneration and non-regeneration modes. Temperatures at various points in the AT system are shown in Figure 80. The temperatures met the cycle targets throughout the cycle. Of particular interest are the bed temperatures for the MFC and the zCSF during regeneration modes. At the 350°C inlet mode (the second regeneration of the cycle shown towards the end of the chart), the bed temperature at the front of the MFC (Bed 1 located 1 inch from the front face) was at 400°C, while at the mid-bed (Bed 2 located approximately 4 inches from the front face) it was at 620°C. This indicates that the majority of the MFC was likely at temperatures above 550°C, sufficient for de$SO_X$ of the MFC. However, at the 300°C inlet mode (the first regeneration shows towards the middle of the cycle), the highest temperature on the MFC was only above 550°C from the mid-bed back. In this case the front bed of the MFC would likely not be fully de-sulfated on these events having been at temperatures below 450°C.

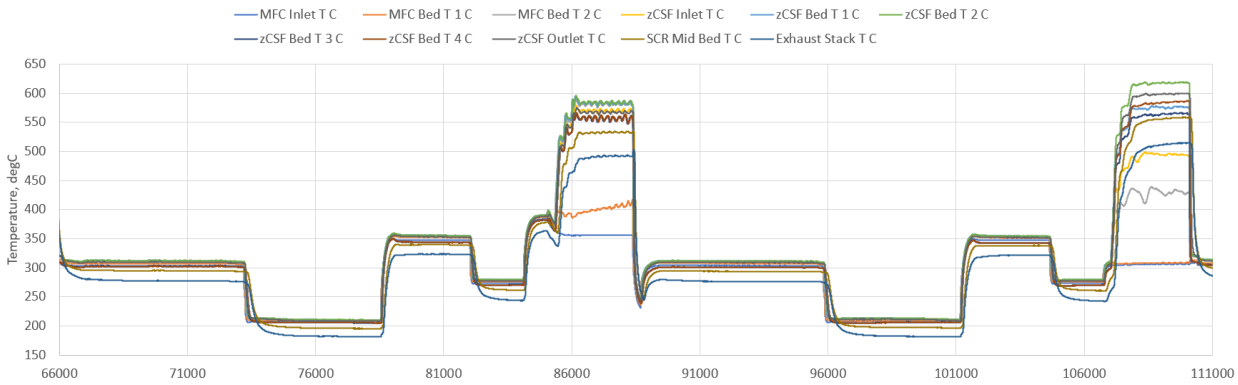



**FIGURE 80. AFTERTREATMENT SYSTEM TEMPERATURES DURING DAAAC AGING CYCLE FOR TIER 5 DEMONSTRATION AGING**

Figure 81 shows an example of $NO_X$ emissions, based on $NO_X$ sensor readings, over a DAAAC cycle from early in the 800-hour aging run. Tailpipe $NO_X$ emissions (in gray) are generally very low throughout the cycle, with significant levels seen only during several spikes during mode transitions. It should be noted that during DAAAC aging, DEF dosing was run at fixed ANR levels representative of the controller results at steady-state, but the model-based controller was not implemented for aging due to aging stand limitations. MFC emissions varied according to the temperatures in accordance with the strategy discussed earlier, with higher reductions at low temperatures and relatively small reductions at high temperatures.

Note that during regeneration, $NO_X$ reduction across the MFC was minimal, as expected during exotherm generation on the MFC. The full burden or regeneration $NO_X$ reduction fell on the downstream SCR, and there was a small amount of tailpipe $NO_X$ present, consistent expectations as discussed below in Section 3.13. Overall, $NO_X$ reduction efficiency during regeneration modes remained in excess of 97% during regenerations over the entire course of

aging. Note that late in the low temperature mode MFC-out $NO_X$ appears to exceed the engine-out level. This is because the initial steady-state ANR setpoint was set too high and there was actual ammonia slip past the MFC, which was detected by the $NO_X$ sensor as $NO_X$ due to the cross-sensitivity of the $NO_X$ sensor to ammonia. This was adjusted later. Note that at the low temperature modes that occur just before regeneration, MFC performance appears to be somewhat degraded, as evidenced by higher $NO_X$ levels, compared to similar modes after regeneration. This provides evidence of on-going sulfation and de$SO_X$ cycling during aging.

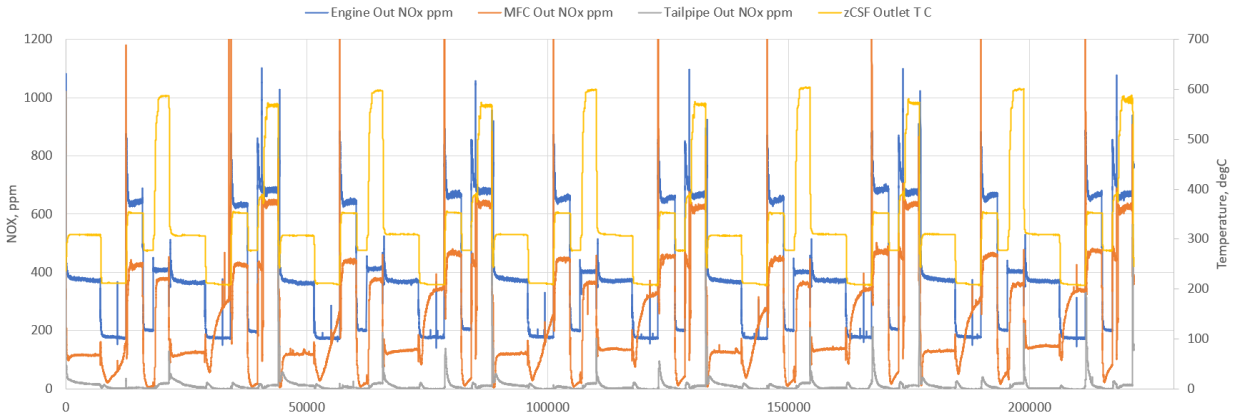



**FIGURE 81. $NO_X$ EMISSIONS OVER DAAAC AGING CYCLE EARLY IN AGING**

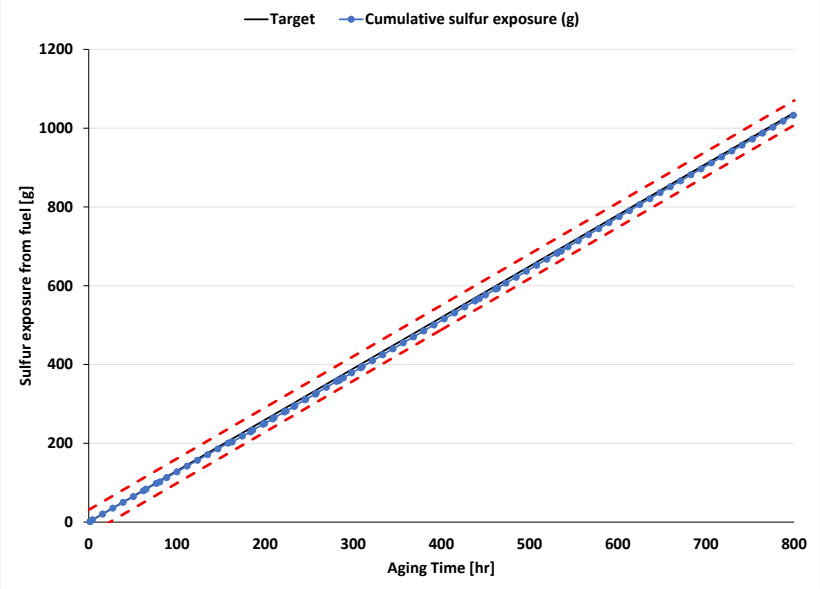
Ash loading on the zCSF was monitored periodically through the 800-hour DAAAC aging run, with three different drain-and-weight events conducted to validate the oil consumption monitoring results. Ash cleaning was not planned during aging unless the ash load exceeded 30 grams/liter, which was not expected during aging. By the end of aging, the final DPF weights indicated an ash loading of 26 grams/liter representing an ash finding ratio of nominally 70 percent. CT-scans indicate a mixture of plug ash and wall ash, although the ash plugs at the end of the filter were relatively small, indicating a majority of wall ash.

Overall, the oil exposure rate during the DAAAC aging run averaged 51 g/hr, slightly below the target of 55 g/hr but still within 10% as required for a DAAAC engine-based aging stand. Oil exposure was 81% from the bulk oil pathway (past the modified piston rings) and 19% from the volatile pathway (doped in fuel). This is consistent with the specifications of the DAAAC protocol which require the volatile pathway to be between 10% and 30% of total oil exposure. The oil exposure was initially 56 g/hr during the first 290 hours of aging but did drop slightly during aging to 44 g/hr during the final 270 hours. The total oil exposure at the end of the 800-hr DAAAC aging run was 43.4 kg. Selected oil properties for the aging oil are given in Table 24. Based on the oil exposure mass and the oil properties, the total exposure of the AT system to Phosphorous was 41.3 grams, or 4.5 grams per liter of SCR displacement on the MFC (not including the ASC layer).

The aftertreatment was exposed to 1033.8 grams of sulfur from fuel over the course of aging, with tracked accumulation of sulfur shown in Figure 82. The accumulation rate for sulfur exposure was well within the DAAAC-specified limits of +/- 3% of the target level throughout the aging run, and the final accumulated sulfur exposure was within 1% of target at the end. An additional 127 grams of sulfur exposure came from the lubricating oil; therefore, the total sulfur exposure for the AT system was 1161 grams. This sulfur exposure equates to 125 grams of sulfur per liter of MFC catalyst, not including the ASC layer.

## TABLE 24. SELECTED OIL PROPERTIES FOR 15W40 OIL USED DURING DAAAC AGING

| ASTM Method | Test Property | Units | Results |
|---|---|---|---|
| D445 at 100°C | Kinematic Viscosity | cSt | 15.99 |
| D445 at 40°C | Kinematic Viscosity | cSt | 130.7 |
| D5185 | Metals by ICP | | |
| | Al | ppm | 1 |
| | Sb | ppm | <1 |
| | Ba | ppm | <1 |
| | B | ppm | 275 |
| | Ca | ppm | 1442 |
| | Cr | ppm | <1 |
| | Cu | ppm | <1 |
| | Fe | ppm | 2 |
| | Pb | ppm | <1 |
| | Mg | ppm | 807 |
| | Mn | ppm | <1 |
| | Mo | ppm | 271 |
| | Ni | ppm | <1 |
| | P | ppm | 952 |
| | Si | ppm | 10 |
| | Ag | ppm | <1 |
| | Na | ppm | <5 |
| | Sn | ppm | <1 |
| | Zn | ppm | 1057 |
| | K | ppm | <5 |
| | Sr | ppm | <1 |
| | V | ppm | <1 |
| | Ti | ppm | <1 |
| | Cd | ppm | <1 |
| D5185 S | Sulfur | wt% | 0.293 |
| | Sulfur | ppm | 2931 |
| D874 | Sulfated Ash | mass % | 1.009 |




## FIGURE 82. ACCUMULATION OF SULFUR EXPOSURE MASS DURING 800-HOUR DAAAC AGING RUN

Following the end of aging and the final weights of the ash loaded zCSF, the filter was removed from the system and ash cleaned via a commercial air-based ash cleaning system. The ash cleaned filter was then given a final CT-scan and weighed to verify cleaning, and then returned to the test cell with the rest of the aged AT system for final tests.

### 3.12 Final 8000-Hour Demonstration Results

Following the completion of the 800-hour DAAAC aging run, equivalent to 8,000 field hours of aging, the final AT system was installed back on the Tier 5 demonstration engine, and preliminary testing was run. Initial test results indicated that performance on the NRTC and RMC cycles showed some degradation but generally looked fairly good, although $N_2O$ emissions were also higher and were above the Tier 4 baseline. However, the LLAC result showed a very large shift and also had very high $N_2O$ emissions. This indicated a significant imbalance between the amount of dosed DEF and the capacity of the aged catalysts. It was apparent from the data that the initial 0-hour calibration for the lower load range was likely too optimistic, and that changes would need to be made to account for the differences.

**TABLE 25. INITIAL TEST RESULTS WITHOUT DSF FOR 8000-HR AGED PARTS WITH 0-HOUR CALIBRATION, CCV**

| Cycle | EO $NO_X$, g/kw-hr | TP $NO_X$, g/kw-hr | $NO_X$ Efficiency, % | $CO_2$, g/kw-hr | Baseline $CO_2$, g/kw-hr | $CO_2$ % Change | TP $N_2O$, g/kw-hr |
|---|---|---|---|---|---|---|---|
| Cold NRTC | 3.7 | 0.119 | 96.8 | 724 | 761 | 4.9 | *0.063* |
| Hot NRTC | 4.1 | 0.007 | 99.8 | 702 | 747 | 6.0 | *0.075* |
| **Composite NRTC** | **4.1** | **0.013** | **99.7** | **703** | **748** | **5.9** | ***0.074*** |
| **RMC C1** | **4.4** | **0.020** | **99.5** | **676** | **699** | **2.9** | **0.048** |
| **LLAC** | ***5.0*** | ***0.086*** | ***98.3*** | ***785*** | ***836*** | ***6.1*** | ***0.347*** |

Figure 83 shows an illustration of the primary issue on the LLAC. With the same storage target calibration at lower temperatures for the MFC that was used for the 0-hour test point, large releases of ammonia are observed at the MFC outlet at the 8000-hr test point, especially later on the cycle. This is also accompanied by large peaks of $N_2O$, and even $NO_X$ peaks as shown in Figure 84 and Figure 85, respectively. This behavior was also observed on the hot-start NRTC, but to a much lesser degree, resulting only in increased $N_2O$, though it was still well below 0.1 g/kw-hr.

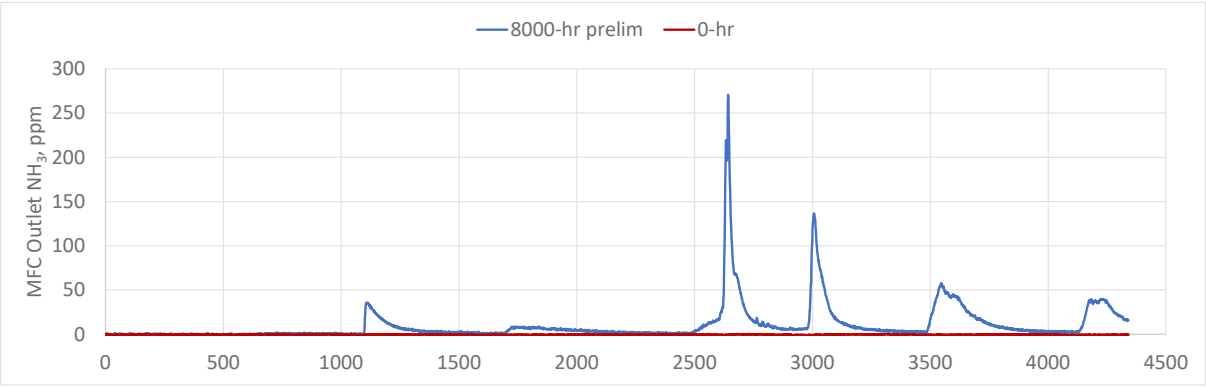



**FIGURE 83. MFC OUTLET AMMONIA ON THE LLAC – 8000-HR INITIAL CALIBRATION VERSUS 0-HR WITHOUT DSF**

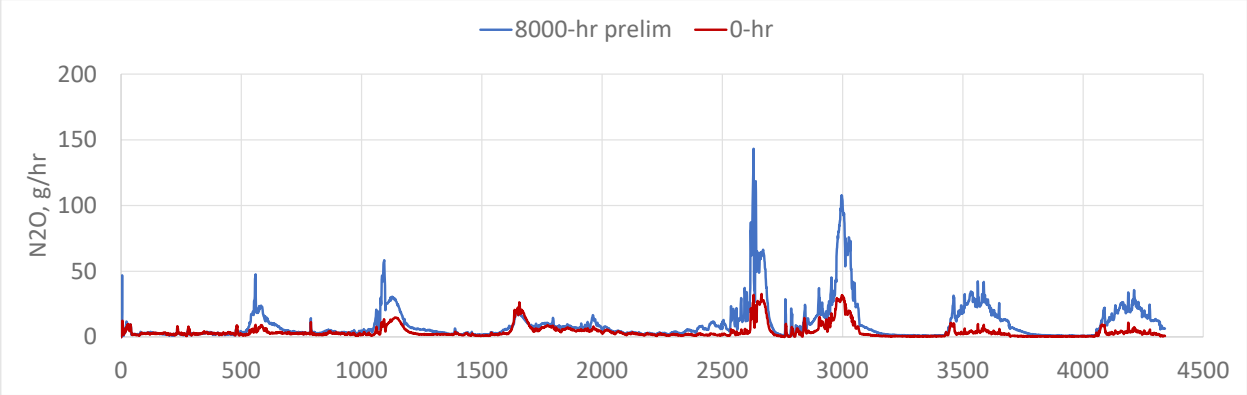



**FIGURE 84. TAILPIPE $N_2O$ EMISSIONS ON THE LLAC - 8000-HR INITIAL CALIBRATION VERSUS 0-HR WITHOUT DSF**

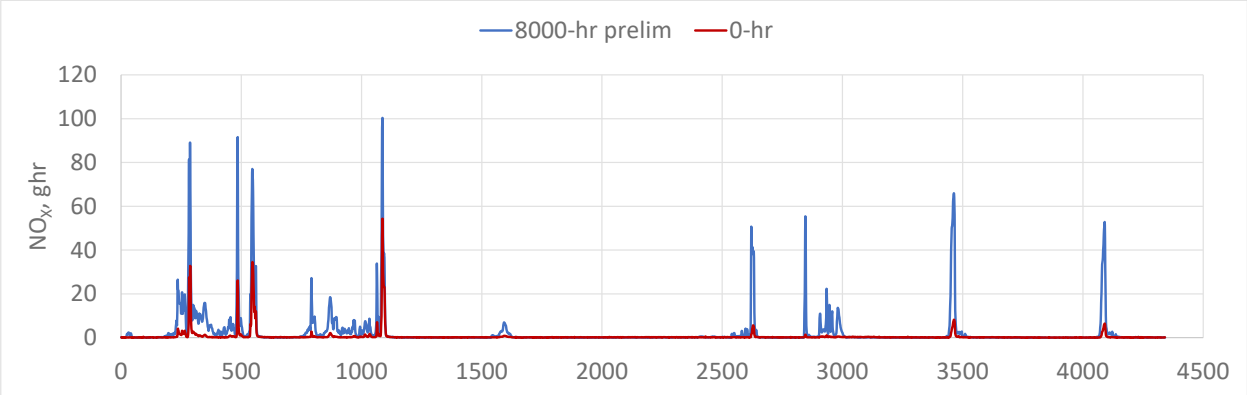



**FIGURE 85. TAILPIPE $NO_X$ EMISSIONS ON THE LLAC - 8000-HR INITIAL CALIBRATION VERSUS 0-HR WITHOUT DSF**

It was apparent from this behavior that while the MFC could still store the same amount of ammonia at low temperatures, it would release that ammonia much more quickly as the temperature increased, indicating that the relationship between storage capacity and temperature had shifted. As a result, storing large amounts of ammonia at the lowest temperatures was no longer feasible, especially over prolonged periods of lower temperatures, such as in the LLAC or LLC. However, aggressive storage targets were still needed for the cold-start NRTC to drive coverage quickly during the early cold-start warmup. In fact, the 0-hour targets had been driven primarily by cold-start need, but a single storage calibration table was used in the strategy for all operations. At the 0-hour point, the catalysts could tolerate this higher storage level, and would release it in a manner that could be digested by the rest of the system. However, with the degraded catalysts, this was no longer the case.

The solution was to separate the cold-start storage targets from the rest of the operation, with the decision to use the cold-start target table being driven by coolant temperature (this was already being done for thermal management by using coolant temperature to divide cold-start and warm-start strategy). With this separation, it was now possible to maintain aggressive storage targets for cold-start and at the same time reduce the warm engine MFC targets to deal with the changed storage curve. This strategy would also help to prevent ammonia slip in prolonged field cycles at lower loads that might be followed by intermittent high load events.

Figure 86 shows the changes in the MFC storage calibration between the 0-hour point and the 8000-hr point. The table axes are temperature (the model average catalyst bed temperature) and inlet $NO_X$ flux. The storage values are values for the coverage fraction, theta, which is the ratio between ammonia storage and the maximum ammonia storage capacity of the catalyst Ω at a reference condition of 175°C. Looking at the 8000-hour tables it can be seen that the targets have been lowered substantially for warm engine operation to values half the original level. However, the cold-start values (highlighted in blue) remain the same as before. The yellow highlighted regions of the table show the temperature range over which ammonia storage on the MFC is ramped down from high to low storage levels to promote passive soot oxidation at higher temperatures, in both cases, and how that region is shifted to lower operating temperatures for the child rating.

T2-Rev34

**MFC (LO-SCR) Team 2 Pkg 2**

| | 1 | 2 | 3 | 4 | 5 | 6 | 7 | 8 | 9 | 10 | 11 | 12 | 13 |
|---|---|---|---|---|---|---|---|---|---|---|---|---|---|
| NOx(g/h)\T | 150 | 210 | 225 | 250 | 275 | 300 | 325 | 350 | 400 | 450 | 500 | 550 | 600 |
| 50 | 0.4 | 0.35 | 0.25 | 0.2 | 0.1 | 0.05 | 0.01 | 0.01 | 0.01 | 0.01 | 0.01 | 0.01 | 0.01 |
| 250 | 0.4 | 0.35 | 0.25 | 0.2 | 0.1 | 0.05 | 0.01 | 0.01 | 0.01 | 0.01 | 0.01 | 0.01 | 0.01 |
| 500 | 0.4 | 0.35 | 0.25 | 0.2 | 0.1 | 0.05 | 0.01 | 0.01 | 0.01 | 0.01 | 0.01 | 0.01 | 0.01 |
| 750 | 0.4 | 0.35 | 0.25 | 0.2 | 0.1 | 0.05 | 0.01 | 0.01 | 0.01 | 0.01 | 0.01 | 0.01 | 0.01 |
| 1000 | 0.4 | 0.35 | 0.25 | 0.2 | 0.1 | 0.05 | 0.01 | 0.01 | 0.01 | 0.01 | 0.01 | 0.01 | 0.01 |
| 1250 | 0.4 | 0.35 | 0.25 | 0.2 | 0.1 | 0.05 | 0.01 | 0.01 | 0.01 | 0.01 | 0.01 | 0.01 | 0.01 |
| 1500 | 0.4 | 0.35 | 0.25 | 0.2 | 0.1 | 0.05 | 0.01 | 0.01 | 0.01 | 0.01 | 0.01 | 0.01 | 0.01 |
| 2000 | 0.4 | 0.35 | 0.25 | 0.2 | 0.1 | 0.05 | 0.01 | 0.01 | 0.01 | 0.01 | 0.01 | 0.01 | 0.01 |
| 3000 | 0.4 | 0.35 | 0.25 | 0.2 | 0.1 | 0.05 | 0.01 | 0.01 | 0.01 | 0.01 | 0.01 | 0.01 | 0.01 |

T2-Rev47 For Hot-start For DSF

**MFC (LO-SCR) Team 2 Pkg 2**

| | 1 | 2 | 3 | 4 | 5 | 6 | 7 | 8 | 9 | 10 | 11 | 12 | 13 |
|---|---|---|---|---|---|---|---|---|---|---|---|---|---|
| NOx(g/h)\T | 150 | 210 | 225 | 250 | 275 | 300 | 325 | 350 | 400 | 450 | 500 | 550 | 600 |
| 50 | 0.17 | 0.15 | 0.13 | 0.11 | 0.09 | 0.05 | 0.01 | 0.01 | 0.01 | 0.01 | 0.01 | 0.01 | 0.01 |
| 250 | 0.17 | 0.15 | 0.13 | 0.11 | 0.09 | 0.05 | 0.01 | 0.01 | 0.01 | 0.01 | 0.01 | 0.01 | 0.01 |
| 500 | 0.17 | 0.15 | 0.13 | 0.11 | 0.09 | 0.05 | 0.01 | 0.01 | 0.01 | 0.01 | 0.01 | 0.01 | 0.01 |
| 750 | 0.17 | 0.15 | 0.13 | 0.11 | 0.09 | 0.05 | 0.01 | 0.01 | 0.01 | 0.01 | 0.01 | 0.01 | 0.01 |
| 1000 | 0.17 | 0.15 | 0.13 | 0.11 | 0.09 | 0.05 | 0.01 | 0.01 | 0.01 | 0.01 | 0.01 | 0.01 | 0.01 |
| 1250 | 0.17 | 0.15 | 0.13 | 0.11 | 0.09 | 0.05 | 0.01 | 0.01 | 0.01 | 0.01 | 0.01 | 0.01 | 0.01 |
| 1500 | 0.17 | 0.15 | 0.13 | 0.11 | 0.09 | 0.05 | 0.01 | 0.01 | 0.01 | 0.01 | 0.01 | 0.01 | 0.01 |
| 2000 | 0.17 | 0.15 | 0.13 | 0.11 | 0.09 | 0.05 | 0.01 | 0.01 | 0.01 | 0.01 | 0.01 | 0.01 | 0.01 |
| 3000 | 0.17 | 0.15 | 0.13 | 0.11 | 0.09 | 0.05 | 0.01 | 0.01 | 0.01 | 0.01 | 0.01 | 0.01 | 0.01 |

T2-Rev47 For Cold-start (same as Rev 34)

**MFC (LO-SCR) Team 2 Pkg 2**

| | 1 | 2 | 3 | 4 | 5 |
|---|---|---|---|---|---|
| NOx(g/h)\T | 150 | 210 | 225 | 250 | 275 |
| 50 | 0.4 | 0.35 | 0.25 | 0.2 | 0.1 |
| 250 | 0.4 | 0.35 | 0.25 | 0.2 | 0.1 |
| 500 | 0.4 | 0.35 | 0.25 | 0.2 | 0.1 |
| 750 | 0.4 | 0.35 | 0.25 | 0.2 | 0.1 |
| 1000 | 0.4 | 0.35 | 0.25 | 0.2 | 0.1 |
| 1250 | 0.4 | 0.35 | 0.25 | 0.2 | 0.1 |
| 1500 | 0.4 | 0.35 | 0.25 | 0.2 | 0.1 |
| 2000 | 0.4 | 0.35 | 0.25 | 0.2 | 0.1 |
| 3000 | 0.4 | 0.35 | 0.25 | 0.2 | 0.1 |

**FIGURE 86. CHANGES TO MFC AMMONIA STORAGE TARGETS FROM 0-HOUR CALIBRATION TO 8000-HOUR CALIBRATION**

An example of this calibration change can be seen comparing ammonia storage targets and actual values over a hot-start NRTC. This is shown in Figure 87 below, with targets shown using dashed lines and actual (modeled) storage values using solid lines. The significant reduction in lower temperature storage on the MFC can be seen in the early NRTC up to about the 400-second mark. At the same time, storage targets were increased by about 15% on the downstream SCR catalysts to help compensate for the increased burden shifted to the downstream catalysts.

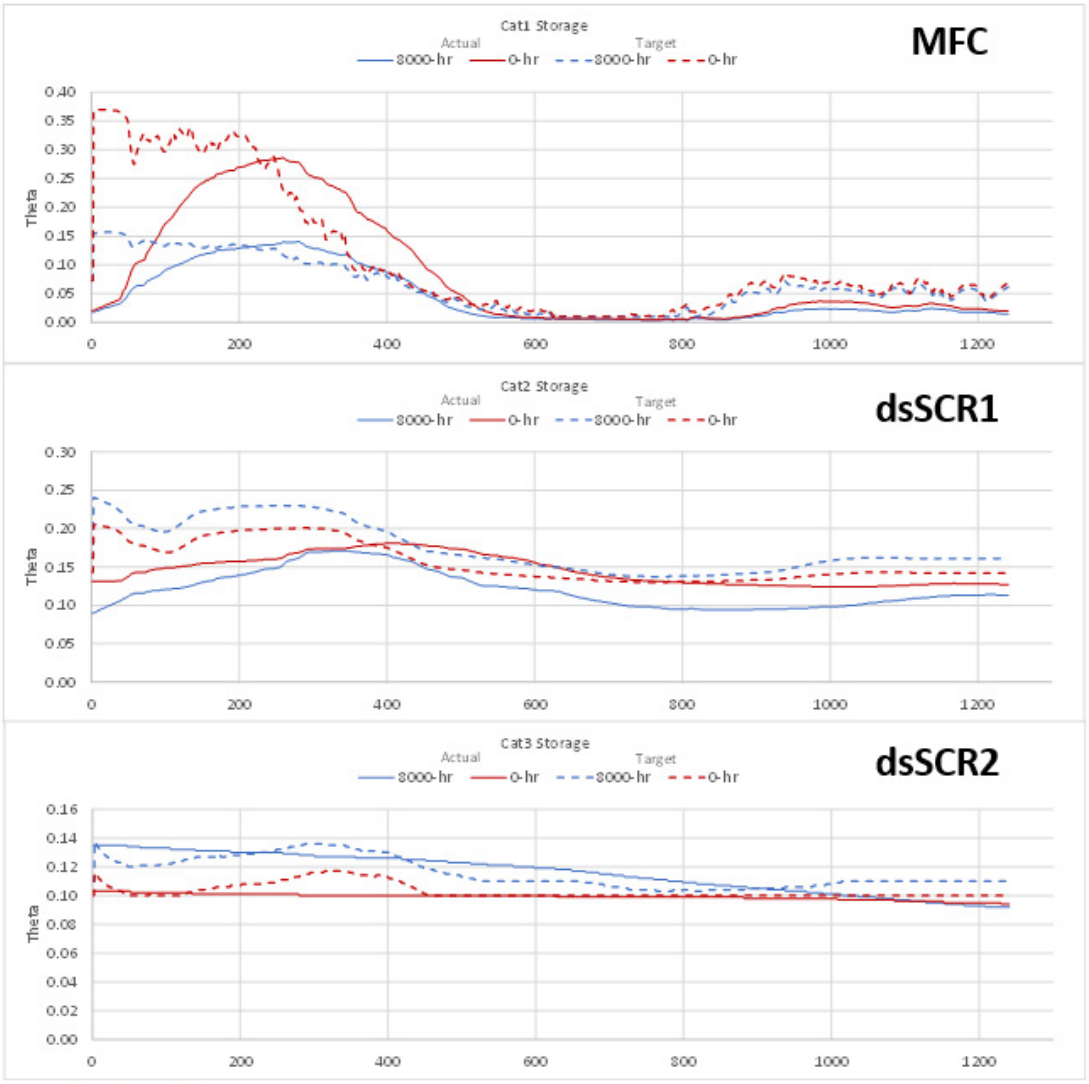



**FIGURE 87. AMMONIA STORAGE TARGETS AND ACTUAL VALUES – BEFORE AND AFTER 8000-HR CALIBRATION CHANGE**

The impact of these storage changes can be seen by comparing the DEF dosing rates for both the upstream and downstream injectors. Figure 88 shows this dosing comparison, with Dosing Rate 1 being for the MFC and Dosing Rate 2 being for the downstream SCR catalysts. A significant reduction in MFC dosing can be seen early in the cycle, especially up before 200 seconds. At the same time, the downstream doser shows an increase due to both increased $NO_X$ flux to the downstream system, and to the small bump in downstream storage targets. On a cycle

basis, the MFC $NO_X$ conversion went from 64% to 56%, as a result of this change, but the difference was successfully absorbed by the downstream system.

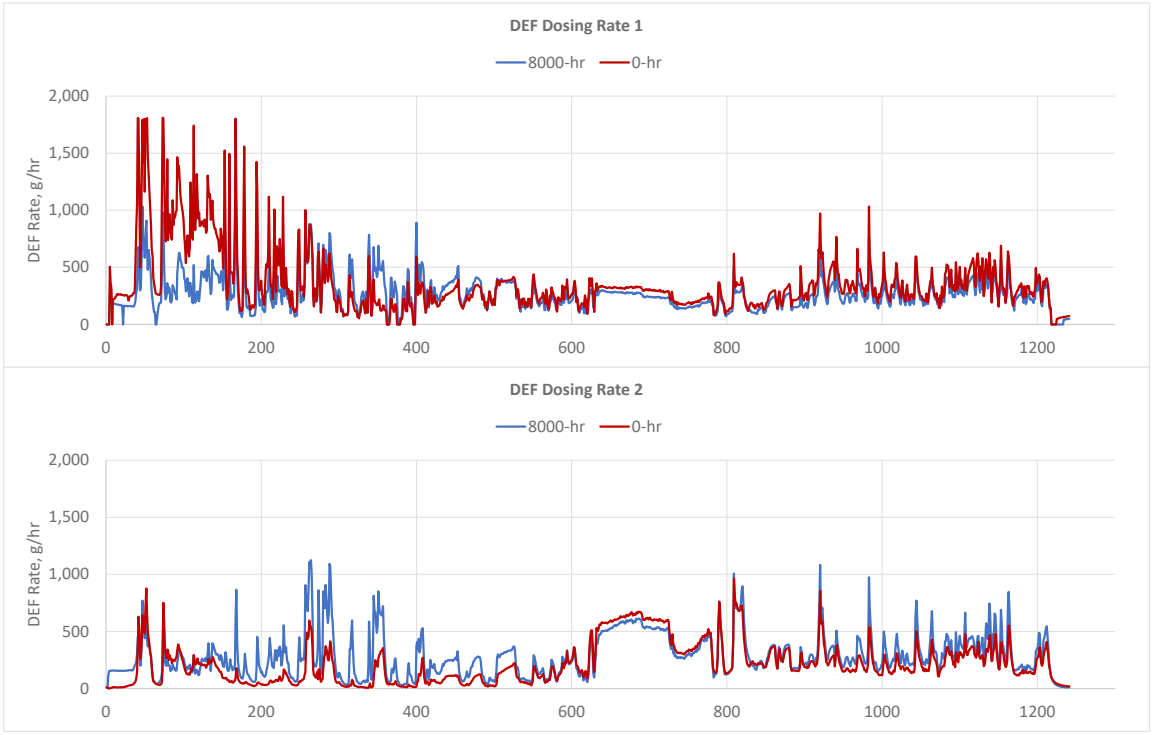



**FIGURE 88. HOT-START NRTC DEF DOSING BEFORE AND AFTER 8000-HR CALIBRATION CHANGE**

Following this calibration strategy change, LLAC tailpipe $NO_X$ emissions were considerably improved, $N_2O$ levels were lowered on most test cycles, and MFC-out ammonia slip was eliminated. Figure 89 shows a comparison of $N_2O$ on the LLAC for the final calibration as compared to the preliminary results with initial calibration. Tailpipe $NO_X$ was reduced from 0.08 g/kw-hr to below 0.02 g/kw-hr. $N_2O$ levels on the hot-start NRTC were also reduced. The final LLC was available for the 8000-hr tests, and so that cycle was also run. There is no 0-hr comparison data for the LLC because the cycle was not yet complete at the time of that testing. Small changes were also made to the thermal management setpoints to help LLAC and LLC emissions, as the 0-hr calibration was likely to be optimistic for the aged catalysts. This did have in impact on the final $CO_2$ emission improvements for both the LLAC and the LLC without DSF.

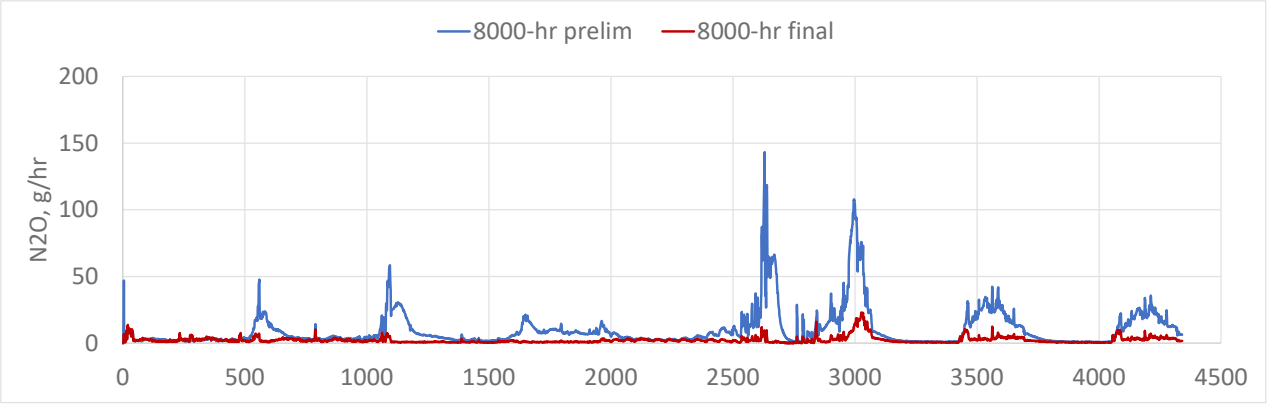



**FIGURE 89. TAILPIPE $N_2O$ EMISSIONS ON THE LLAC - 8000-HR FINAL VERSUS INITIAL CALIBRATION WITHOUT DSF**

Following these changes, the final demonstration triplicate test runs were made both with and without DSF. Tailpipe $NO_X$ emissions without DSF at the 0-hour and 8000-hr test points are shown in Figure 90, while Figure 91 shows $CO_2$ emissions in comparison to the Tier 4 baseline, and Figure 92 shows $N_2O$ emissions in comparison to the baseline. Note that the LLC has a significantly lower duty cycle load factor than the LLAC, which results in higher overall brake-specific $CO_2$ levels. The error bars in Figure 90 represent the standard deviation of the test results, and these are generally in the range of ±0.002 g/kw-hr for the NRTC and RMC, ±0.003 g/kw-hr for the LLAC, and ±0.005 g/kw-hr for the LLC.

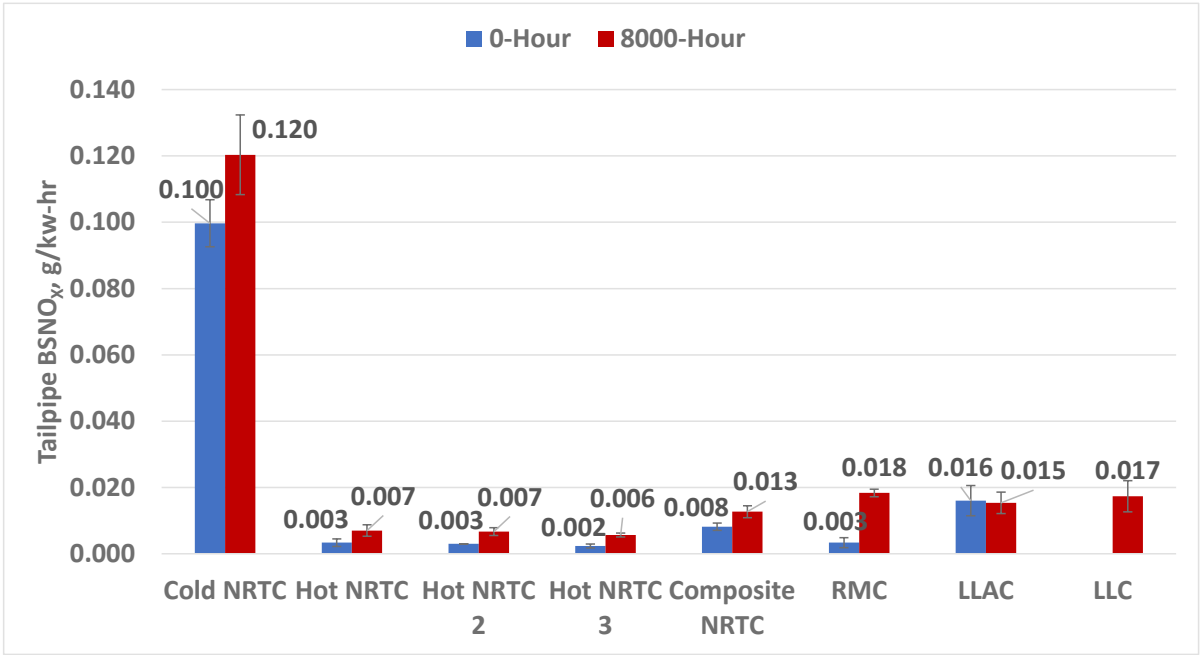



**FIGURE 90. TAILPIPE $NO_X$ EMISSIONS WITHOUT DSF – 8000-HR VERSUS 0-HR, CCV**

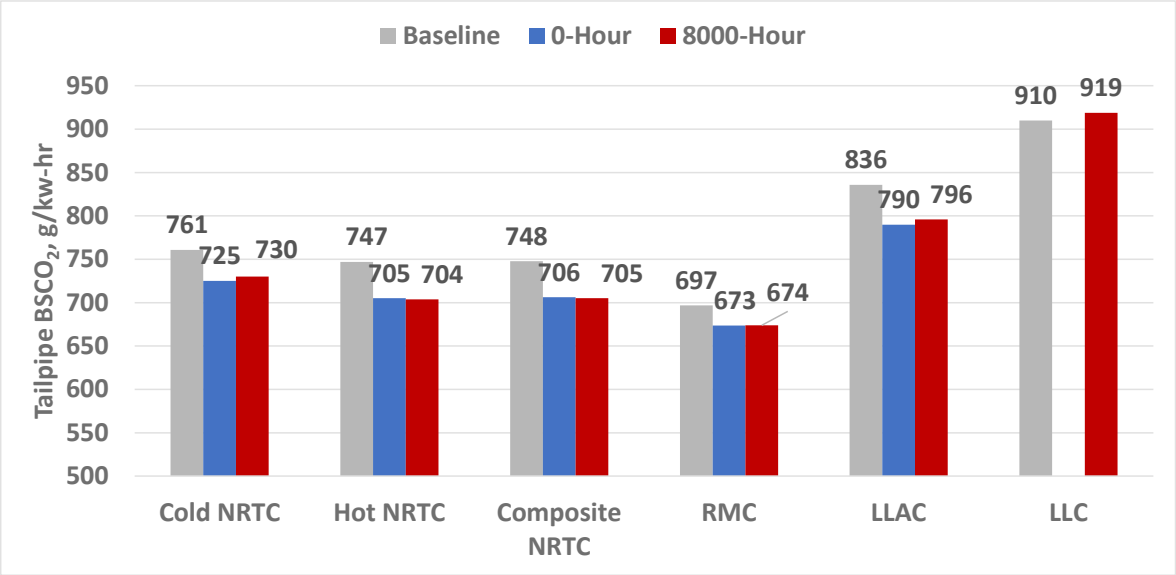



**FIGURE 91. TAILPIPE $CO_2$ EMISSIONS WITHOUT DSF COMPARED TO TIER 4 FINAL BASELINE – 8000-HR VERSUS 0-HR, CCV**

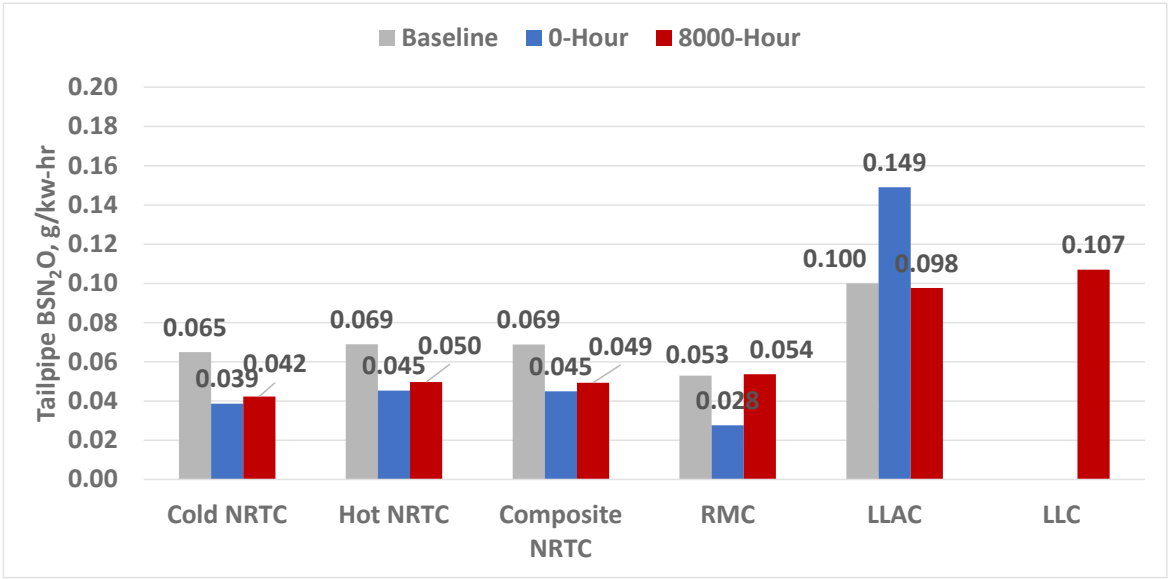



**FIGURE 92. TAILPIPE $N_2O$ EMISSIONS WITHOUT DSF COMPARED TO TIER 4 FINAL BASELINE – 8000-HR VERSUS 0-HR, CCV**

There was some degradation in tailpipe $NO_X$ levels on the NRTC and RMC, with the RMC showing the most significant shift in conversion going from 99.9% $NO_X$ conversion at 0 hours to 99.6% conversion at 8,000 hours. The RMC also showed an increase in $N_2O$, although it was still equivalent to the baseline engine. This movement on the RMC indicates that the aged system had some difficulty with high $NO_X$ flux, indicating that the choice to keep the full displacement with the third brick on the downstream system was likely a good one. Following the calibration changes, $N_2O$ was significantly reduced from the 0-hour level and was now essentially equivalent to the baseline Tier 4 engine.

A comparison of $CO_2$ emissions at FUL versus the Tier 4 baseline engine is shown in Table 26. On the NRTC, the final calibration met the target of 5% to 8.6% $CO_2$ reduction from baseline. In the case of the LLAC, the reduction was somewhat less at the 8000-hr point due to the thermal management changes mentioned above. The demonstration engine with the final calibration did not meet the same reductions in $CO_2$ on the RMC and low load cycles as the 0-hour calibration, due to the changes needed to ensure that $NO_X$ targets could be met at FUL. $N_2O$ emissions at the 8000-hour point were at or below the Tier 4 baseline engine levels, and also well below the 0.15 g/kw-hr cap standard being considered by CARB.

**TABLE 26. $CO_2$ EMISSION RESULTS AT FUL WITHOUT DSF COMPARED TO BASELINE TIER 4 ENGINE**

| | Baseline, g/kw-hr | 8000-hr, g/kw-hr | % Reduction |
|---|---|---|---|
| Cold NRTC | 761 | 730 | 4.1% |
| Hot NRTC | 747 | 704 | 5.8% |
| **Comp NRTC** | **748** | **705** | **5.7%** |
| RMC | 697 | 674 | 3.3% |
| LLAC | 836 | 796 | 4.8% |
| LLC | 910 | 919 | -1.0% |

Figure 93 shows tailpipe PM emissions for both the 0-hour and FUL test points. PM emissions on all cycles are below 0.001 g/kw-hr, which is well below the proposed 0.005 g/kw-hr standard level. The error bars show a one standard deviation, but even with a test result at 3 standard deviations above the mean, that PM result would still be well below a 0.005 g/kw-hr level.

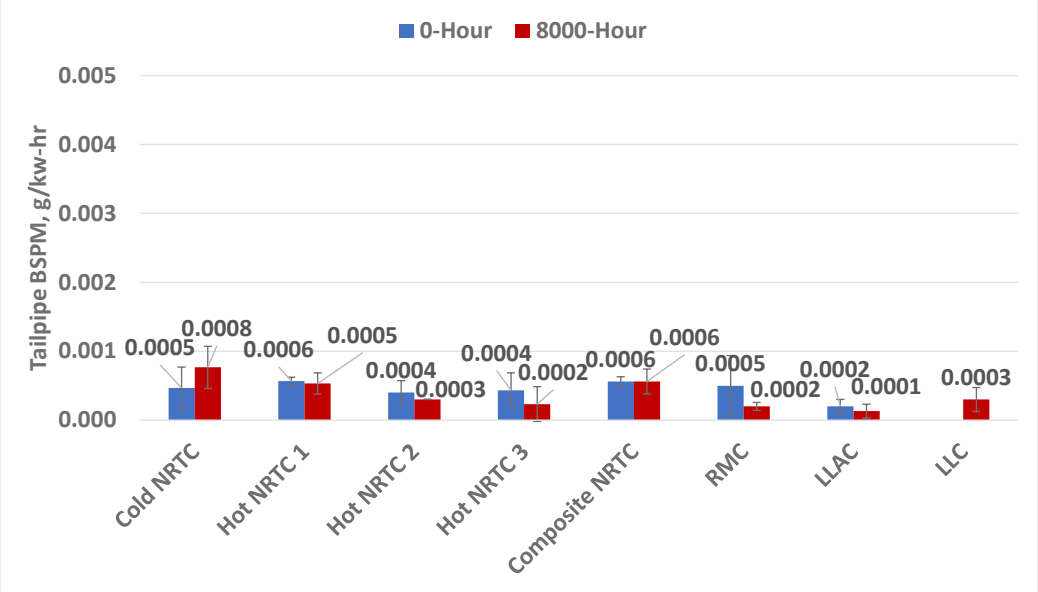



**FIGURE 93. TAILPIPE PM EMISSIONS WITHOUT DSF – 8000-HR VERSUS 0-HR, CCV**

Continuous $NO_X$ data comparisons between 8000-hr and 0-hr tests are shown for the cold-start NRTC, hot-start NRTC, and LLAC in Figure 94, Figure 95, and Figure 96, respectively. Figure 98 shows continuous $NO_X$ data for the LLC, while Figure 98 depicts continuous $NO_X$ data for the RMC. The cold-start data in Figure 94 shows a slight loss of low temperature conversion over the MFC, as well as a small loss of conversion between 225°C and 275°C on the downstream system, resulting in a small additional $NO_X$ breakthrough about 250 seconds into the cold-start. It should be noted that the storage calibration change did not impact cold-start, and therefore storage targets and dosing were the same between 0-hr and 8000-hr tests for the cold NRTC.

Hot-start NRTC data in Figure 95 show the impact of the storage calibration discussed earlier at lower temperatures, with a significant reduction in MFC conversion between 200 and 500 seconds into the hot-start cycle. Most of this load is shifted to the downstream system, as discussed earlier, however, the aged downstream system does not quite have the capability to absorb all of this, resulting in a slightly larger tailpipe $NO_X$ breakthrough between 250 and 300 seconds into the cycle.

LLAC in Figure 96 shows the shift in MFC calibration discussed earlier, with more demand being placed on the downstream SCR. However, at the lower space velocities of the LLAC, the downstream catalyst is able to handle this increased demand, and there was very little change in the overall tailpipe $NO_X$ level.

However, Figure 97 shows continuous $NO_X$ data at the 8000-hr test point for the LLC without DSF. The data shows the balance of conversion through the system over the cycle, mostly relying on the MFC except during the higher load return to service episode between 2100 and 2400 seconds in the cycle, just after the long idle segment. Tailpipe $NO_X$ on this cycle is characterized by a few breakthroughs near the beginning of various return-to-service events, but overall appears well controlled on this cycle. Tailpipe $NO_X$ in the LLC is similar to what was seen on the LLAC.

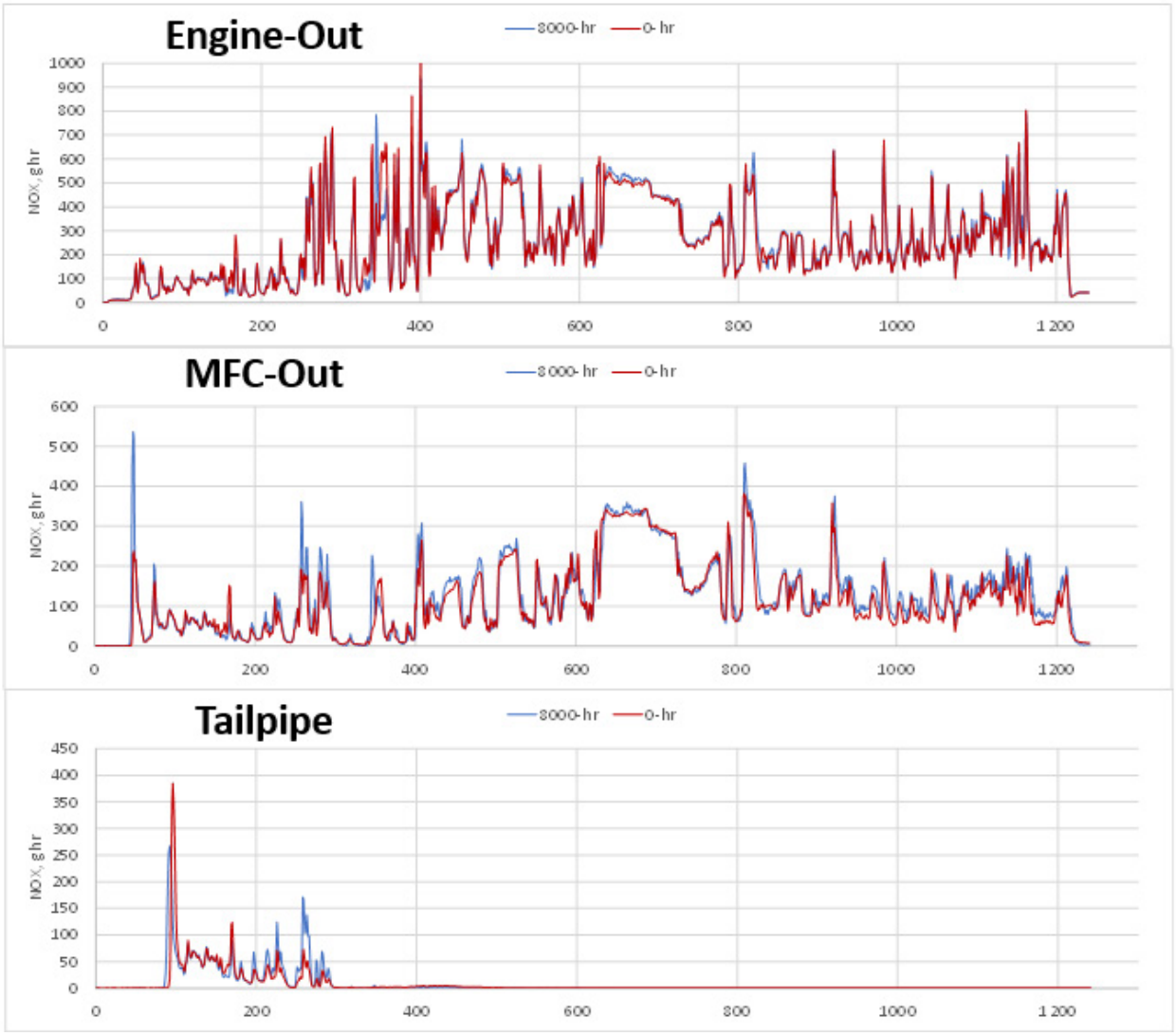



**FIGURE 94. CONTINUOUS COLD-START NRTC $NO_X$ DATA – 8000-HR VERSUS 0-HR WITHOUT DSF, CCV**

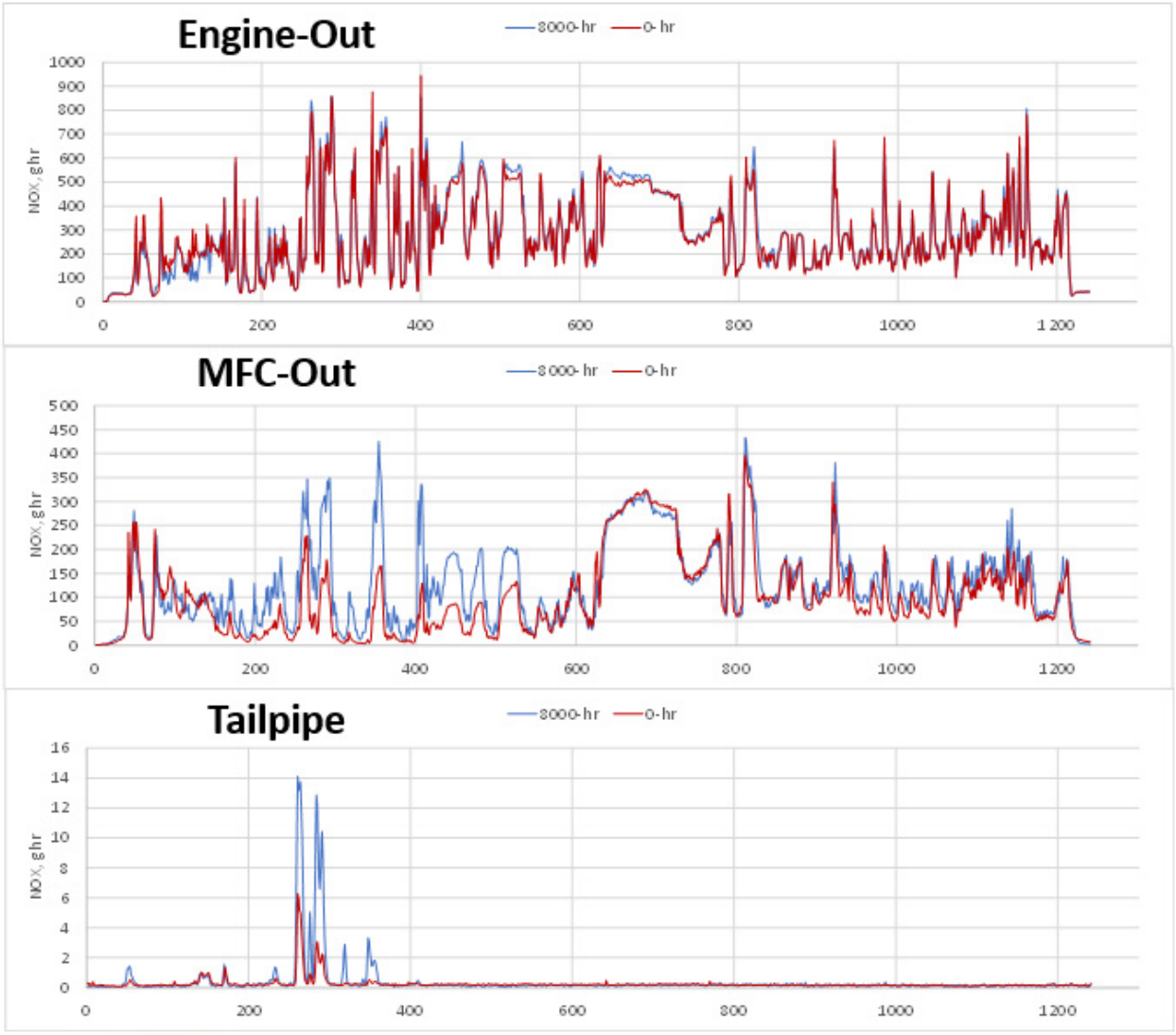



**FIGURE 95. CONTINUOUS HOT-START NRTC $NO_X$ DATA – 8000-HR VERSUS 0-HR WITHOUT DSF, CCV**

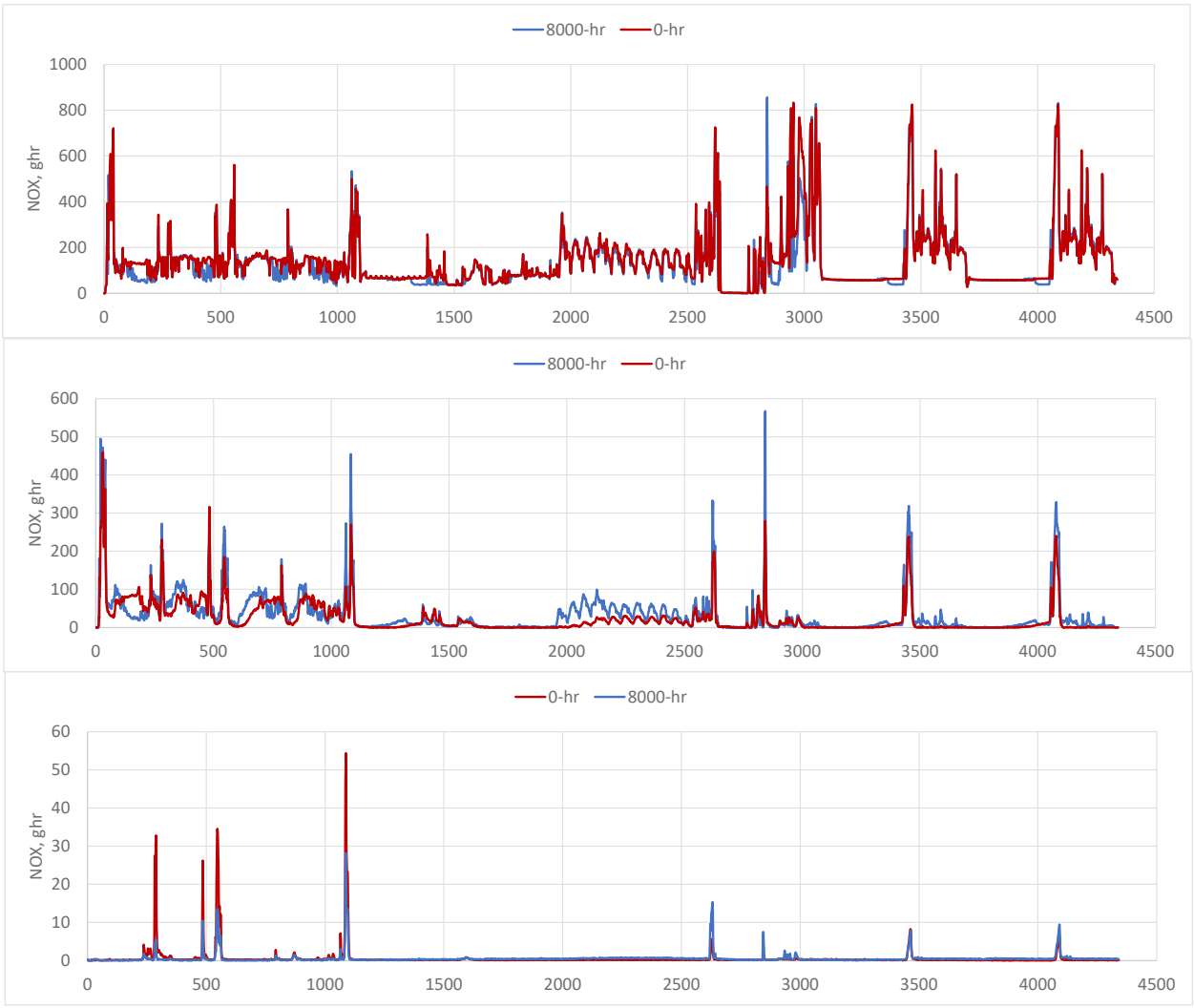



**FIGURE 96. CONTINUOUS LLAC $NO_X$ DATA – 8000-HR VERSUS 0-HR WITHOUT DSF, CCV**

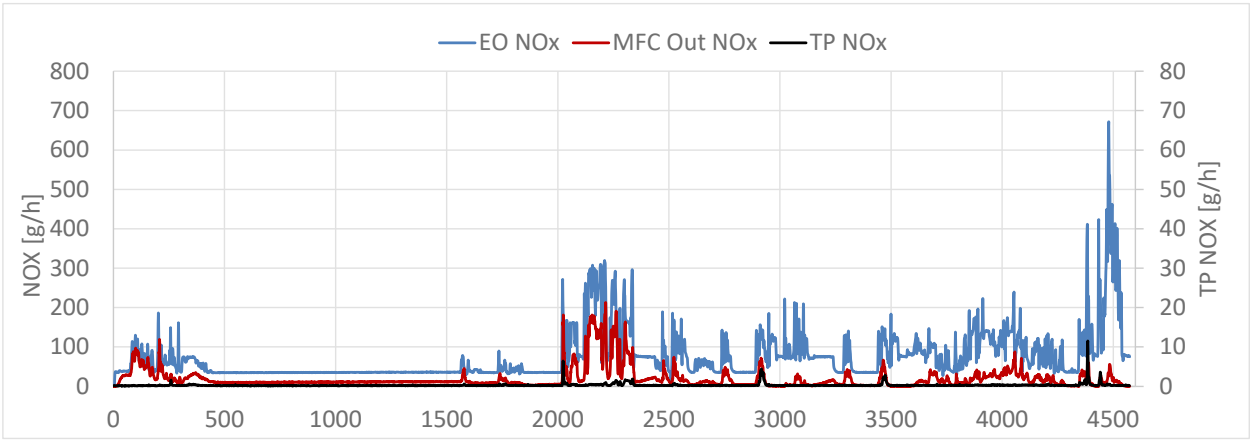



**FIGURE 97. CONTINUOUS LLC $NO_X$ DATA AT THE 8000-HR POINT WITHOUT DSF, CCV**

The RMC showed the largest shift in tailpipe $NO_X$ for all of the test cycles. Figure 97 shows a clear reduction in high temperature, high space velocity (above 75,000 $hr^{-1}$) $NO_X$ conversion across the MFC, although it should be noted that at the high temperature (above 325°C) the calibration is only requesting about 20% $NO_X$ conversion at steady-state. The change in the first non-idle mode is more reflective of the reduced lower temperature storage targets below 250°C, leaving less stored ammonia to deal with the first large change in engine-out $NO_X$. At the same time, the downstream system has lost a small amount of capacity to deal with high $NO_X$ flux under these conditions, and this results in a breakthrough event near 200 seconds, and a more sustained but much lower level but sustained breakthrough at the maximum power mode.




**FIGURE 98. CONTINUOUS RMC $NO_X$ DATA – 8000-HR VERSUS 0-HR WITHOUT DSF, CCV**

At the same time, $N_2O$ emissions on the RMC are significantly higher, though they are still well below the proposed cap of 0.13 g/kw-hr, and thus not problematic. Figure 99 shows a comparison of tailpipe $N_2O$ data on the RMC between the 8000-hr and 0-hr test points. There is a significant shift upwards in $N_2O$, especially in the higher space velocity modes. There was little evidence of $N_2O$ from the MFC (which is not surprising given the under-dosing), which means that the downstream SCR did not have much more headroom to deal with larger amounts of $NO_X$

and ammonia flux through the system. This behavior also likely indicates that the reduced volume SCR would not have been sufficient for the 8000-hour aged catalysts. Selectivity had likely degraded somewhat as well.

It is possible that the calibration could have been adjusted to ask for more $NO_X$ conversion from the MFC in an effort to take the high temperature load off the downstream SCR. However, it was not clear that this would have been completely successful, and such an adjustment would have likely impacted passive soot oxidation on the NRTC in a negative manner. It is also possible that the increased pressure on the downstream system due to the higher $NO_X$ flux and loss of MFC conversion may have revealed a mixing shortfall that was not apparent when the catalyst was less aged. However, there was not enough scope at this point to investigate that possibility.

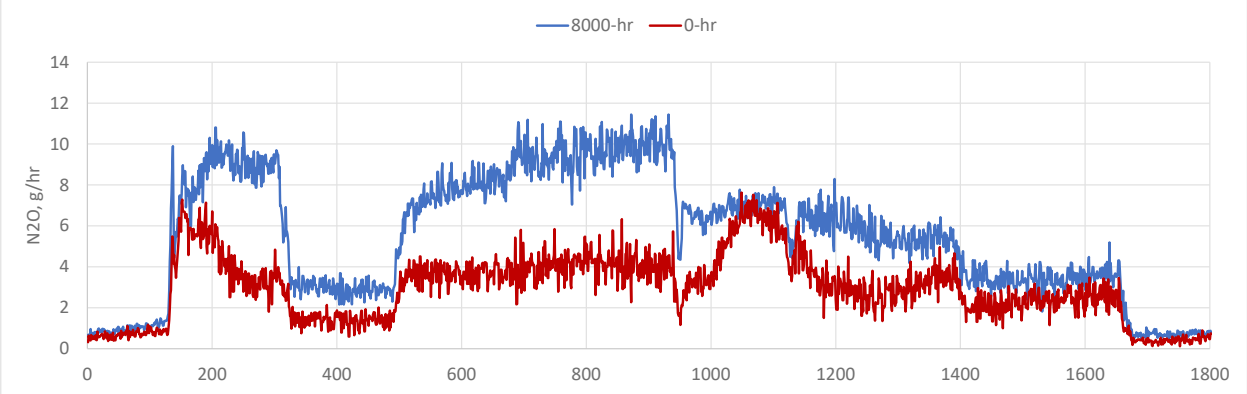



**FIGURE 99. CONTINUOUS RMC TAILPIPE $N_2O$ DATA – 8000-HR VERSUS 0-HR WITHOUT DSF, CCV**

Test results with DSF for the 8000-hr point and 0-hour point are shown in Figure 100 for tailpipe $NO_X$. Figure 101 shows $CO_2$ emissions in comparison to the Tier 4 baseline engine, and Figure 102 shows $N_2O$ emissions compared to the baseline. The Tier 5 system with DSF showed more degradation in the cold-start NRTC, but slightly less on the hot-start NRTC, with the composite being similar to the case without DSF. The RMC still showed are larger degradation than the other cycles, although the 0-hour data point was slightly higher there was still a 0.25% loss of $NO_X$ conversion on the RMC. The LLAC and LLC results were lower with DSF than without DSF but showed very little degradation due to aging (although again the calibration changes do make that comparison more difficult, due to the fact the changes mean that we are no longer looking at a direct performance comparison before and after aging).

Regarding GHG emissions, Table 27 shows a comparison of $CO_2$ emissions for the DSF-enabled Tier 5 demonstration at FUL versus the Tier 4 baseline. With DSF, larger $CO_2$ reductions were seen, with all cycles showing $CO_2$ reductions of 5% to 8.6%, and the LLAC beyond even that level at nearly 11% reduction. $CO_2$ reductions from baseline were 1% larger with DSF on the NRTC and RMC, and 5% larger on low load cycles. $N_2O$ emissions were at or below baseline levels on all cycles, with low load cycles showing particular improvements over the non-DSF case due to the higher exhaust temperatures on the LLAC and LLC.

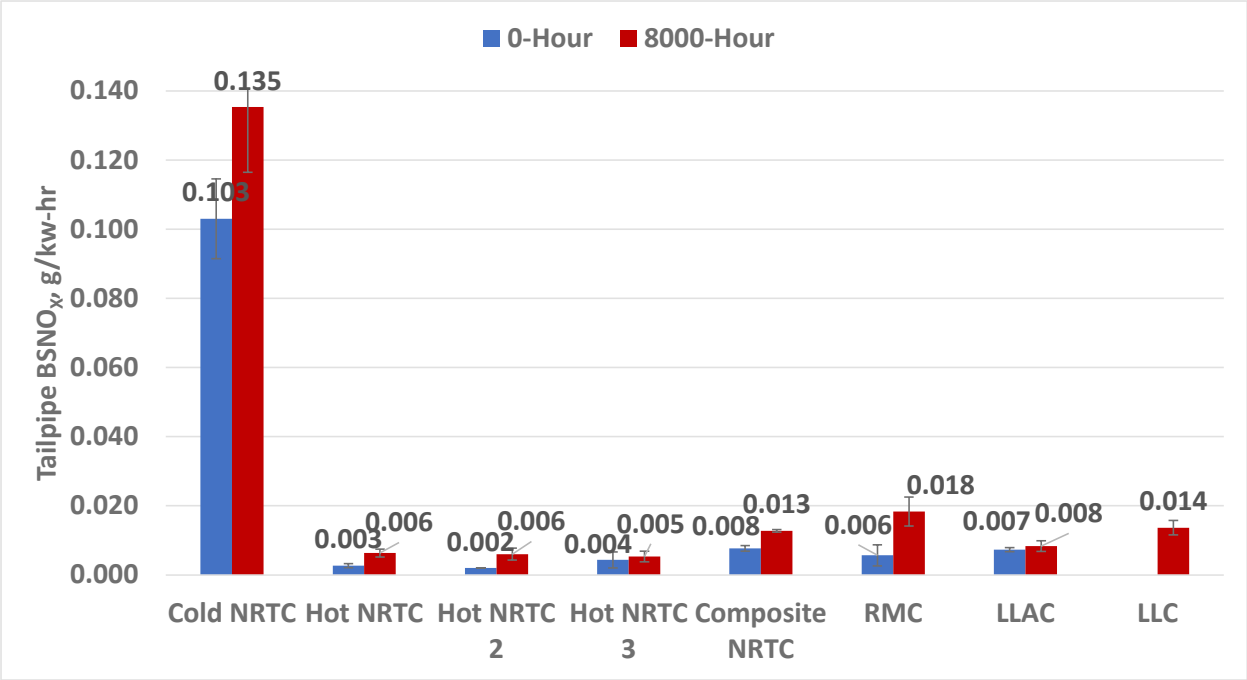



**FIGURE 100. TAILPIPE $NO_X$ EMISSIONS WITH DSF – 8000-HR VERSUS 0-HR, CCV**

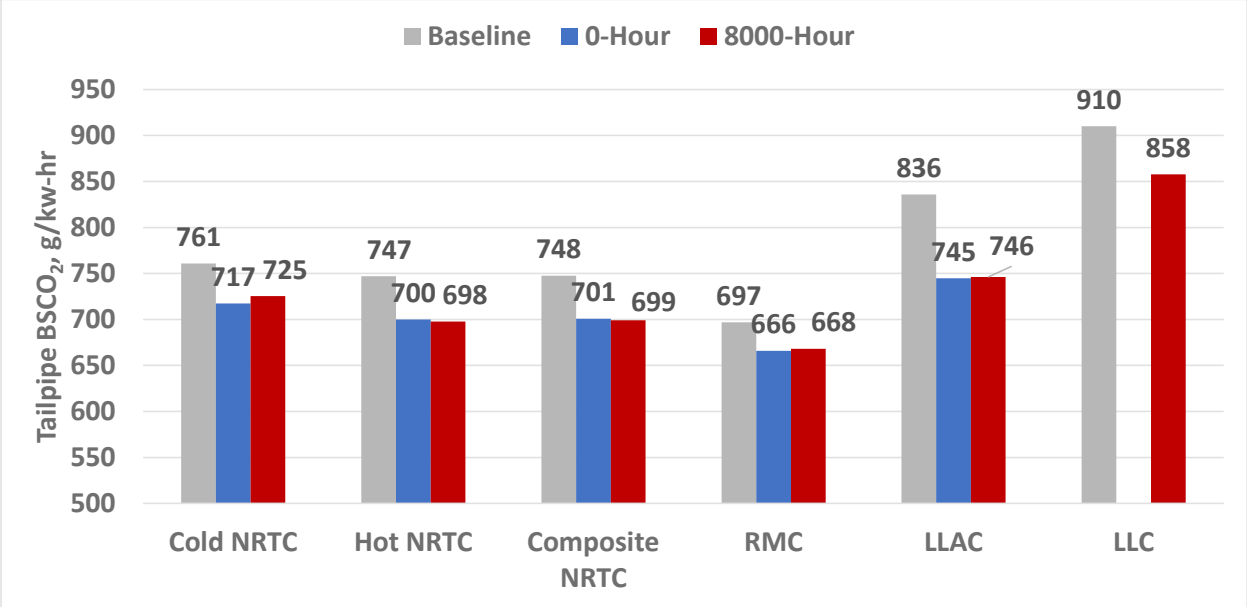



**FIGURE 101. TAILPIPE $CO_2$ EMISSIONS WITH DSF – 8000-HR VERSUS 0-HR, CCV**

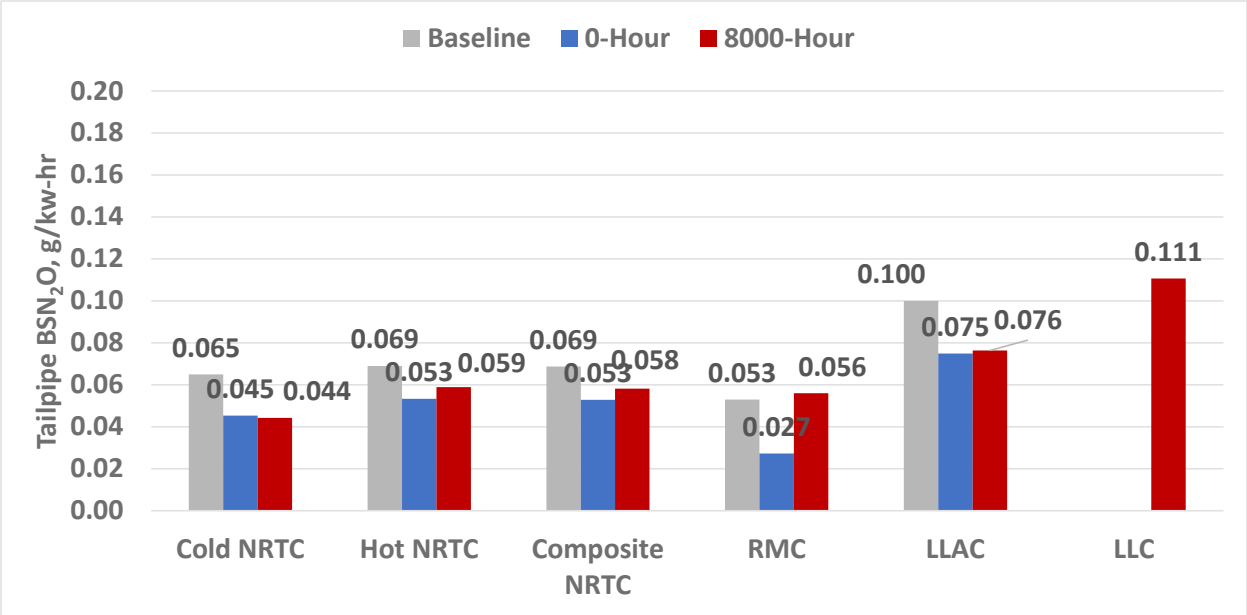



**FIGURE 102. TAILPIPE $N_2O$ EMISSIONS WITH DSF – 8000-HR VERSUS 0-HR, CCV**

**TABLE 27. $CO_2$ EMISSION RESULTS AT FUL WITH DSF COMPARED TO BASELINE TIER 4 ENGINE**

| | Baseline, g/kw-hr | 8000-hr, g/kw-hr | % Reduction |
|---|---|---|---|
| Cold NRTC | 761 | 725 | 4.7% |
| Hot NRTC | 747 | 698 | 6.6% |
| **Comp NRTC** | **748** | **699** | **6.6%** |
| RMC | 697 | 668 | 4.2% |
| LLAC | 836 | 746 | 10.8% |
| LLC | 910 | 858 | 5.7% |

Continuous $NO_X$ data for the various tests cycles run with DSF comparing 8000-hr results and 0-hr results is given in the following series of charts. NRTC cold-start and hot-start $NO_X$ data is shown in Figure 103 and Figure 105, respectively. Note that unlike the case of the hot-start, ammonia storage targets for low temperatures during the cold-start remained similar between the 8000-hr and 0-hr test points. Figure 104 shows ammonia storage targets and actual values for the cold NRTC with DSF, and it can be seen in this chart that ammonia storage was nearly identical at the two test points. However, the $NO_X$ data in Figure 103 shows some loss of low temperature conversion on the MFC after 8000-hrs equivalent aging, despite equivalent dosing and storage. Because this happens in the early cold-start before the downstream SCR has a chance to warm up, cold-start tailpipe $NO_X$ is increased.

The data in Figure 105 indicates some shift to less MFC conversion on the hot-start NRTC, but less so that without DSF because temperatures are hotter, so the change is less apparent. The primary tailpipe $NO_X$ behavior comes for a small breakthrough around the 250-second point in the

cycle, the result of a dip on downstream SCR conversion, down to about 95%. Temperature data given in Figure 106 indicate that this loss of conversion was in the range of 250°C.

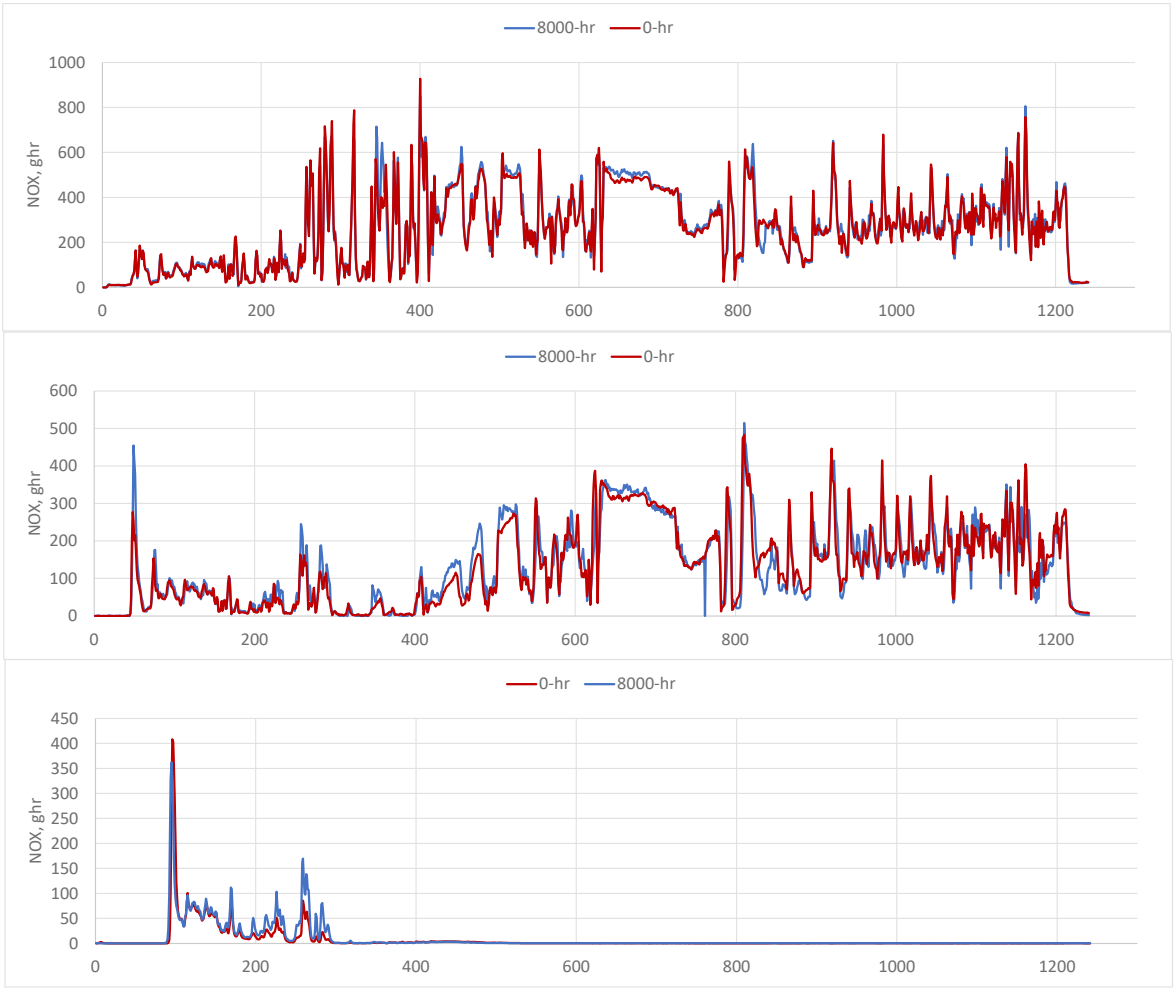



**FIGURE 103. CONTINUOUS COLD-START NRTC $NO_X$ DATA – 8000-HR VERSUS 0-HR WITH DSF, CCV**

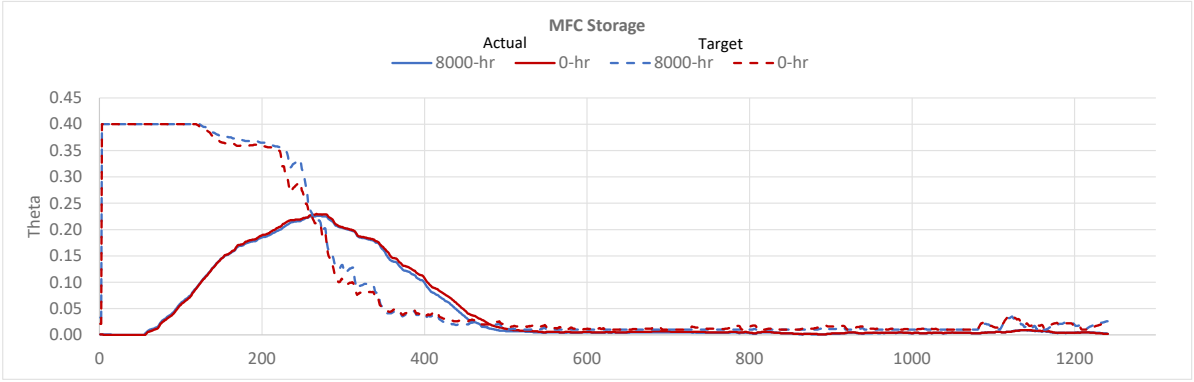



**FIGURE 104. MFC AMMONIA STORAGE FOR COLD-START NRTC WITH DSF AT 8000-HR AND 0-HR TEST POINTS**

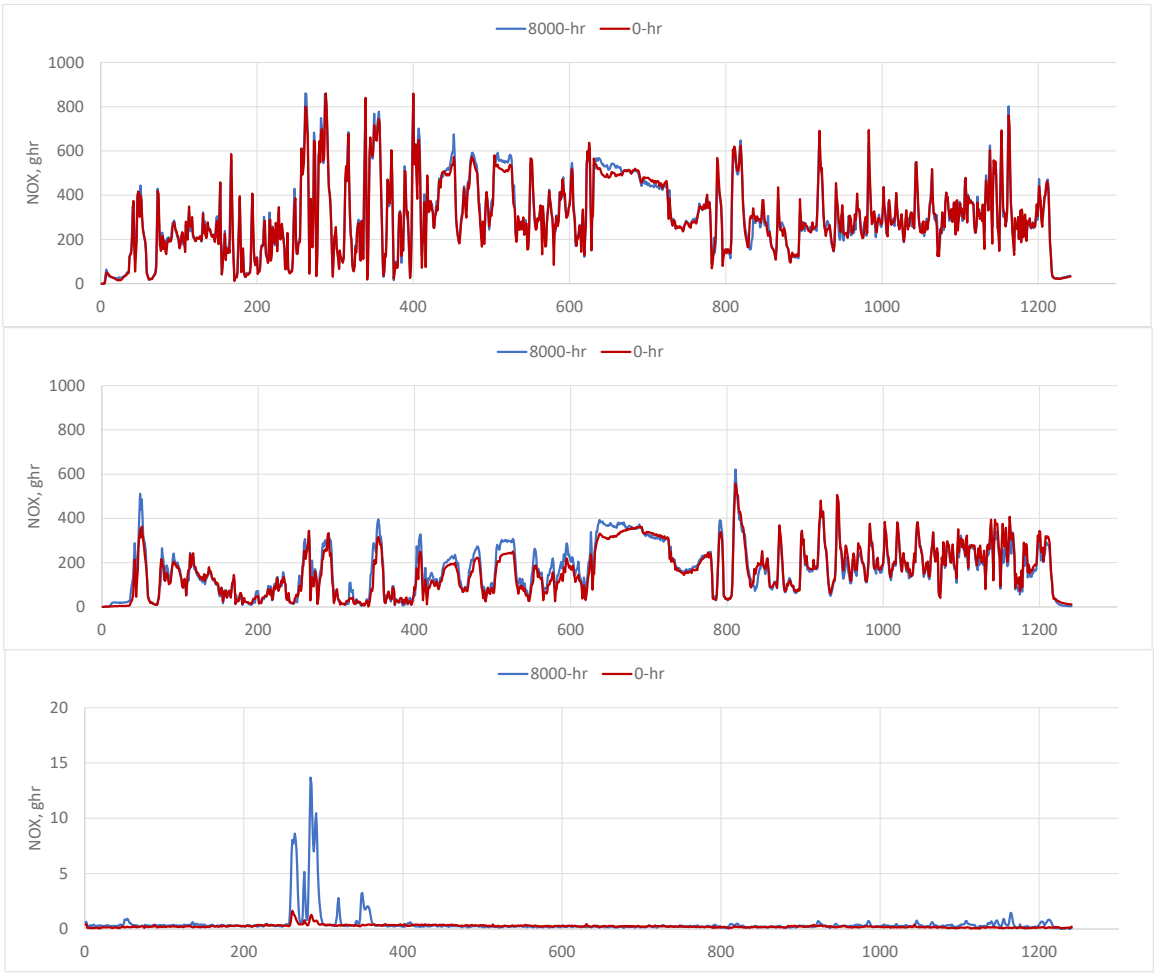



**FIGURE 105. CONTINUOUS HOT-START NRTC $NO_X$ DATA – 8000-HR VERSUS 0-HR WITH DSF, CCV**

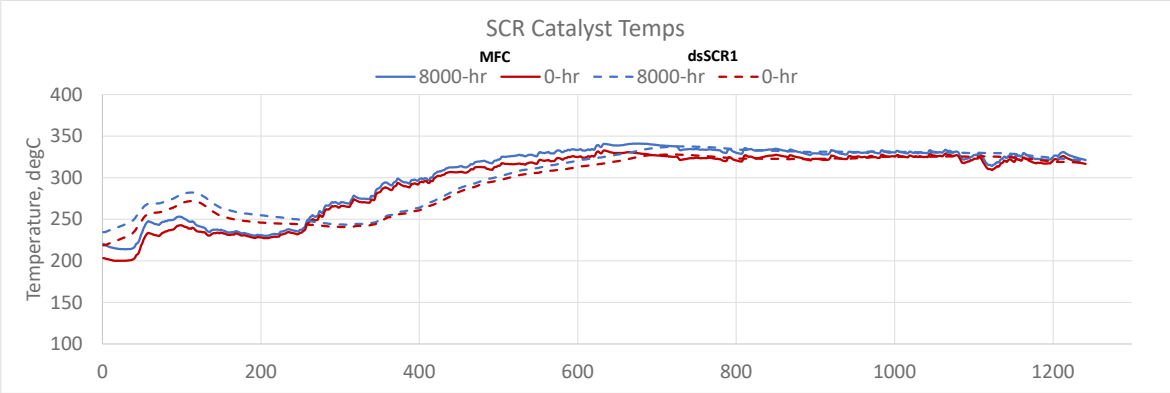



**FIGURE 106. HOT-START NRTC SCR CATALYST TEMPERATURES – 8000-HR VERSUS 0-HR WITH DSF**

Continuous LLAC $NO_X$ data with DSF is given in Figure 107, while MFC NOX conversion is shown in Figure 108. With DSF temperatures were always above 200°C and mostly

above 250°C for the cycle. However, the shift in storage calibration on the MFC is more apparent even with DSF because of the lower overall cycle temperatures. However, the downstream SCR was able to handle this load shift even better than without DSF due to the higher temperatures with DSF.

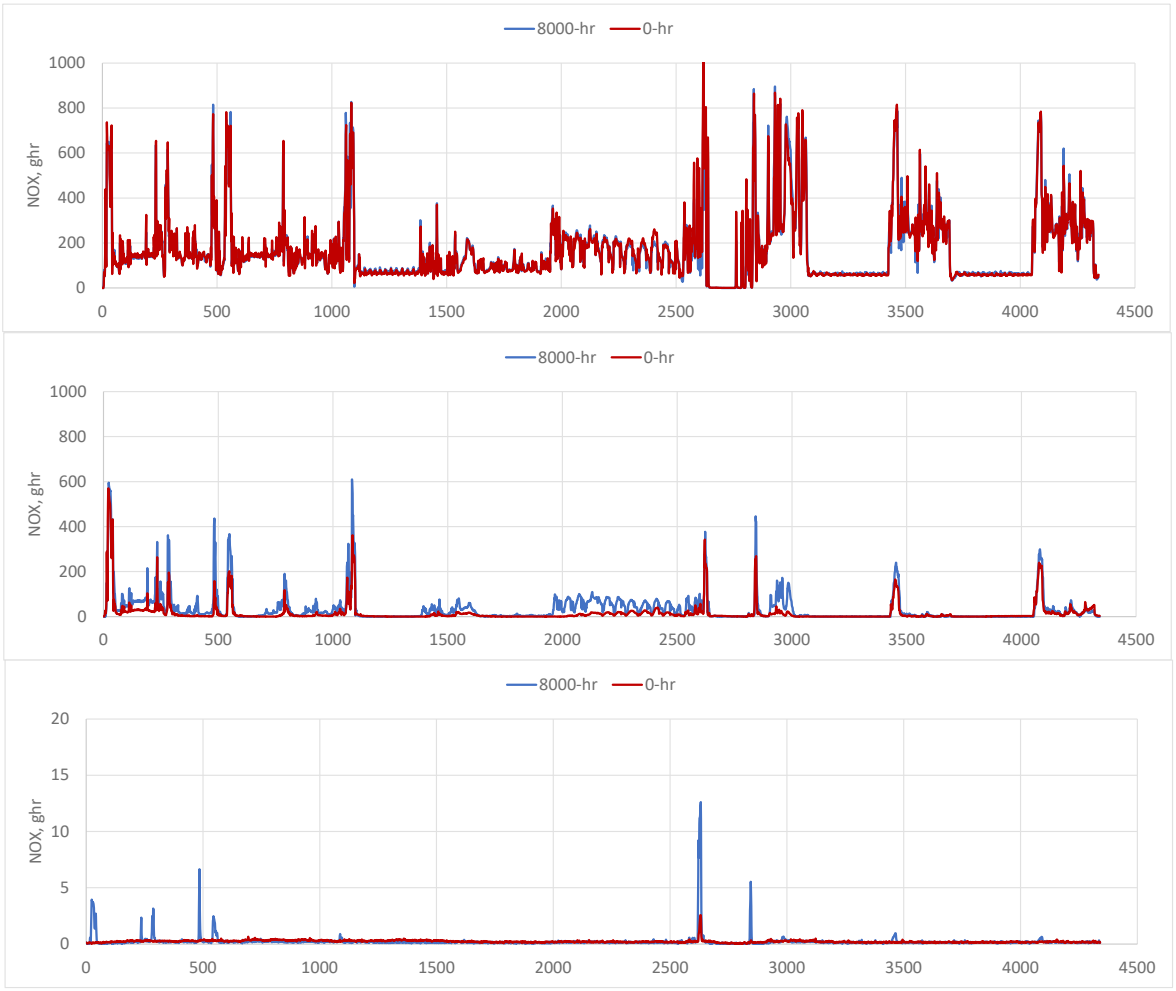



**FIGURE 107. CONTINUOUS LLAC $NO_X$ DATA – 8000-HR VERSUS 0-HR WITH DSF, CCV**




**FIGURE 108. NOX CONVERSION ACROSS MFC ON LLAC – 8000-HR VERSUS 0-HR WITH DSF**

Figure 109 shows only the 8000-hour $NO_X$ data on the LLC, given that there was no 0-hour data due to the cycle not being completed yet. Given the temperature range of the LLC, the majority of $NO_X$ conversion is done by the MFC, other than at the beginning of the cycle when temperatures are higher. The only significant tailpipe $NO_X$ breakthroughs with DSF happen in the return-to-service segment after the long idle (in the range of 2000-seconds), and they are only momentary. The thermal behavior of with DSF on the LLC is shown in Figure 110. The MFC is nearly always above 200°C, even during the long idle, and the rest of the system is below 200°C only at the end of the long idle with the front of the downstream SCR still being over 190°C. The engine is in aggressive thermal management (mode 2) only during the long idle segment itself.

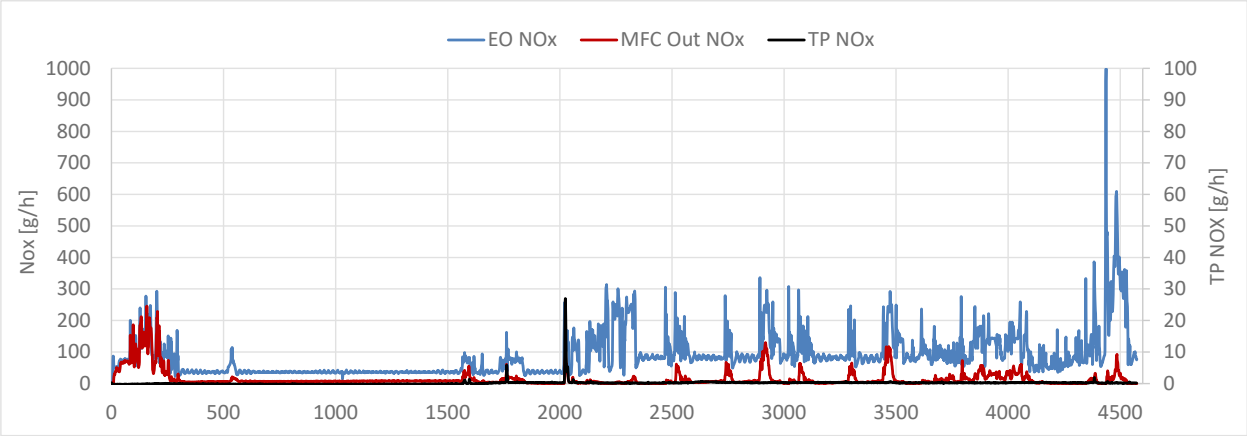



**FIGURE 109. CONTINUOUS LLC $NO_X$ DATA – 8000-HR WITH DSF, CCV**

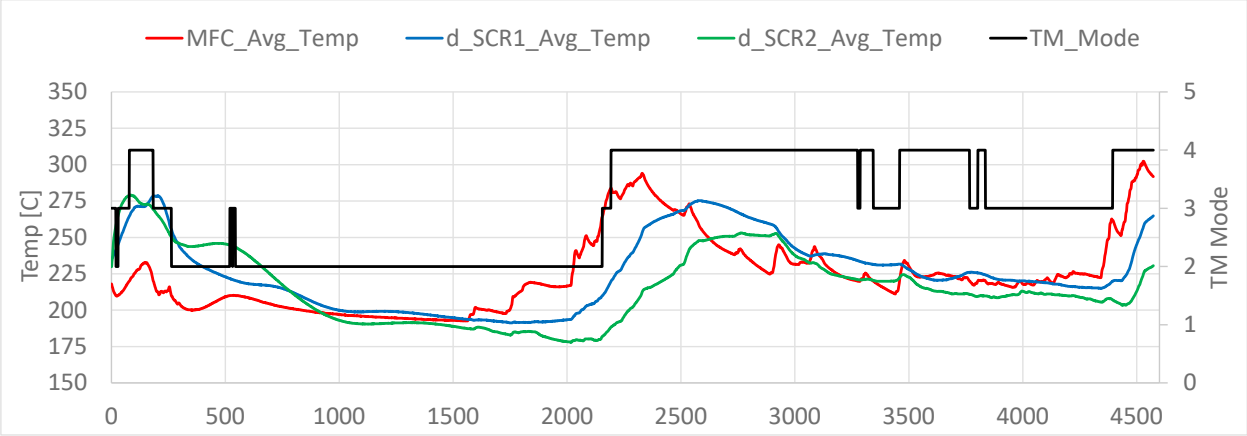



**FIGURE 110. CONTINUOUS LLC TEMPERATURE AND THERMAL MANAGEMENT DATA – 8000-HR WITH DSF, CCV**

Continuous $NO_X$ data for the RMC with DSF, shown in Figure 111, indicates trends very similar to what was seen for the data without DSF. The breakthrough spots on the RMC are also similar, with lower conversion across the MFC and with some downstream system breakthrough occurring under the highest space velocity conditions at the peak torque acceleration, and between 600 and 900 seconds during the high speed high load modes.




**FIGURE 111. CONTINUOUS RMC $NO_X$ DATA – 8000-HR VERSUS 0-HR WITH DSF, CCV**

The impact of DSF on system behavior can be examined further by looking at comparisons of 8000-hour data with and without DSF on the various test cycles. The following charts help to assess that impact, showing $NO_X$ emissions, SCR catalyst temperatures, and thermal management behavior both with and without DSF.

Figure 112 shows these comparisons for the cold-start NRTC cycle. DSF was not enabled until partway through the cold-start NRTC, as it was found that for the Tier 5 system on the NRTC, early cold-start warm-up was better without DSF. Comparing the NRTCs with and without DSF it can be seen that the cycles with DSF stay above 325°C towards the end, rather than cooling off. This does mean the subsequent cycles have less stored ammonia, which has a small impact on the aged cold-start performance on the NRTC with DSF.

Figure 113 shows the hot-start NRTC data with and without DSF. With DSF there is somewhat less conversion across the MFC, due to the higher temperatures that push the transition to relying mostly on the downstream system a little harder. It is also worth noting that with DSF there is no thermal management on the hot NRTC after about the first 30 seconds.




**FIGURE 112. CONTINUOUS COLD-START NRTC DATA – DSF VERSUS NODSF AT 8000 HOURS FUL**

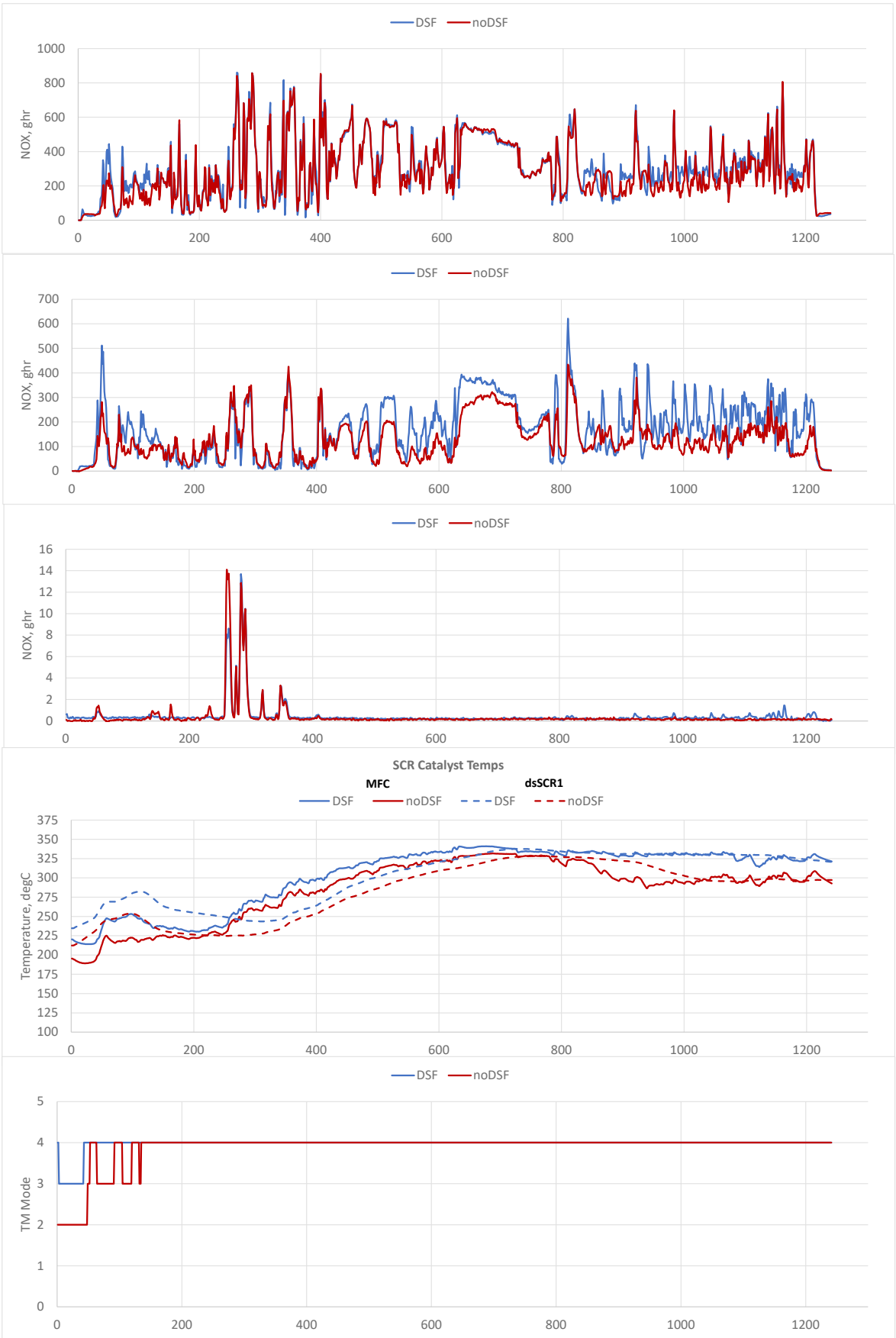



**FIGURE 113. CONTINUOUS HOT-START NRTC DATA – DSF VERSUS NODSF AT 8000 HOURS FUL**

It is on the low load cycles that the difference between runs with and without DSF becomes more apparent. Figure 114 shows the comparison for the LLAC. With DSF, MFC temperatures are as much as 50°C to 75°C in sustained low loads, thought in some cases this is offset by the engine being in thermal management more without DSF. The difference in thermal management behavior is very pronounced, with the engine cycling between all three modes regularly without DSF, while in the case with DSF there is only a short segment of moderate thermal management during the motoring segment in the middle. This results in a very substantial improvement in $CO_2$ and fuel consumption. At the same time, the higher temperatures also lead to lower $N_2O$. The LLAC alternates between conditions where the MFC does most of the work and conditions where it does little. Tailpipe $NO_X$ breakthrough events with DSF are both less common and smaller, leading to lower cycle $NO_X$ emissions.

All of these trends become more pronounced on the LLC, as shown in Figure 115. The engine rarely ever comes out of thermal management without DSF on the LLC, only in a few short segments in the middle and late cycle, and most of the cycle is spent in the aggressive thermal management mode (Mode 2). With DSF however, the engine cycles between all three modes, although it is still in aggressive thermal management through the long idle segment. This leads to an improvement in $BSCO_2$ with DSF of nearly 100 g/kw-hr Most of the tailpipe $NO_X$ breakthroughs are small and less frequent with DSF, but it is worth noting that the initial return actually has a higher $NO_X$ spike. It is worth noting that during the extended idle, the engine is in aggressive thermal management even with DSF, and eventually the aftertreatment system cools to about the same temperature (or a few degrees) cooler that it reaches without DSF, right around 200°C.

The RMC-SET comparison is shown in Figure 116 with and without DSF. Temperatures are higher at idle and the lightest load mode with DSF, but while this shifts the balance of $NO_X$ conversion more to the downstream system, tailpipe $NO_X$ is not affected on a cycle basis. In the end DSF could not do much about the loss of high temperature performance at high space velocity conditions.

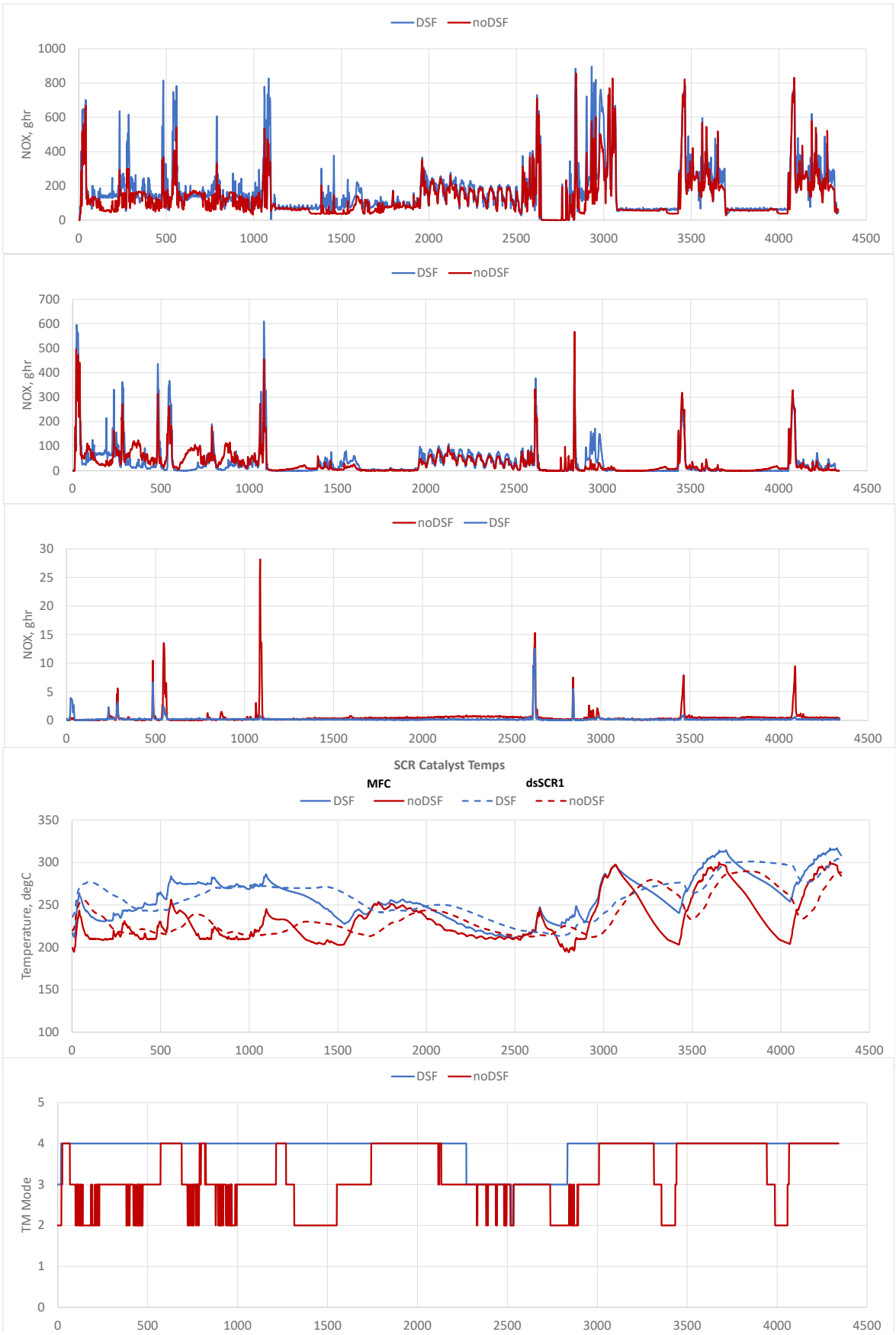



**FIGURE 114. CONTINUOUS LLAC DATA – DSF VERSUS NODSF AT 8000 HOURS FUL**

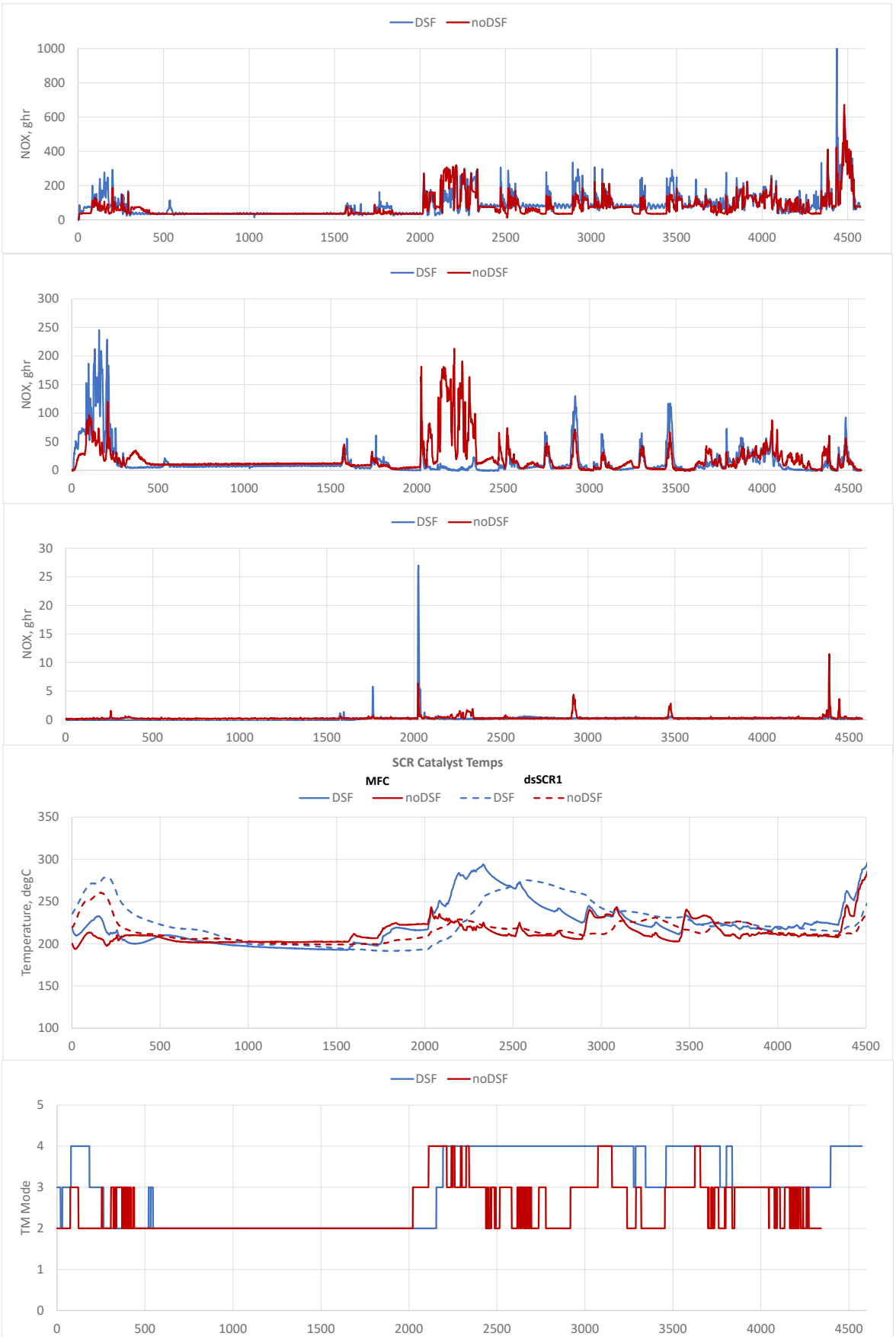



**FIGURE 115. CONTINUOUS LLC DATA – DSF VERSUS NODSF AT 8000 HOURS FUL**

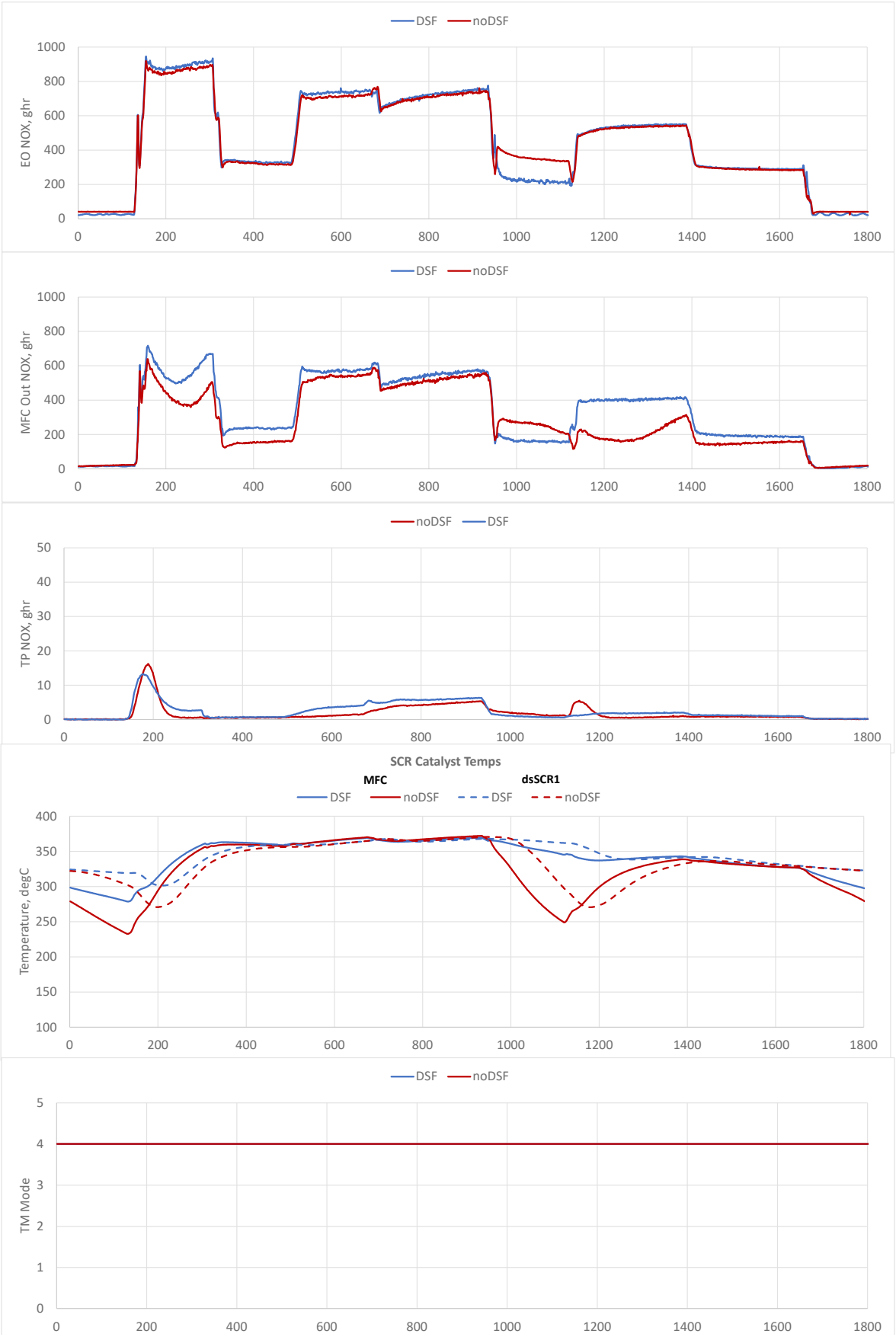



**FIGURE 116. CONTINUOUS RMC DATA – DSF VERSUS NODSF AT 8000 HOURS FUL**

### 3.13 Impact of Infrequent Regeneration Adjustment Factor (IRAF)

A key aspect of compliance measurements is the need to account for the impact of infrequent regeneration events, such as DPF regeneration, on tailpipe emissions. This is required under 40 CFR 1065.680. Although these adjustments are relatively small compared to most current Tier 4 certification levels, they could be quite significant at Low $NO_X$ levels. Therefore, it is important that the system design must maintain good $NO_X$ conversion during regeneration events, otherwise high regeneration emissions could have a serious negative impact on compliance margins. As part of a complete technology demonstration, an assessment of the infrequent regeneration adjustment factor (IRAF) is needed.

Because the development of a transient regeneration controller is not part of the scope of the demonstration program, it is not possible to directly measure emissions during regeneration on transient cycles. Instead the following approach is used to make measurements that will allow projection of the IRAF. Because regeneration does not normally occur during the demonstration emissions tests, it is necessary to calculate and Upward Adjustment Factor (UAF), which is described in 40 CFR 1065.680(a)(1) as follows:

$$UAF_{[cycle]} = EF_{A[cycle]} - EF_{L[cycle]}$$

Eq. 1065.680-1

Where:

$EF_{A[cycle]}$ = the average emission factor over the test segment as determined in paragraph (a)(4) of this section.

$EF_{L[cycle]}$ = measured emissions over a complete test segment in which active regeneration does not occur.

From 40 CFR 1065.680(a)(4) at noted above:

$$EF_{A[cycle]} = F_{[cycle]} \cdot EF_{H[cycle]} + (1.00 - F_{[cycle]}) \cdot EF_{L[cycle]}$$

Eq. 1065.680-3

Where:

$F_{[cycle]}$ = the frequency of the regeneration event during the test segment, expressed in terms of the fraction of equivalent test segments during which active regeneration occurs, as described in paragraph (a)(5) of this section.

$EF_{H[cycle]}$ = measured emissions over the test segment from a complete regeneration event, or the average emission rate over multiple complete test segments with regeneration if the complete regeneration event lasts longer than one test segment.

In order to make this calculation four key parameters must be known:

1. Engine-out emissions during a regeneration event
2. Aftertreatment $NO_X$ conversion capability under regeneration conditions
3. The duration of a regeneration event
4. The period between individual regeneration events

The methodology used to generate each of these parameters is described below. For the Deere 6.8L demo engine, engine out emissions during regeneration were initially projected based on assessing emissions of the baseline engine with the stock AT system during regeneration. A conservative estimate would then utilize the same engine-out emissions, unless it is found that

these are too high to support a reasonable UAF. In that case, a projection is made of what engine-out $NO_X$ levels would need to be lowered to support a workable UAF, and a discussion is included regarding whether such a level is feasible. Generally, regeneration modes often involve operation with either low EGR rates, or no EGR at all. For the NRTC, the engine-out $NO_X$ emission level was 5 g/kw-hr, considerably higher than the normal baseline level of 2.6 g/kw-hr. This helps to ensure sufficient oxygen is always available to deal with the additional post-injected fuel required during regeneration without generating excess soot or causing any issues with long-term DOC fouling.

To determine the $NO_X$ conversion capability of the advanced aftertreatment system, a series of experiments were run at different DPF regeneration temperature targets and different exhaust flow rates. $NO_X$ conversion over zeolite SCR catalysts is generally more difficult at the elevated temperatures seen during regeneration due to parasitic ammonia oxidation, especially in the case of copper-based zeolite SCR catalysts. Therefore, excess ammonia must be injected to sustain high $NO_X$ conversion, in the form of ammonia-to-$NO_X$ ratios (ANR) significantly above 1. The results of these experiments are given below in Figure 117 at low-to-mid space velocity, and in Figure 118 at higher space velocity. Regeneration temperatures at the DPF outlet of 570°C, 585°C, and 600°C were examined. Temperatures below 570°C are not practical because the SCR catalyst downstream of the DPF must reach at least 550°C to ensure good long term de-sulfation ($deSO_X$). At the same time, temperatures above 600°C are not necessary for either $deSO_X$ or soot oxidation, and would likely result in more rapid thermal degradation of the SCR catalysts. In the Stage 3 on-highway work, a regeneration temperature of 600°C was used, but that system also had a LO-SCR to assist in $NO_X$ control under regeneration conditions, and featured HC injection after the LO-SCR. This allowed the LO-SCR which was at lower temperatures during regeneration to handle the bulk of $NO_X$ control under those conditions. However, in a single SCR configuration like the one being examined in this program, this is not the case, therefore it is imperative that the SCR can achieve good $NO_X$ conversion at regeneration temperatures.

### *3.13.1. Team 2 Regeneration Results*

It can be seen from the figures that high $NO_X$ conversion rates, in excess of 90%, can be reached on the Development Aged Team 2 system at only ANR of 4 and higher at temperatures of 570°C. ANR above 4.5 at lower space velocity, and above 4 at higher space velocity is not practical due to limitations of maximum DEF doser flow rate, and limits of how much DEF could be properly mixed and distributed. It should be noted that $NO_X$ conversion was generally better at higher space velocity conditions, due to the fact the parasitic ammonia oxidation rates were lower at those higher exhaust flow rates. At 570°C, these data were used to project a $NO_X$ conversion capability of 93% under regeneration conditions. At 585°C, the projected $NO_X$ conversion capability was only 75%.

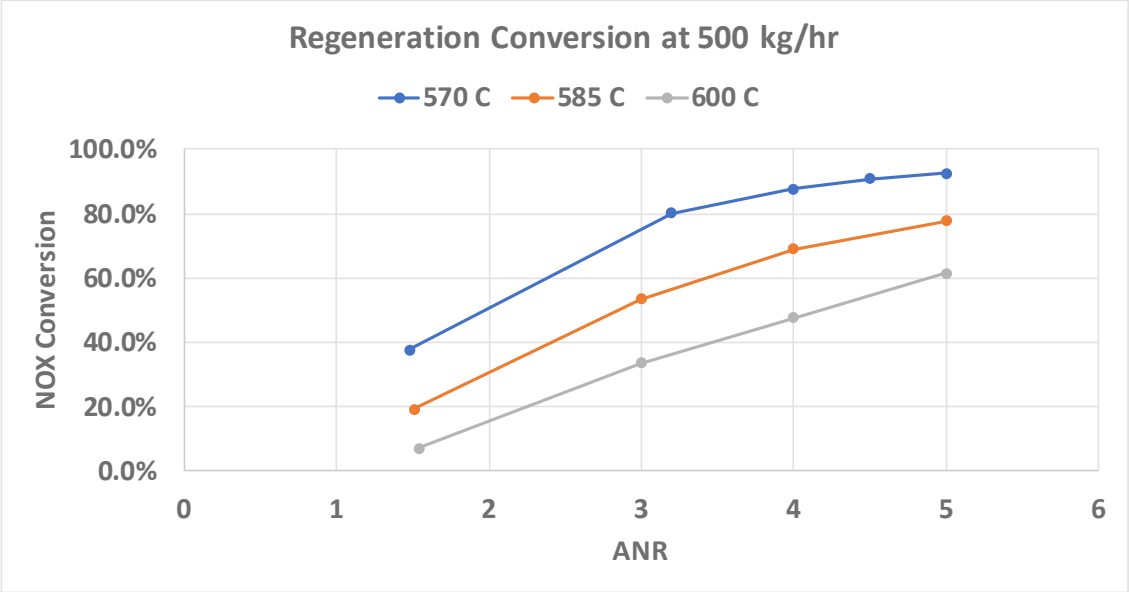



**FIGURE 117. TEAM 2 $NO_X$ CONVERSION UNDER DPF REGENERATION CONDITIONS AT 22.5K $HR^{-1}$ SPACE VELOCITY**

The regeneration duration for the baseline engine was 40 minutes, and the period between regenerations for the baseline engine was every 80 hours. This results in a regeneration frequency of 0.8%. This duration is generally driven by the need for periodic de$SO_X$ of the SCR catalyst. Assessment of the soot loading pressure drop behavior for the Low $NO_X$ system during the three test cycles was made in comparison to the baseline. It was determined that the Low $NO_X$ system would not result in increased engine-out PM and soot loading rates, therefore the baseline characteristics were utilized for the projections. In the case of the NRTC, a slight increase in pressure drop was not seen across multiple repeat cycles, therefore a slightly shorter regeneration period of 68 hours (200 NRTC cycles) was used. For the RMC cycle, good passive soot oxidation is always observed, and the DPF generally keeps itself clean on that cycle. As a result, the base period of 80 hours was used for the RMC cycle. In the case of the LLAC, temperatures are mostly below those required for good passive soot oxidation, therefore a much shorter period of 28 hours (23 LLAC cycles) was utilized for the calculations.

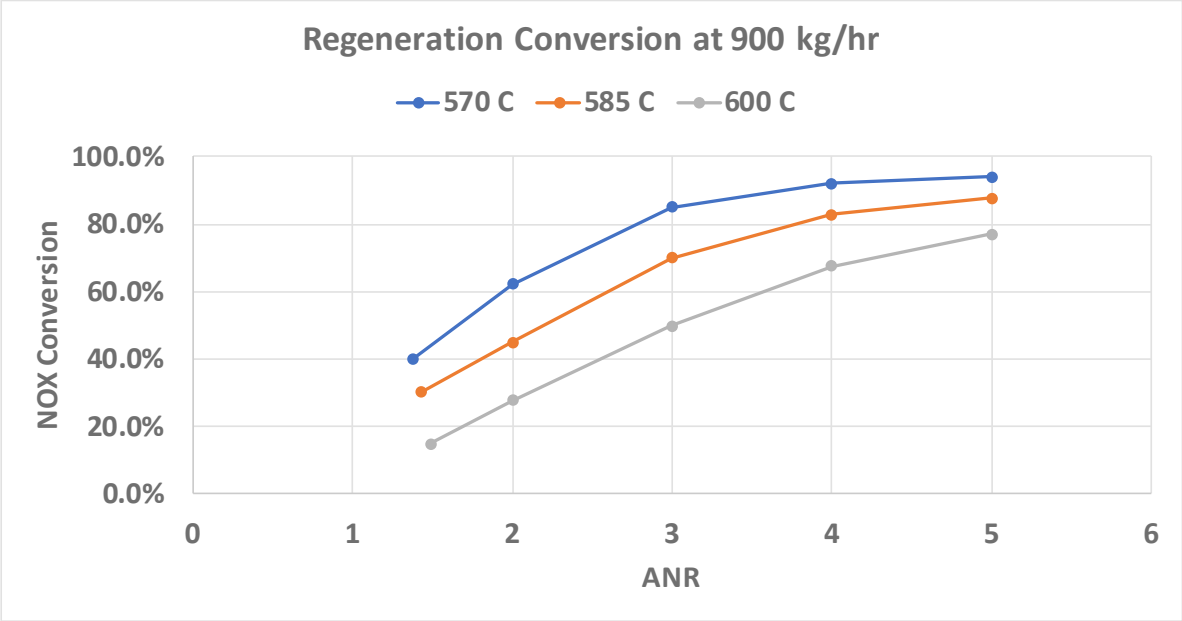



**FIGURE 118. TEAM 2 $NO_X$ CONVERSION UNDER DPF REGENERATION CONDITIONS AT 40K $HR^{-1}$ SPACE VELOCITY**

Using all these parameters as noted above, a projection of the UAF was made using a 570°C target regeneration temperature. Those calculations are summarized below in Figure 119 for the NRTC. The resulting UAF is 0.004 g/kw-hr. A similar projection was made at a 585°C target regeneration temperature, and this calculation is shown in Figure 120.

| | cycles | hours | tp bsnox | wtd mass | | |
|---|---|---|---|---|---|---|
| NRTC | 200 | 68.61 | 0.011 | 0.754722 | grams | |
| Regen NRTC | 2 | 0.69 | 0.350 | 0.240139 | grams | |
| next NRTC | 1 | 0.34 | 0.175 | 0.060035 | grams | |
| total | 203 | 69.6 | | 1.054896 | grams | |
| | | | | *0.01515* | g/kw-hr | |
| | EFL | 0.011 | g/kw-hr | *0.0041* | *g/kw-hr* | |
| | EFH | 0.292 | g/kw-hr | | | |
| | | | | | | |
| | | | | | | |
| **freq (F)** | **0.014778** | 0.014778 | **uaf** | **0.004** | | |

**FIGURE 119. IRAF CALCULATIONS FOR TEAM 2 SYSTEM ON NRTC CYCLE AT 570°C TARGET TEMPERATURE**

Note that at 585°C it was necessary to project that engine-out $NO_X$ levels would stay at 2.4 g/kw-hr during regeneration, which would require the use of EGR during DPF regeneration modes. While this can be done, it is not ideal. However, even with this lower engine-out $NO_X$ level, the much lower $NO_X$ conversion capability of only 75% means that the regeneration cycle emissions are much higher, resulting in a UAF of 0.007 g/kw-hr. This was deemed to be an unsustainably

high UAF at a $NO_X$ standard of 0.04 g/kw-hr, as regeneration emissions alone would actually be higher than all other NRTC emissions, which is problematic for compliance margins. As a result, the 570°C temperature was chosen as the target, and this is the temperature that would be used during the final DAAAC aging protocol in the follow-on program under 20MSC005. Projections were also made for the RMC and LLAC cycles using the 570°C target temperature.

| | cycles | hours | tp bsnox | wtd mass | | |
|---|---|---|---|---|---|---|
| NRTC | 200 | 68.61 | 0.011 | 0.754722 | grams | |
| Regen NRT | 2 | 0.69 | 0.600 | 0.411667 | grams | |
| next NRTC | 1 | 0.34 | 0.300 | 0.102917 | grams | |
| total | 203 | 69.6 | | 1.269306 | grams | |
| | | | | *0.01823* | g/kw-hr | |
| | EFL | 0.011 | g/kw-hr | *0.0072* | *g/kw-hr* | |
| | EFH | 0.500 | g/kw-hr | | | |
| | | | | | | |
| | | | | | | |
| **freq (F)** | **0.014778** | 0.014778 | **uaf** | **0.007** | | |

**FIGURE 120. IRAF CALCULATIONS FOR TEAM 2 SYSTEM ON NRTC CYCLE AT 585°C TARGET TEMPERATURE**

| | cycles | hours | tp bsnox | wtd mass | | |
|---|---|---|---|---|---|---|
| RMC | 160 | 80 | 0.006 | 0.48 | grams | |
| regen rmc | 2 | 1.00 | 0.323 | 0.323167 | grams | |
| total | 162 | 81 | | 0.803167 | grams | |
| | | | | 0.009916 | g/hp-hr | |
| | EFL | 0.0060 | g/hp-hr | 0.0039 | *g/hp-hr* | |
| | EFH | 0.3232 | g/hp-hr | | | |
| | | | | | | |
| | | | | | | |
| **freq (F)** | **0.012346** | 0.012346 | **uaf** | **0.004** | | |

**FIGURE 121. IRAF CALCULATIONS FOR TEAM 2 SYSTEM ON RMC CYCLE**

| | cycles | hours | tp bsnox | wtd mass | | |
|---|---|---|---|---|---|---|
| LLAC | 23 | 27.70861 | 0.047 | 1.302305 | grams | |
| regen LLAC | 1 | 1.204722 | 0.209 | 0.252054 | grams | |
| total | 24 | 28.91333 | | 1.554359 | grams | |
| | | | | 0.053759 | g/hp-hr | |
| | EFL | 0.0470 | g/hp-hr | *0.0068* | *g/hp-hr* | |
| | EFH | 0.2092 | g/hp-hr | | | |
| | | | | | | |
| | | | | | | |
| **freq** | **0.041667** | 0.042 | **uaf** | **0.007** | | |

**FIGURE 122. IRAF CALCULATIONS FOR TEAM 2 SYSTEM ON LLAC CYCLE**

As noted earlier, a DPF outlet temperature of 570°C should produce SCR temperatures at or above 550°C on the SCR, which should be sufficient for long-term de$SO_X$. However, if during the early stages of the DAAAC durability, it is found that this target temperature is not sufficient to adequately control long-term sulfation of the SCR, then a slightly higher target temperature would need to be used, which would result in the need to re-assess these IRAF calculations.

*3.13.2. Team 1 Regeneration Results*

The Team 1 SCR catalysts were also assessed for their capability to reduce $NO_X$ emissions during filter regeneration. Figure 123 shows $NO_X$ conversion versus downstream doser ANR and temperature at low flow rates, while Figure 124 shows the same comparisons at higher exhaust flow rates. Compared to the Team 2 data, it is clear that the Team 1 catalysts display much lower parasitic ammonia oxidation at high temperatures, and therefore a lower ANR is needed to maximize $NO_X$ conversion. In addition, the Team 1 SCR catalysts are able to reach $NO_X$ conversion in excess of 95% under regeneration conditions up to 585°C, and they were able to do this at ANR 3 instead of needed an ANR closer to 4 like the Team 2 SCR catalysts. At a 570°C regeneration temperature, $NO_X$ conversion rates of 97% can be achieved at ANR 3. This is significantly better performance than was apparent for the Team 2 catalysts and was one of the key factors in the selection of the Team 1 downstream SCR catalysts for the final Tier 5 demonstration system.

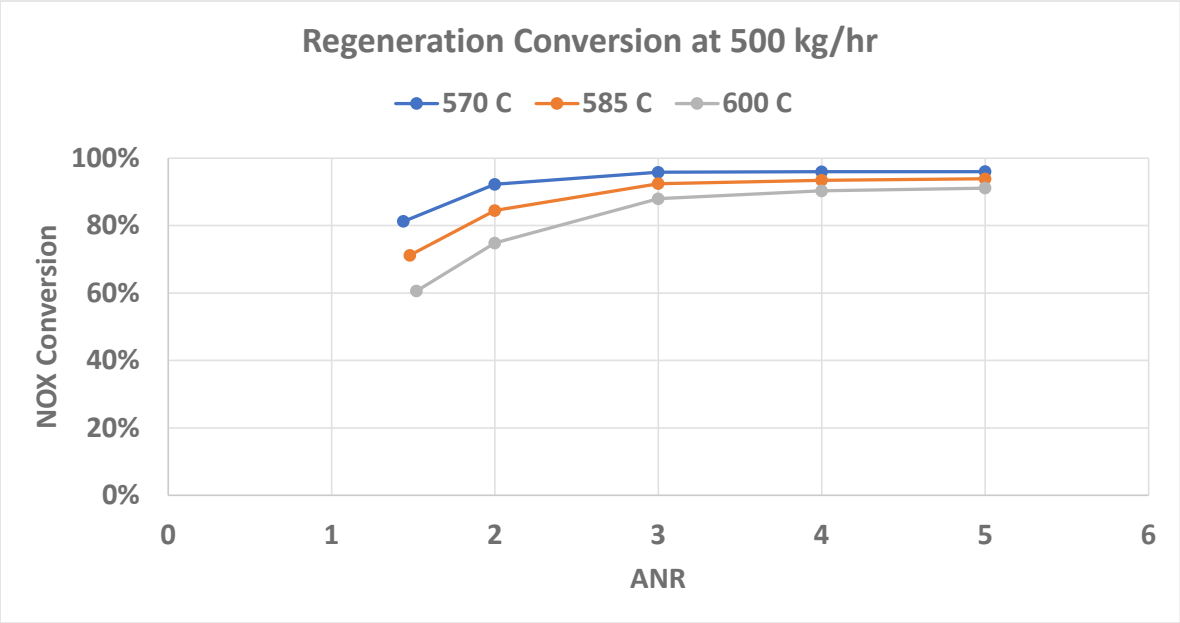



**FIGURE 123. TEAM 1 $NO_X$ CONVERSION UNDER DPF REGENERATION CONDITIONS AT 22.5K $HR^{-1}$ SPACE VELOCITY**

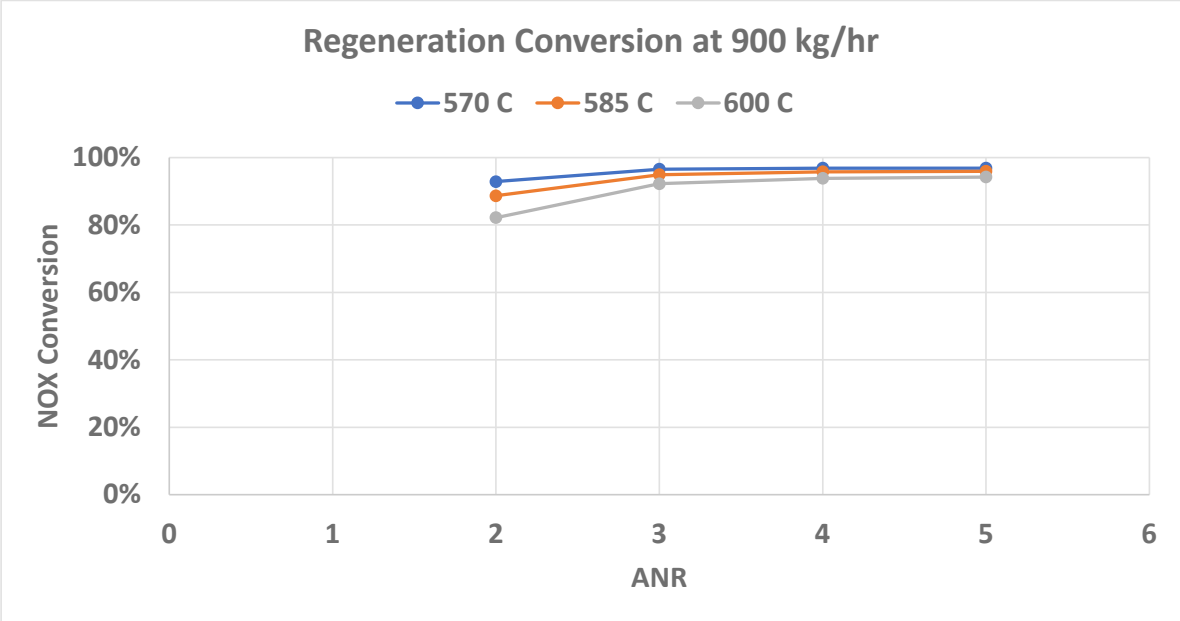



**FIGURE 124. TEAM 1 $NO_X$ CONVERSION UNDER DPF REGENERATION CONDITIONS AT 40K $HR^{-1}$ SPACE VELOCITY**

This improved performance had a significant impact on the IRAF calculations for the UAF on Team 1, and the final Tier 5 system. A conservative $NO_X$ conversion of 96% was used for Team 1 IRAF projections. Similar regeneration intervals were used for each cycle. In addition, once the LLC became available, IRAF calculations were added for the LLC. To support this calculation, and to also make sure that the various calibration changes made at the 8000-hr point did not disturb regeneration behavior, measurements of engine-out soot over all cycles were made using an AVL 483 Micro-Soot Sensors (MSS).

Calculation for UAF for Team 1 SCR catalysts is given in Figure 125 for the NRTC, Figure 126 for the RMC, Figure 127 for the LLAC, and Figure 128 for the LLC, respectively. Note that for all of the cycles, the calculated UAF is roughly half that projected for the Team 2 SCR catalysts. This is due to the higher $NO_X$ conversion efficiency under regeneration conditions, due in large part to lower parasitic ammonia oxidation behavior.

| | cycles | hours | tp bsnox | wtd mass | | |
|---|---|---|---|---|---|---|
| NRTC | 200 | 68.61 | 0.008 | 0.548889 | grams | |
| Regen NRTC | 2 | 0.69 | 0.208 | 0.142711 | grams | |
| next NRTC | 1 | 0.34 | 0.104 | 0.035678 | grams | |
| total | 203 | 69.6 | | 0.727278 | grams | |
| | | | | *0.01044* | g/kw-hr | |
| | EFL | 0.008 | g/kw-hr | *0.0024* | *g/kw-hr* | |
| | EFH | 0.173 | g/kw-hr | | | |
| | | | | | | |
| | | | | | | |
| **freq (F)** | **0.014778** | 0.014778 | **uaf** | **0.002** | | |

**FIGURE 125. IRAF CALCULATIONS FOR TEAM 1 SYSTEM ON NRTC CYCLE AT 570°C TARGET TEMPERATURE**

| | cycles | hours | tp bsnox | wtd mass | | |
|---|---|---|---|---|---|---|
| RMC | 160 | 80 | 0.018 | 1.44 | grams | |
| regen rmc | 2 | 1.00 | 0.213 | 0.212667 | grams | |
| total | 162 | 81 | | 1.652667 | grams | |
| | | | | 0.020403 | g/hp-hr | |
| | EFL | 0.0180 | g/hp-hr | 0.0024 | *g/hp-hr* | |
| | EFH | 0.2127 | g/hp-hr | | | |
| | | | | | | |
| | | | | | | |
| **freq (F)** | **0.012346** | 0.012346 | **uaf** | **0.002** | | |

**FIGURE 126. IRAF CALCULATIONS FOR TEAM 1 SYSTEM ON RMC CYCLE AT 570°C TARGET TEMPERATURE**

| | cycles | hours | tp bsnox | wtd mass | | |
|---|---|---|---|---|---|---|
| LLAC | 28 | 33.73222 | 0.047 | 1.585414 | grams | |
| regen LLAC | 1 | 1.204722 | 0.175 | 0.210699 | grams | |
| total | 29 | 34.93694 | | 1.796113 | grams | |
| | | | | 0.05141 | g/hp-hr | |
| | EFL | 0.0470 | g/hp-hr | *0.0044* | *g/hp-hr* | |
| | EFH | 0.1749 | g/hp-hr | | | |
| | | | | | | |
| | | | | | | |
| **freq** | **0.034483** | 0.034 | **uaf** | **0.004** | | |

**FIGURE 127. IRAF CALCULATIONS FOR TEAM 1 SYSTEM ON LLAC CYCLE AT 570°C TARGET TEMPERATURE**

| | cycles | hours | tp bsnox | wtd mass | | |
|---|---|---|---|---|---|---|
| LLC | 26 | 33.00556 | 0.047 | 1.551261 | grams | |
| regen LLC | 1 | 1.269444 | 0.178 | 0.225651 | grams | |
| total | 27 | 34.275 | | 1.776913 | grams | |
| | | | | 0.051843 | g/hp-hr | |
| | EFL | 0.0470 | g/hp-hr | *0.0048* | *g/hp-hr* | |
| | EFH | 0.1778 | g/hp-hr | | | |
| | | | | | | |
| | | | | | | |
| **freq** | **0.037037** | 0.037 | **uaf** | **0.005** | | |

**FIGURE 128. IRAF CALCULATIONS FOR TEAM 1 SYSTEM ON LLC CYCLE AT 570°C TARGET TEMPERATURE**

As noted earlier, the inclusion of the MFC did not change the target regeneration temperature of 570°C, nor did it impact downstream $NO_X$ efficiency for the Team 1 SCR catalysts in the final Tier 5 configuration. As noted earlier, there was no capability for $NO_X$ reduction on the MFC during regeneration, due to the in-situ oxidation capability and the generation of exotherms across the MFC itself with HC post injection. Therefore, the Team 1 UAF projections were also used for the final demonstration system. Given that, the final UAF values for the Tier 5 Low $NO_X$ demonstration engine are given below in Table 28.

**TABLE 28. FINAL INFREQUENT REGENERATION UAFS FOR TIER 5 DEMONSTRATION ENGINE**

| Cycle | Infrequent Regeneration UAF, g/kw-hr |
|---|---|
| NRTC | 0.002 |
| RMC | 0.002 |
| LLAC | 0.004 |
| LLC | 0.005 |

## 3.13 Assessment of Idle Stop-Start Technology

One of the additional tasks of the scope of 20MSC-005 was to perform an assessment of the potential for stop-start technology to contribute to $NO_X$ and $CO_2$ reduction over off-road duty cycles. The work focused on using the Tier 5 Low $NO_X$ engine to look at the potential of stop-start to provide additional $NO_X$ and $CO_2$ benefits. These tests were run using the Development Aged parts, while the primary system was being DAAAC-aged to FUL.

Unfortunately, most of the current standard offroad duty cycles do not contain significant idle segments that allow for the demonstration of this technology. Some examination was made using the LLAC, but even in that case the segments of actual idle are limited. However, by this point, SwRI was actively engaged in the development of the LLC. Several of the cluster profiles contained significant amounts of idle, and these were leveraged to develop a test cycle which featured varying idle lengths to allow for a proper examination of stop-start technology. The length of long idle segments was varied during some of these tests to examine potential impacts over a wide variety of conditions. The idle test cycle was developed from field operations taken from Cluster 11 and Cluster 3, as discussed in more detail under Section 4 below. The concatenated cycle sequence was repeated twice in a single cycle to allow for different entry conditions. This idle stop-start evaluation cycle is given below in normalized format in Figure 129. The longer idle segments of this cycle are 11 minutes long while many of the shorter ones range from 2 to 3 minutes in duration. This cycle was normally run after a preconditioning similar to the LLAC and LLC, 2 NRTC preconditioning cycles followed by a 20-min engine off soak.

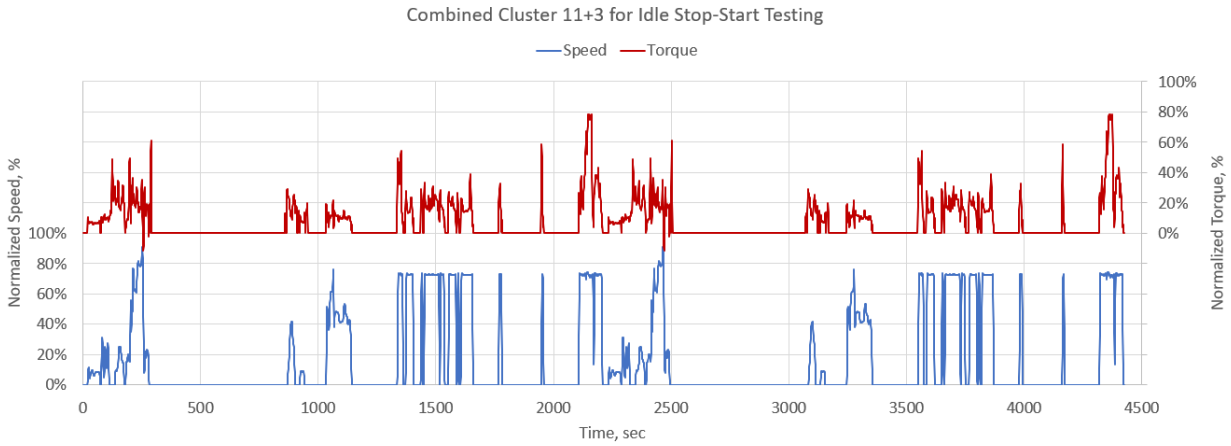



**FIGURE 129. IDLE STOP-START TEST CYCLE – CONCATENATED FROM LOW LOAD CLUSTERS 11 AND 3**

The stop-start idle control functions were added to the Low $NO_X$ controller in the dSPace MAB II. There were two primary configurable parameters. The first parameter was the minimum duration of low idle before engine shutdown would be engaged. The second parameter was a target AT system temperature, below which the engine would re-start to prevent the AT system from cooling down too much. This second parameter was only implemented later in the program to examine some of the longer idle segments.

Some of the stop-start testing was initially conducted with the conventional Team 2 aftertreatment package. Additional testing was later run using the Package 2 system with MFC.

Results for stop-start testing on the LLAC are illustrated in Figure 130. The figure shows LLAC results with the MFC-enabled Package 2 system, with and without stop-start. DSF results without stop-start are also shown for comparison. The minimum idle shut down threshold for this case was 30 seconds, which is about as short as is practical for offroad duty cycles (and may be too short for some applications). The LLAC really only has two true non-working (unloaded) idle events in the later part of the cycle, the ability to demonstrate differences is limited. Still, the impact of stopping the engine can be seen in the slower cool-down of the AT system, though this did depend in part of the thermal management mode the running engine was in during baseline testing without stop-start. However, it can be seen that from an aftertreatment standpoint, temperatures are better preserved by leaving the engine on if the engine has DSF.

A summary of cycle results for these LLAC tests is given in Table 29. Stop-Start had little impact on $NO_X$, but its use did result in a small $CO_2$ reduction over the cycle on the order of 1.5%. For the LLAC, DSF had a much larger impact than Stop-Start, which lower tailpipe $NO_X$ thanks to higher temperatures, and also a larger $CO_2$ benefit of 5%.

**TABLE 29. LLAC EVALUATION RESULTS WITH STOP-START**

| LLAC | Cycle Values | | | | | |
|---|---|---|---|---|---|---|
| Test Conditions | AT System | Work | EO BSNOx | TP BSNOx | NOx Conv Eff | BSCO2 |
| - | - | [g/kW-hr] | [g/kW-hr] | [g/kW-hr] | % | [g/kW-hr] |
| R7423-NoDSF-NoStartStop | T2P2+T1P1 | 34.87 | 5.35 | 0.031 | 99.4 | 776 |
| R7459-NoDSF-wStartStop | T2P2+T1P1 | 34.05 | 5.21 | 0.033 | 99.4 | 764 |
| R7425-wDSF-NoStartStop | T2P2+T1P1 | 34.73 | 5.97 | 0.005 | 99.9 | 743 |

On the other hand, the results of testing on the Cluster 113 idle cycle are shown in Figure 131. Cycle results are summarized in Table 30. This duty cycle, which is based on a combination of a farm tractor working and orchard (for the longer idles) and an excavator (for the more intermittent shorter idle segments) has significantly more opportunity for stop-start to activate. The same 30-second shutdown timer was used for this cycle as was used for the LLAC tests described above. Aftertreatment temperatures remain something of a mixed case with stop-start compared to the normal strategy, but this is mostly due to the intervention of engine thermal management as the system cooled. Still Stop-Start had a definitive impact on $NO_X$, resulting in a reduction in tailpipe $NO_X$ on this cycle of more than 50%, down to below 40 mg/kw-hr. However, as noted earlier, for $NO_X$, leaving the engine running with DSF was more effective, and this produced a tailpipe $NO_X$ level of 20 mg/kw-hr, 75% below the base case.

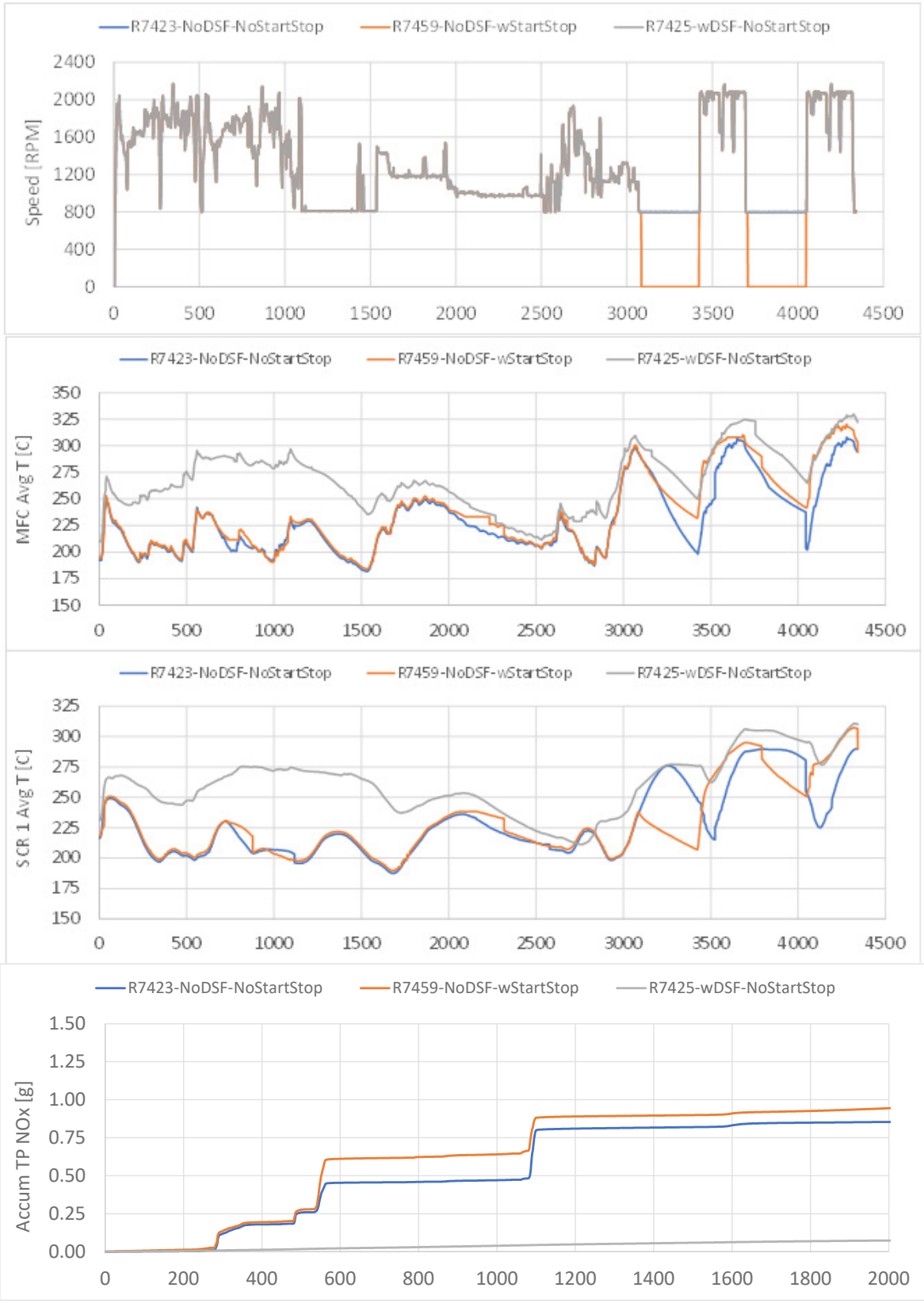



**FIGURE 130. LLAC CYCLES ON MFC-ENALBED SYSTEM – WITH AND WITHOUT STOP-START COMPARED TO DSF**




**FIGURE 131. CLUSTER 113 IDLE CYCLES ON MFC-ENALBED SYSTEM – WITH AND WITHOUT STOP-START COMPARED TO DSF**

**TABLE 30. CLUSTER 113 IDLE CYCLE EVALUATION RESULTS WITH STOP-START ON MFC-ENABLED AT SYSTEM**

| Cluster113 | Cycle Values | | | | | | |
|---|---|---|---|---|---|---|---|
| Test Conditions | AT System | Work | EO BSNOx | TP BSNOx | NOx Conv Eff | BSCO2 | Total CO2 |
| - | - | [g/kW-hr] | [g/kW-hr] | [g/kW-hr] | % | [g/kW-hr] | grams |
| R7441-NoDSF-NoStartStop | T2P2+T1P1 | 16.54 | 5.56 | 0.086 | 98.5 | 938 | 15517 |
| R7447-NoDSF-wStartStop | T2P2+T1P1 | 13.68 | 4.40 | 0.039 | 99.1 | 858 | 11734 |
| R7454-wDSF-NoStartStop | T2P2+T1P1 | 16.23 | 7.00 | 0.020 | 99.7 | 861 | 13981 |

Looking at $CO_2$ emissions however, Stop-Start had a definite edge on this cycle. Not that to compare to the other cycles it is necessary to look at total $CO_2$ mass over the cycle, rather than $BSCO_2$. This is because no work is generated with the engine off and thus this would penalize $BSCO_2$ on the stop-start unfairly. DSF reduces $CO_2$ by 10% on this cycle but Stop-Start results in a 24% reduction in $CO_2$ mass emissions and fuel consumption. It can be seen from these results that the impact of Stop-Start is highly dependent on duty cycle. The Cluster 113 cycle likely represents a "best-case" scenario for Start-Stop.

Longer idle times were also investigated by adding duration to the long idle segments in the Cluster 113 cycle. To do this the idle times were lengthened on the two extended idle segments. The first segment was extended to 40 minutes and the second to 25 minutes. It was noted that after 19 minutes, the aftertreatment had cooled to below the 165°C thresholds for engine restart. Following the restart, even in aggressive thermal management mode, the exhaust never did heat back up above the threshold that would allow it to shut down again. Therefore, the Stop-Start benefit was maximized at that point. It should be noted that based on the field data that was used for the LLC development, idles longer than 40 minutes were exceedingly rare, occur only in the $98^{th}$ percentile of all idle events in terms of duration. Because of the engine restart, the $CO_2$ benefit on this cycle was somewhat smaller, but still significant at 15%.

The Cluster 113 idle cycle was also run on Team 2 conventional aftertreatment package, and cycle results are shown in Table 31. Similarly to the MFC-enabled case, a 22% reduction in $CO_2$ mass was observed. In addition, with this AT system, a somewhat larger improvement in tailpipe $NO_X$ was seen with a reduction of 85%. There was some concern about the impact of the CVS blower in cooling the AT system and thus impacting $NO_X$ emissions artificially. A test case was also running shutting off the CVS blower at each engine shut down, but as seen in the table, this had no significant impact on $NO_X$ and $CO_2$ results on this cycle, alleviating that concern.

**TABLE 31. CLUSTER 113 IDLE CYCLE EVALUATION RESULTS WITH STOP-START ON CONVENTIONAL AT SYSTEM**

| Cluster113 | Cycle Values | | | | | | |
|---|---|---|---|---|---|---|---|
| Test Conditions | AT System | Work | EO BSNOx | TP BSNOx | NOx Conv Eff | BSCO2 | Total CO2 |
| - | - | [g/kW-hr] | [g/kW-hr] | [g/kW-hr] | % | [g/kW-hr] | grams |
| R7509-NoStartStop | T2P2+T1P1 | 16.59 | 4.44 | 0.083 | 98.1% | 1014 | 16822 |
| R7514-wStartStop | T2P2+T1P1 | 13.77 | 3.24 | 0.013 | 99.6% | 950 | 13083 |
| R7517-StartStop-CVSOff | T2P2+T1P1 | 13.78 | 3.19 | 0.019 | 99.4% | 938 | 12923 |

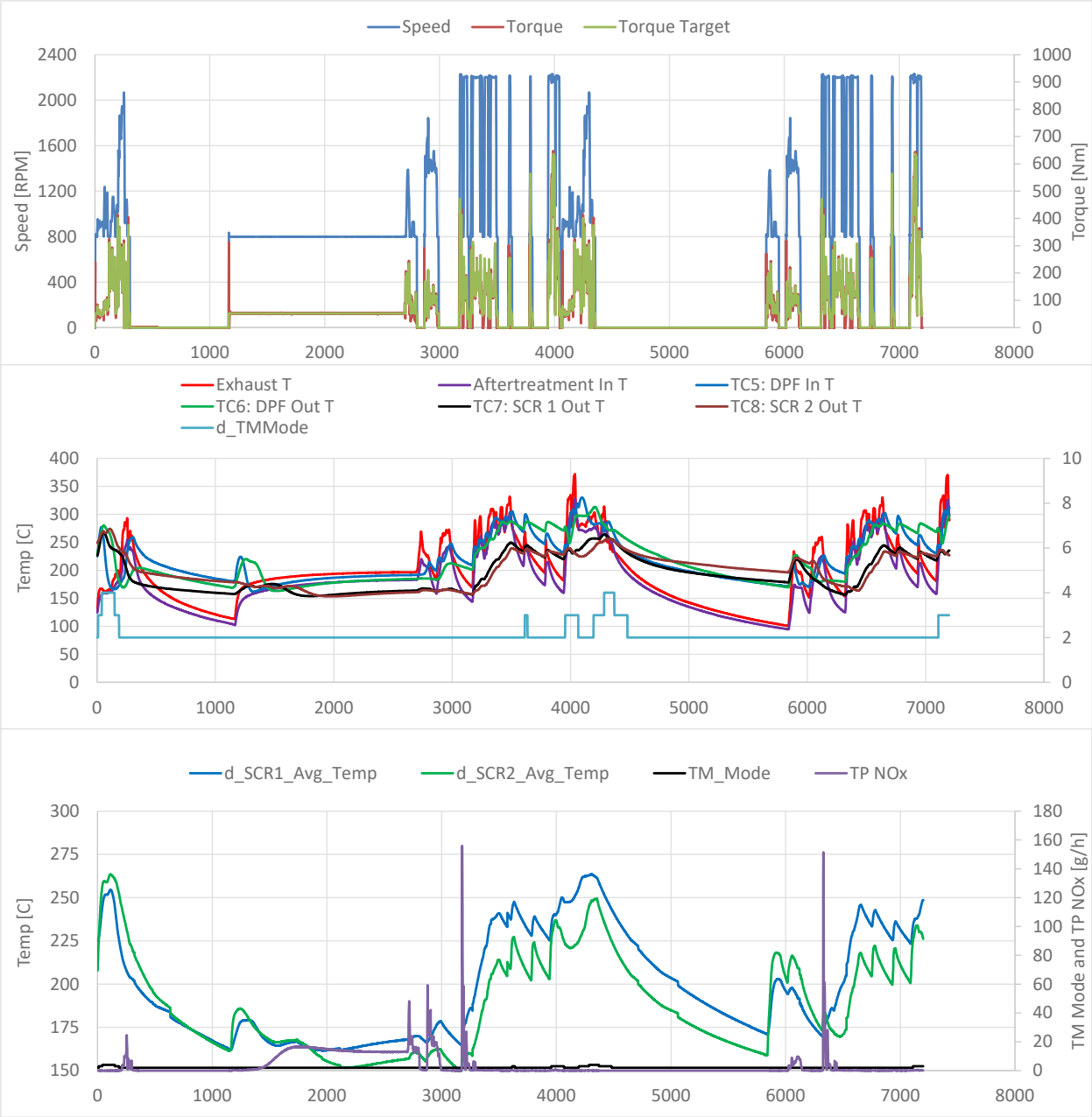



**FIGURE 132. CLUSTER 113 EVALUTION WITH LONGER EXTENDED IDLE MODES (40-MIN AND 25-MIN)**

## 3.14 Low Power Child Rating Tests

Another scope item that was added to the program was the evaluation of the chosen Tier 5 strategy on a lower power child rating of the same engine. A child rating is a lower torque curve calibration on the same hardware within an engine family. Child ratings are of interest here because they share the same absolute thermal mass and heat loss characteristics of the common hardware, but the lower power rating can result in less fuel supplied enthalpy through the system. A similar child rating emissions performance sensitivity evaluation was carried out on the on-highway demonstration, but in the case of the offroad market, many engine families cover a much

wider range of power ratings than is typically seen on the on-highway market. To facilitate this evaluation, SwRI obtained support from John Deere to provide additional torque curves to cover the range of the engine family for this 6068 engine. The available torque curves are show in Figure 133, in comparison to the Base curve used in the program, which was for a 187kw rating.




**FIGURE 133. RANGE OF AVAILABLE CHILD RATINGS FOR THE JOHN DEERE 6068 DEMONSTRATION ENGINE FAMILY**

CARB elected to test only the low power child rating at 126kw, under the reasoning that this was likely to provide a more stringent challenge than a higher power rating, due to lower exhaust temperatures on the same engine platform.

Initial testing was done using the Development Aged parts, while the final parts were still being DAAAC-aged to FUL. These tests allowed an initial look at the impact of the lower power rating, as well as an opportunity to at least begin developing any calibration modifications that might be needed for this rating. These initial tests were run only for the case without DSF. While initial performance numbers look promising there was an issue with the NRTC cycle calibration. Figure 134 shows SCR catalyst temperatures over a hot-start NRTC cycle. As mentioned earlier, an important part of the strategy with the MFC is to back off on MFC conversion as the temperature increases to permit passive soot oxidation to occur. It turned out that with the lower temperatures on the child rating, the system did not reach that tipping point properly and had too much MFC conversion over the NRTC. MFC $NO_X$ conversion on the hot NRTC was 90% rather than the expected 67% over the NRTC. This would not be a workable calibration in the field because it would perform active regenerations far too often as the soot loaded on the filter. Therefore, the calibration was modified to allow for an earlier "roll off" of MFC performance, at lower temperatures. The calibration change is illustrated in Figure 135. As described, the calibration values are in the form of the dimensional coverage ratio theta. The key regions are highlighted in yellow in the two tables. Where the initial calibration had ramped MFC coverage down starting after 250°C through 325°C, the child rating calibration ramped MFC coverage down starting after

225°C through 300°C. With this fix in place, evaluation of the child rating performance could proceed.

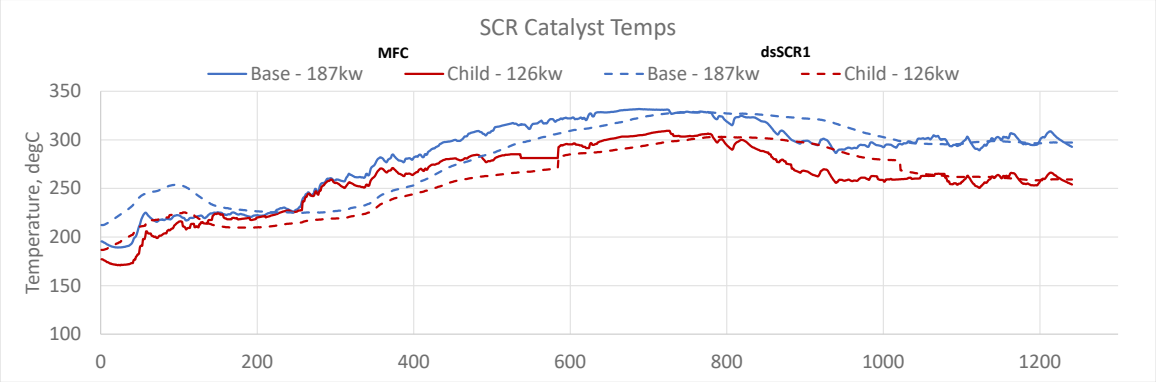



**FIGURE 134. LOW POWER CHILD RATING VERSUS BASE RATING – HOT-START NRTC SCR CATALYST TEMPERAURES**

**187 kw Base Rating**

| | MFC (LO-SCR) Team 2 Pkg 2 | | | | | | | | | | | | | |
|---|---|---|---|---|---|---|---|---|---|---|---|---|---|---|
| | | 1 | 2 | 3 | 4 | 5 | 6 | 7 | 8 | 9 | 10 | 11 | 12 | 13 |
| | NOx(g/h)\T | 150 | 210 | 225 | 250 | 275 | 300 | 325 | 350 | 400 | 450 | 500 | 550 | 600 |
| 1 | 50 | 0.4 | 0.35 | 0.25 | 0.2 | 0.1 | 0.05 | 0.01 | 0.01 | 0.01 | 0.01 | 0.01 | 0.01 | 0.01 |
| 2 | 250 | 0.4 | 0.35 | 0.25 | 0.2 | 0.1 | 0.05 | 0.01 | 0.01 | 0.01 | 0.01 | 0.01 | 0.01 | 0.01 |
| 3 | 500 | 0.4 | 0.35 | 0.25 | 0.2 | 0.1 | 0.05 | 0.01 | 0.01 | 0.01 | 0.01 | 0.01 | 0.01 | 0.01 |
| 4 | 750 | 0.4 | 0.35 | 0.25 | 0.2 | 0.1 | 0.05 | 0.01 | 0.01 | 0.01 | 0.01 | 0.01 | 0.01 | 0.01 |
| 5 | 1000 | 0.4 | 0.35 | 0.25 | 0.2 | 0.1 | 0.05 | 0.01 | 0.01 | 0.01 | 0.01 | 0.01 | 0.01 | 0.01 |
| 6 | 1250 | 0.4 | 0.35 | 0.25 | 0.2 | 0.1 | 0.05 | 0.01 | 0.01 | 0.01 | 0.01 | 0.01 | 0.01 | 0.01 |
| 7 | 1500 | 0.4 | 0.35 | 0.25 | 0.2 | 0.1 | 0.05 | 0.01 | 0.01 | 0.01 | 0.01 | 0.01 | 0.01 | 0.01 |
| 8 | 2000 | 0.4 | 0.35 | 0.25 | 0.2 | 0.1 | 0.05 | 0.01 | 0.01 | 0.01 | 0.01 | 0.01 | 0.01 | 0.01 |
| 9 | 3000 | 0.4 | 0.35 | 0.25 | 0.2 | 0.1 | 0.05 | 0.01 | 0.01 | 0.01 | 0.01 | 0.01 | 0.01 | 0.01 |

**126 kw Child Rating**

| | MFC (LO-SCR) Team 2 Pkg 2 | | | | | | | | | | | | | |
|---|---|---|---|---|---|---|---|---|---|---|---|---|---|---|
| | | 1 | 2 | 3 | 4 | 5 | 6 | 7 | 8 | 9 | 10 | 11 | 12 | 13 |
| | NOx(g/h)\T | 150 | 210 | 225 | 250 | 275 | 300 | 325 | 350 | 400 | 450 | 500 | 550 | 600 |
| 1 | 50 | 0.4 | 0.35 | 0.2 | 0.075 | 0.025 | 0.01 | 0.01 | 0.01 | 0.01 | 0.01 | 0.01 | 0.01 | 0.01 |
| 2 | 250 | 0.4 | 0.35 | 0.2 | 0.075 | 0.025 | 0.01 | 0.01 | 0.01 | 0.01 | 0.01 | 0.01 | 0.01 | 0.01 |
| 3 | 500 | 0.4 | 0.35 | 0.2 | 0.075 | 0.025 | 0.01 | 0.01 | 0.01 | 0.01 | 0.01 | 0.01 | 0.01 | 0.01 |
| 4 | 750 | 0.4 | 0.35 | 0.2 | 0.075 | 0.025 | 0.01 | 0.01 | 0.01 | 0.01 | 0.01 | 0.01 | 0.01 | 0.01 |
| 5 | 1000 | 0.4 | 0.35 | 0.2 | 0.075 | 0.025 | 0.01 | 0.01 | 0.01 | 0.01 | 0.01 | 0.01 | 0.01 | 0.01 |
| 6 | 1250 | 0.4 | 0.35 | 0.2 | 0.075 | 0.025 | 0.01 | 0.01 | 0.01 | 0.01 | 0.01 | 0.01 | 0.01 | 0.01 |
| 7 | 1500 | 0.4 | 0.35 | 0.2 | 0.075 | 0.025 | 0.01 | 0.01 | 0.01 | 0.01 | 0.01 | 0.01 | 0.01 | 0.01 |
| 8 | 2000 | 0.4 | 0.35 | 0.2 | 0.075 | 0.025 | 0.01 | 0.01 | 0.01 | 0.01 | 0.01 | 0.01 | 0.01 | 0.01 |
| 9 | 3000 | 0.4 | 0.35 | 0.2 | 0.075 | 0.025 | 0.01 | 0.01 | 0.01 | 0.01 | 0.01 | 0.01 | 0.01 | 0.01 |

**FIGURE 135. MFC STORAGE CALIBRATION ADJUSTMENTS FROM BASE (187KW) RATING TO CHILD (126KW) RATING**

Table 32 shows selected tailpipe emission results for the 126kw child rating tests. The baseline $CO_2$ levels came from Baseline testing run using the lower power child rating on the Tier 4 final engine. Tailpipe emissions generally looked similar to the 187kw base rating. In fact, the RMC emissions actually looked better, primarily due to lower $NO_X$ flux through the system, but also because the engine was no longer airflow limited at the top end, which meant that the RMC cycle could realize larger efficiency benefits from the revised engine calibration. However, on the LLAC, there was a large increase in the amount of thermal management time needed to maintain

emissions. This resulted in what was an improvement turning into a small CO= penalty on the LLAC for the child rating.

**TABLE 32. TAILPIPE EMISSIONS FOR LOW POWER CHILD RATING WITH DEVELOPMENT AGED PARTS – WITHOUT DSF, CCV**

| Cycle | EO $NO_X$, g/kw-hr | TP $NO_X$, g/kw-hr | $NO_X$ Efficiency, % | $CO_2$, g/kw-hr | Baseline $CO_2$, g/kw-hr | $CO_2$ Percent Reduction | TP $N_2O$, g/kw-hr |
|---|---|---|---|---|---|---|---|
| Cold NRTC | 3.5 | 0.114 | 96.7 | 782 | 805 | 2.9% | 0.051 |
| Hot NRTC | 3.9 | 0.003 | 99.9 | 755 | 810 | 6.8% | 0.053 |
| **Composite NRTC** | **3.9** | **0.009** | **99.8** | **757** | **810** | **6.5%** | **0.053** |
| **RMC C1** | **4.0** | **0.004** | **99.8** | **696** | **745** | **6.6%** | **0.035** |
| **LLAC** | **4.8** | **0.010** | **99.8** | **867** | **871** | **-0.5%** | **0.245** |

With these initial evaluations completed, final child rating tests would be conducted after completion of the 8000-hr emission test points. These tests were done both with and without DSF. A summary of the data without DSF is given in Table 33. There are signs of catalyst degradation as compared to the Development Aged results shown above. The NRTC and RMC both still have a reasonable margin, but the LLAC would be down to a margin (with UAF) of 5-6 mg/kw-hr, and the LLC was significantly above the target level. In addition, due to the extra thermal management demand, both swung to a significant $CO_2$ penalty. In addition, $N_2O$ emissions, although are not proposed to be regulated on these cycles, are still significantly increased above the baseline engine. It should be noted that there was not time or scope available to optimize the calibration in this situation, but it is also clear the optimization alone will not bring the LLC tailpipe $NO_X$ into line with desired targets.

**TABLE 33. TAILPIPE EMISSIONS FOR LOW POWER CHILD RATING WITH 8000-HR DAAAC-AGED PARTS – WITHOUT DSF, CCV**

| Cycle | EO $NO_X$, g/kw-hr | TP $NO_X$, g/kw-hr | $NO_X$ Efficiency, % | $CO_2$, g/kw-hr | Baseline $CO_2$, g/kw-hr | $CO_2$ Percent Reduction | TP $N_2O$, g/kw-hr |
|---|---|---|---|---|---|---|---|
| Cold NRTC | 3.57 | 0.160 | 95.5 | 784 | 805 | 2.6% | 0.059 |
| Hot NRTC | 3.87 | 0.004 | 99.9 | 752 | 810 | 7.2% | 0.053 |
| **Composite NRTC** | **3.86** | **0.012** | **99.7** | **754** | **810** | **6.9%** | **0.053** |
| **RMC C1** | **4.08** | **0.014** | **99.7** | **706** | **745** | **5.2%** | **0.047** |
| **LLAC** | **5.38** | **0.050** | **99.1** | **955** | **871** | **-9.6%** | **0.192** |
| **LLC** | **5.21** | **0.195** | **96.3** | **1041** | **n/a** | **-14.4%** | **0.223** |

A summary of child rating tests with DSF at the 8000-hr test point is given in Table 34. In general, DSF appears to be an effective countermeasure for resolving many of the issues observed with the child rating emissions without DSF. Margins are improved substantially for all cycles, except for the NRTC, wherein tailpipe $NO_X$ actually went up somewhat, but a reasonable margin is still available. RMC margins are improved to be better than the Base rating. Importantly, both low load cycles are now back below targets, with the LLAC having a healthy margin, and the LLC having a smaller margin. However, the LLC $NO_X$ level is now in a range where that margin could likely be improved via optimization. In addition, all cycles now show a $CO_2$ benefit, with the NRTC demonstrating nearly an 8% improvement in $CO_2$ over the baseline engine at this low power rating. Finally, $N_2O$ emissions are below the proposed 0.15 g/kw-hr cap, although the LLAC value could be improved via optimization as well.

**TABLE 34. TAILPIPE EMISSIONS FOR LOW POWER CHILD RATING WITH 8000-HR DAAAC-AGED PARTS – WITH DSF, CCV**

| Cycle | EO $NO_X$, g/kw-hr | TP $NO_X$, g/kw-hr | $NO_X$ Efficiency, % | $CO_2$, g/kw-hr | Baseline $CO_2$, g/kw-hr | $CO_2$ Percent Reduction | TP $N_2O$, g/kw-hr |
|---|---|---|---|---|---|---|---|
| Cold NRTC | 3.66 | 0.173 | 95.3 | 758 | 810 | 6.4% | 0.055 |
| Hot NRTC | 3.89 | 0.009 | 99.8 | 749 | 810 | 7.5% | 0.052 |
| **Composite NRTC** | **3.88** | **0.017** | **99.6** | **750** | **810** | **7.4%** | **0.052** |
| **RMC C1** | **4.13** | **0.008** | **99.8** | **688** | **745** | **7.7%** | **0.048** |
| **LLAC** | **6.32** | **0.016** | **99.7** | **857** | **871** | **1.6%** | **0.149** |
| **LLC** | **5.24** | **0.050** | **99.0** | **895** | **n/a** | **1.6%** | **0.096** |

Although DSF was effective as a countermeasure, it is likely not the only way to improve the situation observed with the non DSF tests, especially on low load cycles. It is likely that inclusion of an e-heater in the system could also help address the situation at lower power, as could the use of an EGR cooler bypass. Both of these measures could also be effective in the field at low ambient temperatures.

More detail on the impact of the child rating on performance is given in the following sets of charts showing continuous data comparing the child rating and the base rating over various cycles. The cold-start NRTC data is shown first in Figure 136 which shows $NO_X$ , SCR catalyst temperatures, and thermal management behavior, and in Figure 137 which shows $NO_X$ conversion over the two SCR catalyst assemblies. It can be seen from these charts that the exhaust temperatures with child rating are considerably lower than for the base rating. On the cold-start NRTC this certainly has the impact of slowing catalysts light-off, though this is primarily on the downstream SCR system, as the MFC still lights off at about the same time as for the base rating. Although tailpipe $NO_X$ is comparable at first, eventually the slower downstream light-off catches up with the system and there are some extra $NO_X$ peaks around 250 seconds that drive the cycle numbers up some. The system stays in thermal management longer, but that is not enough to make up entirely for the loss of exhaust heat with the child rating.

The hot-start NRTC data comparison without DSF is given in Figure 138 for $NO_X$, temperature, and thermal management, and in Figure 139 for $NO_X$ conversion and cumulative $NO_X$. Although child-rating temperatures are lower, they are still above 200°C and mostly above 250°C on the NRTC. Therefore, the NRTC performs well, and in fact the hot NRTC numbers are slightly better with the aged catalysts, due to the lower $NO_X$ flux from the engine. Although downstream performance is a little lower due to lower temperatures early in the cycle, MFC performance is improved due to the lower $NO_X$ flux.

Unlike the case for the higher load cycles like the NRTC and RMC, the lower load cycles appeared to struggle with the low power child rating. The LLAC data comparisons without DSF between the child and base rating are given in Figure 140 for $NO_X$, temperature, and thermal management, and in Figure 141 for $NO_X$ conversion, cumulative tailpipe $NO_X$, and $N_2O$. Exhaust temperatures are clearly lower with the child rating, and while there is definitely more thermal management activity, that is not enough to keep from losing some tailpipe $NO_X$ performance with the 8000-hr aged parts. With the child rating there is some loss of MFC performance evident in Figure 141 due to the lower temperatures, and it is also apparent that the aged downstream SCR catalyst suffers some performance loss at lower temperatures.

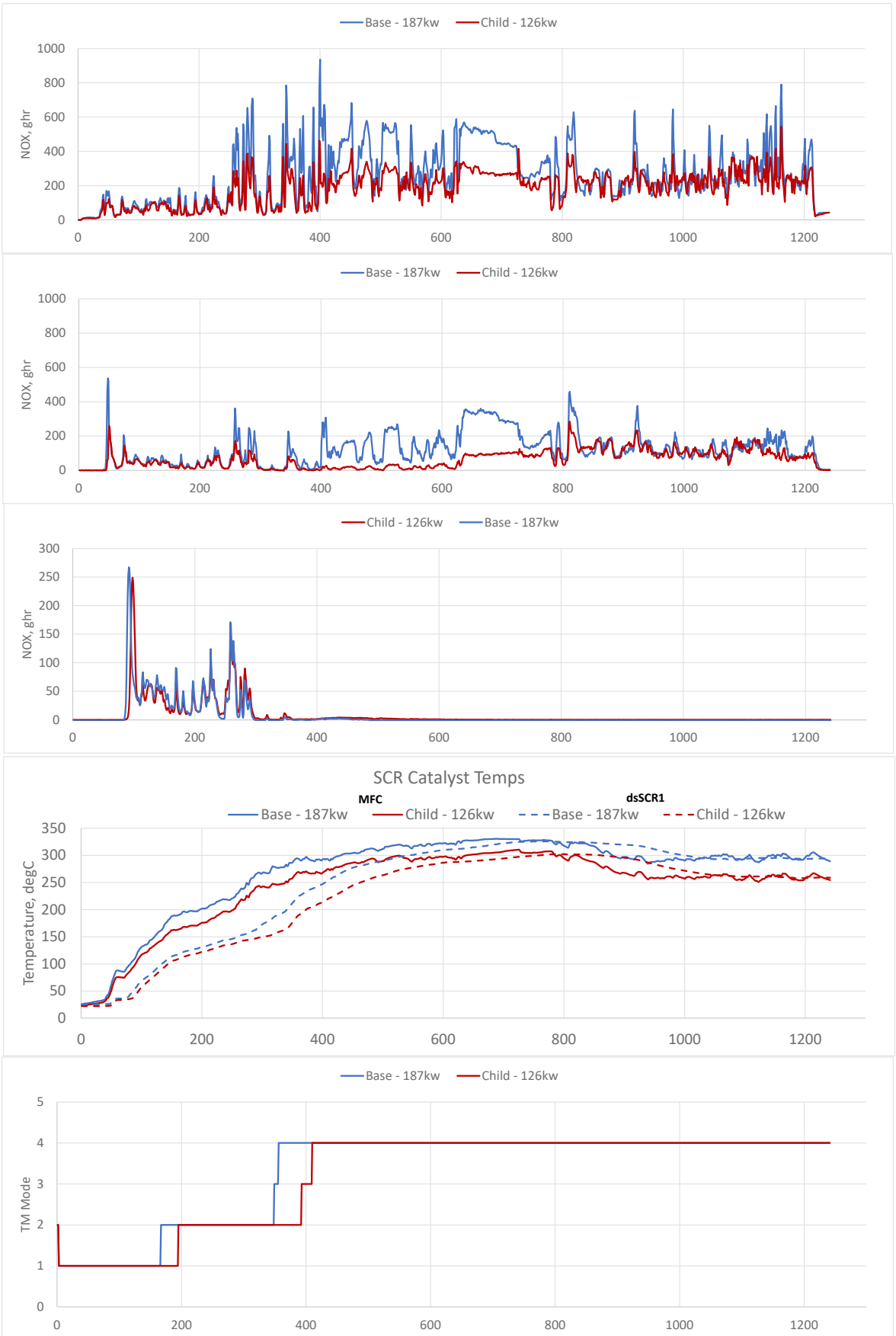



**FIGURE 136. CHILD VS BASE RATING – COLD NRTC BEHAVIOR WITHOUT DSF AT 8000-HR TEST POINT**




**FIGURE 137. CHILD VS BASE RATING – COLD NRTC $NO_X$ CONVERSION AND CUMULATIVE $NO_X$ WITHOUT DSF AT 8000-HR TEST POINT**

As a result, larger and more frequent $NO_X$ breakthroughs are seen in the early, sustained low load portion of the LLAC, as well as larger events during the alternating idle-loaded portion in the late cycle. As a result, tailpipe $NO_X$ increases from 19 to 51 mg/kw-hr over the cycle. The lower temperatures also lead to higher $N_2O$ emissions due to larger return-to-service ammonia releases in the late cycle. This $N_2O$ increase limits the ability to increase dosing to address the $NO_X$ emissions. There may be some ability to adjust thermal management thresholds but it should be noted that this will lead to more $CO_2$ and would likely also cause some $CO_2$ impact on the NRTC as well.

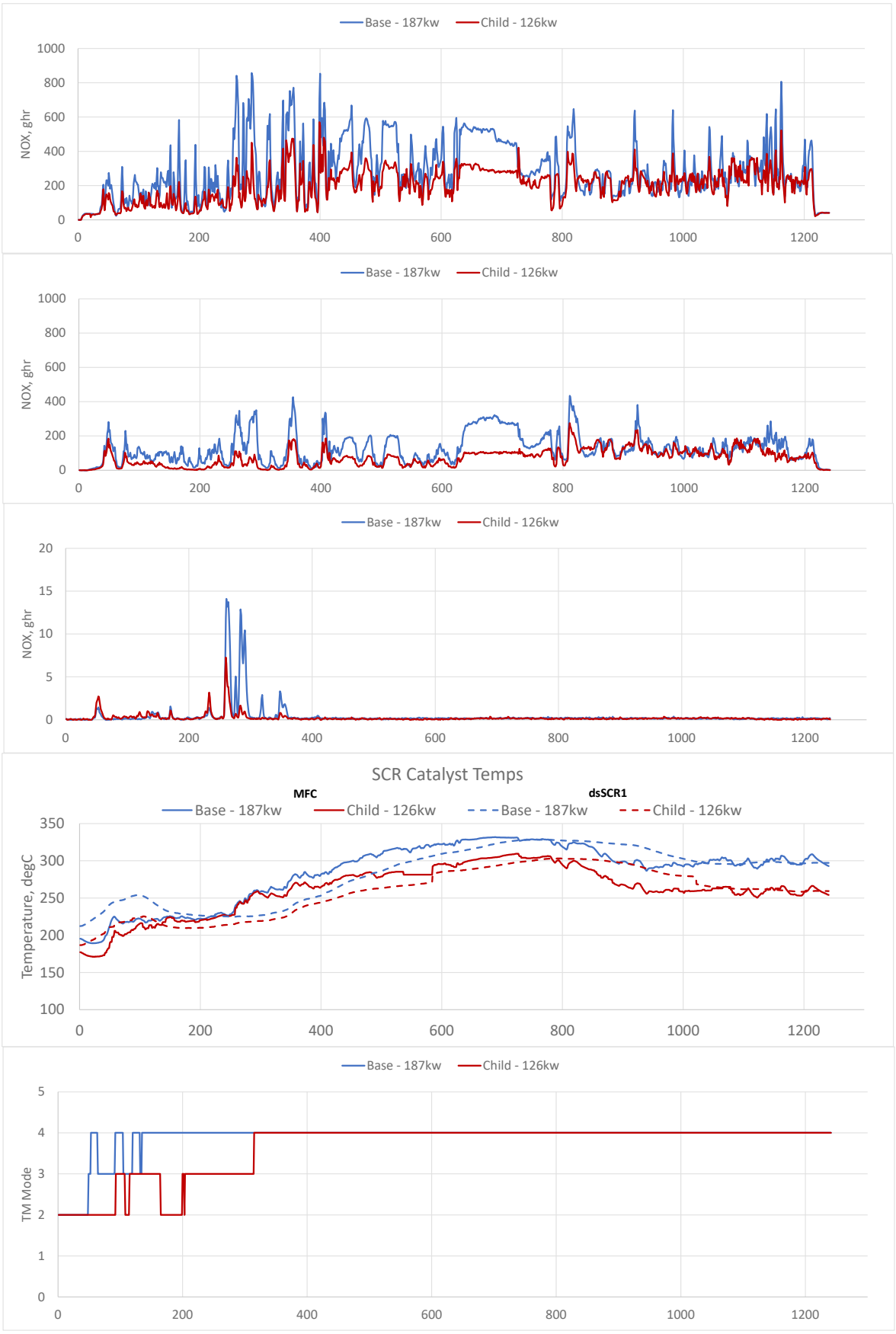



**FIGURE 138. CHILD VS BASE RATING – HOT NRTC BEHAVIOR WITHOUT DSF AT 8000-HR TEST POINT**

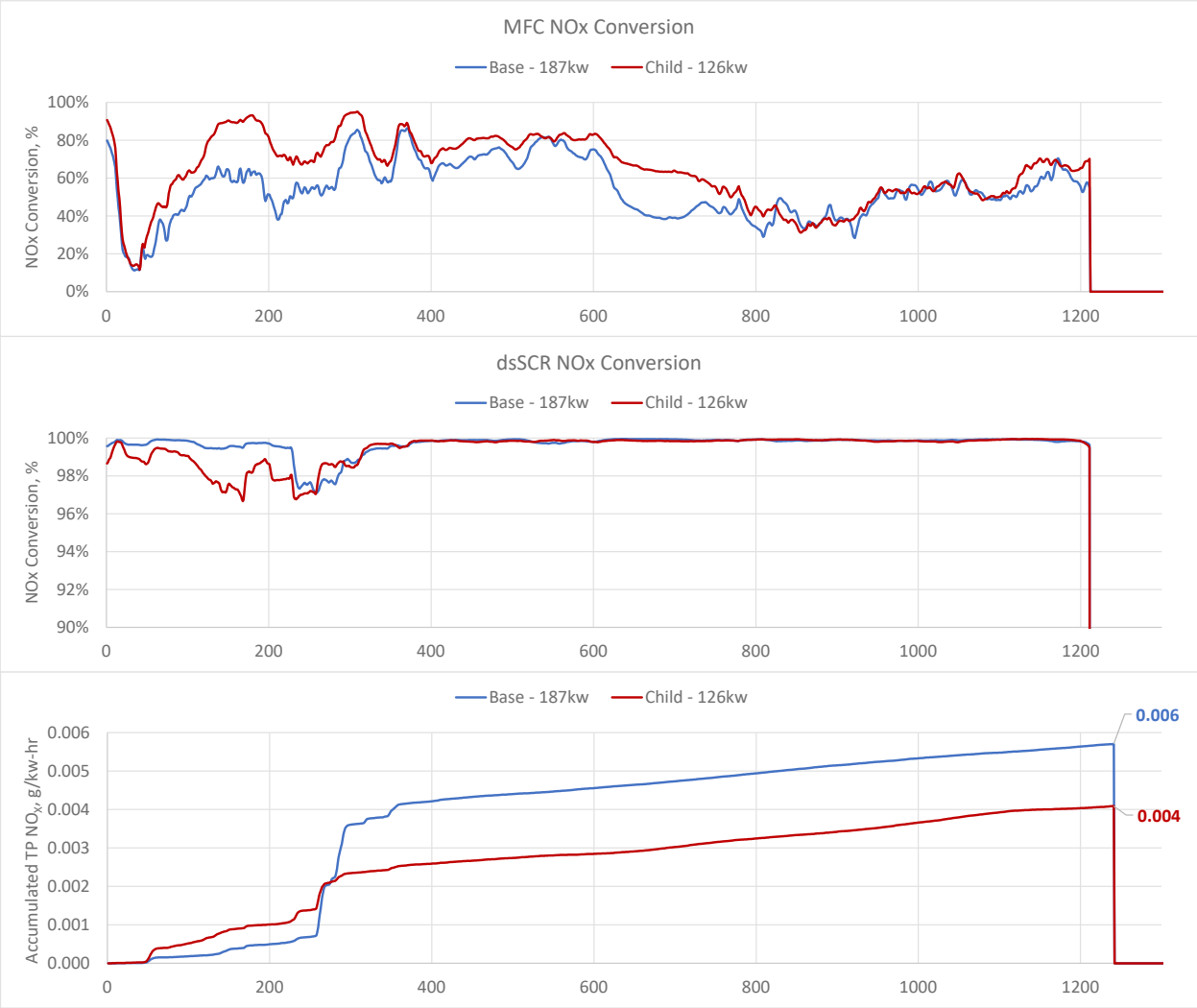



**FIGURE 139. CHILD VS BASE RATING – HOT NRTC $NO_X$ CONVERSION AND CUMULATIVE $NO_X$ WITHOUT DSF AT 8000-HR TEST POINT**

These trends are also observed in the LLC without DSF, but they are even more pronounced. Figure 142 shows $NO_X$, temperature, and thermal management behavior on the LLC, while Figure 143 shows $NO_X$ conversion, cumulative $NO_X$, and $N_2O$ on the LLC. Increased thermal management activity appears to be able to compensate for the lower exhaust temperatures of the child rating in the later part of the LLC, but this is not sufficient for the early part of the LLC which contains the extended idle portion of the cycle. The engine is in the most aggressive thermal management mode, but this is not enough to maintain temperatures compared to the base rating. As a result, SCR temperatures drop below 200°C and in some areas are 30°C lower with the child rating. This has a significant impact on $NO_X$ conversion during that idle and on the return-to-service events that follow that idle, as seen in Figure 143. The child rating also shows few smaller $NO_X$ breakthroughs later in the cycle but is clear that more is needed to bring the LLC back into line without DSF. $NO_X$ is well above the target level at 195 mg/kw-hr and N2O is also increased. Although calibration might improve these results somewhat, it is clear that for the LLC, another technology lever is needed to be able to cover the low power child rating. This could come in the form of DSF, or perhaps something else, such as a small e-heater.

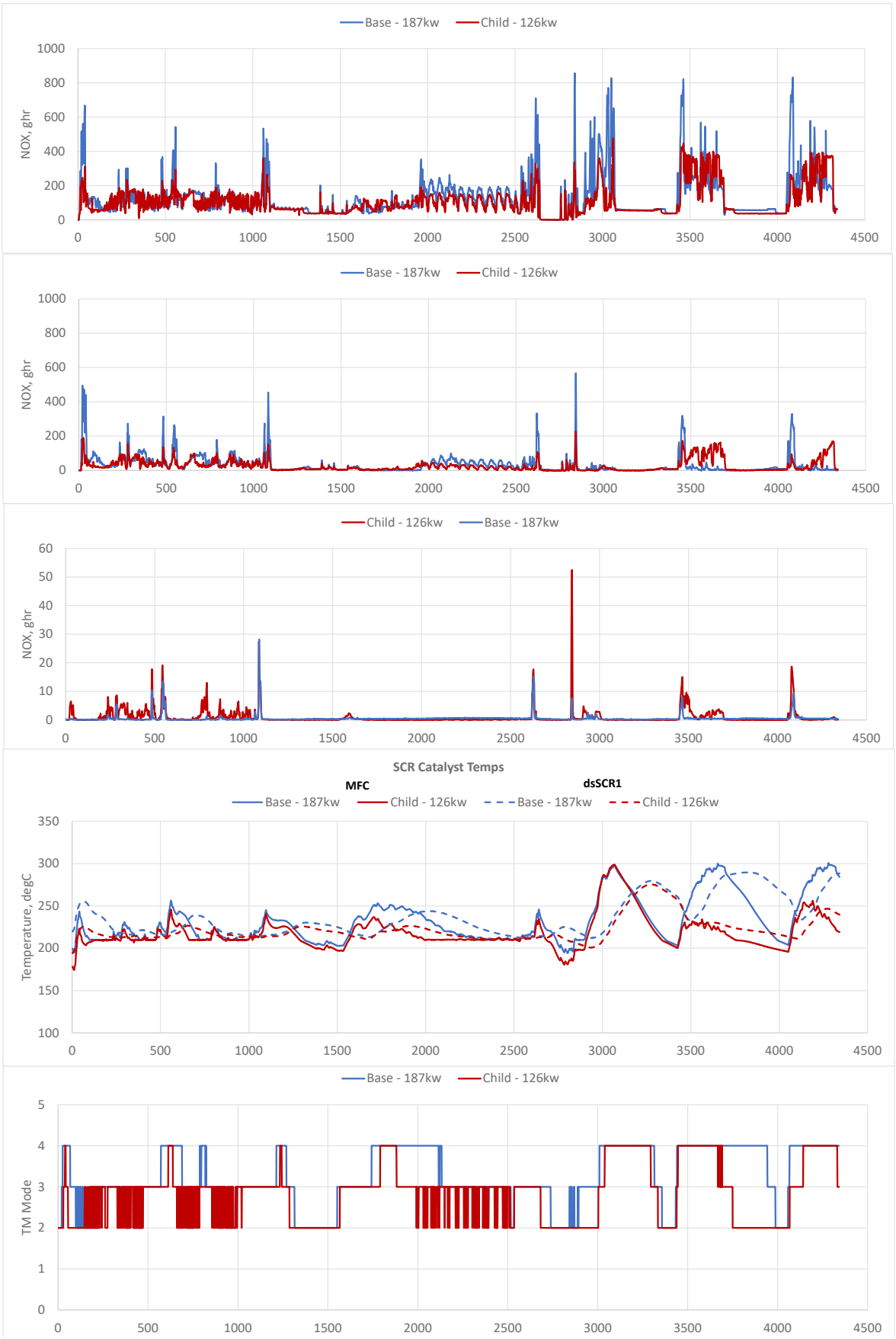



**FIGURE 140. CHILD VS BASE RATING – LLAC BEHAVIOR WITHOUT DSF AT 8000-HR TEST POINT**




**FIGURE 141. CHILD VS BASE RATING – LLAC $NO_X$ CONVERSION, $N_2O$, AND CUMULATIVE $NO_X$ WITHOUT DSF AT 8000-HR TEST POINT**

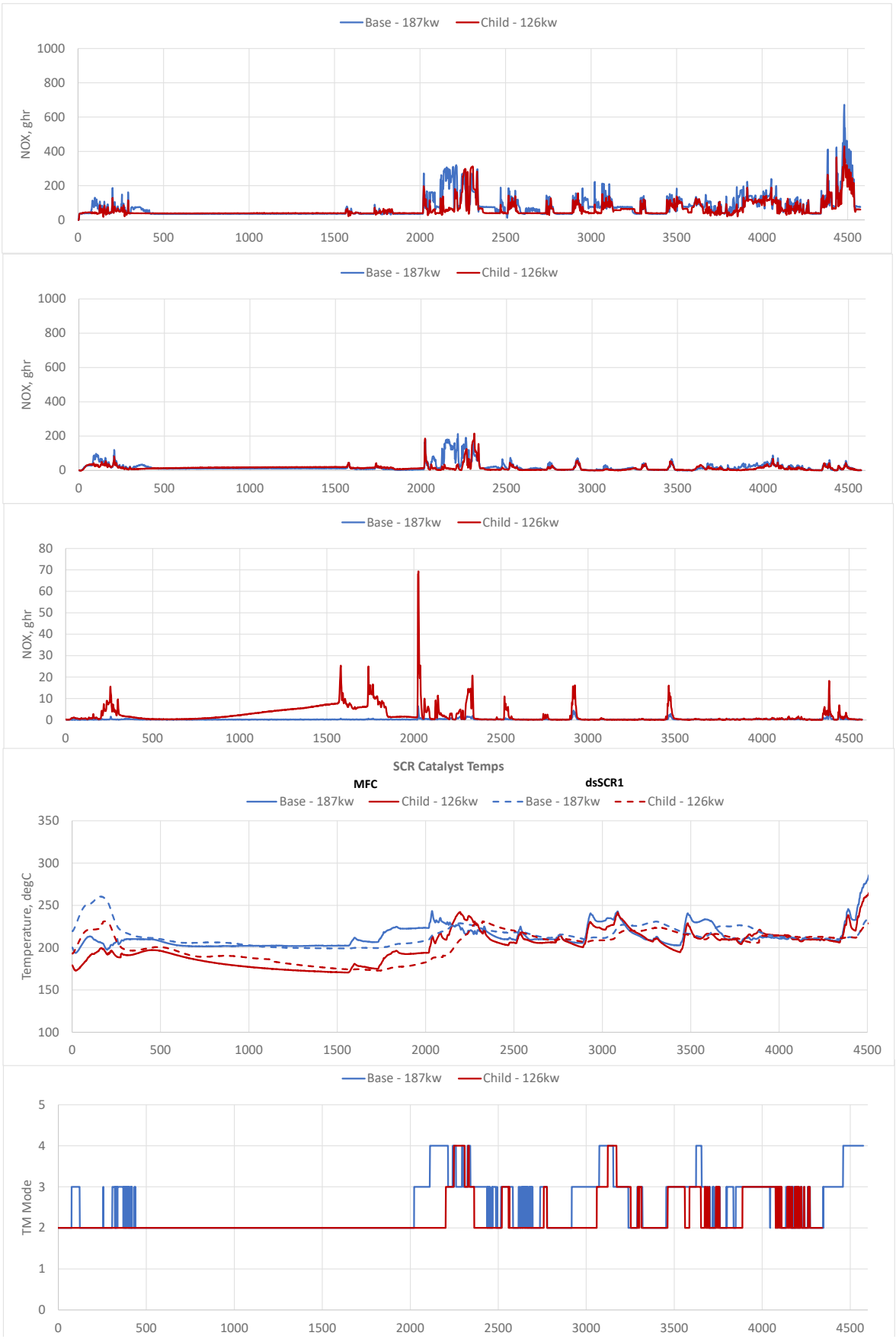



**FIGURE 142. CHILD VS BASE RATING – LLC BEHAVIOR WITHOUT DSF AT 8000-HR TEST POINT**




**FIGURE 143. CHILD VS BASE RATING – LLC $NO_X$ CONVERSION, $N_2O$, AND CUMULATIVE $NO_X$ WITHOUT DSF AT 8000-HR TEST POINT**

With DSF active, however, system performance looks entirely different on the low power child rating. Figure 144 shows system $NO_X$, temperature, and thermal management on the LLAC with DSF comparing the base and child rating. Figure 145 shows $NO_X$ conversion, cumulative $NO_X$, and $N_2O$ for the same comparison. With DSF on the LLAC, while temperatures are still lower with the child rating, SCR catalyst temperature still stays above 200°C for the entire cycle, maintaining high efficiency and much lower $N_2O$ levels. The child rating with DSF has the same tailpipe $NO_X$ as the base rating without DSF, maintaining a healthy compliance margin.

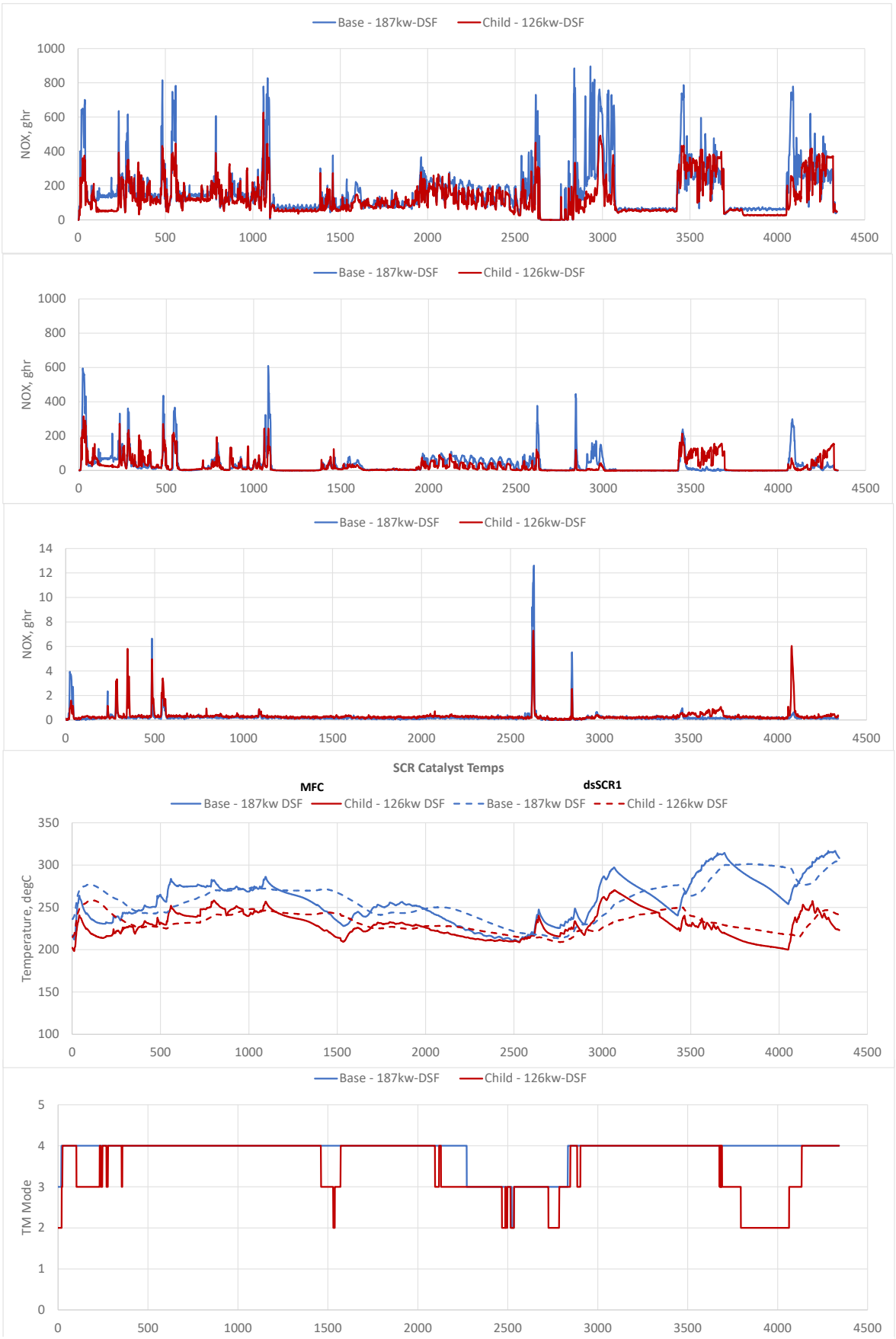



**FIGURE 144. CHILD VS BASE RATING – LLAC BEHAVIOR WITH DSF AT 8000-HR TEST POINT**

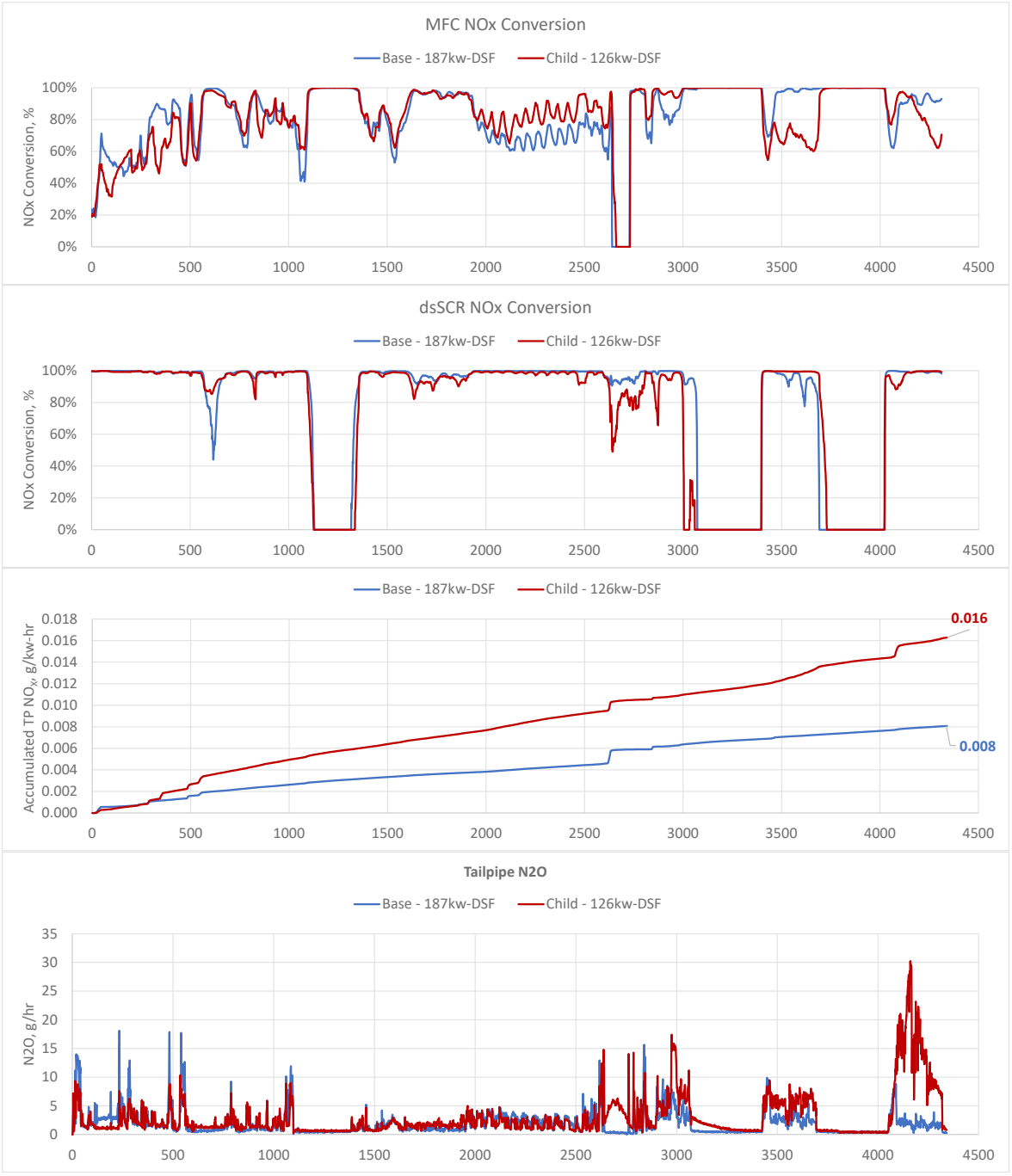



**FIGURE 145. CHILD VS BASE RATING – LLAC $NO_X$ CONVERSION, $N_2O$, AND CUMULATIVE $NO_X$ WITHDSF AT 8000-HR TEST POINT**

Similarly, on the LLC, the use of DSF is effective as a technology lever to offset the impact of the low power child rating on emissions of the FUL-aged system. Figure 146 shows the comparison of base and child ratings on the LLC with DSF in terms of $NO_X$, temperature, and thermal management behavior. Figure 147 shows $NO_X$ conversion, cumulative $NO_X$, and $N_2O$ for the same comparison. While the system still cools off during the early extended idle, this happens much more slowly, so that a dip in conversion only happens at the end of that idle period, and the negative impact on the subsequent return-to-service event is much smaller.

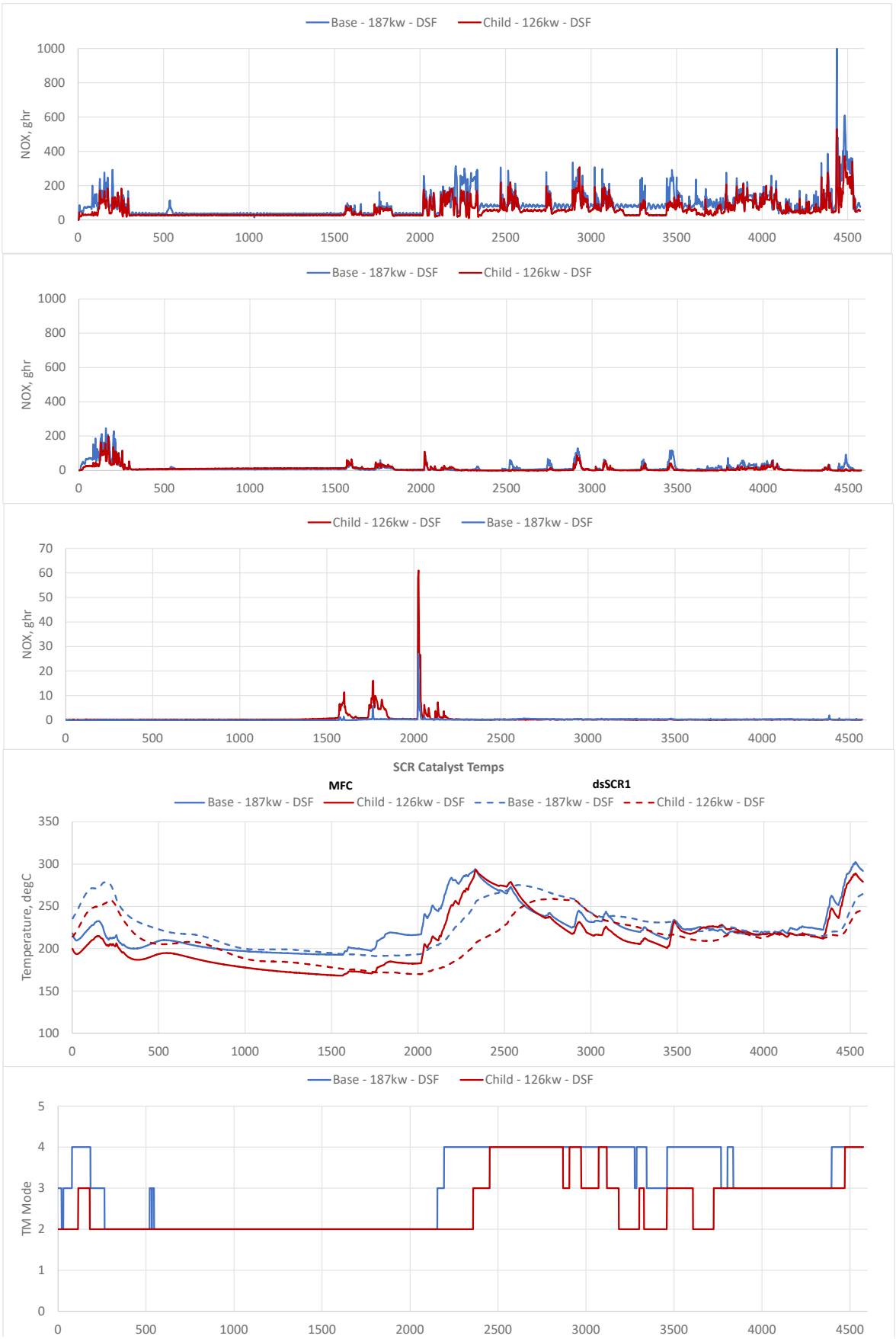



**FIGURE 146. CHILD VS BASE RATING – LLC BEHAVIOR WITH DSF AT 8000-HR TEST POINT**

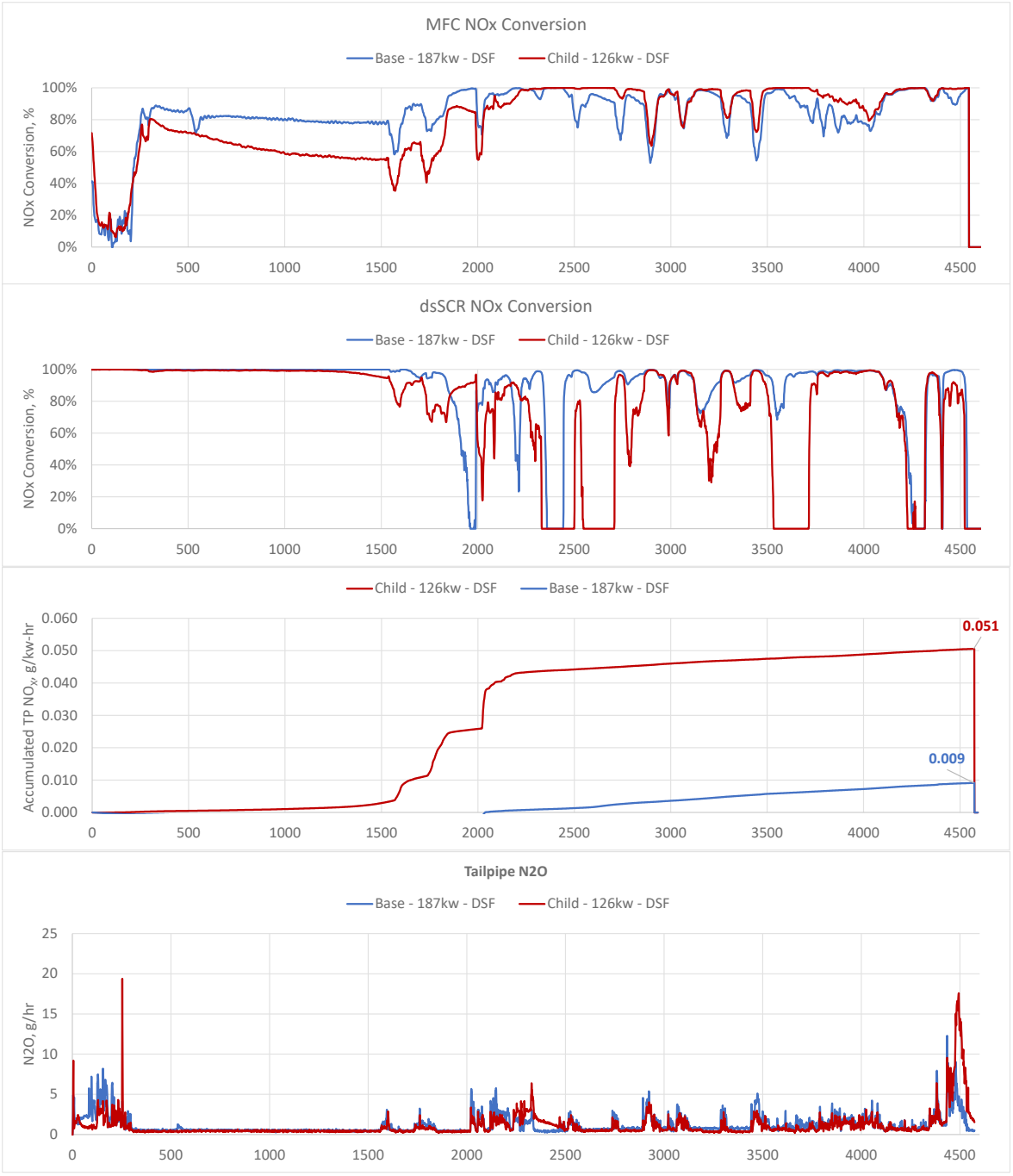



**FIGURE 147. CHILD VS BASE RATING – LLC $NO_X$ CONVERSION, $N_2O$, AND CUMULATIVE $NO_X$ WITHOUT DSF AT 8000-HR TEST POINT**

In addition, all of the late cycle breakthrough events are eliminated as the late cycle SCR temperature is maintained above 200°C. The final cycle value is still increased to 51 mg/kw-hr, which is too high for a comfortable compliance margin, but it is now within the range where additional optimization will likely be enough to create that margin. Finally, with the higher temperatures, the $N_2O$ issues observed without DSF are eliminated. DSF also resulted in a net $CO_2$ improvement, although this was small due to the increased thermal management demand compared to the base rating.

Overall, testing on the low power rating with the 8000-hr DAAAC-aged parts indicated that without DSF, the Low $NO_X$ system did not quite have the reach necessary to cover the full scope of engine family power ratings with end-of-life aged catalysts. It is likely that operations at low ambient temperatures would exacerbate this issue. However, DSF proved to be an effective countermeasure to this problem, such that the Low $NO_X$ system with DSF met all of the Package 2 targets and did so with acceptable levels of $N_2O$.

It should be noted that DSF is not the only potential technology lever to deal with this issue. Given that the primary issue is low load and idle operation, a relatively modest amount of heat would likely also be effective. Some other potential countermeasures could include:

- The use of the EGR cooler bypass. This technology was looked at and not selected because of its limited capability to help temperature beyond idle and very low loads. However, this is exactly where the low power child rating needed further help, so the inclusion of the EGR cooler bypass could be effective, and it would not require energy input.
- Use of a low power e-Heater or heated mixer. It appears that the addition of 20-30° under low and very low exhaust flow conditions would be sufficient to address much of the issue with the low power child rating. This is potentially a good application for a small e-Heater with perhaps only a 2.5kw power capacity mounted just before the downstream DEF mixer/doser. The power requirement is low enough to be compatible with a 24V electrical system, and which would require very little packaging space claim is discussed earlier. There would be some fuel/$CO_2$ costs for this, but optimization of the heater to offset some engine thermal management would likely be able to compensate for that.
- Use of post injection across the MFC/zCSF to generate a small amount of exotherm for additional thermal management. This approach would require no additional hardware, but it would not work below system temperatures of about 265°C due to the risks of HC coking. This means that the system would need to intervene pre-emptively when temperatures were still above that threshold, or perhaps use a small amount of near post-injection to drive temperatures up to that level if the system is otherwise close to that level. However, this approach would need to be active frequently because it would not function once that system had actually cooled down. Therefore, there is a potential for significant fuel consumption and $CO_2$ impact with this approach.

Unfortunately, there was not sufficient time and scope left in the program to implement and examine these countermeasures.

# 4.0 OFF-ROAD LOW LOAD CYCLE (LLC) DEVELOPMENT

This section of the report concerns the development of the new off-road Low Load Cycle (LLC). Although it ultimately has an impact on previously described results, the actual LLC development effort was a separate scope of work that was added to the program as part of Amendment 1 to CARB Contract 20MSC005. Therefore, it is described in a distinct section of this final report.

The off-road LLC was developed using methodology that was initially developed and implemented during the development of the on-highway Low Load Cycle (LLC). This effort is described in detail in the on-highway Stage 2 Low $NO_X$ Program final report [5]. Under that effort, SwRI partnered with the National Renewable Energy Laboratory (NREL) as a subcontractor for the development of the on-highway LLC. That cycle development leveraged a large existing database of on-highway vehicle operations that was available at NREL, which is designated as the FleetDNA database. This data set was supplemented by a data set generated by CE-CERT which involved roughly 100 additional vehicles run in Southern California.

For the on-highway effort, the combined vehicle data was split into manageable windows each consisting of 10 “microtrips” (periods of operation between regions of zero vehicle speed). Each of these windows, which varied in length, became a potential vehicle operation profile, and over 1 million such windows were available in that data set. The windows were characterized by average load, and a distribution of load was developed, allowing for the identification of a “low load” operating region. Common operating modes for windows in that region were identified using a k-means clustering algorithm, and then a number of vehicle profiles were randomly selected from each cluster to be the building blocks of an eventual cycle. A modified version of the EPA GEM model was used to help translate the field data sets into laboratory operation cycles, which were then normalized. Candidate cycles were assembled from these normalized profiles, tested, and refined until a final cycle was developed. The final cycle contained low load operating segments from 6 different vehicles.

For the off-road LLC development, the initial plan was to leverage as much of the same development process as possible. Much of the work of clustering and analysis was performed by CARB staff directly, rather than working with a subcontractor in this case. SwRI provided guidance and input during the initial data analysis and clustering. However, it was anticipated that the methodology used for the development of the on-highway LLC would have to be modified in order to meet the unique demands of the off-road market. Many of these challenges stemmed from the much larger variety of application duty cycles and machine types that are represented in the off-road market, as compared to the on-highway market. The lack of an easy unified operating metric of vehicle speed resulted in the need to modify a number of the analytic processes. In addition, because there is no equivalent to the GEM model for off-road engines, it was necessary to directly employ CAN-recorded operating data for engine speed and load.

The off-road LLC development process was guided by a Steering Committee made up of various industry stakeholders including CARB, EPA, SwRI, EMA, and various off-road engine manufacturers. This group met regularly over the course of a year-and-a-half long period during the development. The Steering Committee provided invaluable feedback, insight, and analysis during the course of the process, helping to ensure a representative and efficient cycle outcome. In particular, the Steering Committee members helped to overcome many of the unique challenges associated with the off-road application data set.

## 4.1 Input Data Sets for LLC Development

Unlike the case of the on-highway LLC development, there was no available existing database of nonroad machine operating data that could be leveraged. Therefore, it was necessary for CARB to engage in a significant data gathering effort. This was primarily done in the form of two large field activity data gathering programs that CARB ran over the 2 years preceding the start of the off-road LLC development. One such program focused on construction machinery under CARB Contract 17RD013, while the other program focused on agricultural equipment under CARB Contract 19RD002. CARB also obtained a significant body of data from a third program which was focused on off-road yard tractors (though the number of engines in that third study was small, necessitating a special data treatment to avoid over-weighting those results). Overall, these CARB data sets contained operating data from 110 different engines, encompassing a wide variety of applications across 24655 hours of equipment operation.

This CARB data set was then augmented by contributions from many of the off-road engine and equipment manufacturers which actively participated as part of the Steering Committee. Data was received from 10 different manufacturers, comprising an additional 130 engines and 932 hours of operation (many of these data sets were much shorter individual runs than the longitudinal data collection in the CARB contracted datasets). These additional data sets proved valuable in further broadening the reach of the input data set in terms of variety of applications and by providing opportunity for manufacturers to further inform the representativeness of the aggregate dataset underpinning this analysis work.

Figure 148 shows a breakdown of applications represented in the data set by machine population. Roughly half of the data came from agricultural tractors, which is consistent with the overall fraction of such tractors in the population of off-road machines in California, as described in the market survey data from the Stage 1 report (Contract 18RD006). Figure 149 shows a histogram of the distribution of engine power levels in the data set, with much of the population falling between 56kw and 450kw. The breadth of the data set helps to ensure the representative nature of the resulting cycle.

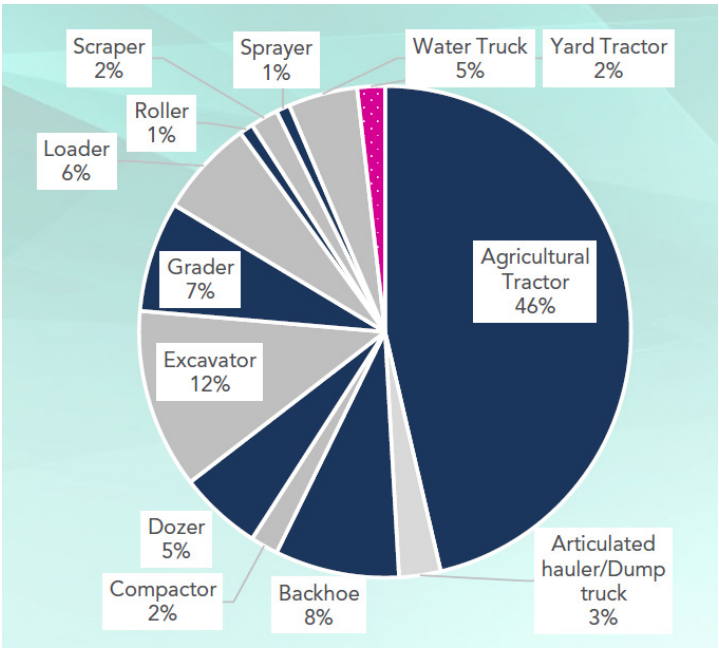



**FIGURE 148. APPLICATION BREAKDOWN IN THE LLC DEVELOPMENT INPUT DATA SET**

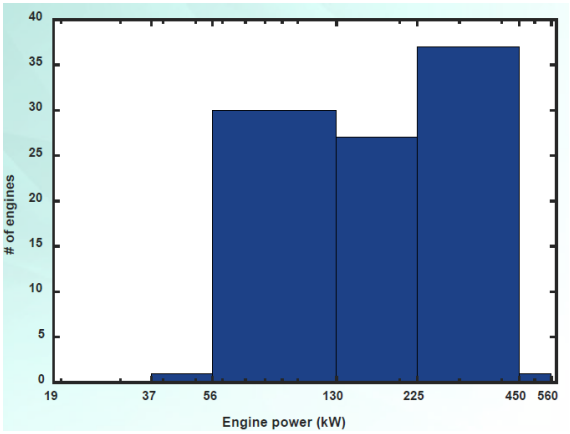



**FIGURE 149. HISTOGRAM OF ENGINE POWER LEVELS IN THE LLC DEVELOPMENT INPUT DATA SET**

## 4.2 Data Windowing

When developing a test cycle to evaluate emission control systems, especially in the case of systems which employ exhaust aftertreatment, duty cycle matters, and engine operating patterns of critically important. It is not enough to simply bin the data on a second-by-second basis according to load. Therefore, it was necessary to mine the data set for segments of engine operation that were long enough to characterize a type of machine operation. As a result, a windowing process was needed to extract these operating "profiles" from the larger data set.

As mentioned earlier, a "microtrip" approach was used in the on-highway program, wherein a microtrip was defined as a period of operation between two periods of zero vehicle

speed. Windows of 10 consecutive microtrips were found to be effective. However, this approach was not easily translated to the off-road data sets, because the universal operating metric of vehicle speed was not available. Instead, for the off-road data, a microtrip was defined as a period or "working" operation between two periods of "non-working" operation. Non-working generally refers to unloaded (i.e. only accessory load) engine idle operation, with other operations being called working. However, in practice, this required the designation of speed and load thresholds for the various engines in the data set to differentiate between working and non-working events. An example of this windowing is shown below in Figure 150, in this case showing windows of 5 microtrips in length, incrementing by 1 microtrip for each new window. This approach generates a large number of unique operating windows, while also ensuring that each window contains enough data to capture a type of operation. Different window sizes were chosen, and a 5 microtip window appeared to work best for the recorded data to balance these needs. The window length in time varied greatly but the average across all windows for which this method was used was 1651 seconds.

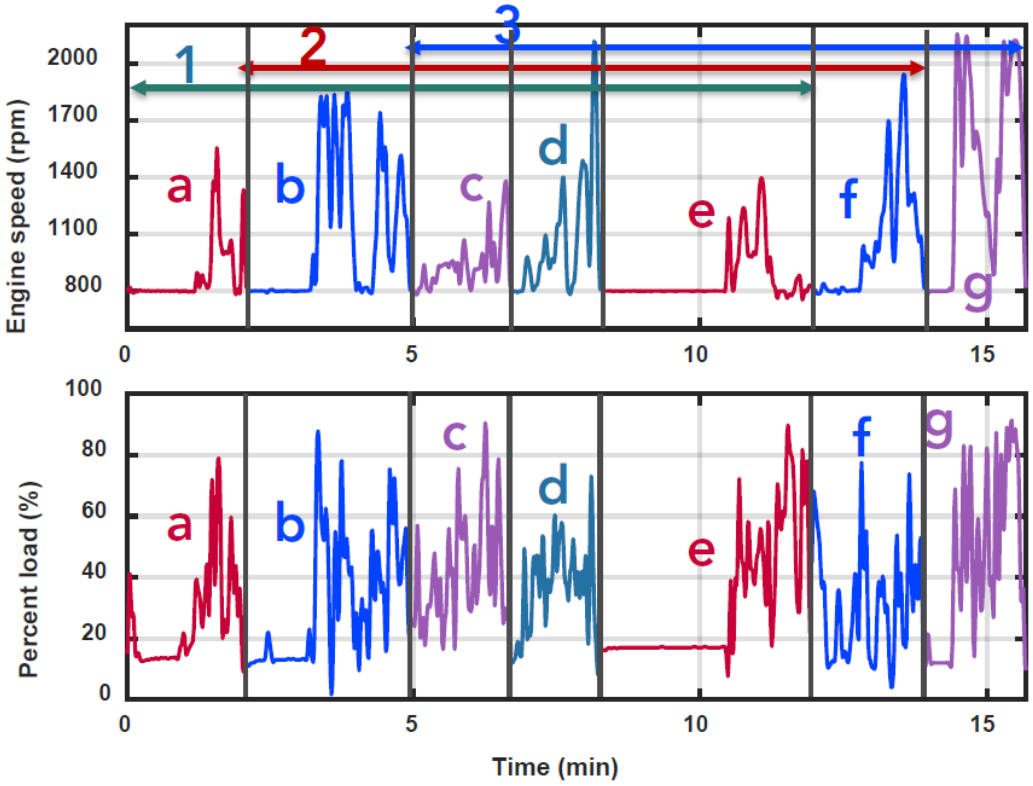



**FIGURE 150. EXAMPLE OF 5-MICROTRIP ANALYSIS ON A MACHINE DATA SEGMENT**

There was a subset of data for which the microtrip-based windowing approach was not usable. This was generally true for a significant portion of the manufacturer supplied data sets, which tended to come in shorter segments, but it was also true for some kinds of engine operation where it was difficult to robustly differentiate working and non-working operations in a consistent manner. For these data sets, a different windowing approach was used, which was originally

developed for the cycle generation process used in the generation of the Nonroad Transient Cycle [13], which was referred to as the "day in the life" method. Instead of microtrips, a fixed time window of 19 minutes was used, incrementing 1 minute at a time. This allowed the generation of a number of useful windows from these shorter data sets, while still being long enough to capture the activity.

At the end of this windowing process, a total of 159,417 individual operating windows were extracted from the data set.

### 4.3 Identification of the Low Load Operating Region

The next key step of the process was to examine the 159,417 windows from the previous step to understand the distribution of engine load in those windows. From that distribution, a region of low load operation would then be designated. It was important that this decision of what constituted low load should not be an arbitrary choice, but rather the result of a consistent, data-driven analysis. It is important in this development to not assume that we "know what low load looks like."

The data windows were analyzed to determine the average engine load within the window using two different metrics. In the first metric, the CAN-recorded Load at Current Speed variable was utilized, and the average of this parameter was taken across each window. For the second metric, the data was processed to determine actual engine power, and then the average power over the window was determined as a fraction of the maximum engine power for the given engine. The data for all the windows was then collected to produce a distribution of load across all data windows. Figure 151 shows the resulting distribution for the first metric, while Figure 152 shows the distribution for the second metric.

In each case, the data indicated a bi-modal distribution. As was done in the on-highway program, this overall distribution could be modeled as a sum of two constituent normal distributions. The figures show the original distribution as the blue dots, and the summed model distribution as the red lines. The two dashed lines show the constituent distributions used to generate the summed model distribution. This general shape was consistent across both metrics, although the actual values were somewhat different. The lower of the two constituent distributions (in terms of load and shown in the green dashed line) was designated as the "Low Load distribution," and the higher of the two (shown in the purple dashed line) as designated as the "NRTC distribution."

Following additional data analysis and Steering Committee input, it was determined that the Low Load operating region would be defined as everything below the $50^{th}$ percentile (median) value of the Low Load distribution. This value was 27% Average Load for the first metric, and 14% of Maximum Power for the second metric. All windows with a load level below either of these two thresholds would be designated as a "Low Load window," and would become part of

the data set that would be used for the k-means clustering analysis in the next step. While both metrics largely overlaid each other on the engine map, the %Average Load metric uniquely included additional high rpm/moderate torque operating points, while the % Maximum Power metric uniquely included additional low rpm/high torque operating points. A total of 52,182 windows were included in this Low Load focus area of the total aggregate data set.

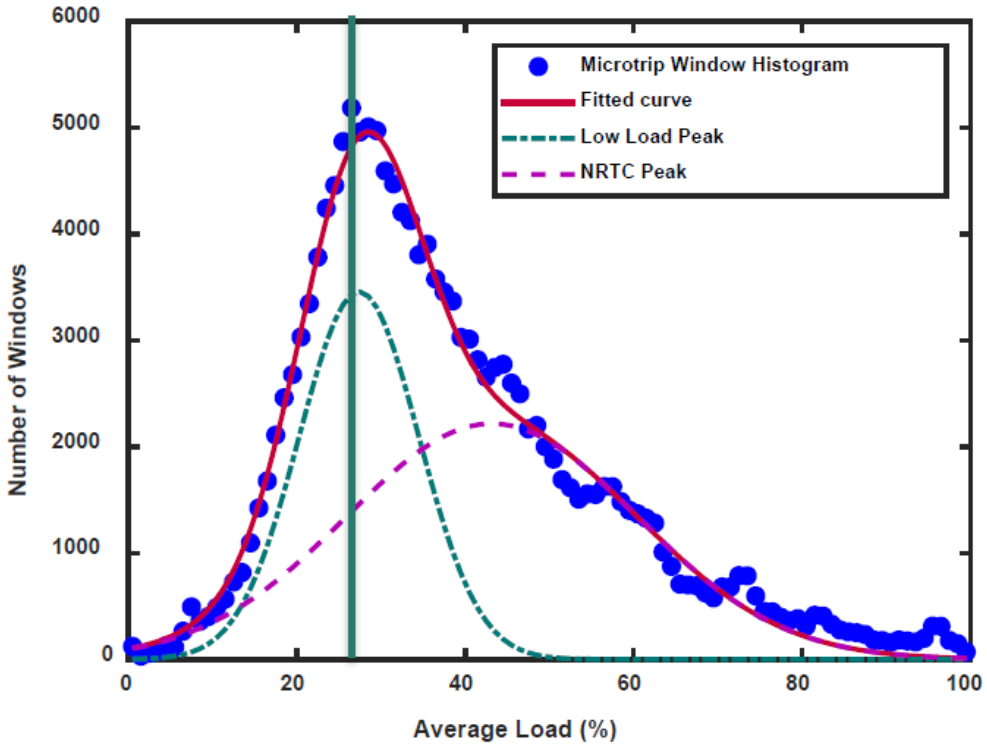



**FIGURE 151. DISTRIBUTION OF WINDOW LOADS USING LOAD AT CURRENT SPEED METRIC**

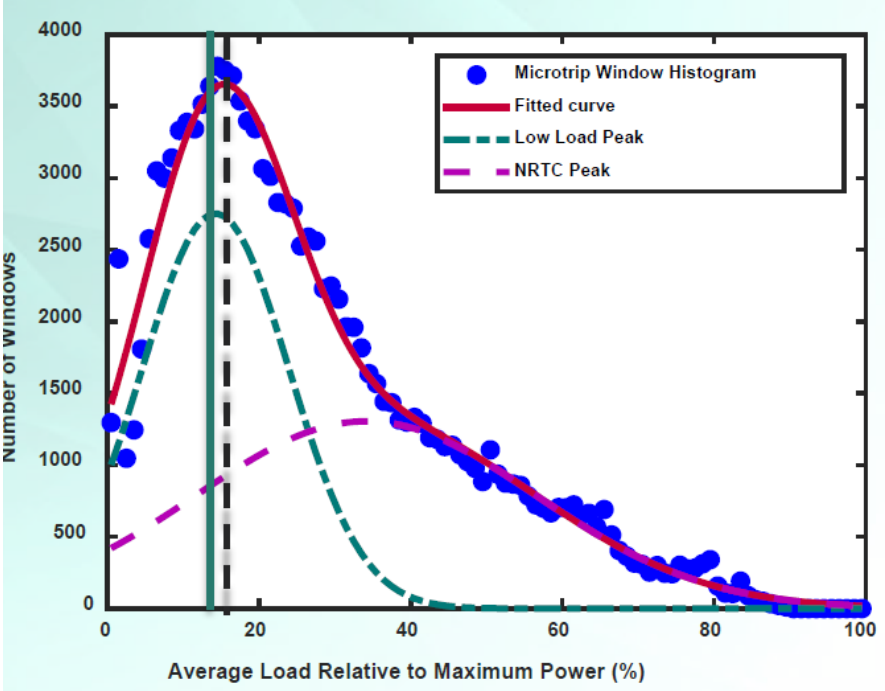



**FIGURE 152. DISTRIBUTION OF WINDOW LOADS USING PERCENT OF MAXIMUM ENGINE POWER METRIC**

## 4.4 k-Means Clustering Analysis to Identify Common Operating Modes

At the conclusion of the previous development step a set of Low Load windows was defined, and the process of selecting profiles could begin. However, it is necessary to have a method to ensure that the profiles eventually selected as building blocks for the LLC are representative of a relatively common form of operation, rather than being from an isolated corner case that is rarely observed in the field. To accomplish this, a method is needed to sort the various profiles into defined groups. The method chosen for this purpose was k-mean clustering, which is the same method that was used by NREL during the on-highway LLC development.

K-means clustering is a method that partitions data into a number (*k)* of groups called clusters based on a set of characteristics. Data points within each cluster are as close as possible to each other, and as far as possible from data in other clusters. Each cluster is defined by its centroid, which is the geometric center of the cluster. The k-means algorithm runs by randomly assigning a group centroids (equal to the number of clusters) and then does repetitive calculations to optimize the positions of the centroids for each characteristic to try to minimize the distance of all the data points to their respective centroids.

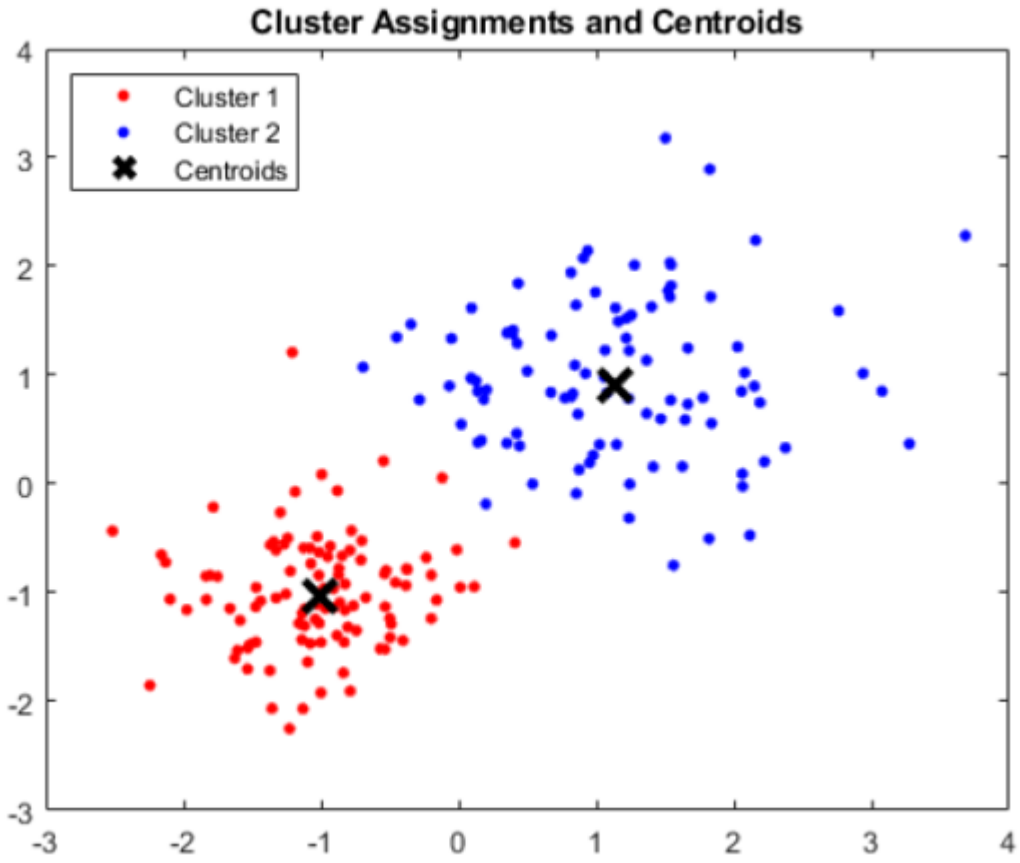



**FIGURE 153. EXAMPLE OF CLUSTERING OUTPUT WITH TWO PARAMETERS AND TWO CLUSTERS**

The number of clusters is a key parameter, and it is necessary to find the optimal number to represent the data set without having too many clusters, which would essentially represent over fitting of the data into a needlessly large number of subgroups. Typically, this decision is made by performing the analysis on a range of different cluster numbers, and then analyzing the result to determine to point where increasing cluster number further provides diminishing returns.

The parameters that were selected for the k-means analysis are given in Table 35, along with the range of those parameters observed in the Low Load data set. The definition of an engine loading event used in this analysis was a load change comparing the current 10 seconds of data to the previous 10 seconds of data. The engine loading ratio is the ratio of increasing load events to decreasing load events in the given window. The 50$^{th}$ Percentile of cumulative Engine Load is essentially the point in time during the window where 50 percent of the accumulated work in that window has been reached (e.g. is the load near the front, the back, or evenly distributed across the window).

**TABLE 35. CLUSTERING PARAMETERS**

| Feature Name | Minimum | Median | 99th percentile |
|---|---|---|---|
| Average Engine Load | 0.02 | 23.03 | 35.95 |
| Maximum Engine Load | 0.56 | 70.87 | 100.47 |
| Median Engine Load | 0.00 | 18.69 | 35.69 |
| Standard Deviation of Engine Load | 0.00 | 10.29 | 28.34 |
| Engine Loading Events per Hour | 0.00 | 327.27 | 1108.42 |
| Engine Loading Ratio | 0.00 | 0.98 | 2.00 |
| % of Low Load (≤25%) Operations | 0.00 | 0.70 | 1.00 |
| % of Sustained (300s) Low Load Operations | 0.00 | 0.20 | 1.00 |
| 50th Percentile of Cumulative Engine Load | 0.00 | 0.51 | 0.80 |

The result of this analysis at different cluster sizes is shown in Figure 154. The figure shows the population of windows in each cluster as a portion of the total for each number of clusters analyzed. An approach to determining the optimal number of clusters to use is to examine the variance as a function of the number of clusters. This is depicted in Figure 155, and this pattern typically shows a curve of decreasing variance. Two approaches are typically used for this kind of analysis. In the first method, which is called the "elbow method," the data is examined visually for the point where the shape of the curve begins to flatten, indicating diminishing returns. For the Low Load data set this method suggests that elbow point at 7 clusters. The other approach is to look where the variance has dropped below 10% of the initial value. For the Low Load data set, 12 clusters are required to reach below the 10% threshold. After examining the results of both data sets and looking at the population data in Figure 154, it was decided to select the 12 cluster solution. It should be noted this is significantly more clusters than were utilized to characterize the on-highway data set, reflecting the much larger variety of operations in off-road machinery.

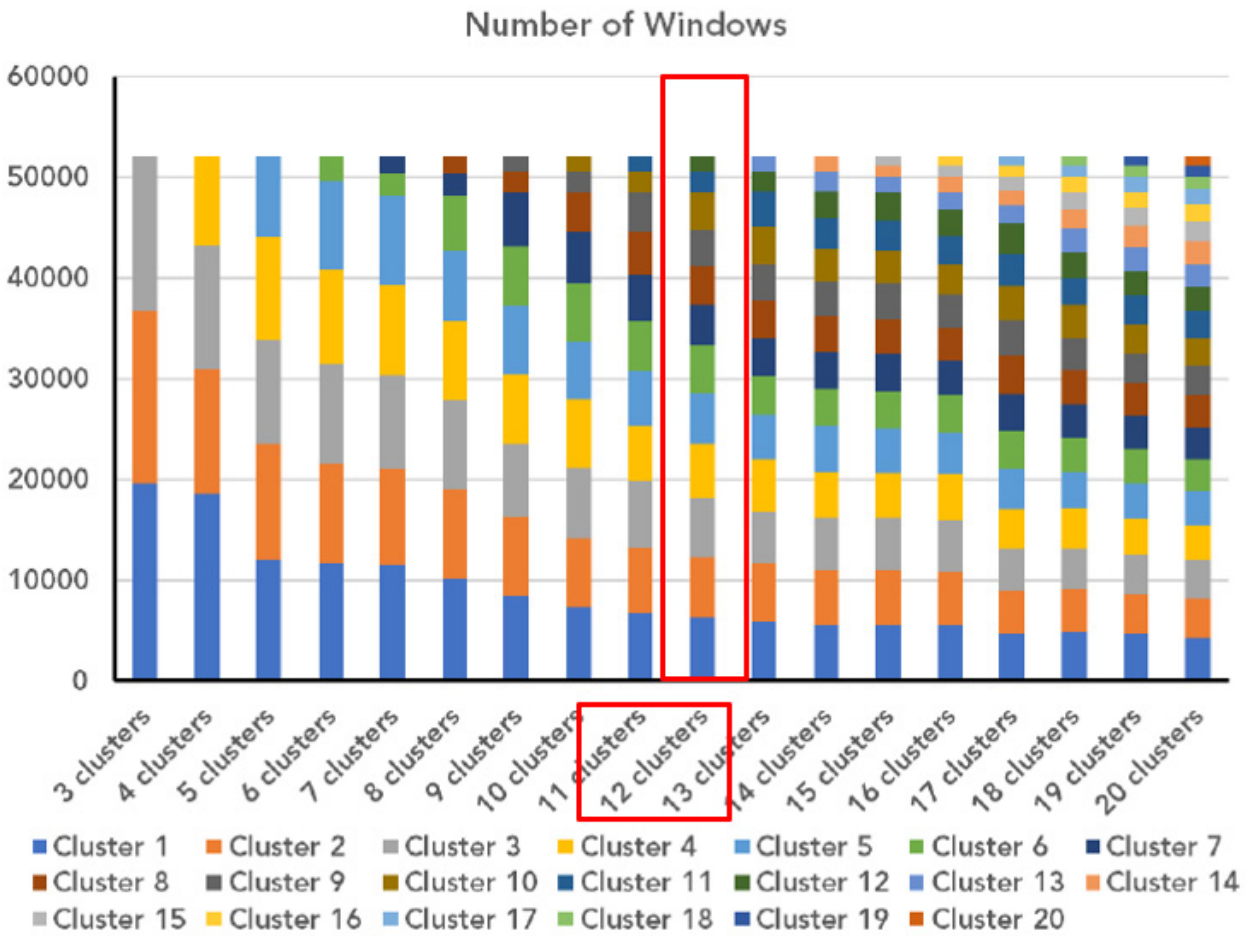



**FIGURE 154. POPULATION OF CLUSTERS VERSUS NUMBER OF CLUSTERS FOR THE LOW LOAD DATA SET**

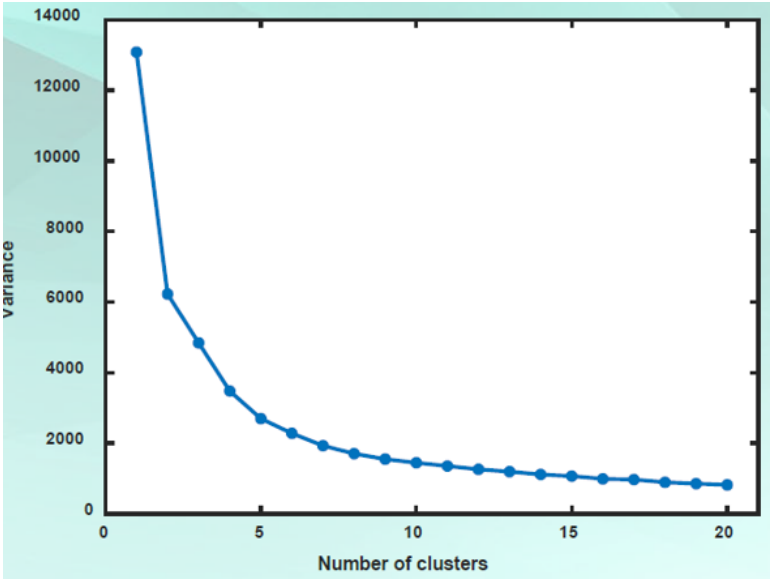



**FIGURE 155. VARIANCE VERSUS NUMBER OF CLUSTERS FOR LOW LOAD DATA SET K-MEANS ANALYSIS**

Table 36 shows the centroid values of all the characteristics used on the k-mean analysis for all 12 of the clusters. The clusters are sorted in order of increasing population in terms of number of windows. The clusters that are highlighted, clusters 4 and 10, represent less than 5% of each of the total population of windows, as well as a small number of engines in the case of cluster 10. Therefore, it was determined that these two clusters would not likely be used for selection of profiles for the final LLC.

**TABLE 36. CENTROID VALUES AND POPULATIONS FOR THE 12 CLUSTERS**

| Original # | Cluster # | Normalized Average Load | Normalized Max. Load | Normalized Median Load | Normalized Std. of Load | Loading Events per Hour | Loading Ratio | Low Load % | Sustained Low Load % | 50th percentile of cumulative load | # of windows | # of engines |
|---|---|---|---|---|---|---|---|---|---|---|---|---|
| 12 | 10 | 0.561 | 0.956 | 0.290 | 0.726 | 0.016 | 0.989 | 0.776 | 0.481 | 0.637 | 1664 | 35 |
| 8 | 4 | 0.327 | 0.318 | 0.316 | 0.092 | 0.017 | 0.981 | 0.985 | 0.926 | 0.628 | 1987 | 85 |
| 9 | 2 | 0.863 | 0.838 | 0.829 | 0.489 | 0.523 | 0.499 | 0.328 | 0.030 | 0.635 | 3673 | 80 |
| 3 | 9 | 0.408 | 0.513 | 0.315 | 0.354 | 0.445 | 0.511 | 0.808 | 0.030 | 0.629 | 3747 | 68 |
| 4 | 1 | 0.602 | 0.495 | 0.582 | 0.198 | 0.198 | 0.545 | 0.763 | 0.050 | 0.631 | 3760 | 100 |
| 6 | 8 | 0.531 | 0.888 | 0.399 | 0.459 | 0.200 | 0.488 | 0.849 | 0.710 | 0.630 | 4062 | 136 |
| 5 | 3 | 0.456 | 0.527 | 0.409 | 0.205 | 0.117 | 0.487 | 0.905 | 0.690 | 0.624 | 4749 | 128 |
| 1 | 12 | 0.684 | 0.894 | 0.510 | 0.643 | 0.752 | 0.507 | 0.636 | 0.032 | 0.636 | 5054 | 89 |
| 10 | 7 | 0.656 | 0.926 | 0.416 | 0.646 | 0.436 | 0.497 | 0.708 | 0.446 | 0.664 | 5245 | 136 |
| 2 | 5 | 0.741 | 0.584 | 0.762 | 0.255 | 0.219 | 0.504 | 0.367 | 0.053 | 0.629 | 5949 | 95 |
| 11 | 6 | 0.675 | 0.722 | 0.595 | 0.388 | 0.476 | 0.485 | 0.627 | 0.015 | 0.632 | 6028 | 107 |
| 7 | 11 | 0.637 | 0.679 | 0.544 | 0.327 | 0.211 | 0.496 | 0.682 | 0.417 | 0.643 | 6264 | 119 |
| | | | | | | | | | Total | | 52182 | |

## 4.5 Idle Related Parameters

The characteristics of idle operation are an important area of consideration in the development of any low load test cycle. Many machines spend a significant amount of operational time on a non-working mode, and during that non-working time they will often be at idle. As a result, it was important to develop an understanding of field idle operation on the data set. Two characteristics of idle in particular were important for cycle development.

The first was an understanding of the distribution of idle durations. This would be helpful in selecting profiles which included significant idle behavior. CARB conducted an analysis of all of the idle (non-working) events in the data set, looking at the duration of each event. For each analysis, a minimum duration was set to remove intermittent idle operations, and to help focus on the distribution of longer or shorter events. The analysis was repeated at several different minimum durations.

The result of this analysis is shown as an empirical cumulative distribution function (ECDF) in Figure 156. Several trends emerge from this distribution that are significant. First, considering minimum idle durations in the range of 30 seconds to 1 minute, the median event appears to be in the range of 2-3 minutes of duration. These are events longer than a brief pause (which the 10-second minimum would represent), but still relatively short in duration. This suggests that for intermittent operations where non-working and working periods alternate frequently, the “typical” idle period is 2 to 3 minutes long.

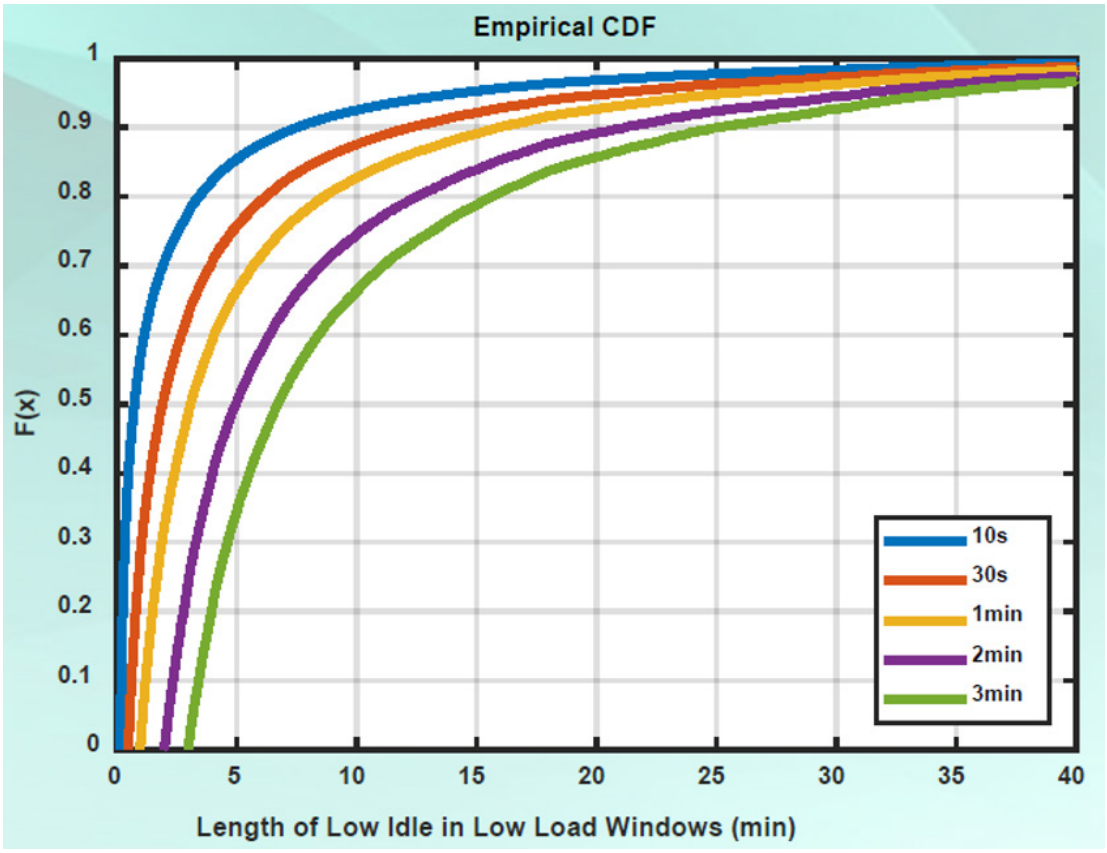



**FIGURE 156. CUMULATIVE EDF OF IDLE DURATION FOR VARIOUS MINIMUM IDLE DURATIONS**

The second observation is that when focusing on longer duration idles above a 2 minute minimum length, the median is still around 5 to 7 minutes, but the 90$^{th}$ percentile is in the range of 20 to 25 minutes. This indicates that in selecting a profile to represent longer idle, a duration in the order of 20 to 25 minutes would be sufficient to cover more than 90 percent of the market. These observations were very useful in helping to guide the selection of a number of profiles that contained idle operation.

Another key piece of information for cycle development was understanding engine load at idle. Off-road engines are often driving significant accessory loads at idle, and the range of idle load can vary significantly by machine application. Given that a portion of the LLC would be at idle, it was necessary to define an appropriate and representative load that would be used under this condition during the test cycle.

CARB staff conducted an analysis of load at the same idle windows used for the duration analysis shown earlier, with the average load across each idle event being used as the data point. To normalize across a wide range of applications and engine sizes, idle load is scaled as a percentage of maximum engine power in this analysis. The distributions of idle load observed in that analysis are depicted again as a set of cumulative EDFs for the various minimum idle durations in Figure 157. It should be noted that in the cases of the 10-second durations, it is likely that the

engine was not fully settled to idle load in some cases due to the short duration, lead to the relatively long tail at the high load end of the ECDF. The other durations actually grouped together very tightly in terms of idle load.

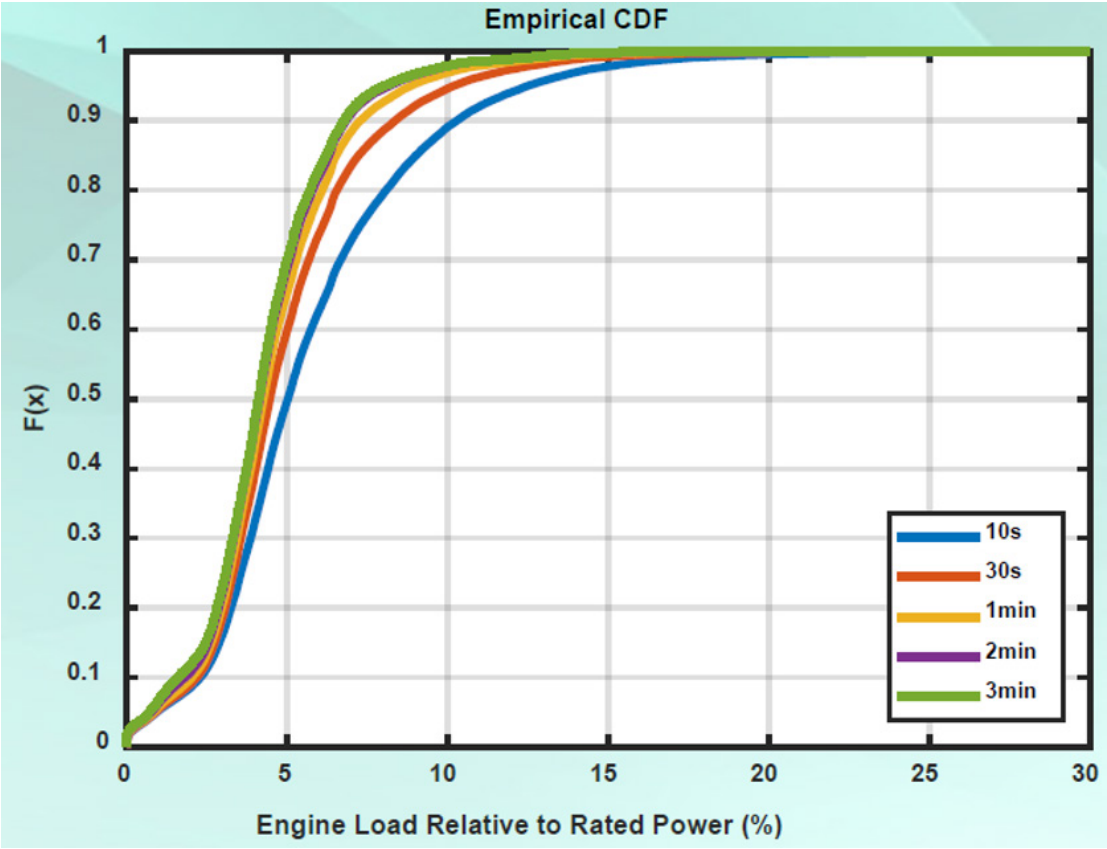



**FIGURE 157. CUMULATIVE EDF FOR IDLE LOAD AT VARIOUS MINIMUM IDLE DURATIONS**

CARB elected to make their determination of idle load based on the 30-second minimum duration ECDF. A summary of key quantiles of the distribution of idle load for this data set is given in Table 37. CARB ultimately chose the 25$^{th}$ percentile to ensure that the LLC testing in the lab would be adequately protective of the majority of field operation from a regulatory standpoint. As a result, during idle on the LLC, an accessory load equivalent to 3.5% of maximum engine power would be utilized.

It was necessary to add this load back in to the cycle at idle because the definition of idle in the normalized cycle is 0 percent speed and 0 percent load. For all other load points, the accessory load is already included in the torque target, but at idle the normalization process effectively wipes away the idle load, setting it to zero. Therefore, it is necessary to add that load back in during denormalization.

**TABLE 37. SELECTED QUANTILES OF IDLE LOAD FOR THE 30-SECOND MINIMUM IDLE DURATION DATA SET**

| Percentile | % of Max Power |
|---|---|
| 10th | 2.6 |
| 25th | 3.5 |
| 50th | 4.6 |
| 75th | 6.2 |
| 90th | 8.6 |

## 4.6 Selection of Profiles from each Cluster

With the clustering analysis complete, the next step was to randomly select a set of profiles from each cluster to begin the process of locating a profile that best represents each cluster. This would yield a set of 10 profiles to serve as the potential building blocks for a low load cycle. Groups of 6 profiles were selected from each cluster at random, choosing profiles from the region of the cluster representing the 10% of profiles in each cluster that were closest to the centroid for that cluster.

Examples of this random selection process are shown in Figure 158 for Cluster 11, which was the most populous cluster by windows, and in Figure 159 for Cluster 6, which was the second most populous cluster by windows. In each case, a characteristic pattern can be observed. Cluster 11 generally appears to feature relatively short activity periods, separated by a relatively long idle periods of more than 10 minutes. By contrast, Cluster 6 features intermittent activity burst separated but short idle periods on the order of 2-3 minutes long. Each of these different activities might be useful, and they should be considered because these patterns occurred more often than any other type of operation in the Low Load data set. In the case of these clusters, such as 6, 11, and 8, which feature idle operations, the idle duration information from the previous analysis was useful in helping to select the appropriate profiles to be used as cycle building blocks.

Ultimately only one profile will be selected for each group. The selected profile is highlighted in green for each group, with the yellow highlighted profiles having also been considered. A number of selection criteria were used to guide the choice of the final profile. One of the key characteristics was the type of application. For each profile, data was examined regarding the number of machines and windows falling into either construction or agricultural activity.

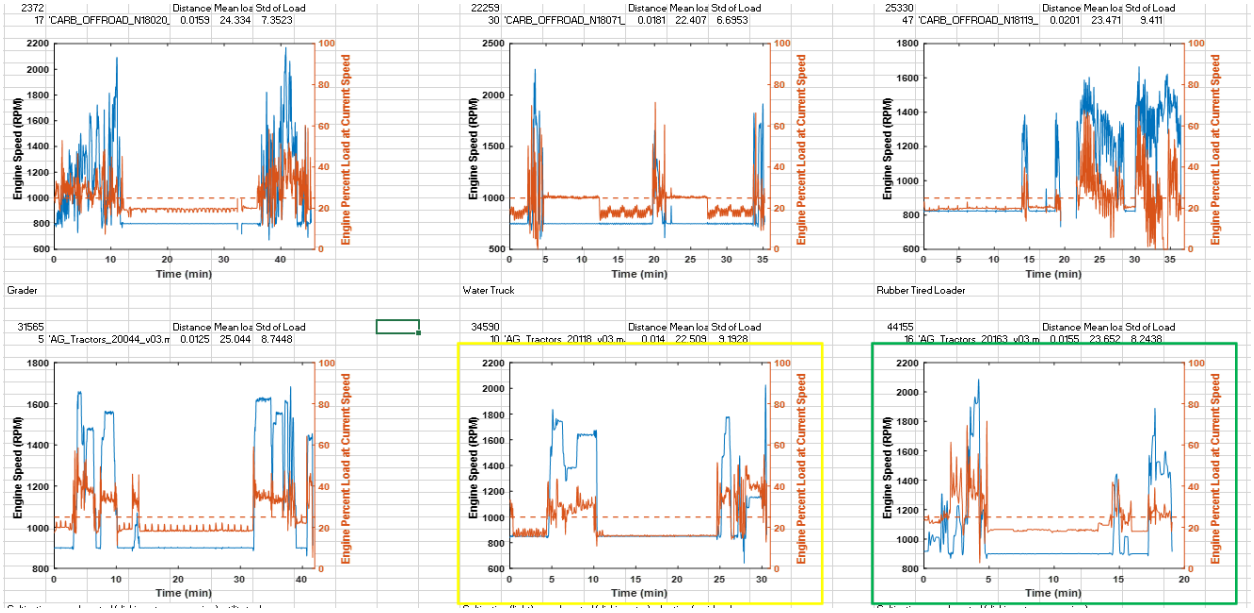



**FIGURE 158. EXAMPLE OF SIX SELECTED PROFILES FOR CLUSTER 11**

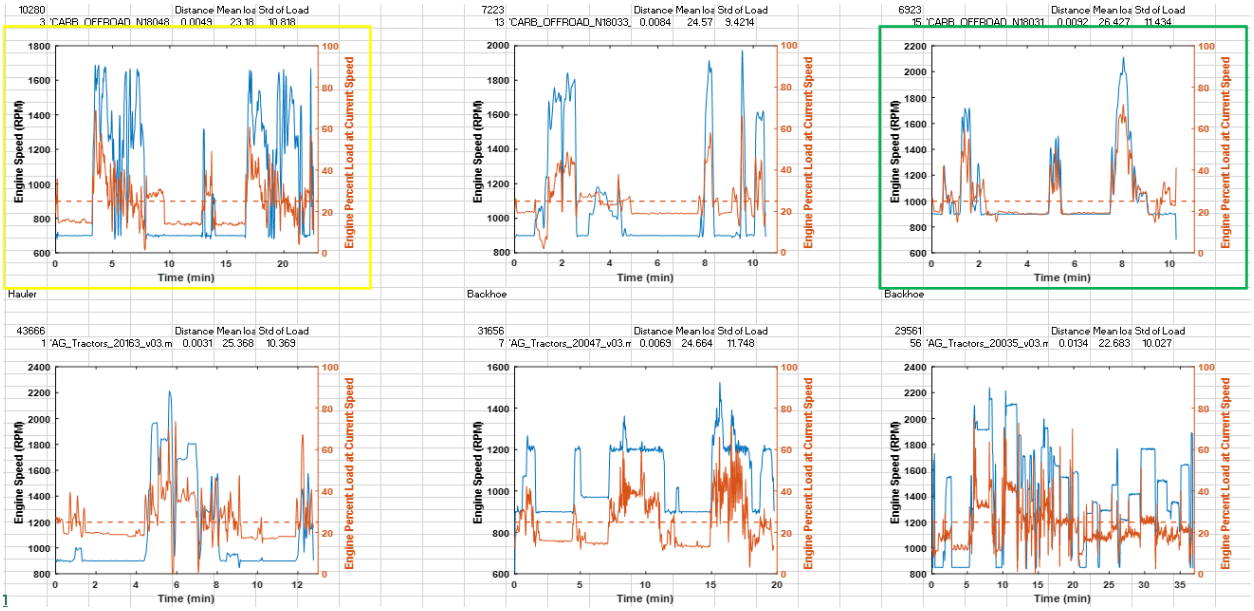



**FIGURE 159. EXAMPLE OF SIX SELECTED PROFILES FOR CLUSTER 6**

An example of this population data is given in Figure 160 for Cluster 11. Although the cluster is relatively evenly proportioned between Ag and Construction by number of engines, there is a clear indication of more operations in Cluster 11 coming from Ag equipment. Therefore, the final choice of profile would be preferably chosen for an agricultural machine (such as a farm tractor).

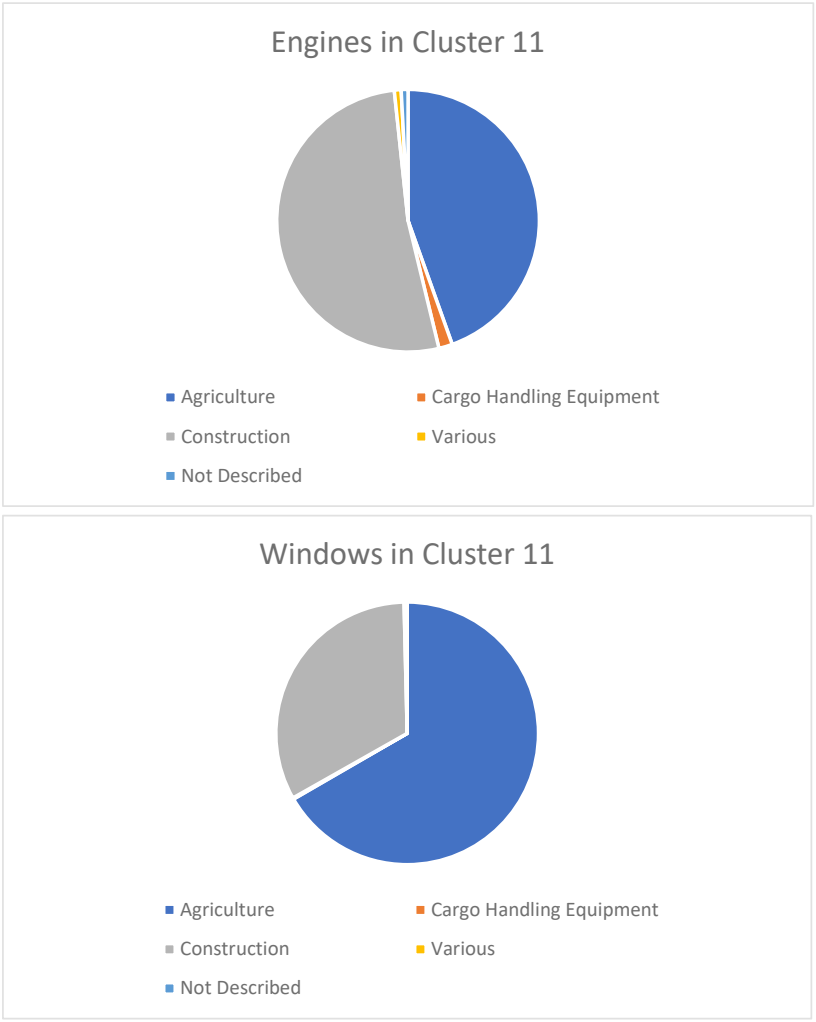



**FIGURE 160. DISTRIBUTION APPLICATION TYPE FOR CLUSTER 11 BY ENGINE POPULATION AND NUMBER OF WINDOWS**

As noted earlier, a single profile was chosen for each cluster that captured the characteristic behavior of that cluster, while at the same time having entry and exit conditions that made it compatible with being assembled into a larger cycle. For the selected profile, additional information was extracted from the data set to identify the behavior prior to the selected profile so that the entry conditions could be maintained in a manner consistent with how the operation had occurred in the field. In some cases, additional profiles were randomly pulled from a given cluster if the initial selection of 6 did not provide any profiles that were suitable for use.

Application information for each of the final selected profiles is given in

Table 38. Each of the profiles was normalized using the appropriate engine torque curve. The profiles were also screened for speed transitions that would not be compatible with running on an engine dynamometer. The final set of normalized profiles is illustrated in Figure 161, and they are also depicted in speed-torque scatterplots in Figure 162. As additional information, the machines for each selected profile are depicted in Figure 163, showing the variety of applications covered by the selected profiles.

## TABLE 38. APPLICATION AND ENGINE INFORMATION FOR SELECTED PROFILE FROM EACH CLUSTER

| Cluster | Profile | Machine | Machine SN | Engine | Engine Power | Application | Category | Application Notes | Start | End | months | Worksite | Worksite Notes |
|---|---|---|---|---|---|---|---|---|---|---|---|---|---|
| 11 | 44155 | 2017 John Deere 5100MH | 1LV5100MLHH101042 | 4045 | 100 HP | Farm Tractor | Ag | High Crop, Orchard, Cultivation and weed control | 4/13/2021 | 7/30/2021 | 3.6 | Farm | 21,000 acres, tomatoes, cotton, alfalfa, onions, almonds, pistachios |
| 6 | 6923 | 2017 John Deere 410-L | 1T0410LXHF310249 | 4045HT096 | 56 - 130 kW | Backhoe | Construction | | 7/25/2019 | 10/31/2019 | 3.27 | | |
| 5 | 27372 | 2012 John Deere 6190R | N/A | 6068 | 190 HP | Farm Tractor | Ag | Cultivation, weed control (disking etc.), planting | | | | Farm | 1600 acres, Tomatoes, Onions, Garlic, Corn, others |
| 7 | 2943 | 2016 Caterpillar 140M3 | CAT0140MAN9J00440 | C9.3 | 256 HP | Grader | Construction | | 1/10/2019 | 2/7/2019 | 0.93 | | |
| 12 | 12924 | 2014 Caterpillar M334 | N/A | C9.3 | 272 HP | Excavator | Construction | | 9/6/2020 | 10/2/2020 | 0.87 | | |
| 3 | 3579 | 2019 Excavator 325FLCR | CAT0325FJNDJ20771 | C4.4 | 161 HP | Excavator | Construction | include the 20 min after please… | 8/28/2019 | 1/23/2020 | 4.93 | | |
| 8 | *23309* | *2020 Caterpillar 450F* | CAT045FCHJR00282 | C4.4 | *142 HP* | *Backhoe* | *Construction* | | 8/31/2021 | 10/7/2021 | 1.53 | | |
| 1 | 26848 | 2016 John Deere 7250R | 1RW7250REHS100006 | 6068RW446 | 250 HP | Farm Tractor | Ag | Cultivation, weed control (disking etc. or spraying), other utility operations | | | | Farm | 9000 acres, ROW CROPS, TOMAOTES, COTTON, GARLIC, LETTUCE, MELONS, ALMONDS |
| 9 | 15285 | 011 Peterbilt Water Truc | 2NP3LN036LM158535 | ISC8.3 350 | 350 HP | Water Truck | Construction | | 8/26/2020 | 9/23/2020 | 0.93 | | |
| 2 | 45552 | 2018 John Deere Tractor | | 4045HLV78 | 100 HP | Farm Tractor | Ag | UCR Ag Tractor | | | | | |
| 4 | 37221 | 2016 John Deere 8370R | 1RW8370RCGD110049 | 6090 | 370 HP | Farm Tractor | Ag | Cultivation (heavy and light), subsoiling, weed control (disking etc.), planting | | | | | 210,00 acres, Processing tomatoes, fresh tomatoes, cotton, alfalfa, onions, almonds, pistachios, watermelons, cantaloupes |

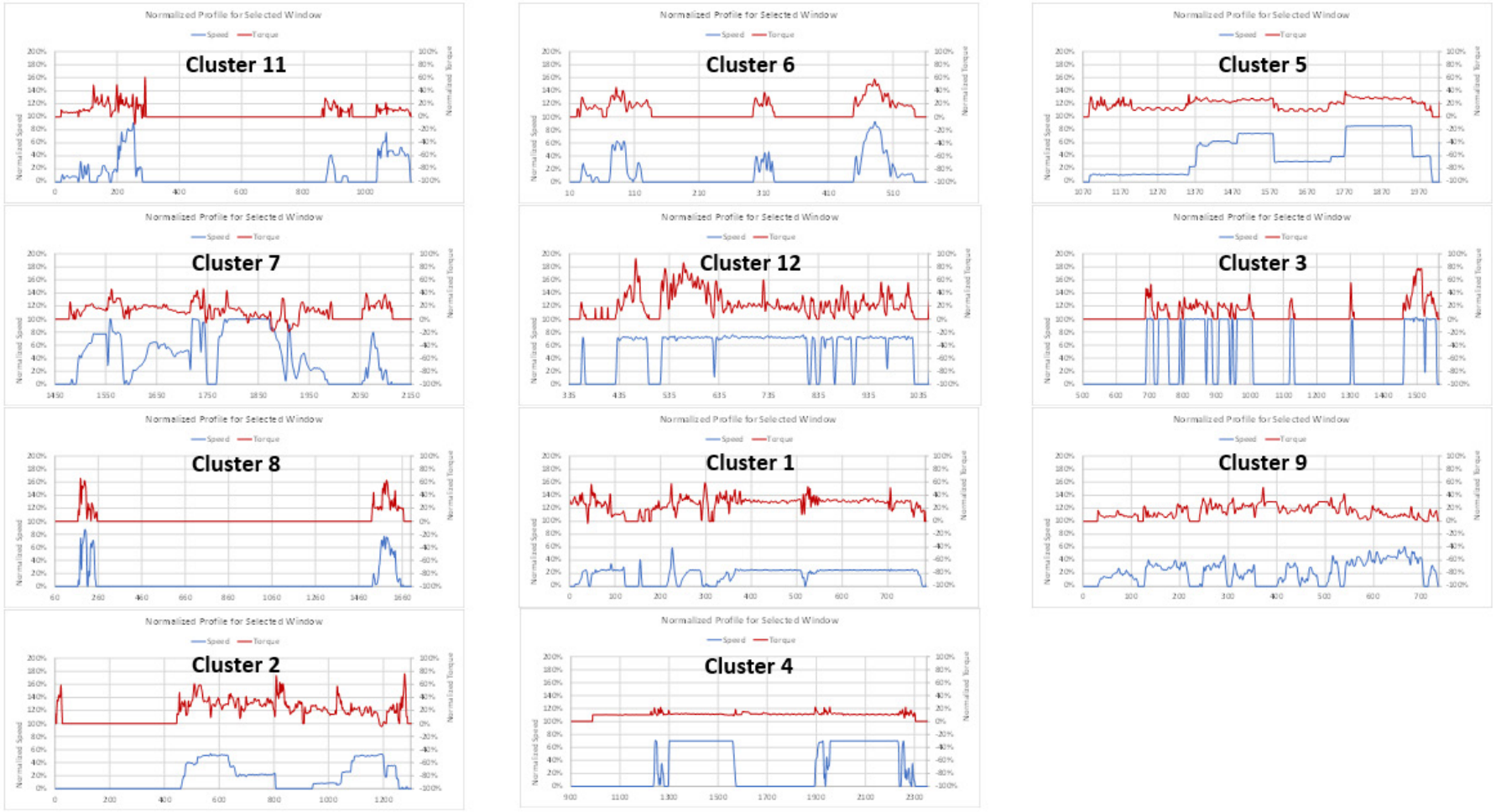



**FIGURE 161. NORMALIZED PROFILES FOR EACH CLUSTER**

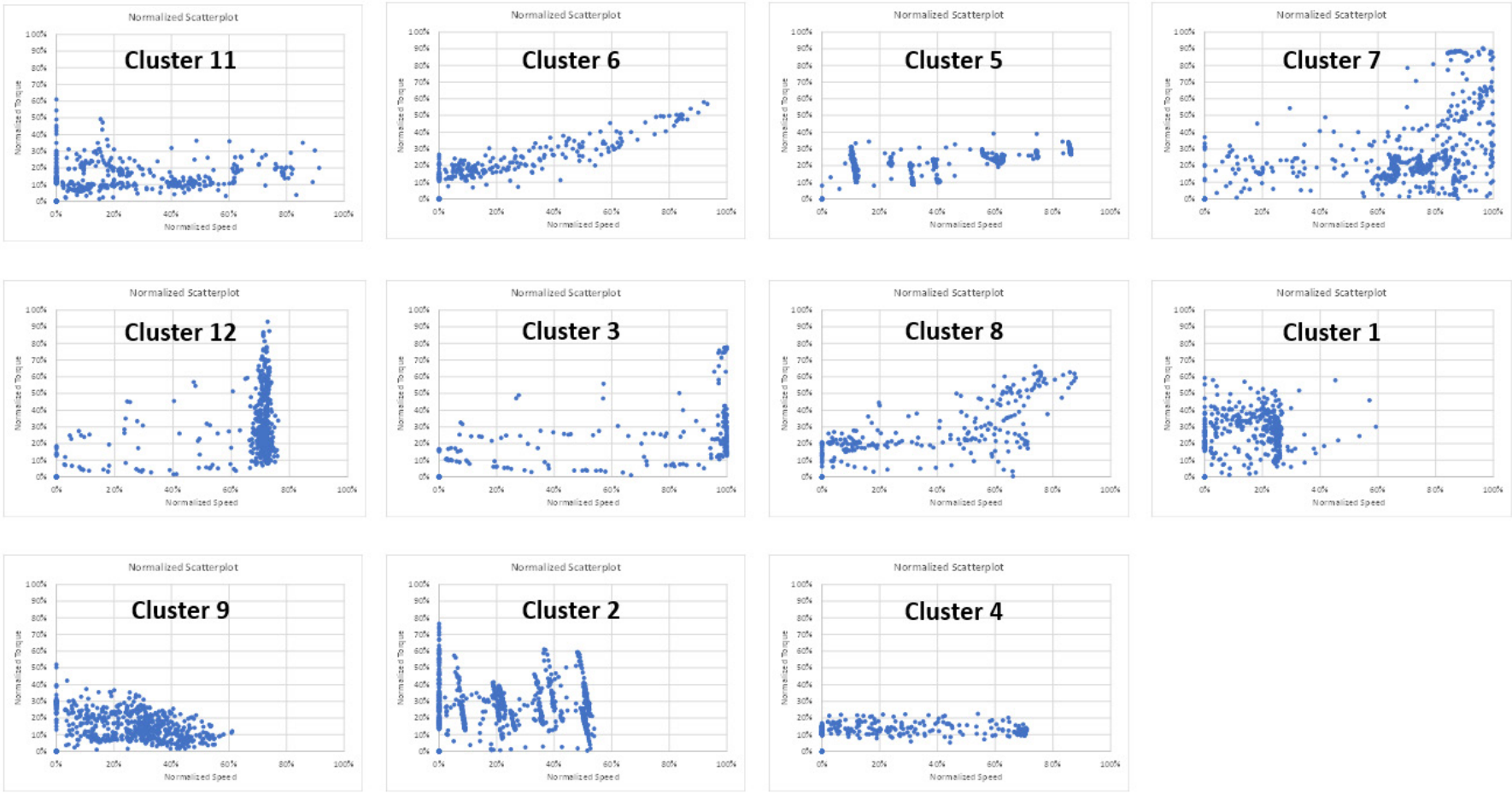



**FIGURE 162. NORMALIZED SPEED-TORQUE SCATTERPLOTS OF SELECTED PROFILES FROM EACH CLUSTER**




**FIGURE 163. MACHINES REPRESENTED BY THE SELECTED PROFILES FOR EACH CLUSTER**

As can be seen in Figure 161 and Figure 162, the selected profiles represent a wide variety of different operating patterns and duty cycles. Both variable speed and constant speed applications are represented within these profiles, as well as both continuous and intermittent load patterns.

## 4.6 Profile Testing

With the individual profiles selected, it was necessary to assess them to understand the characteristic behavior of each profile in the context of a Tier 4 engine. This would help to understand how each profile might contribute to an overall cycle. In addition, it was also important to assess each profile on the engine to ensure that the profiles were all runnable enough on an engine dyno that cycle regression statistics could be met, and the cycle could be run in a repeatable fashion. These runs were conducted using the John Deere 6068 engine for this program, but with that engine in its baseline Tier 4 final configuration.

To do this, the profiles were all run individually. Each profile was run either two or three times, head-to-tail, with no dwell. Before each profile, a preconditioning sequence of two hot-start NRTC cycles was run, with a 20-minute soak between the two cycles. Then after a 20-minute engine-off soak, the profile would be run. This was done because the final cycle was intended to run after the cold-hot NRTC runs during certification testing, following a 20-minute soak. Including this would provide an understanding of how each profile would behave if it was the first one in the final cycle. The repeats would also allow an understanding of the characteristic behavior of each profile after the engine and emissions control system had reached equilibrium with that duty cycle. All of this pieces of information would be important to the process of piecing the building blocks of the individual profiles together into a final cycle.

An example of the data from one of these runs is shown in Figure 164 for the Cluster 6 profile. Given the short duration of the profile, it was repeated 3 times as part of the test run. In looking at the temperature data from the middle plot in the figure, it can be seen that the system was carrying some residual heat left over from the previous hot NRTC test. The lingering impact of that residual heat carried through about the first 400 seconds of the first profile repeat. After that, the system settled into equilibrium with the second and third repeats of the profile. Initially, some $NO_X$ reduction activity is observed through the first profile repeat. However, by the second and third repeat, where the system temperature is now consistently below 250° and spends substantial time below 200°C, there is little sustained $NO_X$ reduction activity. Overall, the profile appears to be a good example of intermittent short burst of working and non-working activity and would be a useful part of examining a sustained low load operation of this kind. Given the short duration, this profile was actually run twice as a segment of the final LLC, which would be longer enough for a system to reach a sustained behavior on this activity.

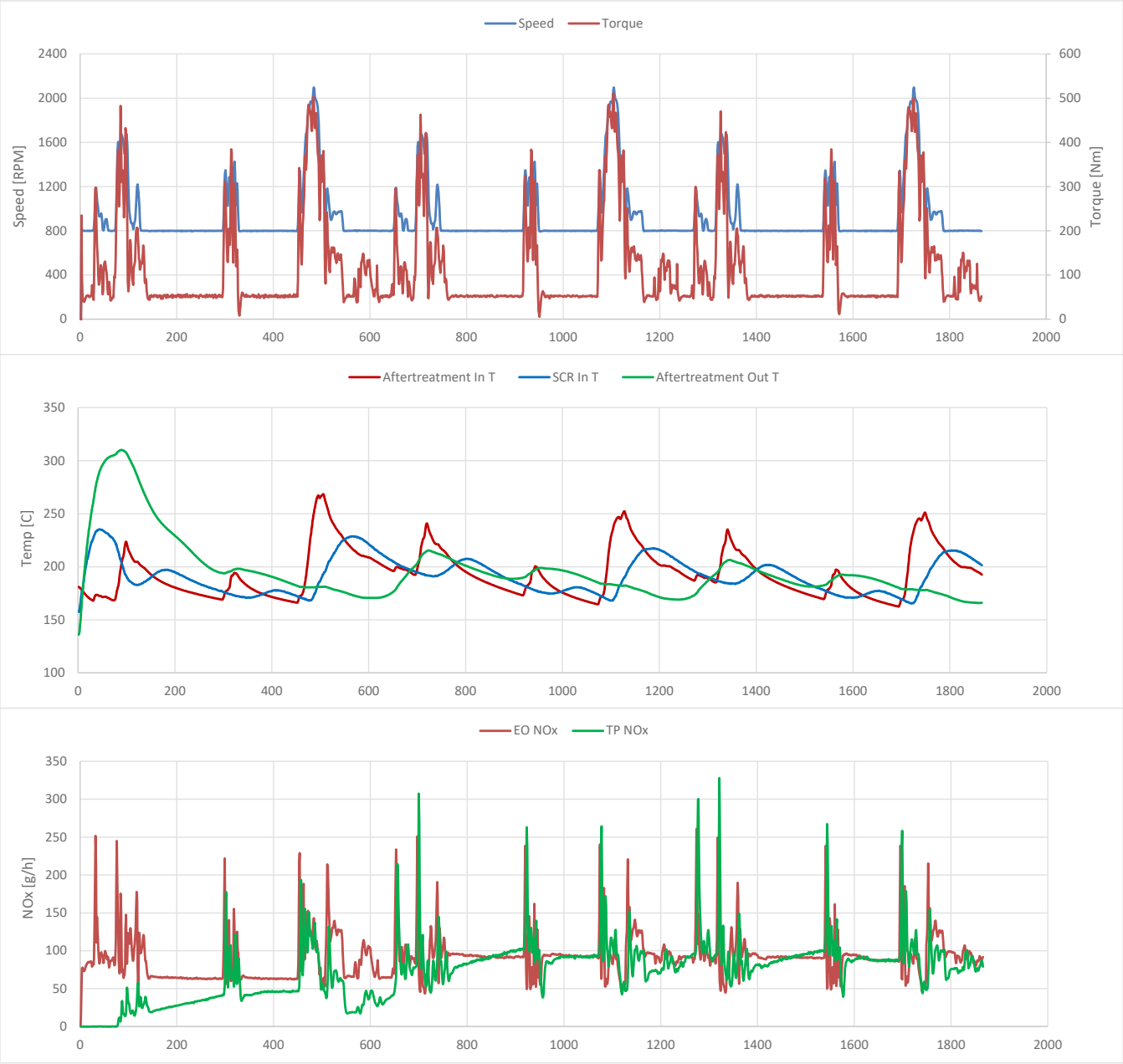



**FIGURE 164. EXAMPLE OF PROFILE TESTING FOR CLUSTER 6 PROFILE ON JOHN DEERE 6068 TIER 4 FINAL ENGINE**

Similar runs were made on all of the Cluster profiles, and that data is included in the report in Appendix B.

Over the course of these runs it was determined that Clusters 2, 4, and 5 were redundant with other clusters and tended to provide a relatively poor assessment of system behavior. In addition, for Clusters 1, 3, and 12, it appeared that a partial run of the profile was sufficient to capture the essence of that behavior, and the remaining portion was likely to be superfluous. These assessments were important to help in shortening the final cycle duration while at the same time

still providing an adequate assessment of low load challenge. With the data from these profile assessments, SwRI had the information to begin the final assembly of candidate cycles.

## 4.7 Candidate Cycle Assembly and Evaluation

Based on the data from the previously discussed profile tests and leveraging prior experience with the assembly of other test cycles, and the on-highway LLC in particular, SwRI assembled multiple sets of candidate LLCs. The initial cycles were tested and evaluated on the engine, and then the resulting data were analyzed to help determine how the cycles behaved and where improvements could be made.

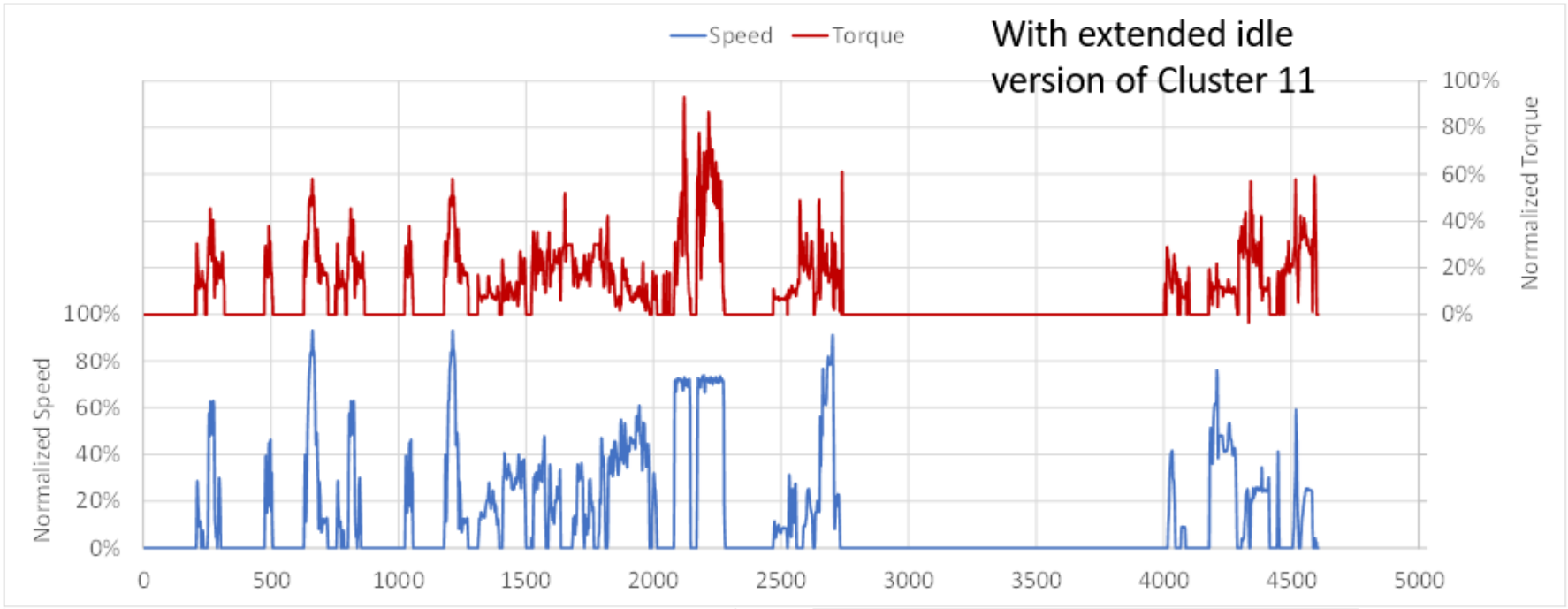
In general, the cycles were assembled to provide examples of three kinds of low load challenges:

- Low load to high load transitions, sometimes called "return-to-service" events. These are typically characterized by a period of non-working operation or low load operation, followed by a transition to high load. Maintaining system readiness for high load events is the primary system challenge for these events.
- High load to low load transitions, sometimes called "cool down" events. These are typically periods of working operation followed by a transition to non-working or idle operation for a period of time. Maintaining system temperature during cool down is the primary system challenge for these events.
- Sustained low load operations. These are characterized by periods of low load that do not feature clear increasing or decreasing load patterns. This can occur due to either sustained segments of very intermittent operation, or sustained period of continuous by low loads. Maintaining system temperature and high efficiency operation is the challenge for these events, as well as being ready for a possible high load transition.

An efficient low load cycle will present examples of each of these challenges and will alternate operations to present these challenges in the most efficient manner possible. Efficiency of cycle construction is important to try to hold down overall cycle duration. Low load operations can potentially lead to very long run times, so assembling a cycle to present challenges is important to help minimize the laboratory burden of the cycle.

Several rounds of candidate cycles were assembled and evaluated as part of this effort. After 13 initial cycles were assembled and evaluated by SwRI, a final set of three "beta" cycles was assembled. These near final form cycles were tested by SwRI on multiple engines, and they were also distributed to Steering Committee member companies to be run on engines in their own test facilities.

The final three candidate cycles, Candidates 14, 15, and 16 are shown in Figure 165, Figure 166, and Figure 167, respectively.




| | | | | | Speed | Torque |
|---|---|---|---|---|---|---|
| Segment | Cluster | Length | Total | | **12%** | **9%** |
| 1 | idle | 180 | 180 | | 0% | 0% |
| 2 | 6 | 1100 | 1280 | | 12% | 10% |
| 3 | 9 | 740 | 2020 | | 22% | 15% |
| 4 | 12 | 431 | 2451 | | 28% | 18% |
| 5 | 11ext | 1837 | 4288 | | 7% | 4% |
| 6 | 1 | 317 | 4605 | | 13% | 22% |

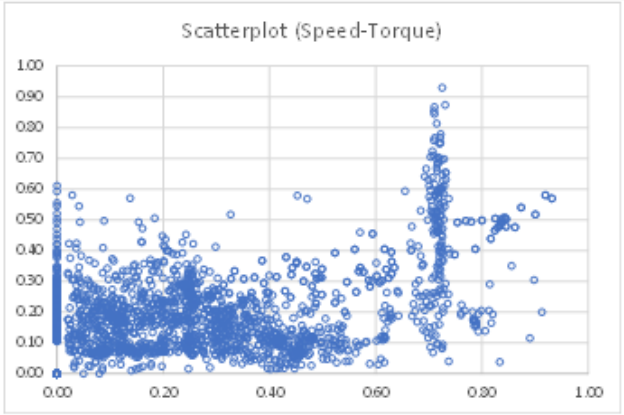
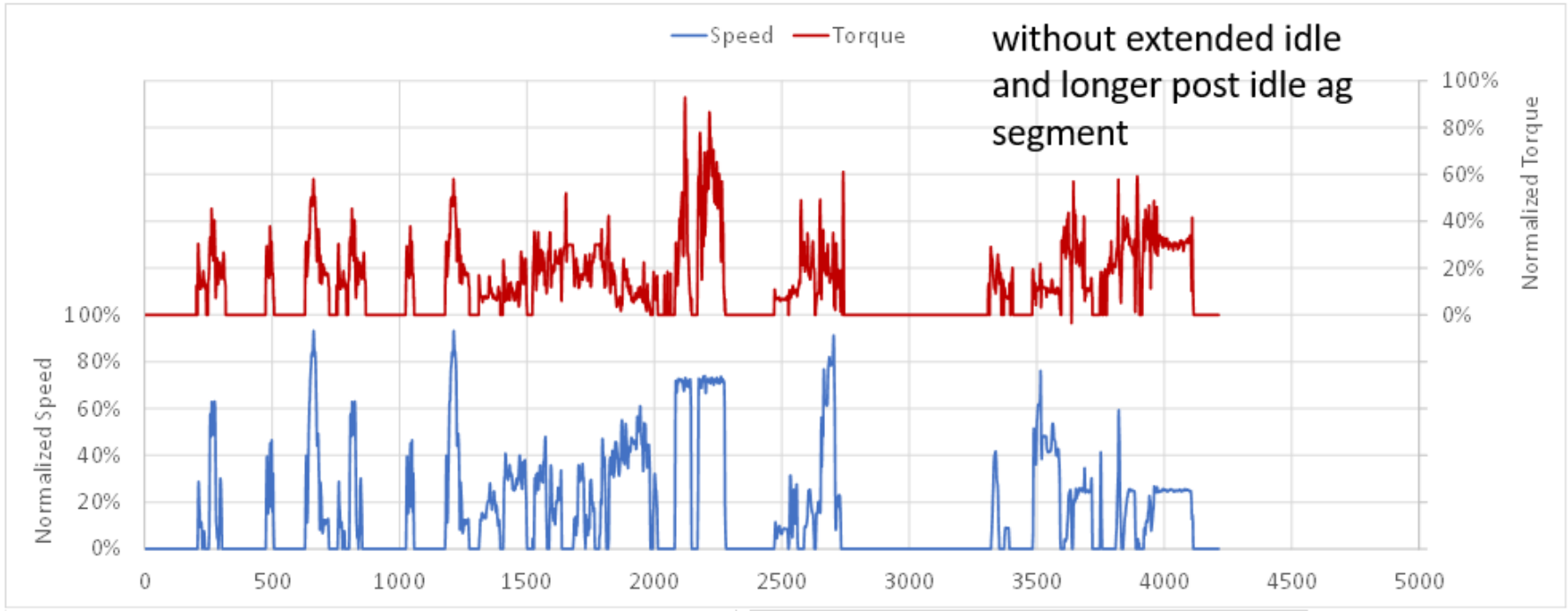



**FIGURE 165. LLC BETA CANDIDATE CYCLE 14**




| | | | | | Speed | Torque |
|---|---|---|---|---|---|---|
| Segment | Cluster | Length | Total | | **15%** | **12%** |
| 1 | idle | 180 | 180 | | 0% | 0% |
| 2 | 6 | 1100 | 1280 | | 12% | 10% |
| 3 | 9 | 740 | 2020 | | 22% | 15% |
| 4 | 12 | 431 | 2451 | | 28% | 18% |
| 5 | 11 | 1143 | 3594 | | 11% | 6% |
| 6 | 1 | 620 | 4214 | | 13% | 21% |

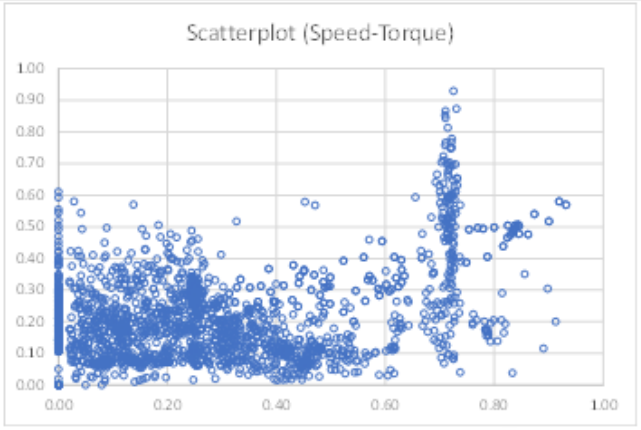
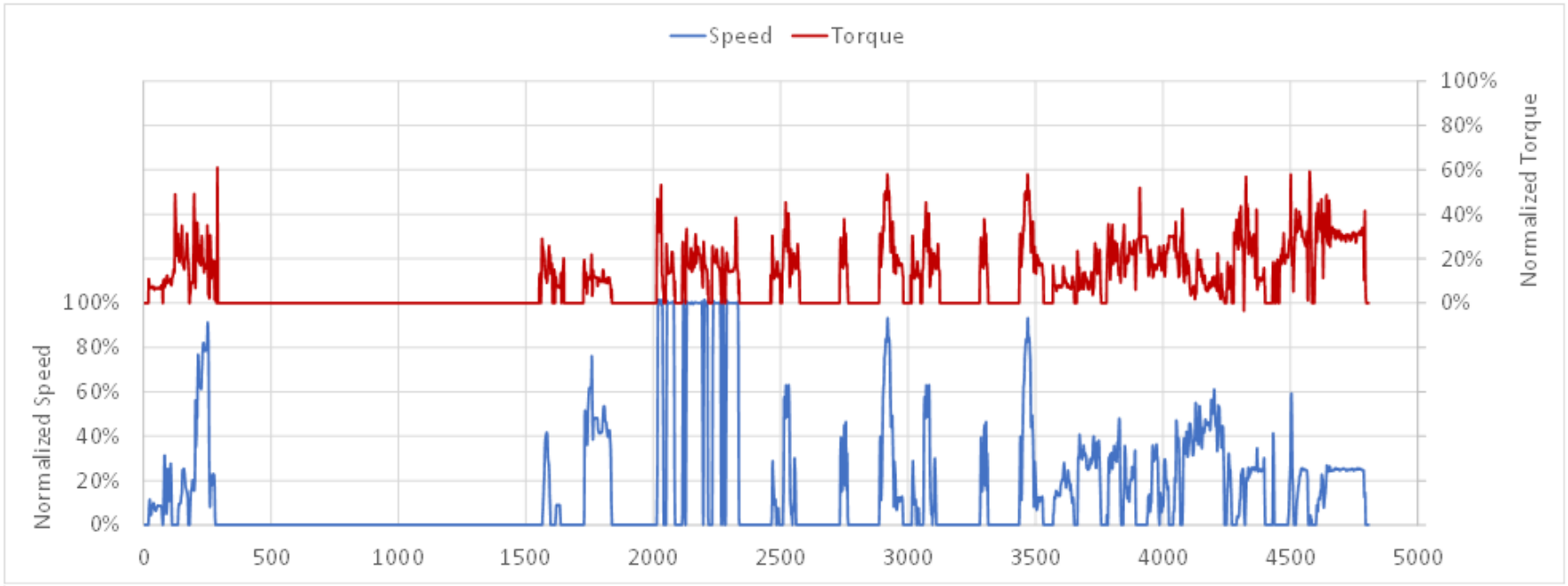



**FIGURE 166. LLC BETA CANDIDATE CYCLE 15**




| | | | | | Speed | Torque |
|---|---|---|---|---|---|---|
| Segment | Cluster | Length | Total | | **15%** | **12%** |
| 1 | idle | 180 | 180 | | 0% | 0% |
| 2 | 6 | 1100 | 1280 | | 12% | 10% |
| 3 | 9 | 740 | 2020 | | 22% | 15% |
| 4 | 12 | 431 | 2451 | | 28% | 18% |
| 5 | 11 | 1143 | 3594 | | 11% | 6% |
| 6 | 1 | 620 | 4214 | | 13% | 21% |

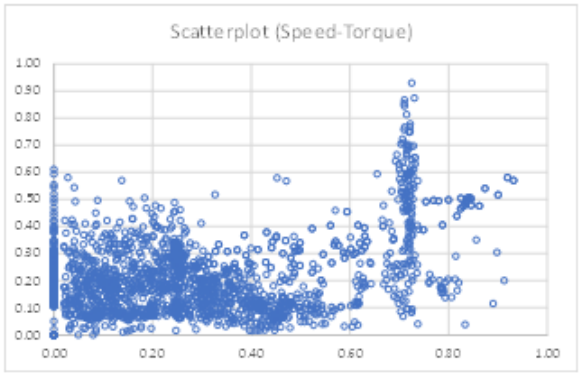



**FIGURE 167. LLC BETA CANDIDATE CYCLE 16**

These final three candidate cycles were also evaluated using the Development Aged parts for the Tier 5 Low $NO_X$ demonstration engine, to get an early look at how much additional calibration effort, if any, might be needed to address these new cycles. In addition, that evaluation was also useful for the final candidate cycle down-selection progress.

As an example, Figure 168 shows data from testing of LLC Candidate 14 on the Baseline Tier 4 Final configuration of the John Deere 6068 engine. Although there are some periods of good $NO_X$ reduction performance, it is clear that overall this engine struggled on this LLC, achieving only about 15% $NO_X$ conversion of the cycle for a tailpipe $NO_X$ level of 6.6 g/kw-hr. Given that this engine was never designed or calibrated for emission control performance over this much lower load cycle, this result is not unexpected.

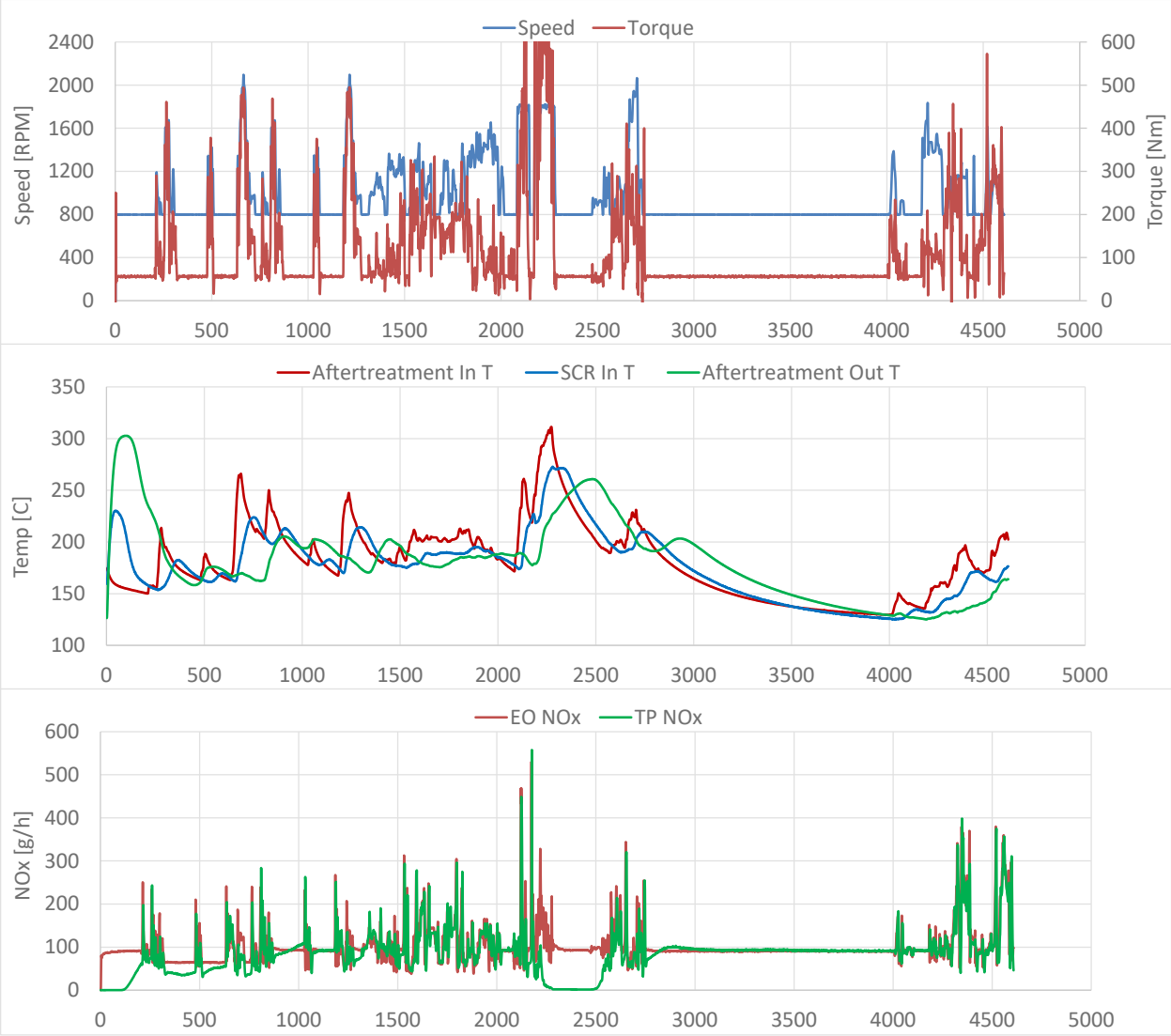



**FIGURE 168. EXAMPLE OF LOW LOAD CYCLE TESTING ON CANDIDATE 14 WITH BASELINE TIER 4 FINAL ENGINE**

Figure 169 shows an example of the same candidate LLC, but this time run on the Tier 5 Low $NO_X$ demonstration configuration using the Development Aged parts. System temperatures are maintained considerably higher, and the use of the upstream SCR in the form of the MFC helps

to maintain low temperature $NO_X$ reduction performance. The Tier 5 demonstration systems achieves 99.6% $NO_X$ reduction over this cycle, for a tailpipe $NO_X$ level of 0.022 g/kw-hr. However, it should also be noted that due to the thermal management associated with improved emission control performance, $CO_2$ emissions were roughly 5% higher on this low load cycle than they were for the baseline engine. It should be noted that these tests were run without the use of DSF or CDA.

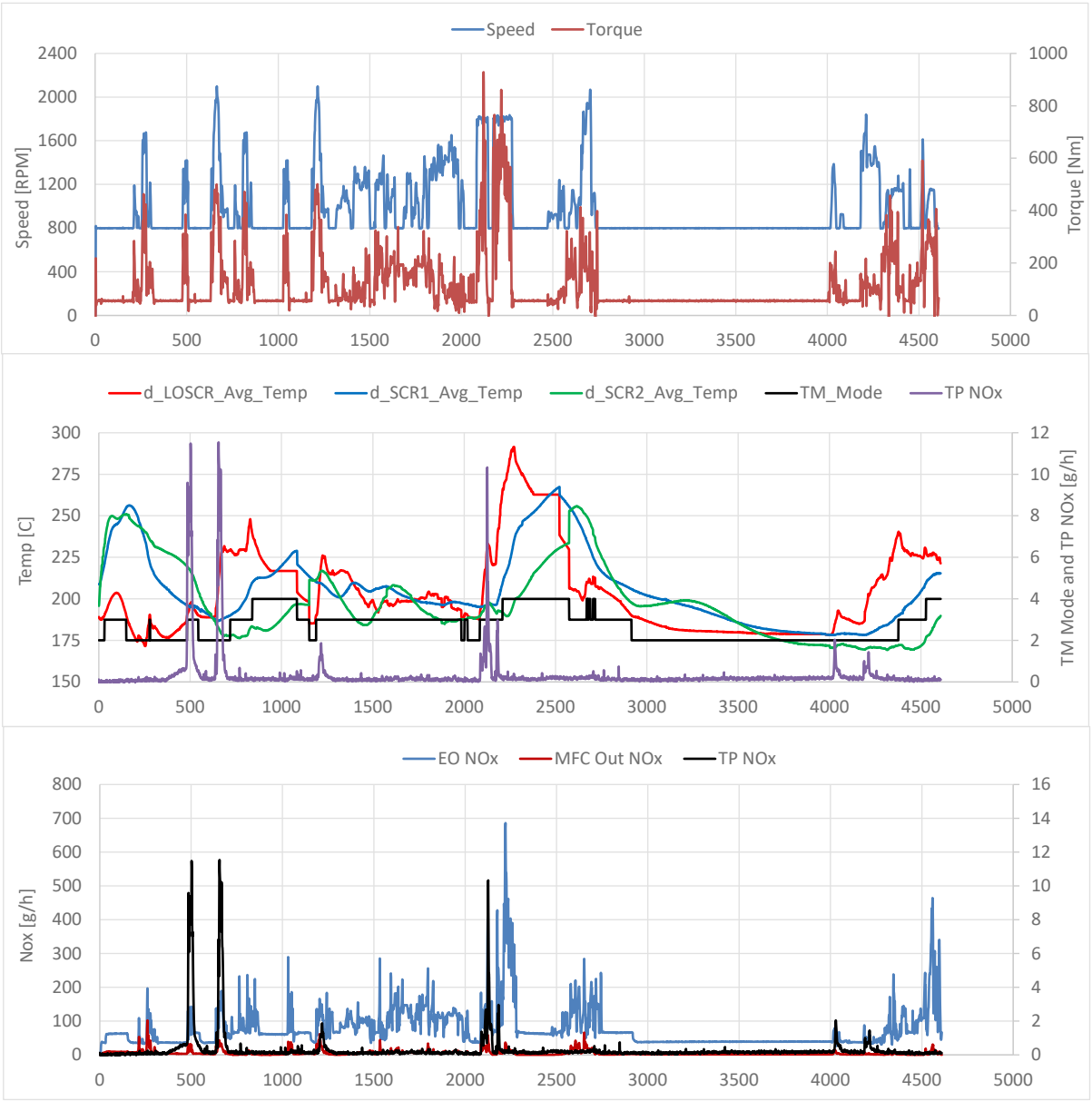



**FIGURE 169. EXAMPLE OF LOW LOAD CYCLE TESTING ON CANDIDATE 14 WITH TEIR 5 LOW $NO_X$ DEMONSRATION ENGINE USING DEVELOPMENT AGED PARTS**

## 4.8 Final Cycle Selection and Cleanup

Information and test data on all three beta candidate cycles was provided to CARB form multiple engines and test laboratories. CARB was also able to evaluate these three cycles in their own laboratory facility in Riverside, CA. It should be noted that across multiple laboratories and several engines of different power ratings, no labs had any particular difficulty running the test cycle. SwRI did observe difficulties with speed regression in one case involving a relatively small engine that was poorly matched to a larger dynamometer with an inertia value too high for that engine. However, this was an exception that should be manageable for any laboratory that is aware of the range of engine sizes that they plan to test.

Ultimately, CARB selected Candidate cycle 16 as the final candidate cycle. However, the aggressive return-to-service event that was part of Cluster 12 and was used in the middle of candidate 14 was also seen as a desirable event that would be useful as part of the final cycle. As a result, the end of Candidate 16 was modified to include this event in place of the ending segment of Cluster 1 operation. This also resulted in a slightly shorter final test cycle. This final iteration of the cycle was termed Candidate 16d.

A final point-by-point review and cleanup was also run on this final cycle, to look for any last issues. Several noisy torque spikes near idle were spotted and removed as being extraneous results of the original normalization process. The final clean, off-road Low Load Cycle that resulted from this progress is shown in Figure 170. The cycle has a duration of 4570 seconds and is intended to be run after the hot-start NRTC of the current certification test sequence, following a 20-minute engine-off soak. If run on its own, precondition should consist of two hot-start NRTC cycles with a 20-minute soak between them, followed by a 20-minute engine off soak. The cycle is run with an accessory load at idle of 3.5% of engine rated maximum power.

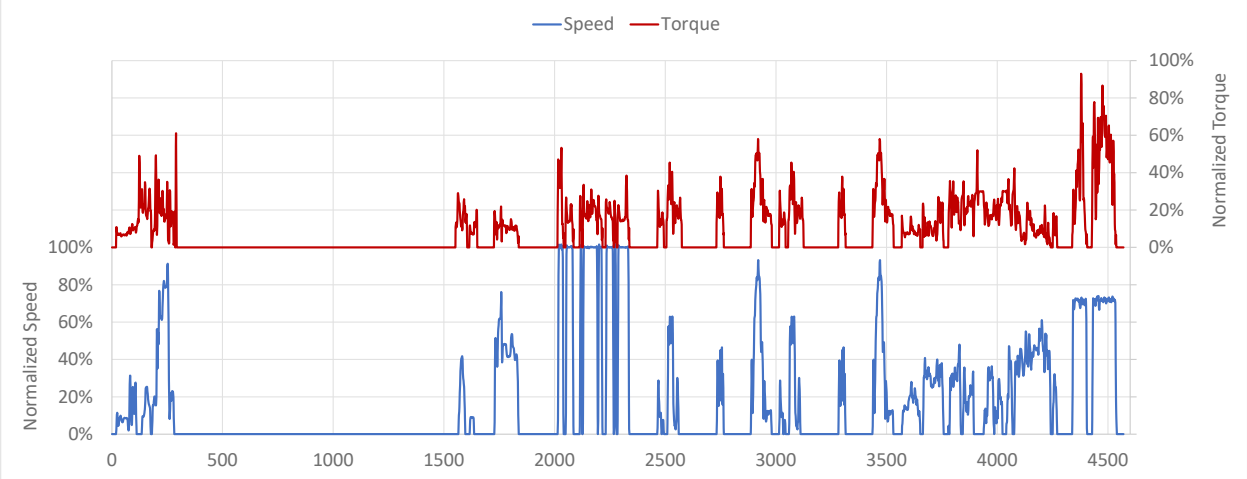



**FIGURE 170. FINAL OFF-ROAD LOW LOAD CYCLE (LLC)**

# 5.0 SUMMARY AND CONCLUSIONS

The objective of this program was to demonstrate the technical feasibility of reaching Low $NO_X$ levels while also reducing $CO_2$ emissions by 5 to 8.6%, while maintaining other GHG emission levels at or below the Tier 4 final baseline engine. The results of this demonstration testing are generally applicable to engines in the range from 56kw to 560kw, and the technologies demonstrated would be applicable across that range. The program goal for Low $NO_X$ was 0.040 g/kw-hr over the NRTC and RMC cycles over full useful life, with LLAC and in-use emissions as low as feasible. The program intent was to reach these targets with technologies that were feasible for production by as early as the 2029+ model year. The results of the program are summarized below, along with conclusions regarding those results with respect to the program targets.

## 5.1 Demonstration Results

A summary of the key demonstration test results is given below in Figure 171 for tailpipe $NO_X$ emissions for both technology packages compared to the Baseline engine. Both packages achieved substantial reductions of 90% in tailpipe $NO_X$ on the NRTC, 75% on the RMC, and more than 99% on the LLAC where tailpipe $NO_X$ was reduced by two orders of magnitude compared to the base Tier 4 engine. It should be noted that the Low $NO_X$ results are parts that have been DAAAC aged to Full Useful Life (FUL), including both thermal and chemical aging, while the Baseline results are from only a de-greened system. Therefore, FUL $NO_X$ reductions would likely be even greater than what is shown here.

A summary of the final tailpipe $BSNO_X$ emissions for the Tier 5 demonstration engine at end-of-life is given in Figure 171, compared to the Baseline Tier 4 Final engine levels (for a de-greened system). These levels represent reductions in tailpipe $NO_X$ on the order of 85% on the NRTC and 70% on the RMC, while the low load cycles are reduced by a factor of 100 to 150 on the LLAC, and nearly 500 on the LLC.

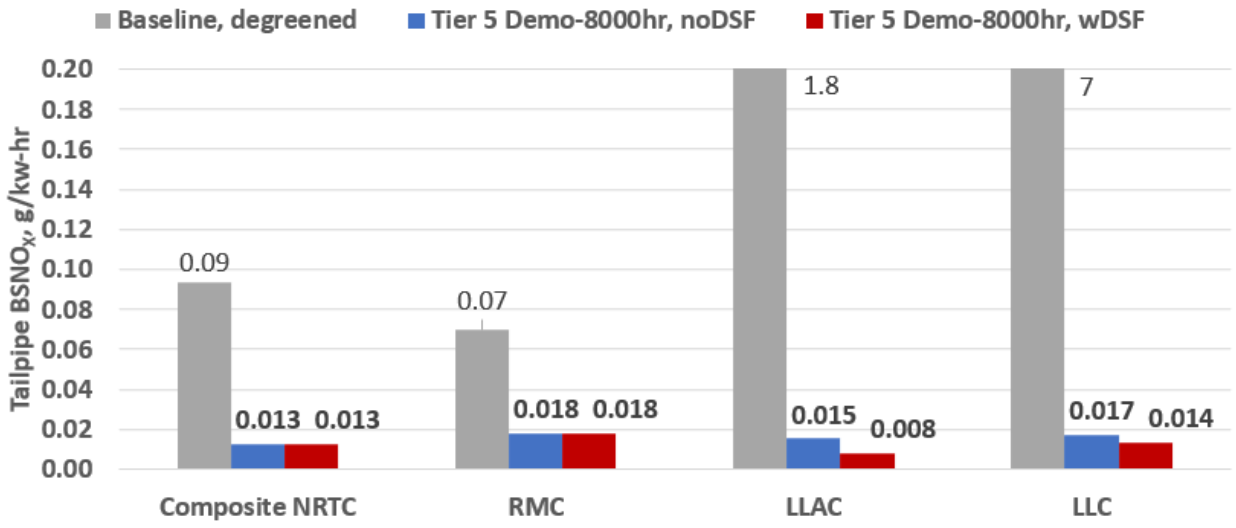



**FIGURE 171. SUMMARY OF TAILPIPE $BSNO_X$ FOR LOW $NO_X$ DEMONSTRATION COMPARED TO BASELINE – WITH AND WITHOUT DSF**

These results were all obtained with an aftertreatment architecture that was similar in concept to the previous on-highway Low $NO_X$ demonstration using a dual SCR, dual DEF dosing approach. However, that architecture was modified to be compatible with offroad duty cycles, and in particular to the challenging demands of packaging these systems in offroad machines. Although this system employs a LO-SCR catalyst, the packaging demands of the offroad market led to the choice of a multi-function catalyst (MFC), which is a LO-SCR that incorporates in-situ oxidation capacity. In this way the MFC can fill the role of both LO-SCR and DOC (partially) in the system. With the MFC up front, a zone-coated catalyzed soot filter (zCSF) helps filter the remainder of the DOC role and the DPF role. Because the MFC+zCSF can replace the DOC+DPF in a conventional architecture, the package size is similar. Another key piece of the architecture for reaching these levels was the adoption of a closed crankcase ventilation (CCV) system, a technology known from On Road and Marine applications.

The final demonstrated $NO_X$ emission levels for the Tier 5 Low $NO_X$ demonstration engine are given in Figure 172 for all the key program test cycles, both with and without the use of DSF. These compliance values are the 8000-hr DAAAC-aged emission results with UAF for infrequent regeneration added in. These are the values that would be compared to the standards, and the proposed Tier 5 standards for engines above 56kw are also shown in the table for reference. For all test cycles it is apparent that a margin of 50% or more is available to the proposed standard levels, with margins of at least 20 mg/kw-hr present on all cycles. The values shown are for a CCV system. If an open crankcase ventilation (OCV) system were used, the values would be 0.01 g/kw-hr higher. Adopting OCV would reduce margins to an uncomfortable degree, but there would still be a margin to any applicable standard in this case.

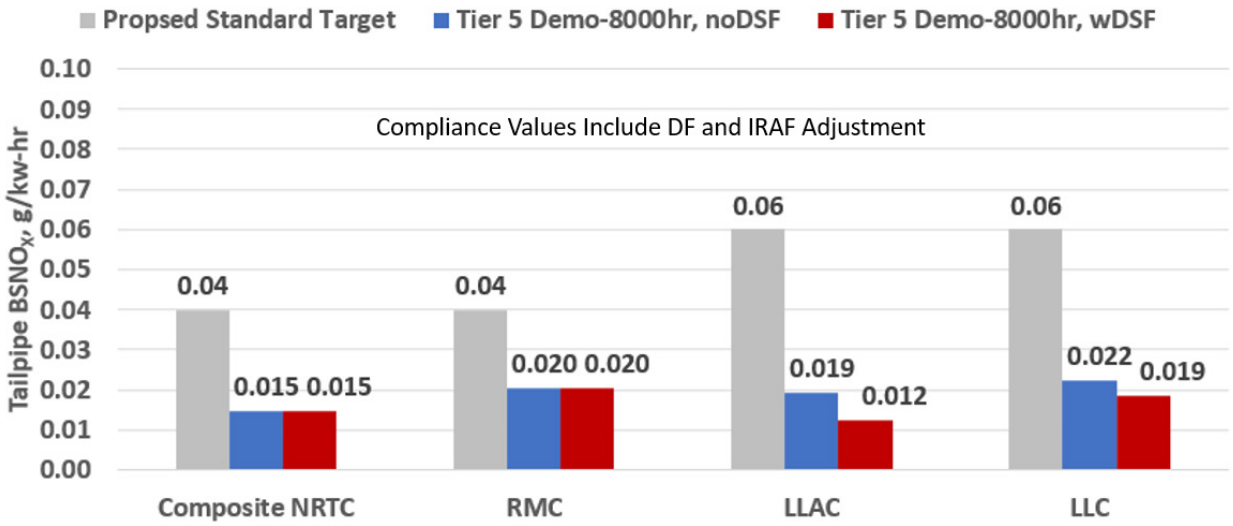



**FIGURE 172. TAILPIPE NOX COMPLIANCE VALUES FOR TIER 5 LOW $NO_X$ DEMONSTRATION ENGINE**

A summary of the key GHG emission impacts for this engine as compared to the Baseline is given in Figure 173 for $CO_2$, and in Figure 174 for $N_2O$. Methane levels are extremely low from this diesel engine, essentially negligible both with and without DSF, and therefore are not shown. For Package 2 the target was a reduction of between 5% and 8.6% from the Baseline, primarily on the NRTC but ideally on other cycles as well. The results indicated $CO_2$ reductions on the order of 6% on the NRTC with DSF adding about 1% to the $CO_2$ reduction. $CO_2$ reductions were smaller on the RMC, where the engine was limited in both airflow and peak cylinder pressure.

For the low load cycles, the LLAC and LLC, there was a significant difference between the DSF and non-DSF results, with the use of DSF contributing to 6 to 7% of additional $CO_2$ reduction over the non DSF case. $N_2O$ emissions for these same tests were at or below the Baseline engine level and were also well below the cap proposed by CARB of 0.15 g/kw-hr over the NRTC.

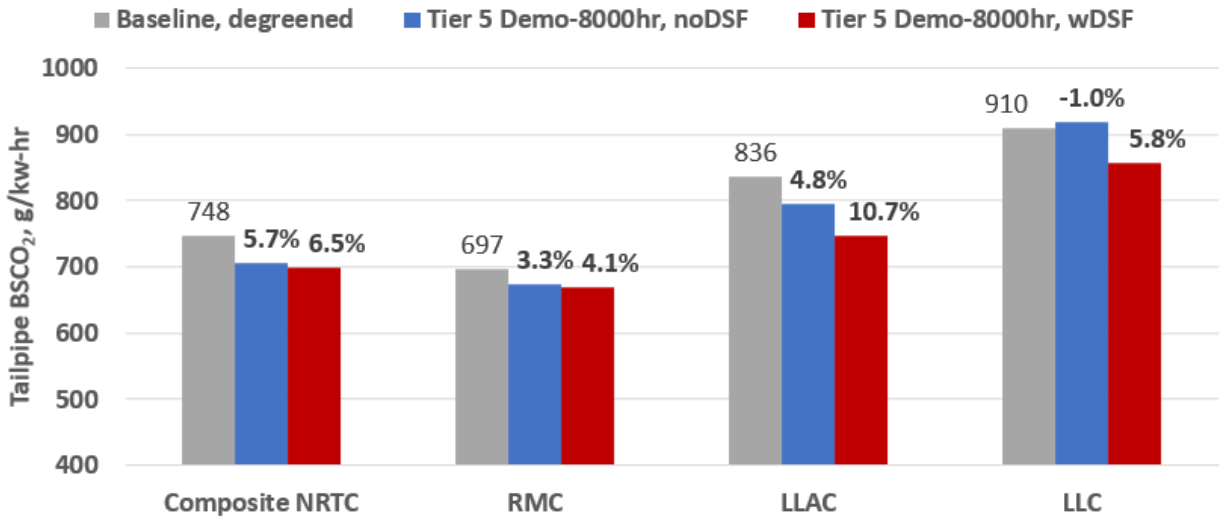



**FIGURE 173. SUMMARY OF TAILPIPE $BSCO_2$ FOR LOW $NO_X$ PACKAGES COMPARED TO BASELINE**

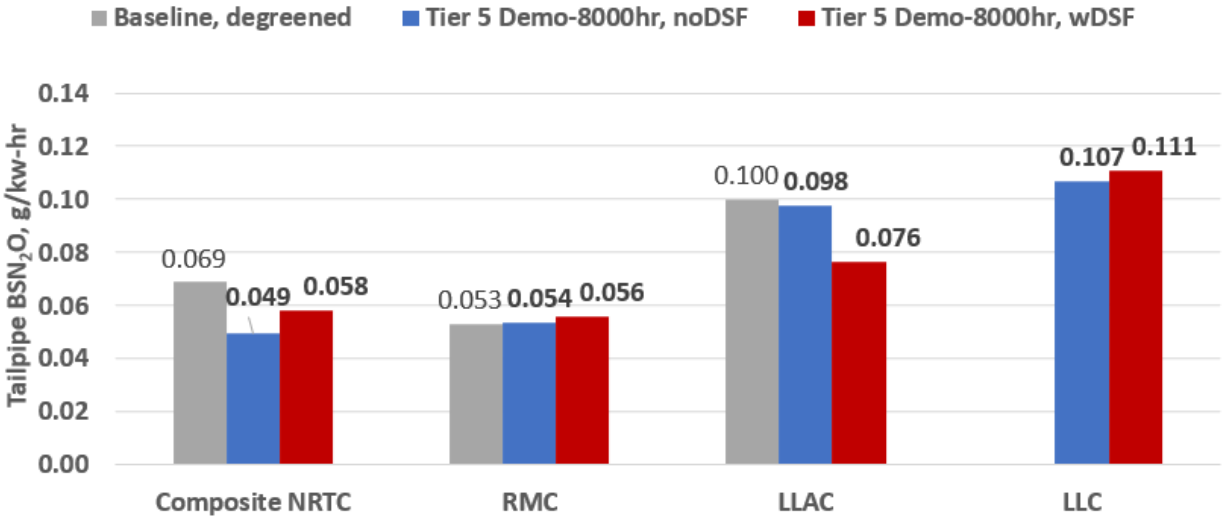



**FIGURE 174. SUMMARY OF TAILPIPE $BSN_2O$ FOR LOW $NO_X$ PACKAGES COMPARED TO BASELINE**

Given the wide range of power ratings available across many offroad engine families, it is important to be able to demonstrate a path to compliance for not only base or parent engine ratings, but also for the various child ratings that might be present in a given engine family. This was examined as part of the program by testing on a low power child rating of 126kw, well below the usual 187kw for this program. A summary of tailpipe $NO_X$ emissions for the base and child ratings is shown in Figure 175. For the NRTC and RMC, tailpipe emissions for the child rating show good NOx compliance potential, However, without DSF the low load cycles (LLAC and LLC) struggled to maintain compliance, showing significant tailpipe $NO_X$ increases. DSF proved to be

a useful technology lever when dealing with the low power child rating, restoring $NO_X$ levels observed under those incrementally more lightly loaded conditions back to expected levels of robust NOx control.

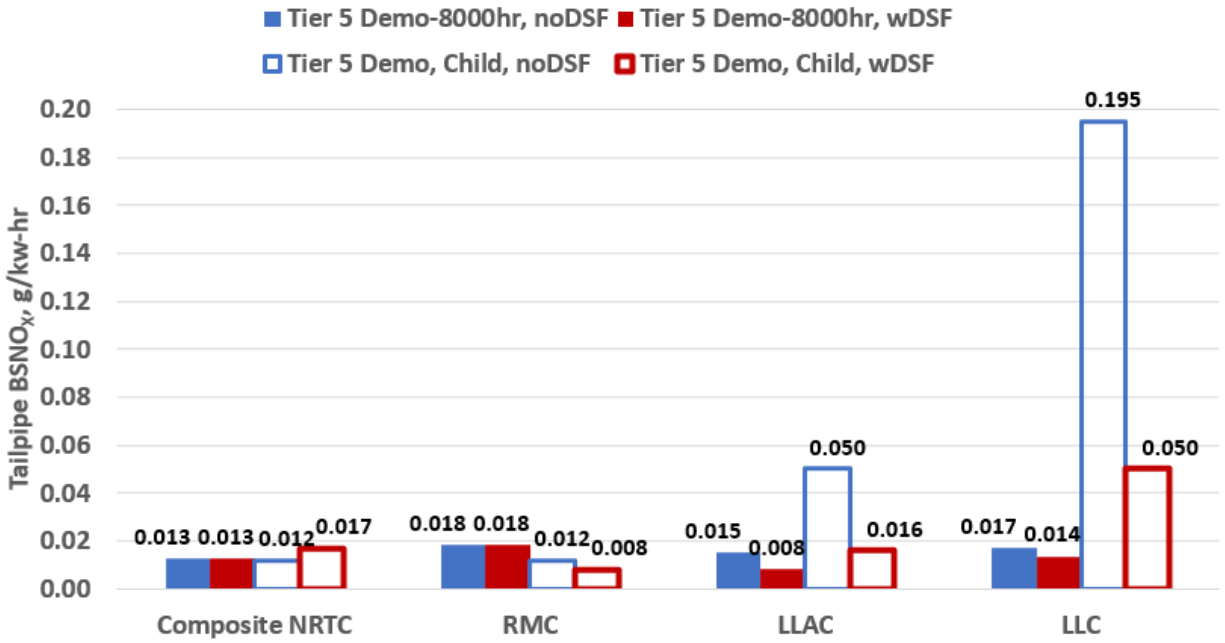



**FIGURE 175. TAILPIPE $NO_X$ EMISSIONS FOR BASE AND CHILD RATINGS – 8000-HR DATA WITH AND WITHOUT DSF**

## 5.2 Additional Discussion of Technology Considerations and Feasibility

The test results discussed above and the projected compliance margins for different technology packages are the primary component of assessing the feasibility of a given set of standards. The emission results document the potential performance of various technology options for meeting the emission targets outlined by possible future standards. However, performance and emissions performance durability are not the only considerations for determining the feasibility of various technologies.

The aftertreatment system packages that were evaluated and produced the results within this report generally consist of technology which is already in production. The basic architecture of the AT systems evaluated is still a conventional DOC+DPF+SCR+ASC arrangement, and conventional (unheated) DEF dosing was still utilized. The catalyst coating technology and formulations represent advancements from current Tier 4 production technology, but some of these formulations are already making their way into production in the on-highway market for the 2021 model year and beyond. In a similar fashion, all of the sensors used in the program are currently available production units.

The engine calibrations produced by SwRI on the base engine were evaluated leveraging help from the program's partner engine manufacturer to address any potential issues in production deployment. Additional performance checks, such as load response tests, were run according to proprietary methodology to document that the modified calibrations maintained acceptable engine performance.

Packaging of the aftertreatment is a significant issue in any market, but it is especially important in the offroad market due to the wide variety of applications that the system must fit into. SwRI worked with canners experienced in fabricating current production offroad aftertreatment systems in developing the technology packages that were examined. Although the systems are larger than current Tier 4 hardware it should be noted that the SCR hardware was only slightly larger at a 12-inch diameter compared to the stock system 11-inch diameter. Overall, the displacement of the SCR system was roughly 22 liters versus the stock system at a little under 20 liters, representing a 14% increase, which was felt to be manageable. The DOC+DPF part of the system was larger but was roughly the same length as the stock system although with a 2.5inch large diameter. Although single module design was used featuring an integrated compact mixer, designs were also available to split the system into two cans for packaging using a small, insulated u-pipe or elbow featuring the DEF doser and mixer. There will be challenges in packaging these larger components, but the overall increase in system size is considerably less than what was seen for the Stage 3 OH program.

The step of moving to a closed crankcase ventilation (CCV) system also requires some discussion with regard to feasibility. It should be noted that while CCV is often employed on smaller diesel engines in the OH market, there are durability risks of long-term turbocharger compressor and intake sensor fouling with adoption CCV. In addition, CCV is already in use on some mining and marine engines, so there is some production experience, albeit in limited application ranges. Improved filtration, including more efficient media, more frequent filter changes, and diagnostics would be required to support CCV adoption on most applications. It should be noted that some of these systems are already in production in other markets. The variation and complexity due to the Offroad market could make this adoption more of a challenge, but one that must be weighed against the difficulties of obtaining similar margin by other hardware means.

The use of cylinder deactivation (CDA) in the form of Dynamic Skip Fire (DSF) provided both $CO_2$ and $NO_X$ benefits, although the amount of benefit varied with duty cycle, as expected. Similar, though perhaps slightly smaller, benefits should be available with more traditional (map-based) CDA. As is the case in the on-highway market, CDA does come with vibration challenges that must be addressed though engineering. This can be done, but it should be noted that the offroad market contains a much wider variety of installation and mounting situations than what is seen for on-highway trucks. This variety means that many more iterations of mounting and machine vibration environments must be evaluated, increasing the complexity of deploying this technology across the full range of engines. This increased complexity could increase the cost associated with adopting the technology, which must be considered along with the fact that the fuel savings are somewhat smaller due to the higher load factor for most offroad applications. Fuel cost is also not as powerful a commercial driver in offroad markets as in on-highway market like Class 8 trucks, due to the smaller quantities of fuel that are burned. However, the trend of increasing diesel fuel costs seen in recent years may offer an additional incentive to off-road diesel engine manufacturers to duly consider this technology as customer demand for better fuel efficiency in the off-road grows.

It should be noted there are a number of other technology options for achieving the Package 2 goals of reducing $CO_2$ by 5% to 8.5%. Several of these options were evaluated for inclusion in this program and the continuing program efforts, but they were not included for reasons of scope and/or budget limitations. These includes options such as:

- Increasing compression ratio higher than the 17.6:1 of the stock engine. It should be noted that OH engines run 19:1 or more, although this requires engine re-design to support much higher peak cylinder pressures.
- Engine friction reduction
- Electrified accessories
- 48V options such as an EGR pump (which allows moving to a more efficient single stage fixed geometry turbocharger), or an e-turbo.

Many of these options have not yet seen as wide an adoption on offroad markets for a variety of reasons including emissions standards that could be easily met without resorting to them, the ease of continuing existing engine designs.

## 6.0 REFERENCES


1. Sharp, C., Webb, C., Neely, G., Carter, M. et al., "Achieving Ultra Low $NO_X$ Emissions Levels with a 2017 Heavy-Duty On-Highway TC Diesel Engine and an Advanced Technology Emissions System - Thermal Management Strategies," SAE Int. J. Engines 10(4):1697-1712, 2017.
2. Sharp, C., Webb, C., Yoon, S., Carter, M. et al., "Achieving Ultra Low $NO_X$ Emissions Levels with a 2017 Heavy-Duty On-Highway TC Diesel Engine - Comparison of Advanced Technology Approaches," SAE Int. J. Engines 10(4):1722-1735, 2017.
3. Sharp, C., Webb, C., Neely, G., Sarlashkar, J. et al., "Achieving Ultra Low $NO_X$ Emissions Levels with a 2017 Heavy-Duty On-Highway TC Diesel Engine and an Advanced Technology Emissions System - $NO_X$ Management Strategies," SAE Int. J. Engines 10(4):1736-1748, 2017U.S. Department of Transportation, "Summary of Fuel Economy Performance," NHTSA, NVS-220, Apr. 28, 2011.
4. Stage 1 Final Report: Evaluating Technologies and Methods to Lower Nitrogen Oxide Emissions from Heavy-Duty Vehicles, CARB Agreement 13-312, April 2017, https://ww2.arb.ca.gov/sites/default/files/classic//research/apr/past/13-312.pdf.
5. Stage 2 Final Report: Heavy-Duty Engine Low-load Emission Control Calibration, Low-load Test Cycle Development, and Evaluation of Engine Broadcast Torque and Fueling Accuracy during Low-load Operation, CARB Contract 15MSC010, December, 2019, https://www.arb.ca.gov/lists/com-attach/1-hdomnibus2020-VDdXMFIhU2IAWQIw.pdf.
6. Stage 3 Final Report: Further Development and Validation of Technologies to Lower Oxides of Nitrogen Emissions from Heavy Duty Vehicles, CARB Contract 16MSC010, January, 2021, https://www.arb.ca.gov/lists/com-attach/79-hdomnibus2020-Uj4AaQB2Aj8FbAhw.pdf.
7. Off-Road Diesel Low-Emission Demo for Nitrogen Oxides ($NO_x$), Particulate Matter (PM) - Off-Road Low $NO_X$ Demonstration Stage 1, and Toxics, CARB Contract 18RD006, April 2021, https://ww2.arb.ca.gov/sites/default/files/2022-03/18RD006.pdf.
8. Next Tier Off-Road Diesel Aftertreatment Technology Fabrication and Optimization – Off-Road Low $NO_X$ Demonstration Stage 2, CARB Contract 19RD025, December 2022.
9. CARB Tier 5 Off-Road Meetings and Workshops, October 30 and 31, 2023, https://ww2.arb.ca.gov/our-work/programs/tier-5/meetings-workshops
10. Eakle, S., Zavala, B., and Sharp, C., "The DAAAC Protocol: A Procedure for Developing Accelerated Aging Cycles for Diesel Aftertreatment," 2022-01–1017, 2022, doi:10.4271/2022-01-1017.
11. Zavala, B., Vats, S., and Eakle, S., "The Diesel Aftertreatment Accelerated Aging Cycle Protocol: An Advanced Aftertreatment Case Study," SAE Technical Paper 2020-01-2210, 2020, https://doi.org/10.4271/2020-01-2210.
12. Gordon, B. 12th CLEERS Workshop. The DAAAC Protocol for Accelerated Aging of Diesel Aftertreatment Systems. Dearborn. 2012.
13. Webb, C.C., "Nonroad Data Analysis and Composite Cycle Development," Final Report prepared for the Environmental Protection Agency, September 1997.

# APPENDIX A - EMISSION DATA SUMMARIES FOR ALL TEST POINTS

## TABLE A-1. DETAILED TAILPIPE EMISSIONS FOR 0-HOUR TESTING WITHOUT

| | | NRTC | | | | | | | LLAC | RMC |
|---|---|---|---|---|---|---|---|---|---|---|
| | | Cold | Hot 1 | Hot 2 | Hot 3 | Composite | Hot-Avg | Hot-SD | | |
| | | Set 1 | | | | | | | | |
| Run No | | 7748 | 7749 | 7750 | 7751 | n/a | | | 7752 | 7729 |
| THC | g/kw-hr | 0.008 | 0.000 | 0.000 | 0.000 | 0.000 | 0.000 | 0.000 | 0.000 | 0.007 |
| NMHC | g/kw-hr | 0.008 | 0.000 | 0.000 | 0.000 | 0.000 | 0.000 | 0.000 | 0.000 | 0.006 |
| CO | g/kw-hr | 0.262 | 0.027 | 0.026 | 0.024 | 0.039 | 0.026 | 0.002 | 0.062 | 0.014 |
| NOx | g/kw-hr | 0.092 | 0.004 | 0.003 | 0.002 | 0.008 | 0.003 | 0.001 | 0.015 | 0.005 |
| PM | g/kw-hr | 0.0008 | 0.0006 | 0.0005 | 0.0004 | 0.0006 | 0.0005 | 0.0001 | 0.0003 | 0.0002 |
| CO2 | g/kw-hr | 738.1 | 710.1 | 708.0 | 706.7 | 711.5 | 708.3 | 1.72 | 806.7 | 660.4 |
| Work | g/kw-hr | 24.03 | 23.96 | 23.92 | 23.89 | 23.96 | 23.92 | 0.033 | 34.87 | 51.81 |
| N2O | g/kw-hr | 0.032 | 0.038 | 0.038 | 0.038 | 0.038 | 0.038 | 0.000 | 0.159 | 0.027 |
| | Set 2 | | | | | | | | | |
| Run No | | 7759 | 7760 | 7761 | 7762 | n/a | | | 7763 | 7765 |
| THC | g/kw-hr | 0.012 | 0.000 | 0.000 | 0.000 | 0.001 | 0.000 | 0.000 | 0.000 | 0.000 |
| NMHC | g/kw-hr | 0.012 | 0.000 | 0.000 | 0.000 | 0.001 | 0.000 | 0.000 | 0.000 | 0.000 |
| CO | g/kw-hr | 0.284 | 0.011 | 0.026 | 0.025 | 0.025 | 0.021 | 0.008 | 0.061 | 0.016 |
| NOx | g/kw-hr | 0.101 | 0.002 | 0.003 | 0.002 | 0.007 | 0.003 | 0.001 | 0.012 | 0.002 |
| PM | g/kw-hr | 0.0004 | 0.0006 | 0.0005 | 0.0007 | 0.0006 | 0.0006 | 0.0001 | 0.0002 | 0.0003 |
| CO2 | g/kw-hr | 734.1 | 706.9 | 707.5 | 705.6 | 708.2 | 706.7 | 0.93 | 806.6 | 659.8 |
| Work | g/kw-hr | 24.02 | 23.97 | 23.93 | 23.92 | 23.97 | 23.94 | 0.026 | 34.87 | 51.84 |
| N2O | g/kw-hr | 0.042 | 0.052 | 0.050 | 0.049 | 0.052 | 0.050 | 0.002 | 0.150 | 0.027 |
| | Set 3 | | | | | | | | | |
| Run No | | 7768 | 7769 | 7770 | 7771 | n/a | | | 7772 | 7773 |
| THC | g/kw-hr | 0.010 | 0.000 | 0.000 | 0.000 | 0.001 | 0.000 | 0.000 | 0.002 | 0.000 |
| NMHC | g/kw-hr | 0.010 | 0.000 | 0.000 | 0.000 | 0.001 | 0.000 | 0.000 | 0.002 | 0.000 |
| CO | g/kw-hr | 0.274 | -0.037 | 0.022 | 0.024 | -0.021 | 0.003 | 0.035 | 0.060 | 0.019 |
| NOx | g/kw-hr | 0.106 | 0.004 | 0.003 | 0.001 | 0.009 | 0.002 | 0.001 | 0.021 | 0.003 |
| PM | g/kw-hr | 0.0002 | 0.0005 | 0.0002 | 0.0002 | 0.0005 | 0.0003 | 0.0002 | 0.0001 | 0.0010 |
| CO2 | g/kw-hr | 731.4 | 700.1 | 701.2 | 699.3 | 701.7 | 700.2 | 0.93 | 803.5 | 660.4 |
| Work | g/kw-hr | 24.00 | 23.96 | 23.94 | 23.91 | 23.96 | 23.94 | 0.022 | 34.88 | 51.84 |
| N2O | g/kw-hr | -0.003 | 0.000 | 0.000 | 0.000 | 0.000 | 0.000 | 0.000 | 0.000 | 0.000 |

## TABLE A-2. DETAILED ENGINE-OUT EMISSIONS FOR 0-HOUR TESTING WITHOUT DSF

| | | NRTC | | | | | | | | |
|---|---|---|---|---|---|---|---|---|---|---|
| | | Cold | Hot 1 | Hot 2 | Hot 3 | Composite | Hot-Avg | Hot-SD | LLAC | RMC |
| | Set 1 | | | | | | | | | |
| Run No | | 7748 | 7749 | 7750 | 7751 | n/a | | | 7752 | 7729 |
| THC | g/kw-hr | 0.17 | 0.06 | 0.08 | 0.08 | 0.07 | 0.08 | 0.01 | 0.37 | 0.06 |
| NMHC | g/kw-hr | 0.17 | 0.08 | 0.06 | 0.08 | 0.09 | 0.08 | 0.01 | 0.36 | 0.06 |
| CO | g/kw-hr | 1.40 | 1.30 | 1.36 | 1.34 | 1.31 | 1.33 | 0.03 | 1.55 | 0.30 |
| NOx | g/kw-hr | 3.66 | 4.06 | 4.03 | 4.05 | 4.04 | 4.04 | 0.01 | 5.03 | 4.36 |
| CO2 | g/kw-hr | 750.4 | 720.2 | 720.8 | 718.8 | 721.7 | 720.0 | 1.0 | 812.4 | 680.2 |
| | Set 2 | | | | | | | | | |
| Run No | | 7759 | 7760 | 7761 | 7762 | n/a | | | 7763 | 7765 |
| THC | g/kw-hr | 0.00 | 0.00 | 0.00 | 0.00 | 0.00 | 0.00 | 0.00 | 0.00 | 0.06 |
| NMHC | g/kw-hr | 0.18 | 0.08 | 0.06 | 0.08 | 0.00 | 0.07 | 0.01 | 0.00 | 0.06 |
| CO | g/kw-hr | 1.36 | 1.31 | 1.30 | 1.32 | 0.00 | 1.31 | 0.01 | 0.00 | 0.32 |
| NOx | g/kw-hr | 3.65 | 4.02 | 4.03 | 4.03 | 0.00 | 4.02 | 0.01 | 0.00 | 4.29 |
| CO2 | g/kw-hr | 742.3 | 714.8 | 716.7 | 715.0 | 716.2 | 715.5 | 1.0 | 806.6 | 677.6 |
| | Set 3 | | | | | | | | | |
| Run No | | 7768 | 7769 | 7770 | 7771 | n/a | | | 7772 | 7773 |
| THC | g/kw-hr | 0.00 | 0.00 | 0.00 | 0.00 | 0.00 | 0.00 | 0.00 | 0.00 | 0.06 |
| NMHC | g/kw-hr | 0.18 | 0.08 | 0.06 | 0.07 | 0.00 | 0.07 | 0.01 | 0.00 | 0.06 |
| CO | g/kw-hr | 1.31 | 1.25 | 1.29 | 1.27 | 0.00 | 1.27 | 0.02 | 0.00 | 0.32 |
| NOx | g/kw-hr | 3.67 | 4.04 | 4.05 | 4.05 | 0.00 | 4.05 | 0.01 | 0.00 | 4.34 |
| CO2 | g/kw-hr | 740.5 | 710.4 | 709.7 | 709.0 | 711.9 | 709.7 | 0.7 | 803.0 | 676.1 |

## TABLE A-3. DETAILED TAILPIPE EMISSOINS FOR 0-HOUR TESTING WITH DSF

| | | NRTC | | | | | | | | |
|---|---|---|---|---|---|---|---|---|---|---|
| | | Cold | Hot 1 | Hot 2 | Hot 3 | Composite | Hot-Avg | Hot-SD | LLAC | RMC |
| | | Set 1 | | | | | | | | |
| Run No | | 7703 | 7704 | 7705 | 7706 | n/a | | | 7707 | 7710 |
| THC | g/kw-hr | 0.013 | 0.018 | 0.046 | 0.024 | 0.018 | 0.029 | 0.014 | 0.021 | 0.000 |
| NMHC | g/kw-hr | 0.013 | 0.018 | 0.045 | 0.023 | 0.018 | 0.029 | 0.014 | 0.021 | 0.000 |
| CO | g/kw-hr | 0.313 | 0.015 | 0.013 | 0.014 | 0.030 | 0.014 | 0.001 | 0.111 | 0.016 |
| NOx | g/kw-hr | 0.102 | 0.003 | 0.002 | 0.002 | 0.008 | 0.003 | 0.000 | 0.008 | 0.003 |
| PM | g/kw-hr | 0.0002 | 0.0009 | 0.0008 | 0.0005 | 0.0009 | 0.0007 | 0.0002 | 0.0001 | 0.0004 |
| CO2 | g/kw-hr | 725.7 | 698.8 | 698.5 | 696.0 | 700.1 | 697.8 | 1.54 | 756.1 | 651.6 |
| Work | g/kw-hr | 23.90 | 23.93 | 23.88 | 23.86 | 23.92 | 23.89 | 0.035 | 34.77 | 51.82 |
| N2O | g/kw-hr | 0.034 | 0.043 | 0.048 | 0.048 | 0.043 | 0.046 | 0.003 | 0.071 | 0.023 |
| | Set 2 | | | | | | | | | |
| Run No | | 7732 | 7733 | 7734 | 7735 | n/a | | | 7719 | 7738 |
| THC | g/kw-hr | 0.010 | 0.000 | 0.000 | 0.000 | 0.000 | 0.000 | 0.000 | 0.000 | 0.000 |
| NMHC | g/kw-hr | 0.010 | 0.000 | 0.000 | 0.000 | 0.000 | 0.000 | 0.000 | 0.000 | 0.000 |
| CO | g/kw-hr | 0.308 | 0.029 | 0.027 | 0.018 | 0.043 | 0.025 | 0.006 | 0.134 | 0.017 |
| NOx | g/kw-hr | 0.115 | 0.007 | 0.001 | 0.003 | 0.012 | 0.003 | 0.003 | -0.006 | 0.005 |
| PM | g/kw-hr | 0.0007 | 0.0011 | 0.0012 | 0.0010 | 0.0011 | 0.0011 | 0.0001 | 0.0003 | 0.0005 |
| CO2 | g/kw-hr | 726.7 | 702.3 | 700.4 | 701.5 | 703.5 | 701.4 | 0.95 | 761.8 | 652.3 |
| Work | g/kw-hr | 23.99 | 23.92 | 23.89 | 23.87 | 23.92 | 23.89 | 0.026 | 34.76 | 51.83 |
| N2O | g/kw-hr | 0.034 | 0.043 | 0.042 | 0.044 | 0.043 | 0.043 | 0.001 | 0.052 | 0.026 |
| | Set 3 | | | | | | | | | |
| Run No | | 7776 | 7777 | 7778 | 7779 | n/a | | | 7780 | 7782 |
| THC | g/kw-hr | 0.012 | 0.000 | 0.000 | 0.000 | 0.001 | 0.000 | 0.000 | 0.000 | 0.000 |
| NMHC | g/kw-hr | 0.012 | 0.000 | 0.000 | 0.000 | 0.001 | 0.000 | 0.000 | 0.000 | 0.000 |
| CO | g/kw-hr | 0.292 | 0.025 | 0.028 | 0.028 | 0.039 | 0.027 | 0.001 | 0.104 | 0.017 |
| NOx | g/kw-hr | 0.092 | 0.003 | 0.002 | 0.003 | 0.007 | 0.002 | 0.000 | 0.007 | 0.009 |
| PM | g/kw-hr | 0.0003 | 0.0006 | 0.0006 | 0.0009 | 0.0006 | 0.0007 | 0.0002 | 0.0002 | 0.0001 |
| CO2 | g/kw-hr | 727.7 | 701.4 | 702.2 | 699.5 | 702.7 | 701.0 | 1.36 | 761.6 | 653.2 |
| Work | g/kw-hr | 24.02 | 23.96 | 23.93 | 23.91 | 23.96 | 23.93 | 0.025 | 34.78 | 51.87 |
| N2O | g/kw-hr | 0.066 | 0.079 | 0.077 | 0.069 | 0.078 | 0.075 | 0.005 | 0.102 | 0.032 |

## TABLE A-4. DETAILED ENGINE-OUT EMISSIONS FOR 0-HOUR TESTING WITH DSF

| | | NRTC | | | | | | | | |
|---|---|---|---|---|---|---|---|---|---|---|
| | | Cold | Hot 1 | Hot 2 | Hot 3 | Composite | Hot-Avg | Hot-SD | LLAC | RMC |
| | | Set 1 | | | | | | | | |
| Run No | | 7703 | 7704 | 7705 | 7706 | n/a | | | 7707 | 7710 |
| THC | g/kw-hr | 0.15 | 0.05 | 0.06 | 0.06 | 0.05 | 0.06 | 0.01 | 0.10 | 0.05 |
| NMHC | g/kw-hr | 0.14 | 0.06 | 0.05 | 0.06 | 0.07 | 0.06 | 0.01 | 0.09 | 0.05 |
| CO | g/kw-hr | 1.91 | 1.95 | 2.01 | 2.01 | 1.95 | 1.99 | 0.04 | 1.40 | 0.28 |
| NOx | g/kw-hr | 3.77 | 4.31 | 4.31 | 4.31 | 4.28 | 4.31 | 0.00 | 5.84 | 4.19 |
| CO2 | g/kw-hr | 737.5 | 708.9 | 707.7 | 707.5 | 710.4 | 708.1 | 0.8 | 767.5 | 671.0 |
| | | Set 2 | | | | | | | | |
| Run No | | 7732 | 7733 | 7734 | 7735 | n/a | | | 7719 | 7738 |
| THC | g/kw-hr | 0.00 | 0.00 | 0.00 | 0.00 | 0.00 | 0.00 | 0.00 | 0.00 | 0.06 |
| NMHC | g/kw-hr | 0.15 | 0.07 | 0.05 | 0.07 | 0.00 | 0.06 | 0.01 | 0.00 | 0.06 |
| CO | g/kw-hr | 1.48 | 1.53 | 1.54 | 1.53 | 0.00 | 1.53 | 0.01 | 0.00 | 0.27 |
| NOx | g/kw-hr | 3.83 | 4.34 | 4.35 | 4.35 | 0.00 | 4.35 | 0.00 | 0.00 | 4.27 |
| CO2 | g/kw-hr | 725.1 | 700.4 | 701.2 | 698.2 | 701.7 | 700.0 | 1.6 | 768.9 | 672.2 |
| | | Set 3 | | | | | | | | |
| Run No | | 7776 | 7777 | 7778 | 7779 | n/a | | | 7780 | 7782 |
| THC | g/kw-hr | 0.00 | 0.00 | 0.00 | 0.00 | 0.00 | 0.00 | 0.00 | 0.00 | 0.06 |
| NMHC | g/kw-hr | 0.16 | 0.08 | 0.06 | 0.07 | 0.00 | 0.07 | 0.01 | 0.00 | 0.06 |
| CO | g/kw-hr | 1.66 | 1.55 | 1.67 | 1.60 | 0.00 | 1.61 | 0.06 | 0.00 | 0.28 |
| NOx | g/kw-hr | 3.77 | 4.28 | 4.27 | 4.29 | 0.00 | 4.28 | 0.01 | 0.00 | 4.16 |
| CO2 | g/kw-hr | 724.3 | 697.3 | 697.5 | 696.0 | 698.7 | 697.0 | 0.8 | 763.6 | 670.0 |

## TABLE A-5. DETAILED TAILPIPE EMISSIONS FOR 8000-HR TESTING WITHOUT DSF

| | | NRTC | | | | | | | | | |
|---|---|---|---|---|---|---|---|---|---|---|---|
| | | Cold | Hot 1 | Hot 2 | Hot 3 | Composite | Hot-Avg | Hot-SD | LLAC | RMC | LLC |
| | | Set 1 | | | | | | | | | |
| Run No | | 8052 | 8053 | 8054 | 8055 | n/a | | | 8056 | 8057 | 8049 |
| THC | g/kw-hr | 0.014 | 0.000 | 0.000 | 0.001 | 0.001 | 0.000 | 0.001 | 0.009 | 0.000 | 0.000 |
| NMHC | g/kw-hr | 0.014 | 0.000 | 0.000 | 0.001 | 0.001 | 0.000 | 0.001 | 0.009 | 0.000 | 0.000 |
| CO | g/kw-hr | 0.361 | 0.105 | 0.132 | 0.119 | 0.117 | 0.118 | 0.014 | 0.082 | 0.015 | 0.058 |
| NOx | g/kw-hr | 0.132 | 0.006 | 0.013 | 0.010 | 0.013 | 0.010 | 0.003 | 0.019 | 0.019 | 0.020 |
| PM | g/kw-hr | 0.0011 | 0.0004 | 0.0003 | 0.0002 | 0.0004 | 0.0003 | 0.0001 | 0.0001 | 0.0002 | 0.0005 |
| CO2 | g/kw-hr | 730.9 | 701.5 | 699.8 | 698.5 | 702.9 | 699.9 | 1.51 | 807.4 | 657.6 | 913.3 |
| Work | g/kw-hr | 24.11 | 24.00 | 24.02 | 23.98 | 24.01 | 24.00 | 0.021 | 34.84 | 51.83 | 20.21 |
| N2O | g/kw-hr | 0.042 | 0.049 | 0.053 | 0.054 | 0.049 | 0.052 | 0.003 | 0.096 | 0.054 | 0.113 |
| | Set 2 | | | | | | | | | | |
| Run No | | 8073 | 8074 | 8075 | 8076 | n/a | | | 8077 | 8099 | 8103 |
| THC | g/kw-hr | 0.001 | 0.000 | 0.000 | 0.000 | 0.000 | 0.000 | 0.000 | 0.003 | 0.000 | 0.000 |
| NMHC | g/kw-hr | 0.001 | 0.000 | 0.000 | 0.000 | 0.000 | 0.000 | 0.000 | 0.003 | 0.000 | 0.000 |
| CO | g/kw-hr | 0.340 | 0.101 | 0.108 | 0.102 | 0.112 | 0.104 | 0.004 | 0.078 | 0.015 | 0.086 |
| NOx | g/kw-hr | 0.108 | 0.006 | 0.006 | 0.005 | 0.011 | 0.006 | 0.001 | 0.014 | 0.017 | 0.021 |
| PM | g/kw-hr | 0.0005 | 0.0007 | 0.0003 | 0.0002 | 0.0007 | 0.0004 | 0.0003 | 0.0001 | 0.0002 | 0.0003 |
| CO2 | g/kw-hr | 729.6 | 706.7 | 707.2 | 707.1 | 707.8 | 707.0 | 0.27 | 816.8 | 664.7 | 933.9 |
| Work | g/kw-hr | 24.05 | 24.02 | 24.03 | 24.02 | 24.02 | 24.02 | 0.004 | 34.84 | 51.84 | 19.95 |
| N2O | g/kw-hr | 0.041 | 0.048 | 0.052 | 0.052 | 0.048 | 0.051 | 0.002 | 0.081 | 0.054 | 0.189 |
| | Set 3 | | | | | | | | | | |
| Run No | | 8093 | 8094 | 8096 | 8097 | n/a | | | 8098 | 8141 | 8161 |
| THC | g/kw-hr | 0.010 | 0.000 | 0.000 | 0.000 | 0.001 | 0.000 | 0.000 | 0.007 | 0.000 | 0.005 |
| NMHC | g/kw-hr | 0.010 | 0.000 | 0.000 | 0.000 | 0.001 | 0.000 | 0.000 | 0.007 | 0.000 | 0.000 |
| CO | g/kw-hr | 0.353 | 0.098 | 0.107 | 0.108 | 0.111 | 0.104 | 0.006 | 0.091 | 0.013 | 0.059 |
| NOx | g/kw-hr | 0.121 | 0.009 | 0.008 | 0.006 | 0.015 | 0.008 | 0.002 | 0.013 | 0.022 | 0.012 |
| PM | g/kw-hr | 0.0004 | 0.0004 | 0.0005 | 0.0003 | 0.0004 | 0.0004 | 0.0001 | 0.0001 | 0.0002 | 0.0001 |
| CO2 | g/kw-hr | 742.3 | 706.7 | 707.1 | 707.0 | 708.5 | 706.9 | 0.24 | 818.0 | 658.0 | 917.6 |
| Work | g/kw-hr | 24.11 | 24.03 | 24.01 | 24.01 | 24.03 | 24.01 | 0.011 | 34.82 | 51.86 | 19.94 |
| N2O | g/kw-hr | 0.042 | 0.052 | 0.054 | 0.055 | 0.052 | 0.054 | 0.002 | 0.116 | 0.051 | 0.101 |

## TABLE A-6. DETAILED ENGINE-OUT EMISSIONS FOR 8000-HR TESTING WITHOUT DSF

| | | NRTC | | | | | | | | | |
|---|---|---|---|---|---|---|---|---|---|---|---|
| | | Cold | Hot 1 | Hot 2 | Hot 3 | Composite | Hot-Avg | Hot-SD | LLAC | RMC | LLC |
| | Set 1 | | | | | | | | | | |
| Run No | | 8052 | 8053 | 8054 | 8055 | n/a | | | 8056 | 8057 | 8049 |
| THC | g/kw-hr | 0.18 | 0.06 | 0.08 | 0.08 | 0.06 | 0.07 | 0.01 | 0.33 | 0.06 | 0.54 |
| NMHC | g/kw-hr | 0.17 | 0.08 | 0.06 | 0.08 | 0.08 | 0.07 | 0.01 | 0.33 | 0.06 | 0.53 |
| CO | g/kw-hr | 1.26 | 1.14 | 1.15 | 1.18 | 1.15 | 1.16 | 0.02 | 1.52 | 0.32 | 2.06 |
| NOx | g/kw-hr | 3.60 | 4.03 | 3.99 | 4.00 | 4.00 | 4.00 | 0.02 | 4.58 | 4.37 | 4.84 |
| CO2 | g/kw-hr | 744.0 | 714.4 | 710.7 | 711.7 | 715.9 | 712.2 | 1.9 | 809.8 | 679.0 | 915.1 |
| | Set 2 | | | | | | | | | | |
| Run No | | 8073 | 8074 | 8075 | 8076 | n/a | | | 8077 | 8099 | 8103 |
| THC | g/kw-hr | 0.00 | 0.00 | 0.00 | 0.00 | 0.00 | 0.00 | 0.00 | 0.00 | 0.05 | 0.00 |
| NMHC | g/kw-hr | 0.15 | 0.07 | 0.05 | 0.07 | 0.00 | 0.07 | 0.01 | 0.00 | 0.05 | 0.00 |
| CO | g/kw-hr | 1.26 | 1.15 | 1.17 | 1.16 | 0.00 | 1.16 | 0.01 | 0.00 | 0.30 | 0.00 |
| NOx | g/kw-hr | 3.70 | 4.11 | 4.13 | 4.11 | 0.00 | 4.12 | 0.01 | 0.00 | 4.38 | 0.00 |
| CO2 | g/kw-hr | 747.5 | 719.8 | 719.6 | 719.5 | 721.2 | 719.6 | 0.2 | 824.1 | 685.7 | 936.2 |
| | Set 3 | | | | | | | | | | |
| Run No | | 8093 | 8094 | 8096 | 8097 | n/a | | | 8098 | 8141 | 8161 |
| THC | g/kw-hr | 0.00 | 0.00 | 0.00 | 0.00 | 0.00 | 0.00 | 0.00 | 0.00 | 0.06 | 0.00 |
| NMHC | g/kw-hr | 0.17 | 0.08 | 0.06 | 0.08 | 0.00 | 0.07 | 0.01 | 0.00 | 0.06 | 0.00 |
| CO | g/kw-hr | 1.25 | 1.14 | 1.17 | 1.15 | 0.00 | 1.15 | 0.01 | 0.00 | 0.33 | 0.00 |
| NOx | g/kw-hr | 3.40 | 4.08 | 4.08 | 4.10 | 0.00 | 4.09 | 0.01 | 0.00 | 4.33 | 0.00 |
| CO2 | g/kw-hr | 755.1 | 717.5 | 718.3 | 719.3 | 719.4 | 718.4 | 0.9 | 820.5 | 676.3 | 912.1 |
| MSS PM | g/kw-hr | 0.105 | 0.079 | 0.083 | 0.078 | 0.013 | 0.080 | 0.003 | 0.084 | 0.016 | 0.128 |

## TABLE A-7. DETAILED TAILPIPE EMISSIONS FOR 8000-HOUR TESTING WITH DSF

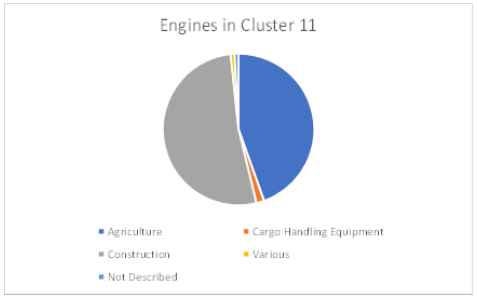
| | | NRTC | | | | | | | | | |
|---|---|---|---|---|---|---|---|---|---|---|---|
| | | Cold | Hot 1 | Hot 2 | Hot 3 | Composite | Hot-Avg | Hot-SD | LLAC | RMC | LLC |
| | Set 1 | | | | | | | | | | |
| Run No | | 8022 | 8023 | 8024 | 8025 | n/a | | | 8026 | 8029 | 8060 |
| THC | g/kw-hr | 0.019 | 0.000 | 0.000 | 0.000 | 0.001 | 0.000 | 0.000 | 0.008 | 0.000 | 0.000 |
| NMHC | g/kw-hr | 0.018 | 0.000 | 0.000 | 0.000 | 0.001 | 0.000 | 0.000 | 0.006 | 0.000 | 0.000 |
| CO | g/kw-hr | 0.342 | 0.059 | 0.060 | 0.058 | 0.073 | 0.059 | 0.001 | 0.090 | 0.015 | 0.075 |
| NOx | g/kw-hr | 0.131 | 0.007 | 0.008 | 0.004 | 0.013 | 0.006 | 0.002 | 0.007 | 0.017 | 0.009 |
| PM | g/kw-hr | 0.0008 | 0.0003 | 0.0007 | 0.0004 | 0.0003 | 0.0005 | 0.0002 | 0.0001 | 0.0001 | 0.0002 |
| CO2 | g/kw-hr | 720.3 | 691.4 | 690.2 | 689.4 | 692.8 | 690.3 | 1.01 | 751.8 | 650.4 | 814.1 |
| Work | g/kw-hr | 23.99 | 23.96 | 23.85 | 23.86 | 23.96 | 23.89 | 0.060 | 34.74 | 51.58 | 19.92 |
| N2O | g/kw-hr | 0.050 | 0.057 | 0.061 | 0.061 | 0.057 | 0.060 | 0.002 | 0.094 | 0.049 | 0.076 |
| | Set 2 | | | | | | | | | | |
| Run No | | 8063 | 8064 | 8065 | 8066 | n/a | | | 8067 | 8068 | 8114 |
| THC | g/kw-hr | 0.009 | 0.000 | 0.000 | 0.000 | 0.000 | 0.000 | 0.000 | 0.000 | 0.000 | 0.000 |
| NMHC | g/kw-hr | 0.008 | 0.000 | 0.000 | 0.000 | 0.000 | 0.000 | 0.000 | 0.000 | 0.000 | 0.000 |
| CO | g/kw-hr | 0.335 | 0.071 | 0.072 | 0.060 | 0.084 | 0.068 | 0.006 | 0.103 | 0.015 | 0.084 |
| NOx | g/kw-hr | 0.119 | 0.007 | 0.005 | 0.005 | 0.012 | 0.005 | 0.001 | 0.008 | 0.023 | 0.013 |
| PM | g/kw-hr | 0.0001 | 0.0003 | 0.0007 | 0.0004 | 0.0003 | 0.0005 | 0.0002 | 0.0001 | 0.0001 | 0.0001 |
| CO2 | g/kw-hr | 742.0 | 700.7 | 699.5 | 698.0 | 702.8 | 699.4 | 1.34 | 765.4 | 656.9 | 841.4 |
| Work | g/kw-hr | 23.85 | 23.95 | 23.91 | 23.90 | 23.94 | 23.92 | 0.027 | 34.72 | 51.85 | 19.82 |
| N2O | g/kw-hr | 0.038 | 0.057 | 0.061 | 0.061 | 0.056 | 0.060 | 0.002 | 0.067 | 0.053 | 0.146 |
| | Set 3 | | | | | | | | | | |
| Run No | | 8083 | 8085 | 8086 | 8087 | n/a | | | 8088 | 8111 | 8158 |
| THC | g/kw-hr | 0.019 | 0.000 | 0.001 | 0.000 | 0.001 | 0.000 | 0.001 | 0.012 | 0.000 | 0.027 |
| NMHC | g/kw-hr | 0.019 | 0.000 | 0.001 | 0.000 | 0.001 | 0.000 | 0.001 | 0.002 | 0.000 | 0.001 |
| CO | g/kw-hr | 0.356 | 0.109 | 0.113 | 0.104 | 0.122 | 0.109 | 0.005 | 0.111 | 0.017 | 0.105 |
| NOx | g/kw-hr | 0.156 | 0.005 | 0.005 | 0.007 | 0.012 | 0.005 | 0.001 | 0.010 | 0.015 | 0.016 |
| PM | g/kw-hr | 0.0007 | 0.0002 | 0.0003 | 0.0001 | 0.0002 | 0.0002 | 0.0001 | 0.0002 | 0.0002 | 0.0002 |
| CO2 | g/kw-hr | 729.4 | 701.7 | 700.3 | 700.2 | 703.0 | 700.7 | 0.82 | 771.0 | 658.3 | 825.2 |
| Work | g/kw-hr | 23.99 | 23.94 | 23.92 | 23.90 | 23.94 | 23.92 | 0.017 | 34.71 | 51.86 | 19.59 |
| N2O | g/kw-hr | 0.045 | 0.059 | 0.061 | 0.061 | 0.058 | 0.060 | 0.001 | 0.068 | 0.048 | 0.085 |

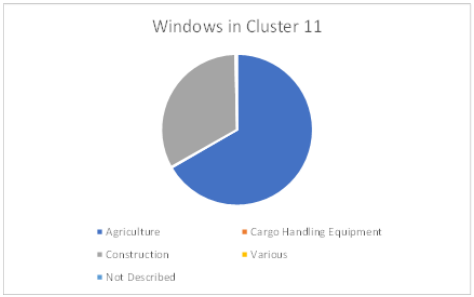
## TABLE A-8. DETAILED ENGINE-OUT EMISSIONS FOR 8000-HR TESTING WITH DSF

| | | NRTC | | | | | | | | | |
|---|---|---|---|---|---|---|---|---|---|---|---|
| | | Cold | Hot 1 | Hot 2 | Hot 3 | Composite | Hot-Avg | Hot-SD | LLAC | RMC | LLC |
| | | Set 1 | | | | | | | | | |
| Run No | | 8022 | 8023 | 8024 | 8025 | n/a | | | 8026 | 8029 | 8060 |
| THC | g/kw-hr | 0.15 | 0.05 | 0.06 | 0.06 | 0.05 | 0.06 | 0.01 | 0.09 | 0.05 | 0.17 |
| NMHC | g/kw-hr | 0.15 | 0.07 | 0.05 | 0.06 | 0.07 | 0.06 | 0.01 | 0.09 | 0.05 | 0.17 |
| CO | g/kw-hr | 1.35 | 1.21 | 1.23 | 1.25 | 1.22 | 1.23 | 0.02 | 1.11 | 0.29 | 1.48 |
| NOx | g/kw-hr | 3.82 | 4.26 | 4.27 | 4.27 | 4.24 | 4.27 | 0.00 | 5.59 | 4.19 | 5.58 |
| CO2 | g/kw-hr | 734.3 | 703.7 | 702.6 | 700.2 | 705.2 | 702.2 | 1.8 | 756.7 | 671.2 | 823.8 |
| | | Set 2 | | | | | | | | | |
| Run No | | 8063 | 8064 | 8065 | 8066 | n/a | | | 8067 | 8068 | 8114 |
| THC | g/kw-hr | 0.00 | 0.00 | 0.00 | 0.00 | 0.00 | 0.00 | 0.00 | 0.00 | 0.05 | 0.00 |
| NMHC | g/kw-hr | 0.15 | 0.06 | 0.04 | 0.06 | 0.00 | 0.05 | 0.01 | 0.00 | 0.05 | 0.00 |
| CO | g/kw-hr | 1.38 | 1.23 | 1.25 | 1.24 | 0.00 | 1.24 | 0.01 | 0.00 | 0.27 | 0.00 |
| NOx | g/kw-hr | 3.32 | 4.41 | 4.39 | 4.40 | 0.00 | 4.40 | 0.01 | 0.00 | 4.34 | 0.00 |
| CO2 | g/kw-hr | 759.7 | 712.4 | 709.8 | 709.3 | 714.8 | 710.5 | 1.7 | 770.4 | 677.5 | 847.0 |
| | | Set 3 | | | | | | | | | |
| Run No | | 8083 | 8085 | 8086 | 8087 | n/a | | | 8088 | 8111 | 8158 |
| THC | g/kw-hr | 0.00 | 0.00 | 0.00 | 0.00 | 0.00 | 0.00 | 0.00 | 0.00 | 0.05 | 0.00 |
| NMHC | g/kw-hr | 0.17 | 0.06 | 0.04 | 0.06 | 0.00 | 0.05 | 0.01 | 0.00 | 0.05 | 0.00 |
| CO | g/kw-hr | 1.33 | 1.30 | 1.27 | 1.28 | 0.00 | 1.28 | 0.01 | 0.00 | 0.27 | 0.00 |
| NOx | g/kw-hr | 3.87 | 4.37 | 4.38 | 4.39 | 0.00 | 4.38 | 0.01 | 0.00 | 4.34 | 0.00 |
| CO2 | g/kw-hr | 739.4 | 710.9 | 711.6 | 709.4 | 712.3 | 710.6 | 1.1 | 773.5 | 678.5 | 824.4 |
| MSS PM | g/kw-hr | 0.122 | 0.104 | 0.118 | 0.112 | 0.016 | 0.111 | 0.007 | 0.082 | 0.015 | 0.082 |

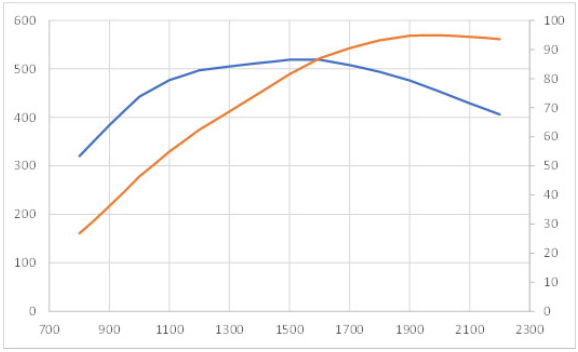
# APPENDIX B – SUMMARY OF INDIVIDUAL TEST RESULTS FOR LOW LOAD CYCLE CLUSTER

# Cluster 11 Profile 44155 – What Machine Is It ?




- 2017 John Deere 5100MH Tractor
- 2017 T4F 4045 – 95kw (from torque curve)
- 12% of total windows
- 50% of total engines

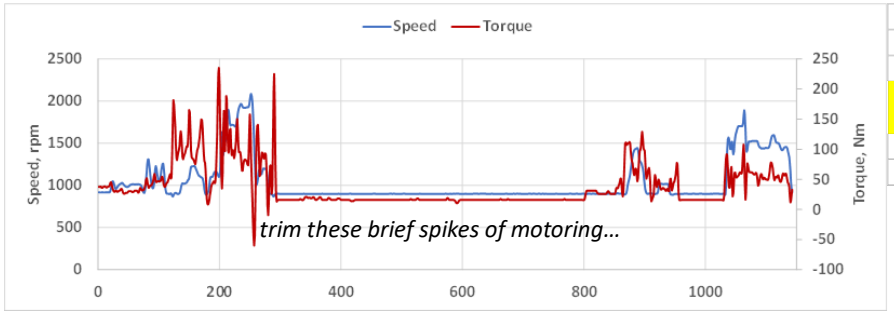


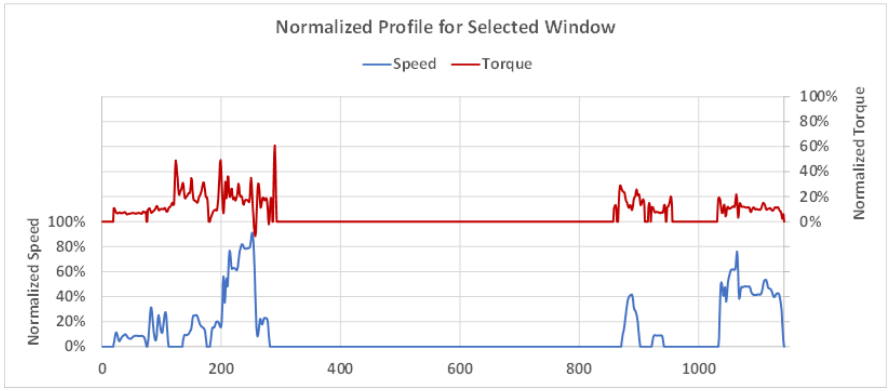



| Cluster # | Normalized Average Load | Normalized Max. Load | Normalized Median Load | Normalized Std. of Load | Loading Events per Hour | Loading Ratio | Low Load % | Sustained Low Load % | 50th percentile of cumulative load | # of windows | # of engines |
|---|---|---|---|---|---|---|---|---|---|---|---|
| 11 | 0.637 | 0.679 | 0.544 | 0.327 | 0.211 | 0.496 | 0.682 | 0.417 | 0.643 | 6264 | 119 |

| Cluster | Profile | Machine | Machine SN | Engine | Engine Power | Application | Category | Application Notes | Start | End | months | Worksite | Worksite Notes |
|---|---|---|---|---|---|---|---|---|---|---|---|---|---|
| 11 | 44155 | 2017 John Deere 5100MH | 1LV5100MLHH101042 | 4045 | 100 HP | Farm Tractor | Ag | High Crop, Orchard, Cultivation and weed control | 4/13/2021 | 7/30/2021 | 3.6 | Farm | 21,000 acres, tomatoes, cotton, alfalfa, onions, almonds, pistachios |

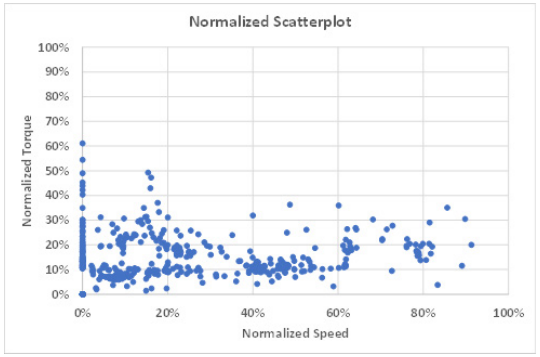
# Cluster 11 Profile 44155




| | | | |
|---|---|---|---|
| 0.099987 | Average normalized speed | | |
| 0.058559 | Average normalized load | | |
| | | | |
| 0 | start | 0.106603 | Average normalized speed in window |
| 1143 | end | 0.059306 | Average normalized load window |
| | | 0.082994 | Average noramlized load in last 300 secs of window |
| | | 0.070472 | Average noramlized load in firs 120 secs of window |

- Central idle is 579 secs long (about 10 mins)
  - 86th percentile of all idles longer than 30 secs



# Cluster 11 – 89Nm Idle



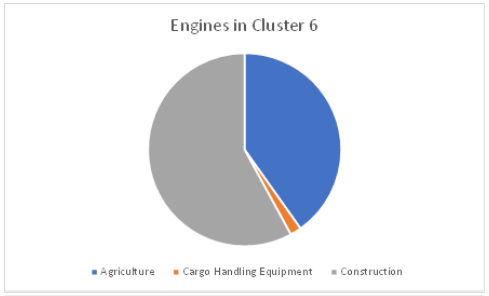

- Comparing initial behavior vs second repeat it takes about 180 secs for the AT system to fully remove the residual NRTC heat
- At 6% average load current system temperatures are low and NOX performance is poor
  - Much of cycle is below DEF injection temperature
- End of idle ROS unaffected by initial condition
- Is this idle long enough for a long idle challenge on LLC ?

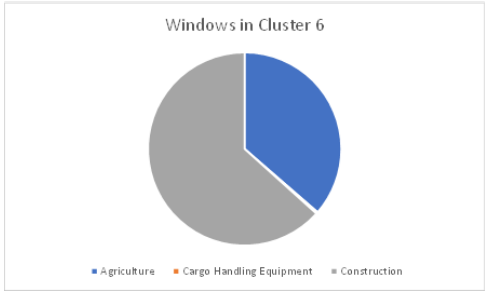
# Cluster 11 – 52Nm Idle



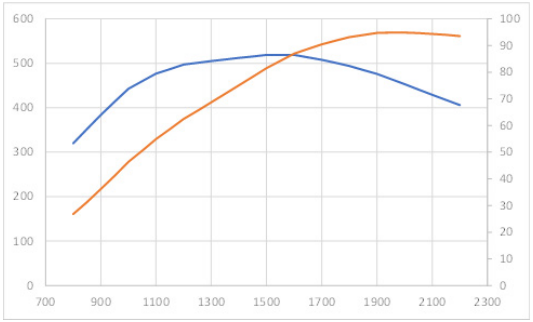

- Lower idle load did result in marginally lower temperatures, but performance was not much worse
- Return-to-service challenge was not impact by idle load difference in this case

# Cluster 6 Profile 6923 – What Machine Is It ?




- 2017 John Deere 410-L Backhoe
- 2017 T4F 4045– 95kw (from torque curve)
- 12% of total windows
- 45% of total engines



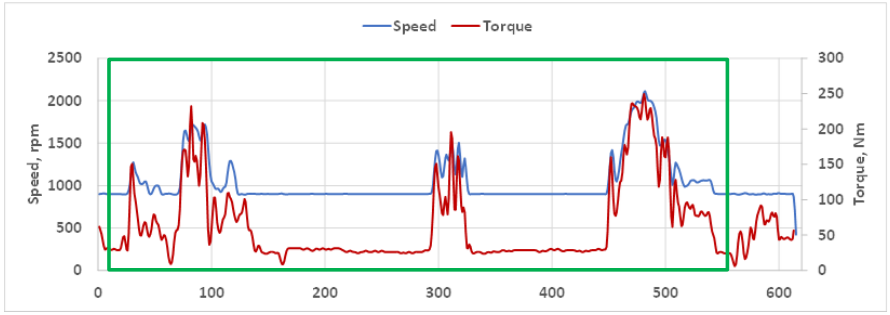


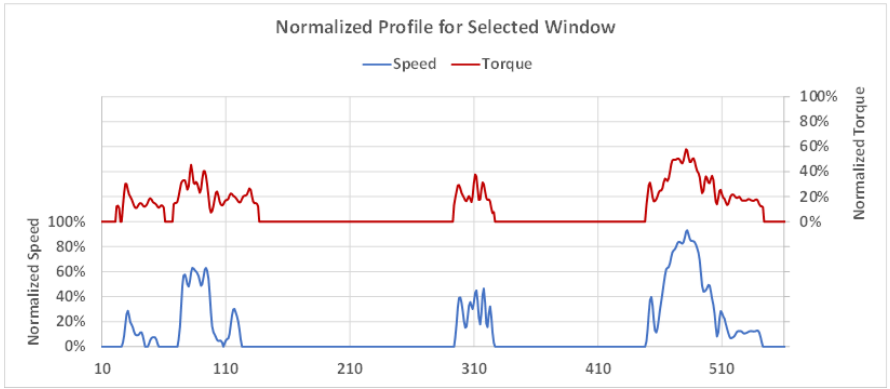


| Cluster # | Normalized Average Load | Normalized Max. Load | Normalized Median Load | Normalized Std. of Load | Loading Events per Hour | Loading Ratio | Low Load % | Sustained Low Load % | 50th percentile of cumulative load | # of windows | # of engines |
|---|---|---|---|---|---|---|---|---|---|---|---|
| 6 | 0.675 | 0.722 | 0.595 | 0.388 | 0.476 | 0.485 | 0.627 | 0.015 | 0.632 | 6028 | 107 |

| Processed | Data to SwRI | Cluster | Profile | Machine | Machine SN | Engine | Engine Power | Application | Category | Application Notes | Start | End | months | Worksite | Worksite Notes |
|---|---|---|---|---|---|---|---|---|---|---|---|---|---|---|---|
| y | y | 6 | 6923 | 2017 John Deere 410-L | 1T0410LXHF310249 | 4045HT096 | 56 - 130 kW | Backhoe | Construction | | 7/25/2019 | 10/31/2019 | 3.27 | | |

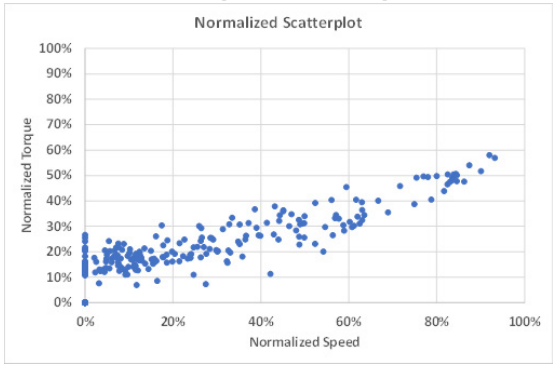
# Cluster 6 Profile 6923




| | | | |
|---|---|---|---|
| **0.10653** | Average normalized speed | | |
| **0.103067** | Average normalized load | | |
| | | | |
| 10 | start | **0.118733** | Average normalized speed in window |
| 560 | end | **0.101378** | Average normalized load window |
| | | **0.114797** | Average noramlized load in last 300 secs of window |
| | | **0.169892** | Average noramlized load in firs 120 secs of window |

- Shorter operating segments punctuated by shorter idles (2-3 mins each)
- We could repeat this profile...

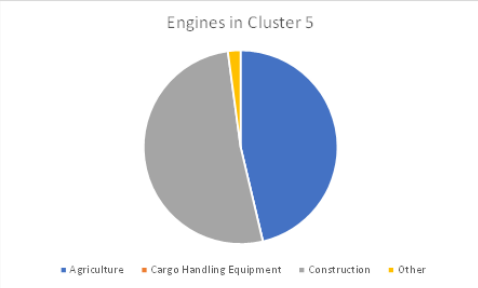


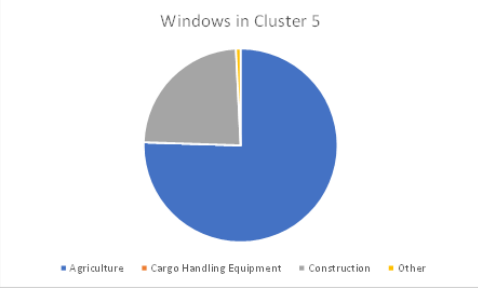
# Cluster 6 – 52Nm Idle



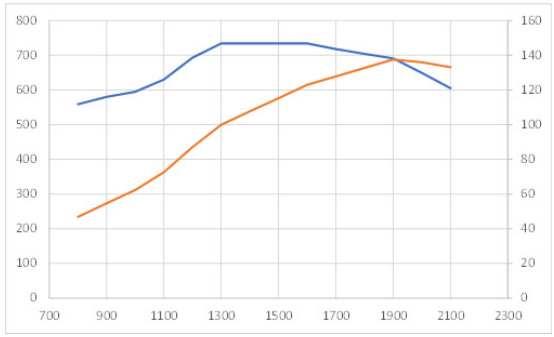

- Intermittent operation and short idles
  - Good candidate for "sustained low load" challenge ?
- Idle events are in median length area in duration
  - This profile is short so it could be looped twice to provide a good challenge event…

# Cluster 5 Profile 27372 – What Machine Is It ?




- John Deere 6190R Tractor
- 6068 – 142kw (from torque curve)
- 11% of total windows
- 40% of total engines

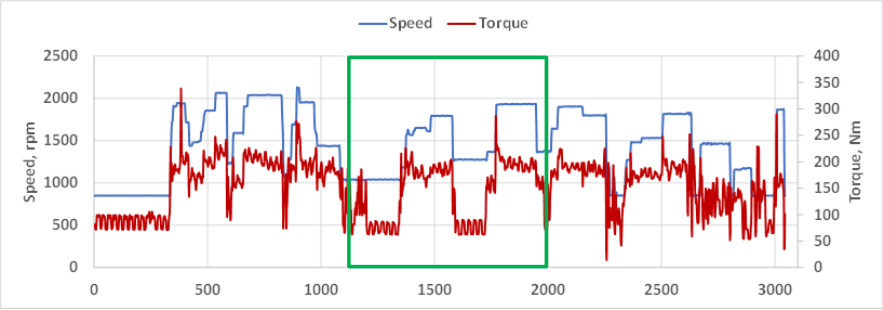


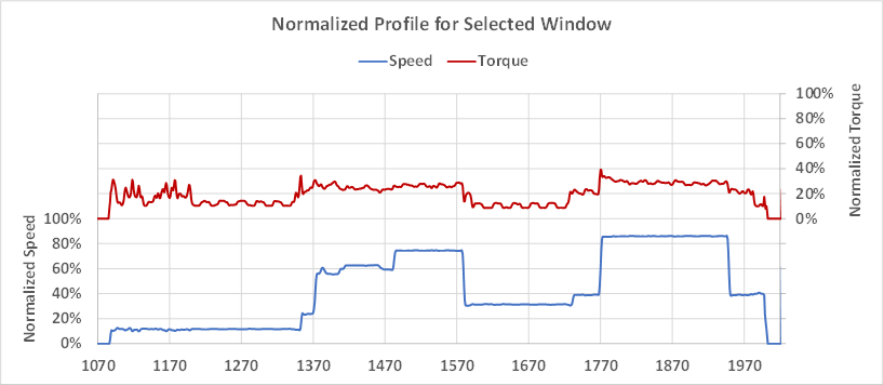



| Cluster # | Normalized Average Load | Normalized Max. Load | Normalized Median Load | Normalized Std. of Load | Loading Events per Hour | Loading Ratio | Low Load % | Sustained Low Load % | 50th percentile of cumulative load | # of windows | # of engines |
|---|---|---|---|---|---|---|---|---|---|---|---|
| 5 | 0.741 | 0.584 | 0.762 | 0.255 | 0.219 | 0.504 | 0.367 | 0.053 | 0.629 | 5949 | 95 |

| Cluster | Profile | Machine | Machine SN | Engine | Engine Power | Application | Category | Application Notes | Start | End | months | Worksite | Worksite Notes |
|---|---|---|---|---|---|---|---|---|---|---|---|---|---|
| 5 | 27372 | 2012 John Deere 6190R | N/A | 6068 | 190 HP | Farm Tractor | Ag | Cultivation, weed control (disking etc.), planting | | | | Farm | 1600 acres, Tomatoes, Onions, Garlic, Corn, others |

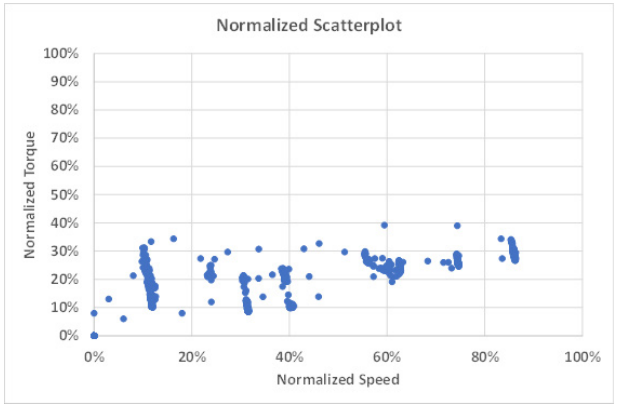
# Cluster 5 Profile 27372




| | | | |
|---|---|---|---|
| **0.459423** | Average normalized speed | | |
| **0.199325** | Average normalized load | | |
| | | | |
| 1070 | start | **0.431105** | Average normalized speed in window |
| 2020 | end | **0.196615** | Average normalized load window |
| | | **0.239765** | Average noramlized load in last 300 secs of window |
| | | **0.166448** | Average noramlized load in firs 120 secs of window |

- This profile is unique in operation, but we don't need the whole ting just a representative piece from the middle
- Starts with slightly elevated PTO then alternating higher and lower load…

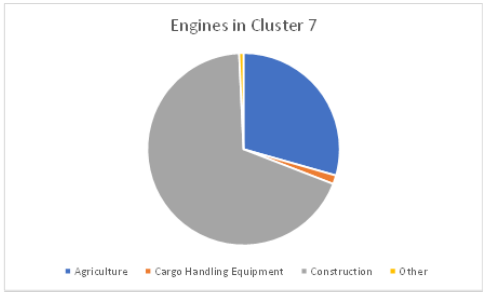


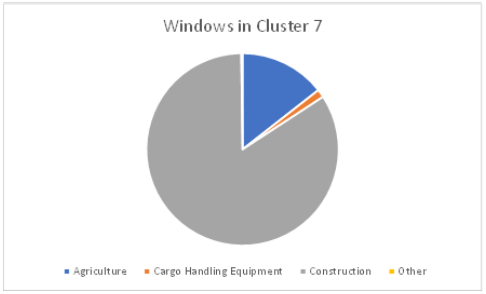
# Cluster 5 – 52Nm Idle



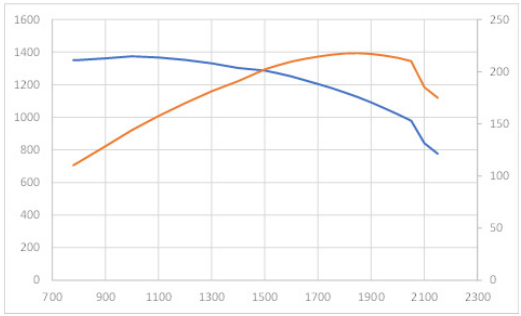

- This profile is at the higher end of the "low load" range (~20% average load)
- Contrast versus previous two we are actually warming after the NRTC+soak
- Generally good controls on current system but RoS is on edge
  - return to service at 300/1250 depends on previous entry condition

# Cluster 7 Profile 2943 – What Machine Is It ?




- Caterpillar 140M3 Motor Grader
- C9.3 – 218kw (from torque curve)
- 10% of total windows
- 57% of total engines



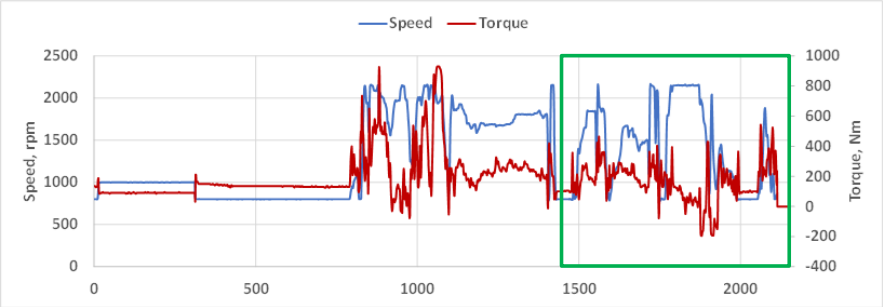


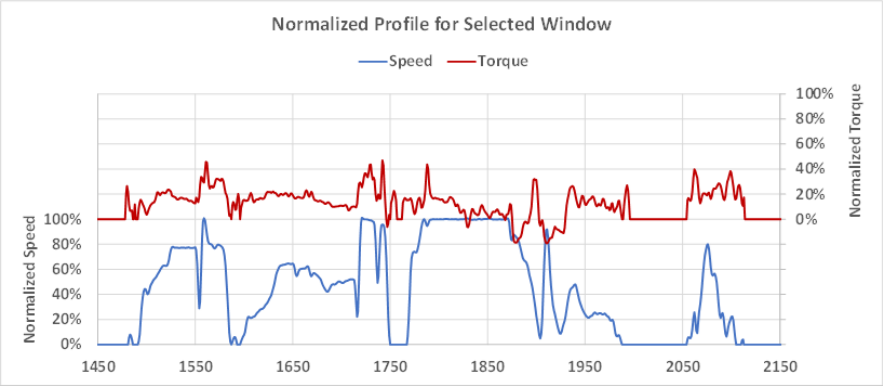


| Cluster # | Normalized Average Load | Normalized Max. Load | Normalized Median Load | Normalized Std. of Load | Loading Events per Hour | Loading Ratio | Low Load % | Sustained Low Load % | 50th percentile of cumulative load | # of windows | # of engines |
|---|---|---|---|---|---|---|---|---|---|---|---|
| 7 | 0.656 | 0.926 | 0.416 | 0.646 | 0.436 | 0.497 | 0.708 | 0.446 | 0.664 | 5245 | 136 |

| Cluster | Profile | Machine | Machine SN | Engine | Engine Power | Application | Category | Application Notes | Start | End | months | Worksite | Worksite Notes |
|---|---|---|---|---|---|---|---|---|---|---|---|---|---|
| 7 | 2943 | 2016 Caterpillar 140M3 | CAT0140MAN9J00440 | C9.3 | 256 HP | Grader | Construction | | 1/10/2019 | 2/7/2019 | 0.93 | | |

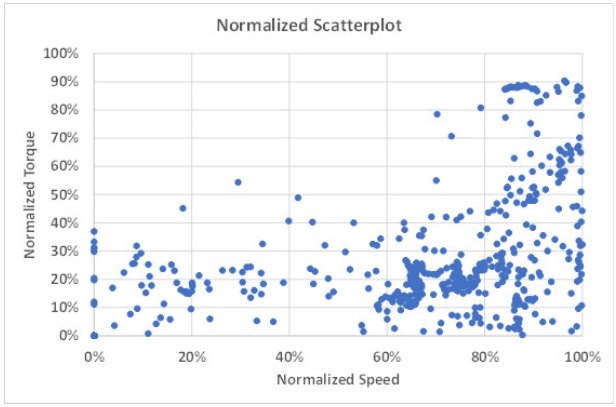
# Cluster 7 Profile 2943



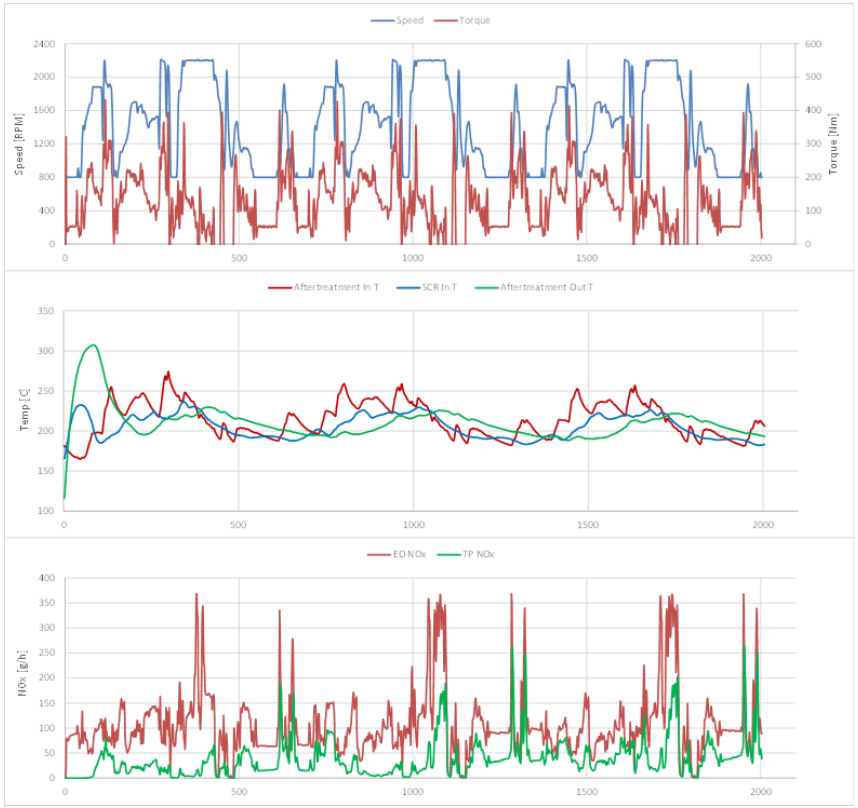




| | | | | | | | |
|---|---|---|---|---|---|---|---|
| **0.238225** | Average normalized speed | | | | | | |
| **0.118563** | Average normalized load | | | | | | |
| | | | | | | | |
| 1450 | start | **0.455995** | Average normalized speed in window | | | | |
| 2150 | end | **0.122941** | Average normalized load window | | | | |
| 700 | secs | **0.081246** | Average noramlized load in last 300 secs of window | | | | |
| 11.66667 | min | **0.134195** | Average noramlized load in firs 120 secs of window | | | | |

- Later segment pulled to better match overall load
- High-speed, light load segments
  - Contains small portion of high-speed motoring

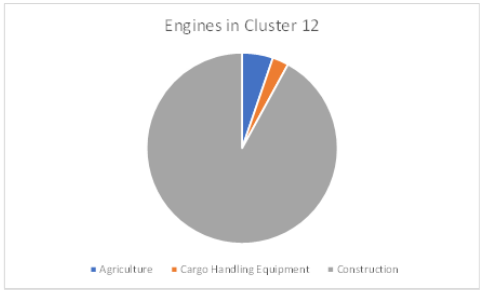


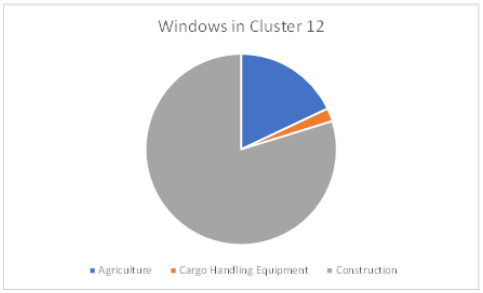
# Cluster 7 – 52Nm Idle



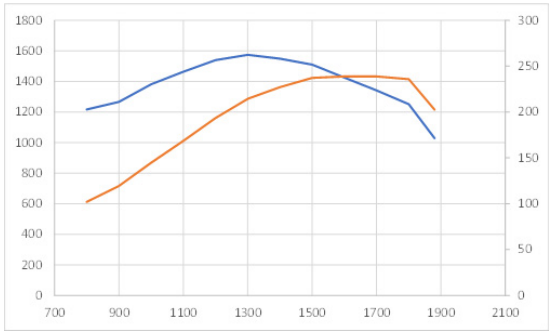

- This profile appears about mid-range (12% average load)
- Very different operating profile from any previous
  - Possibly also useful for sustained low load
- Previous condition impact gone after only 120 secs
- Control is on the edge
  - Some conversion but not full controls

# Cluster 12 Profile 12924 – What Machine Is It ?




- Caterpillar 336F Excavator
- 2014 T4F C9.3– 239kW (from torque curve)
- 10% of total windows
- 37% of total engines



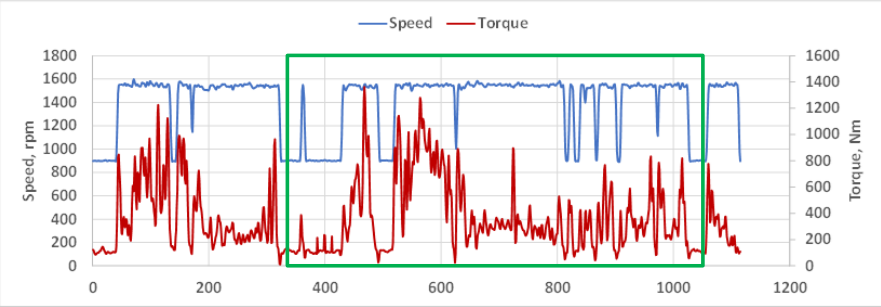


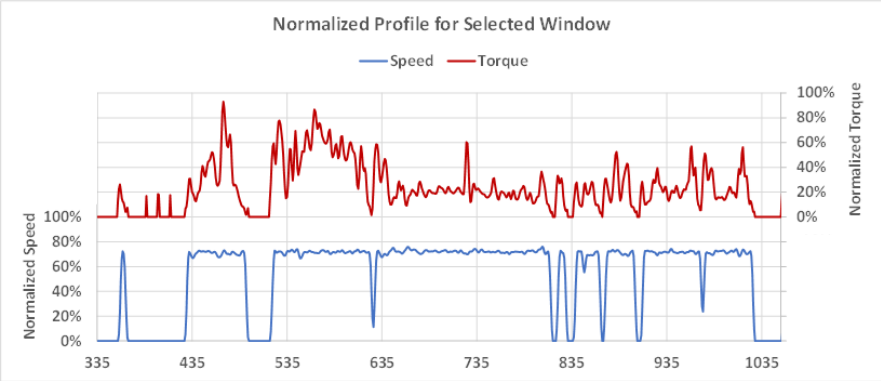


| Cluster # | Normalized Average Load | Normalized Max. Load | Normalized Median Load | Normalized Std. of Load | Loading Events per Hour | Loading Ratio | Low Load % | Sustained Low Load % | 50th percentile of cumulative load | # of windows | # of engines |
|---|---|---|---|---|---|---|---|---|---|---|---|
| 12 | 0.684 | 0.894 | 0.510 | 0.643 | 0.752 | 0.507 | 0.636 | 0.032 | 0.636 | 5054 | 89 |

| Cluster | Profile | Machine | Machine SN | Engine | Engine Power | Application | Category | Application Notes | Start | End | months | Worksite | Worksite Notes |
|---|---|---|---|---|---|---|---|---|---|---|---|---|---|
| 12 | 12924 | 2014 Caterpillar 336F | N/A | C9.3 | 272 HP | Excavator | Construction | | 9/6/2020 | 10/2/2020 | 0.87 | | |

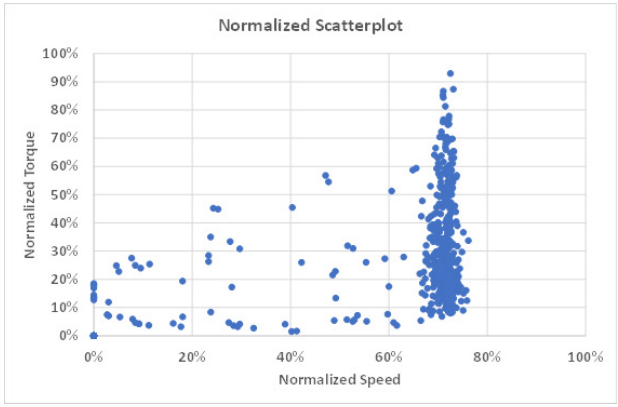
# Cluster 12 Profile 12924




| | | | | | | |
|---|---|---|---|---|---|---|
| **0.551552** | Average normalized speed | | | | | |
| **0.230834** | Average normalized load | | | | | |
| | | | | | | |
| 335 | start | **0.534972** | Average normalized speed in window | | | |
| 1055 | end | **0.230109** | Average normalized load window | | | |
| | | **0.185096** | Average noramlized load in last 300 secs of window | | | |
| | | **0.082162** | Average noramlized load in firs 120 secs of window | | | |

- Could be a good low-to-high load transition as it enters from a previous light load
- High speed sustained part load
  - but still around 20% average…so not too low…
- Can we shorten further by stopping at 835 secs ?

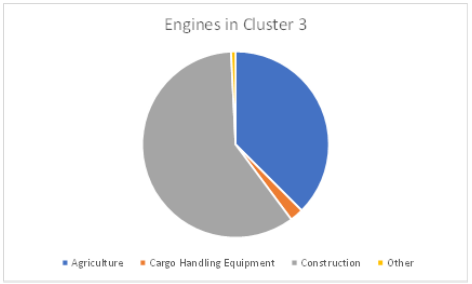


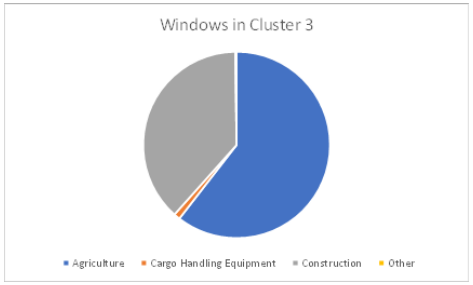
# Cluster 12 – 52Nm Idle



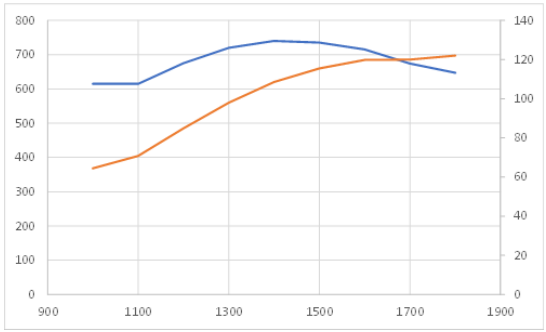

- This profile in near the high end of the load range (23%)
- High load at front and remaining load does not result in much cooling
- Emission control system is always in range
  - This profile does not have any substantial cooling opportunities

# Cluster 3 Profile 3579 – What Machine Is It ?




- Caterpillar 325FLCR Excavator
- 2019 T4F C4.4– 120kW (from torque curve)
- 9% of total windows
- 54% of total engines



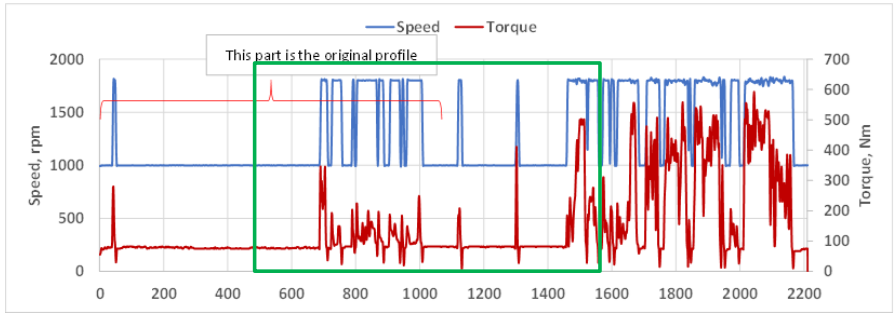


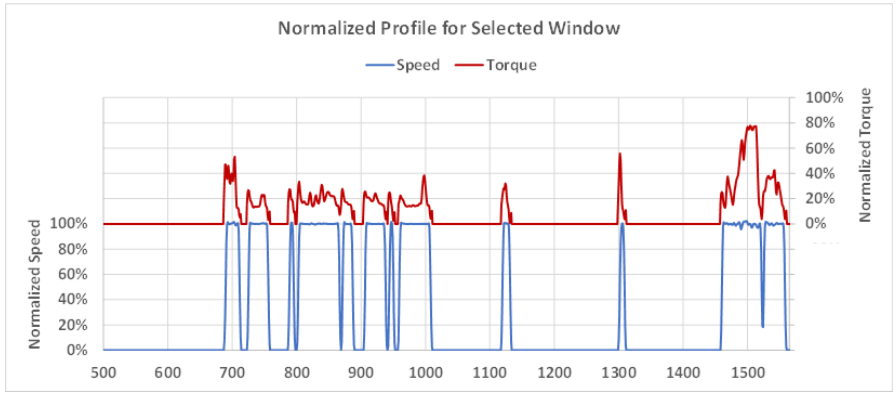


| Cluster # | Normalized Average Load | Normalized Max. Load | Normalized Median Load | Normalized Std. of Load | Loading Events per Hour | Loading Ratio | Low Load % | Sustained Low Load % | 50th percentile of cumulative load | # of windows | # of engines |
|---|---|---|---|---|---|---|---|---|---|---|---|
| 3 | 0.456 | 0.527 | 0.409 | 0.205 | 0.117 | 0.487 | 0.905 | 0.690 | 0.624 | 4749 | 128 |

| Cluster | Profile | Machine | Machine SN | Engine | Engine Power | Application | Category | Application Notes | Start | End | months | Worksite | Worksite Notes |
|---|---|---|---|---|---|---|---|---|---|---|---|---|---|
| 3 | 3579 | 2019 Excavator 325FLCR | CAT0325FJNDJ20771 | C4.4 | 161 HP | Excavator | Construction | include the 20 min after please... | 8/28/2019 | 1/23/2020 | 4.93 | | |

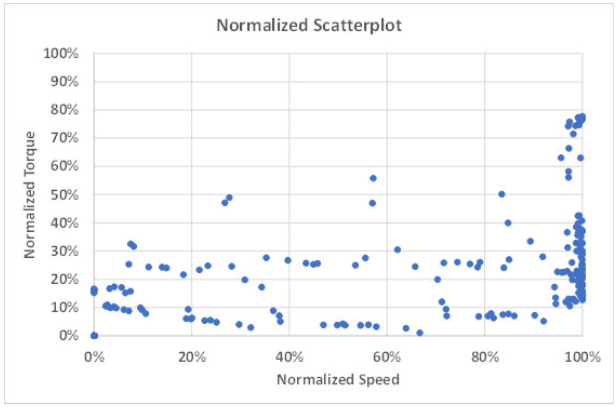
# Cluster 3 Profile 3579




| | | | |
|---|---|---|---|
| 0.218992 | Average normalized speed | | |
| 0.049653 | Average normalized load | | |
| | | | |
| 500 | start | 0.319733 | Average normalized speed in window |
| 1565 | end | 0.089371 | Average normalized load window |
| 1065 | secs | 0.138918 | Average noramlized load in last 300 secs of window |
| 17.75 | min | 0 | Average noramlized load in firs 120 secs of window |

- Another version of high speed light load but this one is lighter load than Cluster 12
- If we reached earlier (before profile we could use the long idle segment (~ 11mins), but we already have one and we don't need two of those in the cycle…



# Cluster 3 – 89Nm Idle



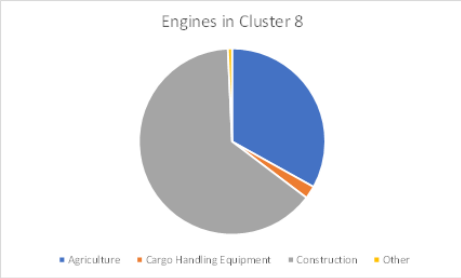

- Lower-to-middle load ~ 9%
- Intermittent long-short idle alternating
- Short early load, then cooling off period after that
  - This might be a good return-to-service followed by cooldown for next event
- May pair well following other sustained low load

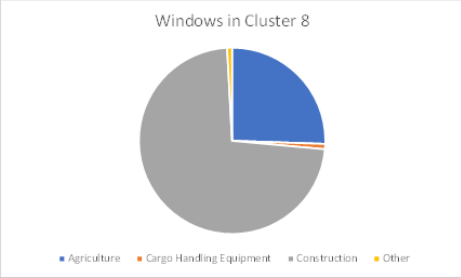
# Cluster 3 – 52Nm Idle



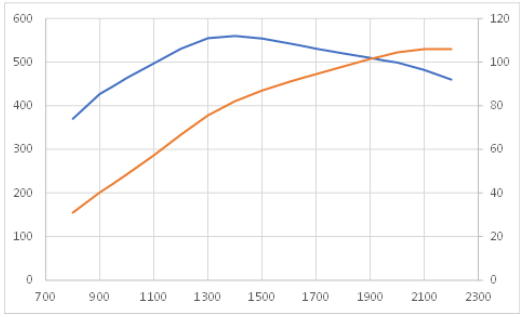

- Lower-to-middle load ~ 9%
- Intermittent long-short idle alternating
- Lower load promotes some more cooling but performance impact is small
- Short early load, then cooling off period after that
  - This might be a good return-to-service followed by cooldown for next event

# Cluster 8 Profile 23309 – What Machine Is It ?




- Caterpillar 450F Backhoe
- 2020 T4F C4.4– 105kW (from torque curve)
- 9% of total windows
- 54% of total engines





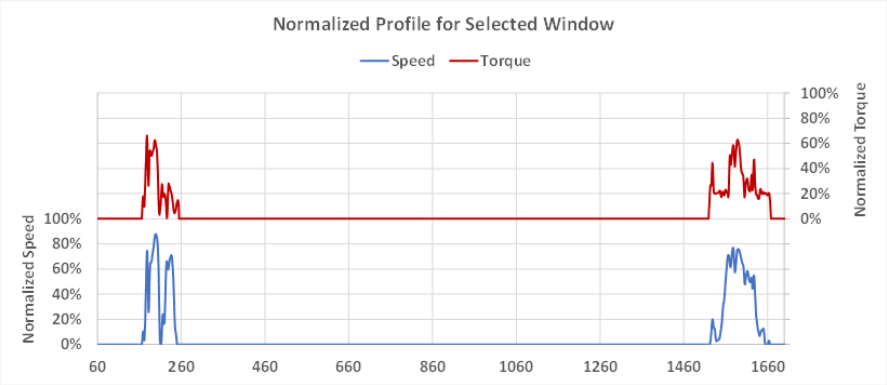


| Cluster # | Normalized Average Load | Normalized Max. Load | Normalized Median Load | Normalized Std. of Load | Loading Events per Hour | Loading Ratio | Low Load % | Sustained Low Load % | 50th percentile of cumulative load | # of windows | # of engines |
|---|---|---|---|---|---|---|---|---|---|---|---|
| 8 | 0.531 | 0.888 | 0.399 | 0.459 | 0.200 | 0.488 | 0.849 | 0.710 | 0.630 | 4062 | 136 |

| Cluster | Profile | Machine | Machine SN | Engine | Engine Power | Application | Category | Application Notes | Start | End | months | Worksite | Worksite Notes |
|---|---|---|---|---|---|---|---|---|---|---|---|---|---|
| 8 | *23309* | *2020 Caterpillar 450F* | CAT045FCHJR00282 | C4.4 | *142 HP* | *Backhoe* | *Construction* | | 8/31/2021 | 10/7/2021 | 1.53 | | |

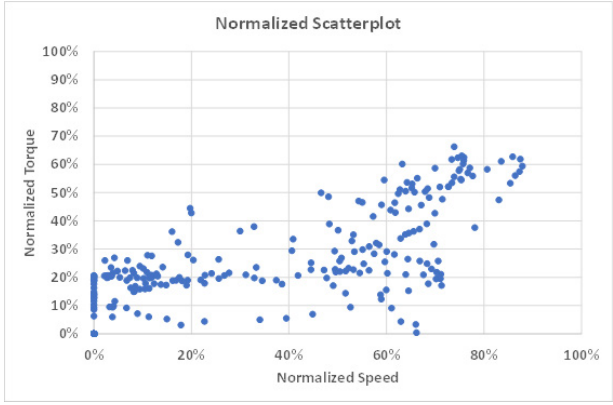
# Cluster 8 Profile 23309



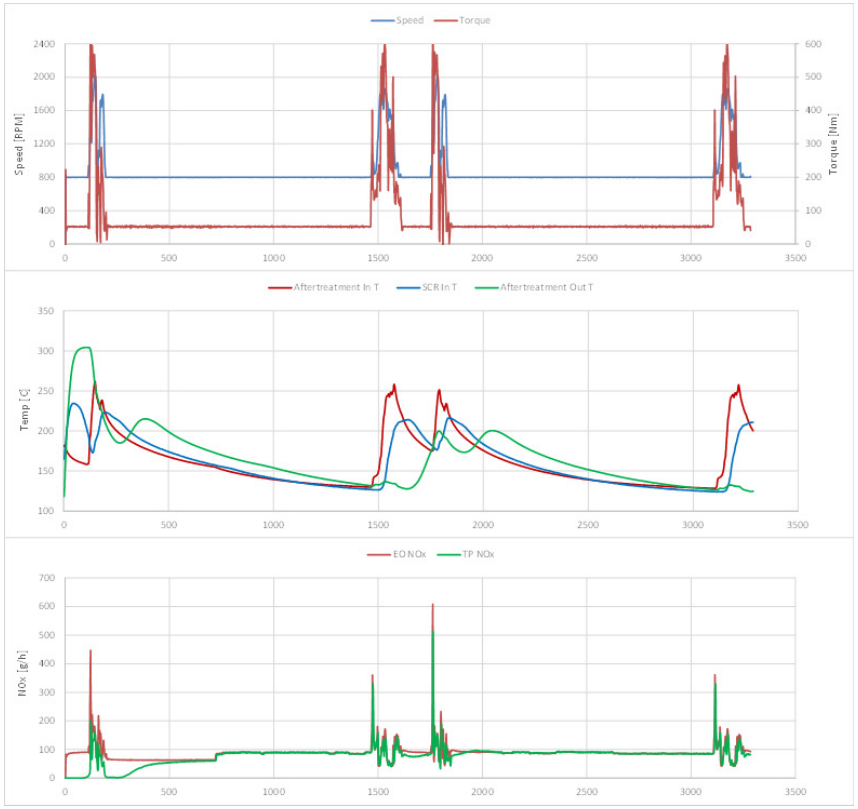




| | | | | | | | |
|---|---|---|---|---|---|---|---|
| **0.035646** | Average normalized speed | | | | | | |
| **0.02374** | Average normalized load | | | | | | |
| | | | | | | | |
| 60 | start | **0.055283** | Average normalized speed in window | | | | |
| 1700 | end | **0.040944** | Average normalized load window | | | | |
| 1640 | secs | **0.14324** | Average noramlized load in last 300 secs of window | | | | |
| 27.33333 | min | **0.037195** | Average noramlized load in firs 120 secs of window | | | | |

- This is another long central idle (similar to Cluster 11 but it is 21 minutes long)
  - 95th percentile of idle lengths > 30 secs (90th percentile > 2 mins
- But…this profile is 27 minutes long…

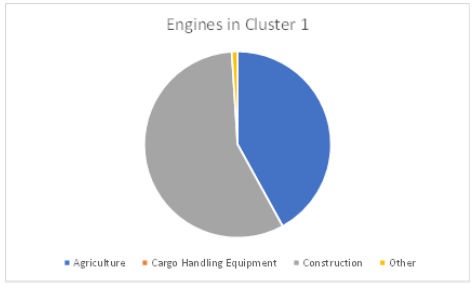


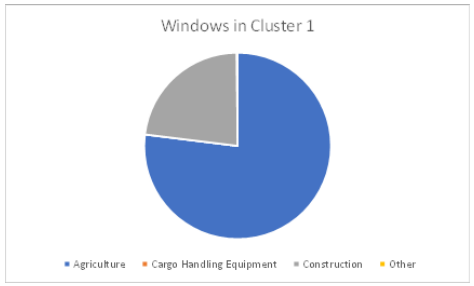
# Cluster 8 – 52Nm Idle



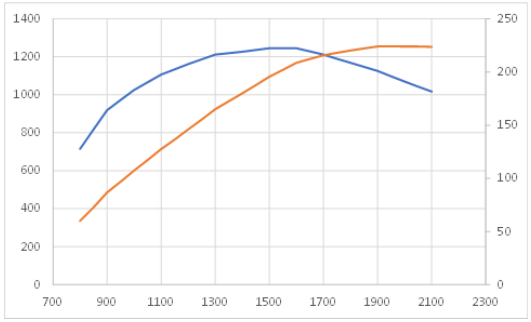

- Is this long idle needed in the LLC ?
- Return-to-service not impacted
- Likely avoids any need to separate extended idle test if there is one
- This is a lot of cycle time to spend
  - How much gain over Cluster 11 ?

# Cluster 1 Profile 37922 – What Machine Is It ?




- John Deere 7250R Tractor
- 2016 T4F 6068 – 220kW (from torque curve)
- 7% of total windows
- 42% of total engines

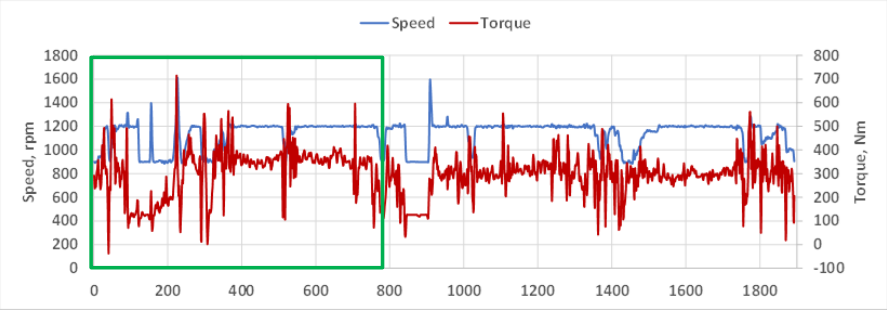


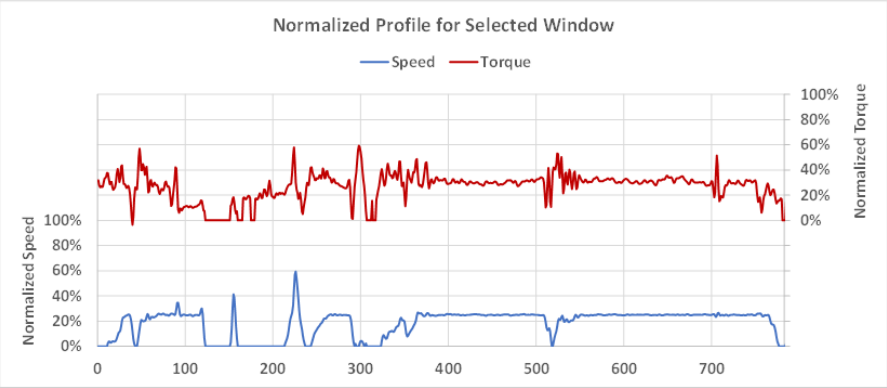



| Cluster # | Normalized Average Load | Normalized Max. Load | Normalized Median Load | Normalized Std. of Load | Loading Events per Hour | Loading Ratio | Low Load % | Sustained Low Load % | 50th percentile of cumulative load | # of windows | # of engines |
|---|---|---|---|---|---|---|---|---|---|---|---|
| 1 | 0.602 | 0.495 | 0.582 | 0.198 | 0.198 | 0.545 | 0.763 | 0.050 | 0.631 | 3760 | 100 |

| Cluster | Profile | Machine | Machine SN | Engine | Engine Power | Application | Category | Application Notes | Start | End | months | Worksite | Worksite Notes |
|---|---|---|---|---|---|---|---|---|---|---|---|---|---|
| 1 | 26848 | 2016 John Deere 7250R | 1RW7250REHS100006 | 6068RW446 | 250 HP | Farm Tractor | Ag | Cultivation, weed control (disking etc. or spraying), other utility operations | | | | Farm | 9000 acres, ROW CROPS, TOMAOTES, COTTON, GARLIC, LETTUCE, MELONS, ALMONDS |

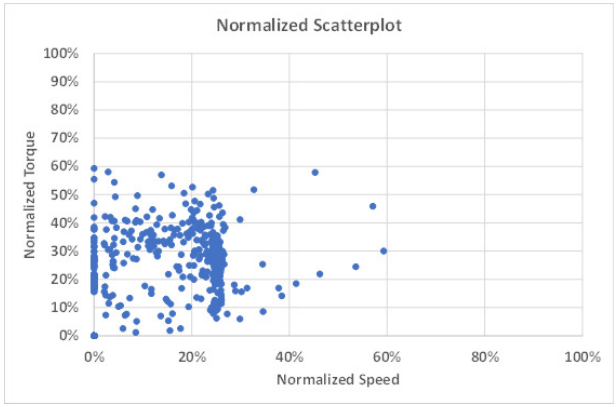
# Cluster 1 Profile 37922




| | | | | | | | |
|---|---|---|---|---|---|---|---|
| **0.187511** | Average normalized speed | | | | | | |
| **0.248511** | Average normalized load | | | | | | |
| | | | | | | | |
| 0 | start | **0.175397** | Average normalized speed in window | | | | |
| 900 | end | **0.246487** | Average normalized load window | | | | |
| | | **0.212162** | Average noramlized load in last 300 secs of window | | | | |
| | | **0.247347** | Average noramlized load in firs 120 secs of window | | | | |

- Initial lower load segment then higher load
  - Mix of variable speeds and steady-state speed
- Short early part captures most of what we want
- On the higher load end of the segments…
- Possibly good after lower load segment…

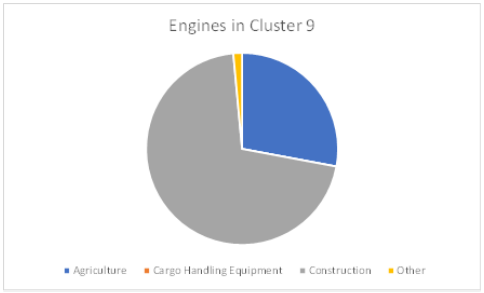


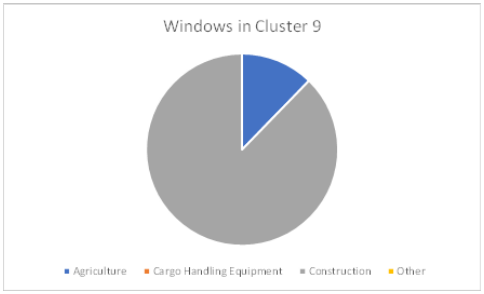
# Cluster 1 – 52Nm Idle



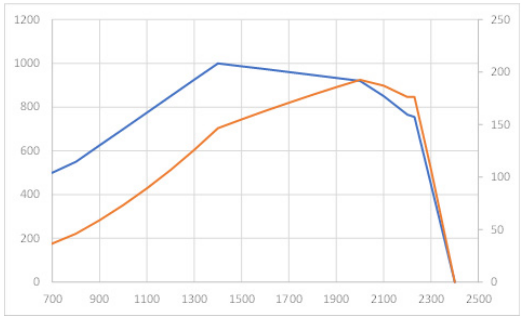

- Another profile near higher end of load profile (23%)
- This is constant speed low load but at intermediate speed rather than high speed
  - A different kind of operation from other high load portions
- Performance on Tier 4 is on edge and comes in and out of high conversion
- Profile is short so one run may make sense after lower load segment if this kind of operation needs to be represented

# Cluster 9 Profile 15285 – What Machine Is It ?




- 2011 Peterbilt Water Truck
- Cummins ISC 8.3 193kw (from torque curve)
- 7% of total windows
- 29% of total engines

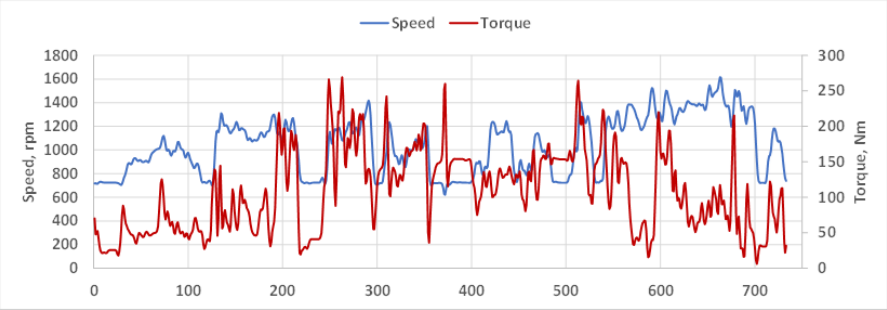





| Cluster # | Normalized Average Load | Normalized Max. Load | Normalized Median Load | Normalized Std. of Load | Loading Events per Hour | Loading Ratio | Low Load % | Sustained Low Load % | 50th percentile of cumulative load | # of windows | # of engines |
|---|---|---|---|---|---|---|---|---|---|---|---|
| 9 | 0.408 | 0.513 | 0.315 | 0.354 | 0.445 | 0.511 | 0.808 | 0.030 | 0.629 | 3747 | 68 |

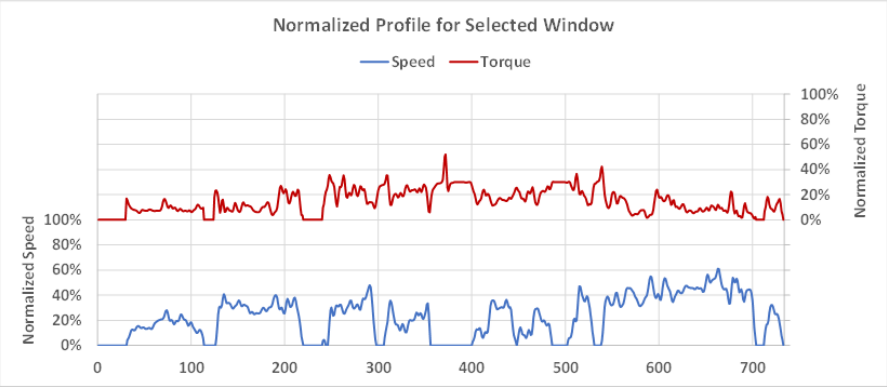
| Cluster | Profile | Machine | Machine SN | Engine | Engine Power | Application | Category | Application Notes | Start | End | months | Worksite | Worksite Notes |
|---|---|---|---|---|---|---|---|---|---|---|---|---|---|
| 9 | 15285 | 2011 Peterbilt Water Truck | 2NP3LN036LM158535 | ISC8.3 350 | 350 HP | Water Truck | Construction | | 8/26/2020 | 9/23/2020 | 0.93 | | |

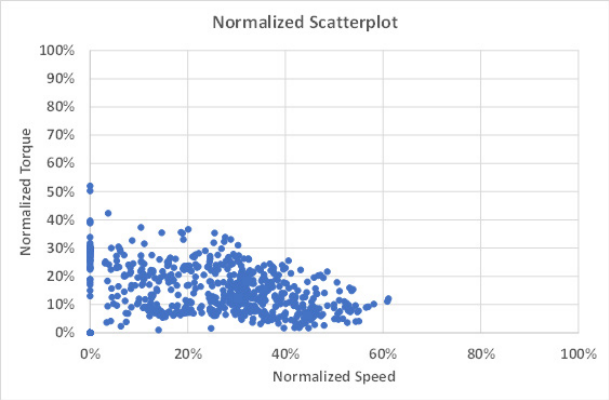
# Cluster 9 Profile 15285




| | | | |
|---|---|---|---|
| **0.223166** | Average normalized speed | | |
| **0.14647** | Average normalized load | | |
| | | | |
| 0 | start | **0.223166** | Average normalized speed in window |
| 734 | end | **0.14647** | Average normalized load window |
| 734 | secs | **0.146314** | Average noramlized load in last 300 secs of window |
| 12.23333 | min | **0.061008** | Average noramlized load in firs 120 secs of window |

- Different form of operation from most others
- Looks a lot more like on-highway operation
- Sustained lower loads rather than alternating high-low…



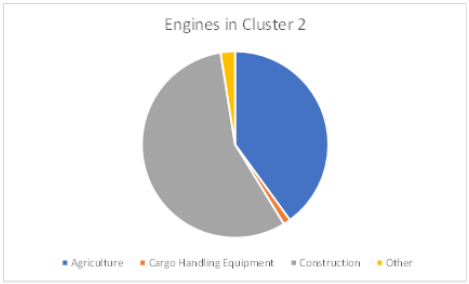



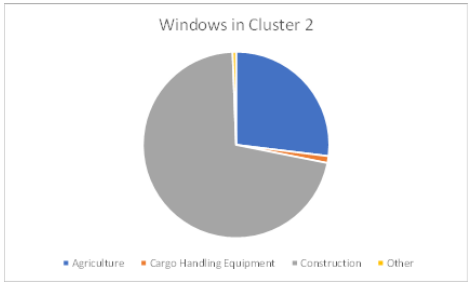
# Cluster 9 – 52Nm Idle



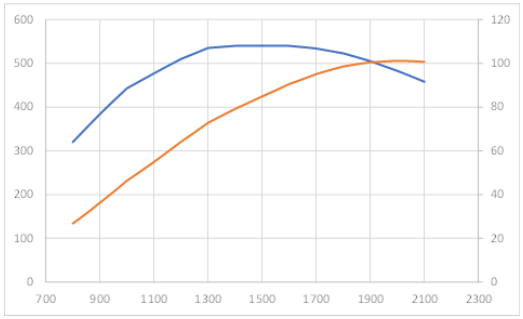

- Mid-load profile at ~ 15%
- This profile looks much more like an on-highway profile
  - May represent nonroad machines that have some road driving…
- Sustained low load performance
- Mostly below range of Tier 4f system after residual heat from NRTC+soak is gone
- Short profile so could be matched with a different one under a sustained low load segment to try provide different operating profiles

# Cluster 2 Profile 45552 – What Machine Is It ?



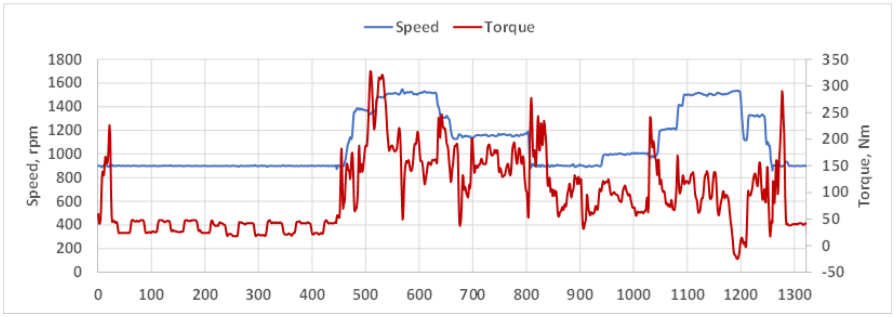

- 2018 John Deere Tractor (need more info…)
- John Deere 4045100kw (from torque curve)
- 7% of total windows
- 34% of total engines

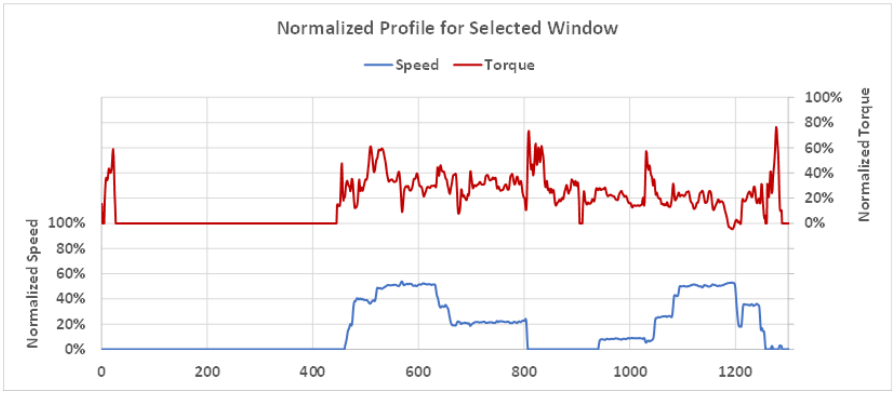



| Cluster # | Normalized Average Load | Normalized Max. Load | Normalized Median Load | Normalized Std. of Load | Loading Events per Hour | Loading Ratio | Low Load % | Sustained Low Load % | 50th percentile of cumulative load | # of windows | # of engines |
|---|---|---|---|---|---|---|---|---|---|---|---|
| 9 | 0.408 | 0.513 | 0.315 | 0.354 | 0.445 | 0.511 | 0.808 | 0.030 | 0.629 | 3747 | 68 |

| Cluster | Profile | Machine | Machine SN | Engine | Engine Power | Application | Category | Application Notes | Start | End | months | Worksite | Worksite Notes |
|---|---|---|---|---|---|---|---|---|---|---|---|---|---|
| 2 | 45552 | 2018 John Deere Tractor | | 4045HLV78 | 100 HP | Farm Tractor | Ag | UCR Ag Tractor | | | | | |

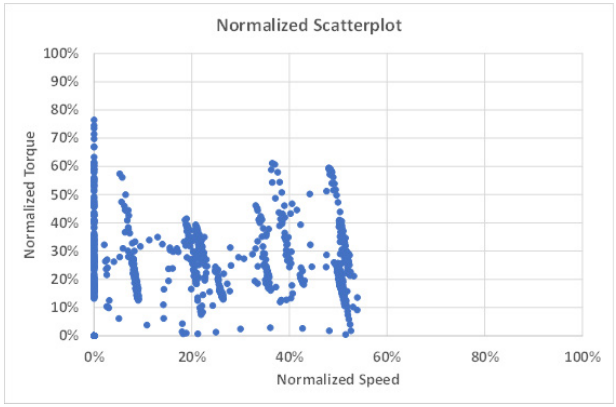
# Cluster 2 Profile 45552



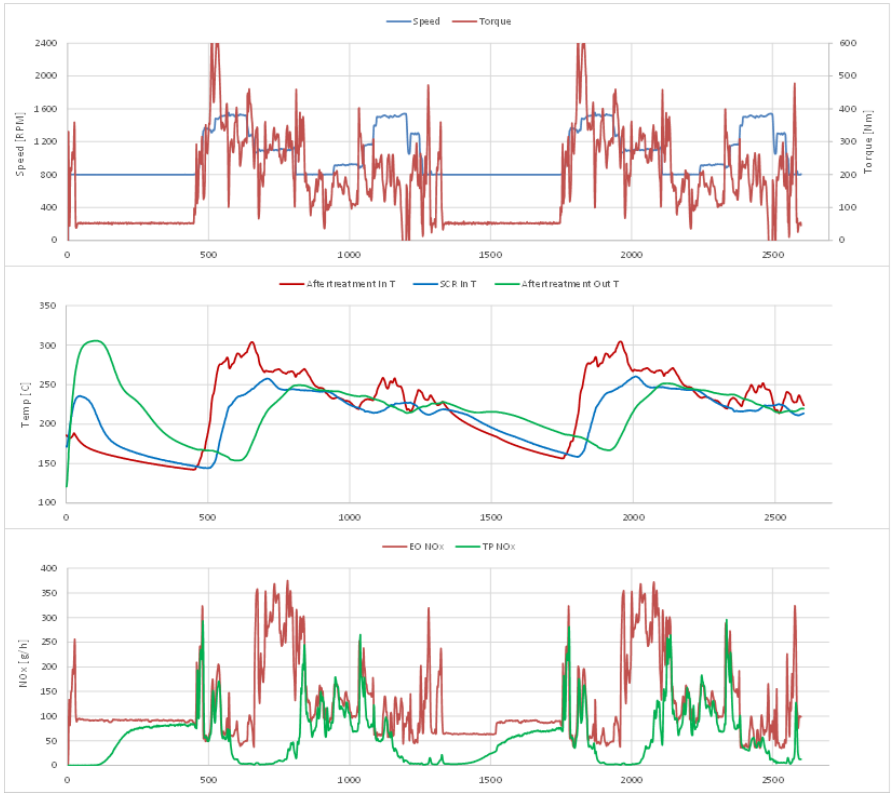




| | | | |
|---|---|---|---|
| **0.124385** | Average normalized speed | | |
| **0.180374** | Average normalized load | | |
| | | | |
| 0 | start | **0.161983** | Average normalized speed in window |
| 1300 | end | **0.180175** | Average normalized load window |
| 1300 | secs | **0.189854** | Average noramlized load in last 300 secs of window |
| 21.66667 | min | **0.06823** | Average noramlized load in firs 120 secs of window |

- Initial idle at ~7 min (intermediate to others)
  - 85th percentile over 30 secs
- Is this unique from others…
  - Speed pattern is different

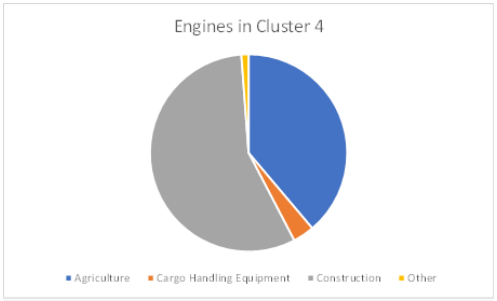


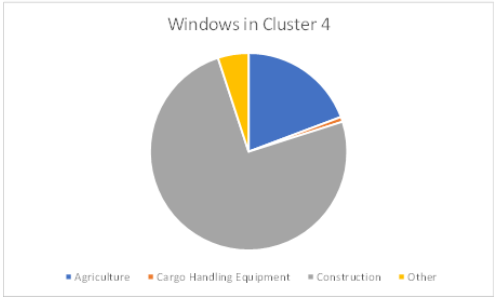
# Cluster 2 – 52Nm Idle



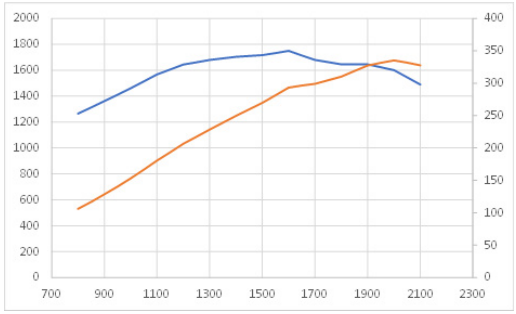

- Mid-to-high end of load range (18%)
- Alternating idle and return-to-service, but longer period than previous profiles
- Tier 4f system comes in and-out of range
  - aggressive return-to-service but then some cooling
- Profile is short so one run may make sense after lower load segment if this kind of operation needs to be represented

# Cluster 4 Profile 37221 – What Machine Is It ?




- 2016 John Deere 8370R
- John Deere 6090 330kw (from torque curve)
- 4% of total windows
- 36% of total engines



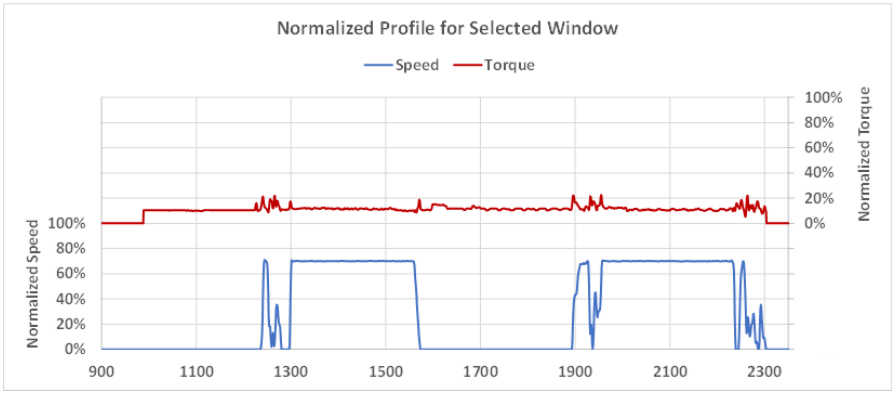



| Cluster # | Normalized Average Load | Normalized Max. Load | Normalized Median Load | Normalized Std. of Load | Loading Events per Hour | Loading Ratio | Low Load % | Sustained Low Load % | 50th percentile of cumulative load | # of windows | # of engines |
|---|---|---|---|---|---|---|---|---|---|---|---|
| 4 | 0.327 | 0.318 | 0.316 | 0.092 | 0.017 | 0.981 | 0.985 | 0.926 | 0.628 | 1987 | 85 |

| Cluster | Profile | Machine | Machine SN | Engine | Engine Power | Application | Category | Application Notes | Start | End | months | Worksite | Worksite Notes |
|---|---|---|---|---|---|---|---|---|---|---|---|---|---|
| 4 | 37221 | 2016 John Deere 8370R | 1RW8370RCGD110049 | 6090 | 370 HP | Farm Tractor | Ag | Cultivation (heavy and light), subsoiling, weed control (disking etc.), planting | | | | | 210,00 acres, Processing tomatoes, fresh tomatoes, cotton, alfalfa, onions, almonds, pistachios, watermelons, cantaloupes |

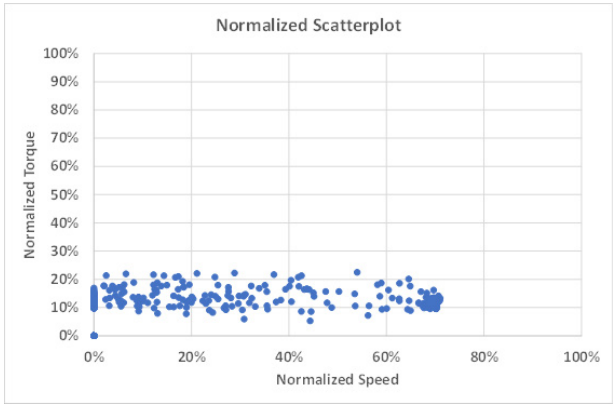
# Cluster 4 Profile 37221



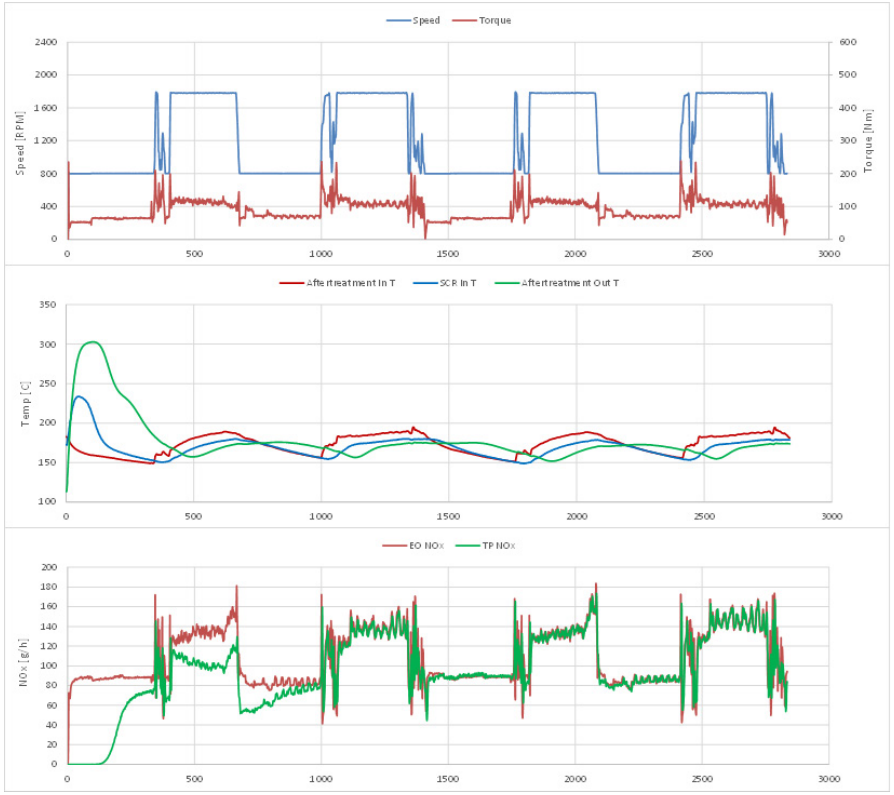




| | | | |
|---|---|---|---|
| **0.053818** | Average normalized speed | | |
| **0.074453** | Average normalized load | | |
| | | | |
| 900 | start | **0.30945** | Average normalized speed in window |
| 2315 | end | **0.107592** | Average normalized load window |
| 1415 | secs | **0.107642** | Average noramlized load in last 300 secs of window |
| 23.58333 | min | **0.027895** | Average noramlized load in firs 120 secs of window |

- Early longer idle at 17 min but do we need another one of these
- This has varying speeds but sustained low torque
  - Different from others
- But this is low population in our data set so do we need this kind of operation ?



# Cluster 4 – 52Nm Idle




- Low-to-Middle of load range (10% load)
- Alternating idle and load but the loaded portions are still high-speed low load
  - Not much heating this profile is more of a sustained low load profile
  - Longer period between load changes
- Tier 4f emission system is mostly out of range after loss of initial residual heat from NRTC+soak
- This is a very low population cluster
  - Do we need this (as opposed to Cluster 2 above ?)